THE INVESTIGATION AND PRACTICAL APPLICATION OF VIBRATION THEORIES TO DETECT CUP NICKS ON TAPERED ROLLER BEARINGS

Marlé Fernandes 0305263X

A research report submitted to the Faculty of Engineering and the Built Environment, University of the Witwatersrand, in partial fulfillment of the requirements for the degree of Master of Science in Engineering.

Johannesburg, 2013

DECLARATION

I, Marlé Fernandes (0305263X) am registered for Course EMC007. I herewith submit the following research report "*The Investigation and Practical Application of Vibration Theories to Detect Cup Nicks on Tapered Roller Bearings*" in partial fulfillment of the degree of Master of Science.

I hereby declare the following:

- I am aware that plagiarism (the use of someone else's work without their permission and/or without acknowledging the original source) is wrong
- I confirm that the work submitted herewith for assessment in the above course is my own unaided work, except where I have explicitly indicated otherwise
- This task has not been submitted before, either individually or jointly, for any course requirement, examination or degree at this or any other tertiary educational institution
- I have followed the required conventions in referencing the thoughts and ideas of others
- I understand that the University of the Witwatersrand may take disciplinary action against me if it can be shown that this task is not my own unaided work or that I have failed to acknowledge the source of the ideas or words in my writing in this task
- This project was completed with the financial and resource support of The Timken Company

Signature: _____ Date: _____

ABSTRACT

Timken South Africa manufacture and assemble AP tapered roller bearings which are used on rail journals. These are also assembled in numerous other facilities worldwide. The bearings are large and cumbersome to handle. On the assembly line there is no method of detecting the presence of cup (outer ring) nicks during the assembly process. A nick is a displacement of metal of very small size on the raceways. High spots of metal also exist. They are most frequently caused during the assembly of bearings. Cup nicks are known for repeat customer complaints due to rough rotation. The presence of the nick can induce premature fatigue spalling on the raceways, thus compromising the life of the bearing. Accelerometers were mounted on nicked and non-nicked cups and were analysed by completing Fast Fourier Transforms and Power Spectral Densities (PSD) while the assembly was rotated in a Lateral Machine. When analyzing the results with a PSD it was found that it was possible to define a baseline for a good defect-free bearing at different sampling rates. These were then transposed onto the PSD's of defective nicked bearings and it was found that the nicked bearings could be distinguished as having exceeded baseline limits. The frequencies at which this trigger occurred were not the associated bearing frequencies calculated for the ball pass outer frequencies. The energy associated with the rollers rotating over the nicked portion of the raceway excites frequencies with sufficient energy to transpose into the machine running frequency range as well natural frequencies of the bearing components. Different severity nicks were detectable as well as roller-spaced and non-roller-spaced nicks. The nicks with high spots excited the most energy. Tests were performed to show that a cone (inner ring) nick was also detectable by exceeding the baseline limit. Testing performed showed that the limits were also applicable when the accelerometer was mounted on a machine component and not directly on the cup. Recommendations include the implementation of the testing on the production line to increase the sample size of acceptable bearings for the baseline definition. The data analysis method can be fully automated to compare measured results to set limits in a reasonable time frame to not compromise production output. Nicks are detectable as long as a whole spectrum of frequencies is considered in the baseline limits and detection is not reliant on one defined frequency.

ACKNOWLEDGMENTS

The author wishes to acknowledge the Timken Company for the financial resources and support in the endeavor to complete this investigation, Terrance Frangakis for the leadership and guidance as a supervisor and TLC Engineering Solutions for the free use of their CMS software.

TABLE OF CONTENTS

LIST OF FIGURES

LIST OF TABLES

NOMENCLATURE

Symbol	Description	Unit
α	Cup Included Angle	[rad]
B	Filter Bandwidth of Analogue Signal Analysis	[Hz]
B_e	Resolution Bandwidth	[Hz]
C	Damping	[Ns/m]
d	Roller Diameter	[m]
D	Pitch Diameter	[m]
D1	Nicked Bearing	[-]
D2	Nicked Bearing	[-]
D3	Nicked Bearing	[-]
D4	Nicked Bearing	[-]
D5	Non Nicked Bearing	[-]
D6	Nicked Bearing	[-]
f_a	Shaft Frequency	[Hz]
f_b	Ball Frequency	[Hz]
f_c	Cage Frequency	[Hz]
f_o	Outer Defect Frequency	[Hz]
f_i	Inner Defect Frequency	[Hz]
f_r	Rolling Element Defect Frequency	[Hz]
$F_{unbalanced}$	Force due to unbalanced mass	[N]
k	Spring Stiffness	[N/m]

M	Mass	[kg]
n	Number of rollers	[-]
N	Number of Equally Spaced Samples	[-]
r	Radius	[m]
t	Instantaneous Time	[s]
T	Duration of the measurement	[s]
ω	Angular Frequency	[rad/s]

1. INTRODUCTION

1.1 Overview

1.1.1 Introduction to Timken

Timken is an international company that manufactures and supplies various types of bearings including tapered, spherical, cylindrical and ball bearings. Additionally, they specialise in a large range of friction management solutions. In South Africa they produce a range of bearings called the All Purpose (AP) bearing used on railway wagon axles with sizes ranging from class B to class E. The South African branch is the only manufacturer of class C and D bearings. These bearings are supplied to the local rail industries, industrial applications as well as customers in other countries. The AP tapered roller bearings are assembled in approximately five Timken locations in the world and are used worldwide as journal rail bearings in most countries with a rail infrastructure. The assembly facilities worldwide have similar equipment and the processes involved in assembly of bearings is mostly identical. The Timken Company has extensive market share across the world in the rail industry and thus the bearings are prolific across the global in most rail applications including high speed passenger trains, underground railway systems, as well as freight and cargo applications.

Bearings allow axial and radial loads to be transmitted from a rotating element such as a shaft to a non-rotating element such as a wagon bogey. Bearings usually consist of an outer race (cup), an inner race (cone) and rolling elements (balls or rollers). They are designed to tight dimensional tolerances and have ground surface finishes in order to ensure a high reliability during operation, where they are exposed to high loads and loading cycles.

A particular problem associated with larger AP bearings is “nicks” (small indentations or gouges) on the bearing races (cups) which arise during assembly of the bearings which, in certain processes, involves manual handling of fairly heavy components or sub-assemblies.

1.1.2 Motivation and problem statement

When nicks are present on a bearing race it results in rough turning, audible noise, early fatiguing of raceways, and ultimately results in premature failure of the bearing. This results in unsatisfied customers and a poor image of Timken. While the problem is a quality control issue, there are numerous instances where, even with good quality control, defects of this nature may still occur in the production line. Currently there is no mechanism for nick detection besides visual methods. To visually detect nicks is not practical as they often occur during the assembly process and thus cannot be viewed once the bearing is assembled.

This research concerns detection of the cup nicks during the bearing assembly stage as a means of preventing premature bearing failure and customer complaints. The proposed approach will be to assess the feasibility of using vibration condition monitoring techniques applied during one particular stage of the bearing assembly process, when the bearings are tested in the Lateral Machine (in order to determine the correct bench end-play and install a spacer). One particular size of bearings is proposed in the research, namely the All Purpose (AP) bearing, class D. This is due to its availability as a result of high production volumes in South Africa.

1.2 Research Questions

1. Is it feasible to detect cup nicks in class D AP bearing during the bearing assembly stage using standard vibration condition monitoring techniques?
2. Is it feasible to detect cup nicks when the bearings are placed in the Lateral Machine during bench end-play measurement?
3. If vibration is measureable is there a correlation between vibration amplitude and size of the cup nicks?
4. Is it feasible to detect cup nicks during the assembly stage rather than when the bearings are fully assembled (so as to reduce or eliminate rework)?

1.3 Objectives

The following are the objectives of the research undertaken in this report.

i. Set up a vibration condition monitoring system to be used on AP bearings being tested for bench end-play on the Lateral Machine.

ii. Test bearings with and without cup nicks (of known sizes) in order to detect and identify frequencies of vibration associated with the nicks (if present), and verify the repeatability of test results.

iii. Determine the effect of sampling parameters (such as testing duration and sampling frequency) on the amplitude of vibration of a nicked and non-nicked bearing.

iv. Determine amplitudes of vibration of bearings with cup nicks and determine whether there is a correlation with nick sizes. If so, determine what range of nick sizes are detectable.

v. Determine if different bearing parameters such as bearing bench end-play affect amplitudes of vibration and additional frequencies.

vi. Investigate the effect on frequency and amplitude of vibration of the bearings if the nicks are roller-spaced or not.

vii. Evaluate the variation in vibration amplitude obtained for varying transducer mounting positions on the bearing cup, relative to the location of known nicks.

viii. Assess the suitability of detection of cup nicks in the bearing production environment on a Lateral Machine.

The introductory chapter has shown the need for the research to detect cup nicks on the assembly line as the presence of nicks could induce premature failure. Nicks occur most often due to handling damage. AP bearings are used extensively across the world on rail journals as a result of the extensive market share that Timken has in this particular bearing application and thus there would be large industry benefit in finding a method to detect cup nicks. The testing will be conducted in the Timken South Africa (Benoni) assembly plant, and will be conducted on class D bearings at this time due to the high availability of this part number within the production facility. The testing will be limited to the vibration detection possible on the Lateral Machine.

2 LITERATURE REVIEW

This chapter will discuss the basic bearing nomenclature and geometry associated with the AP bearing. This will lead to relevant information regarding vibration fundamentals and the use of condition monitoring equipment and techniques in measuring vibration within the industry. Specific mention will be given to the techniques associated with bearing fault detection. Case studies will be discussed on how standard bearing vibration techniques are applied to detect bearing faults. The previous work done on detecting cup nicks within the Timken assembly environment will be explained and discussed to broaden the understanding of why the undertaken research is necessary to better understand cup nick detection within the bearing assembly line.

2.1 Bearing Nomenclature and Geometry

2.1.1 Bearing nomenclature

Figure 2-1 shows a general arrangement of an AP (All Purpose) bearing. This is a pre-lubricated, preassembled package bearing. AP Bearings are mostly used for rail wheel journals and also in some industrial applications. Timken South Africa manufactures class B, C, D and E bearings (between four and six inch bores), but assembles most of the other sizes (bore up to seven inches).

Figure 2-1 – General bearing arrangement (The Timken Company)

The assembled bearing consists of an outer ring (cup) on which two sets of taper rollers act. Two inner races (cones) transmit radial and axial loads through the taper rollers to the outer race or vice versa. A spacer separates the two cones in such a manner that the desired mounted end-play can be achieved within the assembly. Assembled bearings also have seals and ancillary components to retain grease and prevent environmental contamination within the application.

Figure 2-2 shows a cross section of a typical bearing assembly with some basic nomenclature.

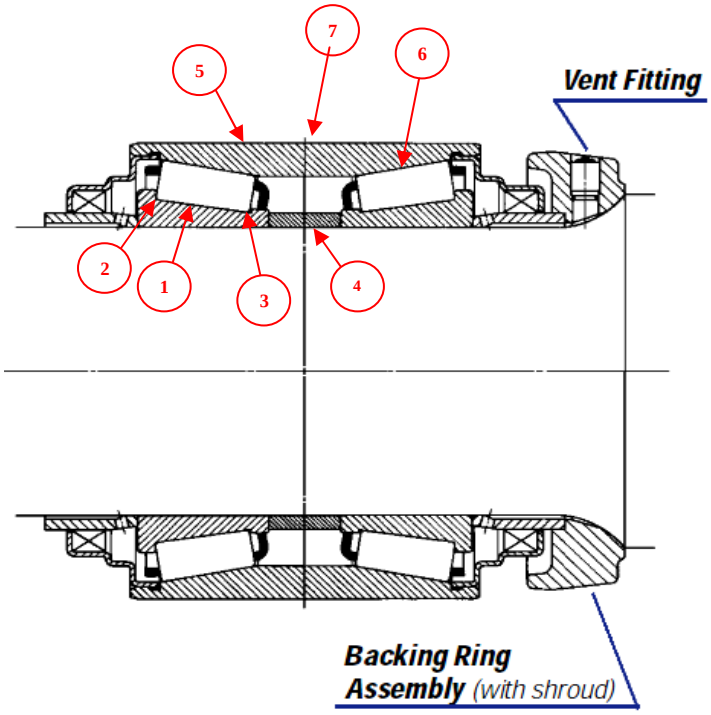

1. Cone (Inner Ring) Race
2. Cone Large Rib
3. Cone Small Rib
4. Cone Spacer
5. Cup OD (Outer Ring)
6. Cup Race
7. Track

Figure 2-2 - Bearing assembly nomenclature (The Timken Company)

2.1.2 Cup nicks

A nick is a defect that occurs in bearings due to in-process handling damage. They can occur as a result of a variety of factors within the manufacturing facility but most commonly occur in the assembly process when operators put the cone into the cup at an angle and force the cone into the cup (see Figure 2-3). This causes a ‘nick’ in the cup material which is the removal or scraping of material pointed towards the large end of the race, which can result in raised metal at the furthest point of the nick in severe cases. Due

to this action a nick is normally felt by a finger nail and if raised metal is present it is easily felt by touch. The indented material normally has a shiny appearance. Nicks are also created by general handling damage and do not only occur on the raceways. They can be small, i.e. appear only as a visual defect, but not cause any displacement of metal. In some circumstances it is found that nicks cause smooth raised metal. Alternatively the nick could potentially cause rough 'jagged' shears of metal. This is all dependent on the nature of the handling damage. Nicks are not only present in isolation but commonly roller-spaced nicks are found. The exact roller spacing is resembled in the nicks on the cup raceways, showing that it is caused by the rollers impacting the cup race during assembly.

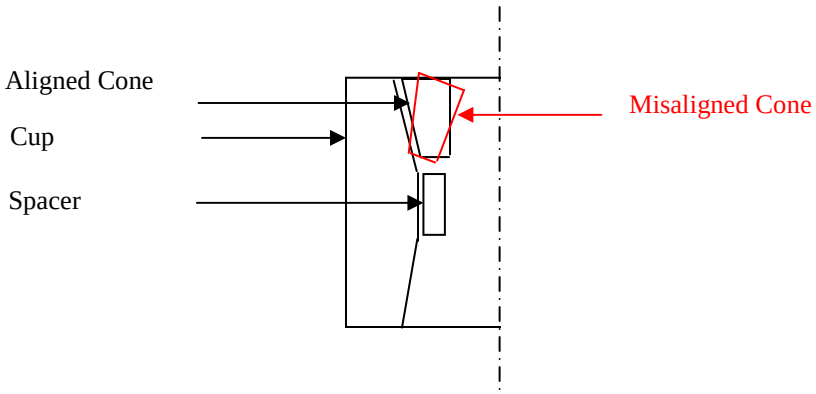

Figure 2-3 – Typical method in which cup nicks are created

Figure 2-4 shows typical examples of raceway nicks. This particular bearing was returned from a customer, opened, washed and cleaned and inspected. Large nicks have been encircled and these particular nicks have been stained as well. Nicks are not always this dark. The lines in the photograph are not as a result of grease smearing but due to another damage mode which is not in the project scope.

Figure 2-4 – Nicks in two different cup raceways

The initial consequences of nicks on a bearing are rough turning and noise when installed in the application. As previously mentioned this is bad for the customers as it could immediately sounds as if the bearing is defective. Additionally with the modern industrial focus on Noise, Vibration and Harshness monitoring (NVH) this is not an acceptable bearing feature.

When the nick is not detected before installation into the application the high spots, caused by the nick, can induce high stresses as the rollers roll over these points. These high stress concentration points can lead to premature fatigue of the raceway and this will result in spalling of the raceway. Spalling is the dominant mode of failure of rolling elements of a bearing. It is caused when a fatigue crack appears below the surface and when it propagates towards the surface a piece of metal breaks away to leave a pit or a spall (Tandon & Choudhury, 1999). Thus spalling is the phenomenon where bearing material pits or flakes away. Typical spalling that could occur due to nicks is Point Surface Origin (PSO) of which photos are shown in Figure 2-5.

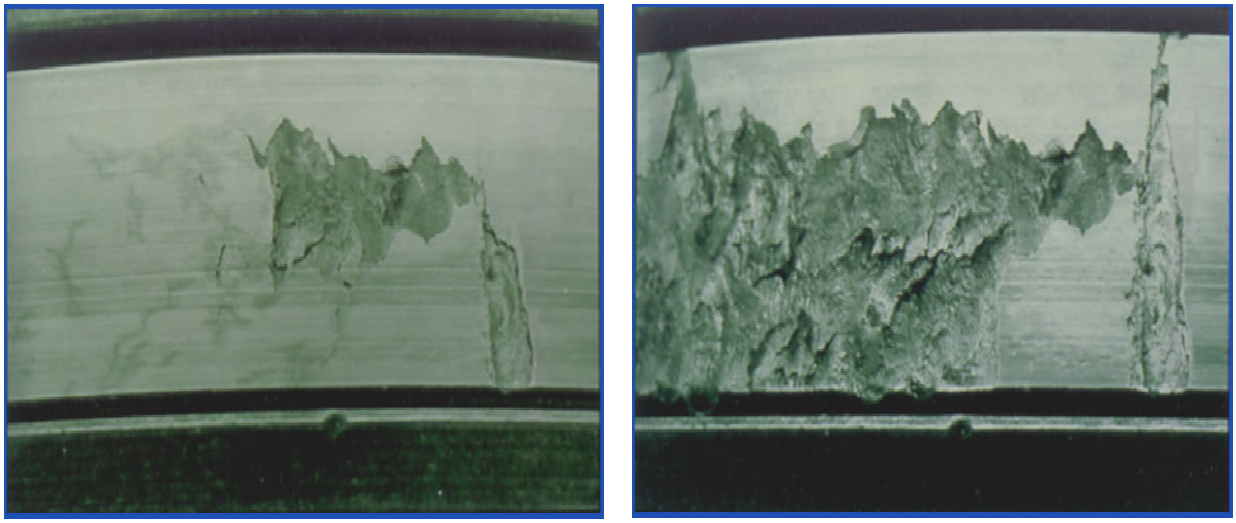

Figure 2-5 – PSO spalling shown through progressive deterioration

Normal occurrences of spalling exist in bearings due to standard fatigue of raceways when the life of the bearing has been overextended. It can also be expected that the bearing can operate with small spalls for a certain period of time. However, it takes millions of revolutions to produce spalling of the magnitude shown in Figure 2-5. It should be noted that once severe spalling has begun the condition of the bearing will start deteriorating as the flaked off material from the spalls will remain within the bearing assembly and is likely to create spalls of a different origin elsewhere in the bearing. When spalling gets to a state as shown the bearing will not only be rough, very noisy and rattle but the fit of the bearing will be compromised and the assembly in which the bearing is used will most likely be clearly unfit for further use. Bearings, however, will not necessarily seize up due to this condition.

The current Timken corporate standard allows a nick on a cup and cone raceway to be maximum 1.02mm (length) x 0.25mm (width) in size. No nicks that have raised metal are permitted and only one nick per quadrant is acceptable on the raceway surface (The Timken Company, 2011). However, in practice when nicks are seen the bearings are mostly scrapped as a matter of course.

2.2 Vibration Fundamentals

2.2.1 Introduction

A simple definition of vibration is the motion of a machine or its parts back and forth from a position of rest. Alternatively it is defined as a motion that repeats itself after an interval of time (Rao, 2004). To be able to extract useful information from a vibration signal given off by a machine component or bearing it is important to first understand the characteristics that define a vibration signal (Scheffer, 2010).

The simplest example by which to explain vibration is that of a system with a spring, a mass and a damper, such as a dashpot. These three elements make up the three fundamental properties that are present in all vibration scenarios and these are Mass (*M*), Stiffness (*k*) and Damping (*C*). All vibration systems are made up of a means for storing potential energy, a spring, the storage of kinetic energy, through a mass and inertia, and a means by which the energy is gradually lost, a damper (Rao, 2004). This is illustrated in Figure 2-6.

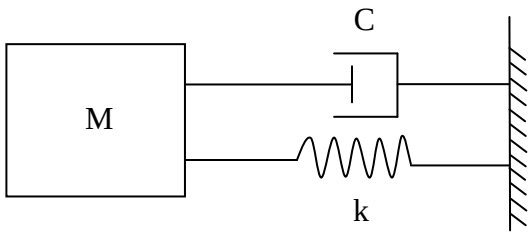

Figure 2-6 – Basic vibrational system

When considering a rotational system with an unbalanced mass the vibrational force produced by the unbalanced mass, *Mu*, is represented by:

$$F_{unbalanced} = Mu \cdot r \cdot \omega^2 \cdot \sin(\omega t) \tag{2-1}$$

where

t is the time [s],

ω is the angular frequency [rad/s],

r is the fixed radius of the unbalanced mass [m].

The matching restraining force generated by the three fundamental characteristics is then

$$(M \times a) + (C \times v) + (k \times d) = 0 \qquad (2\text{-}2)$$

where a is the acceleration [$m.s^{-2}$],

v is the velocity [$m.s^{-1}$],

d is the displacement. [m].

When the system is in equilibrium the restraining and vibrational forces will be equal. However, conditions are normally changing and as some factors increase others decrease, resulting in a net variation in the sum of all forces.

The three different types of motion variables: displacement, velocity and acceleration, are all present in a situation in which vibration occurs. These three properties are, however, more prominent at different frequency levels. For example at lower frequencies displacement has a more gradual slope in the relationship between displacement and frequency, i.e. the change in displacement with frequency is less (Figure 2-7). At medium frequencies, 30Hz to 1000Hz velocity is found to be almost constant. At high frequencies, 1000Hz to 10,000Hz, acceleration is mostly constant (Seippel, 1983). Thus it is good practice that displacement is used for measurements at lower frequency ranges and acceleration is more suited at higher frequencies. Most machinery operates at frequencies where velocity is most prominent and thus velocity is often the most common form of vibration measurement and analysis (Scheffer, 2010). However, modern

accelerometers have the ability to be responsive across all frequency ranges when they are specified correctly for the intended application.

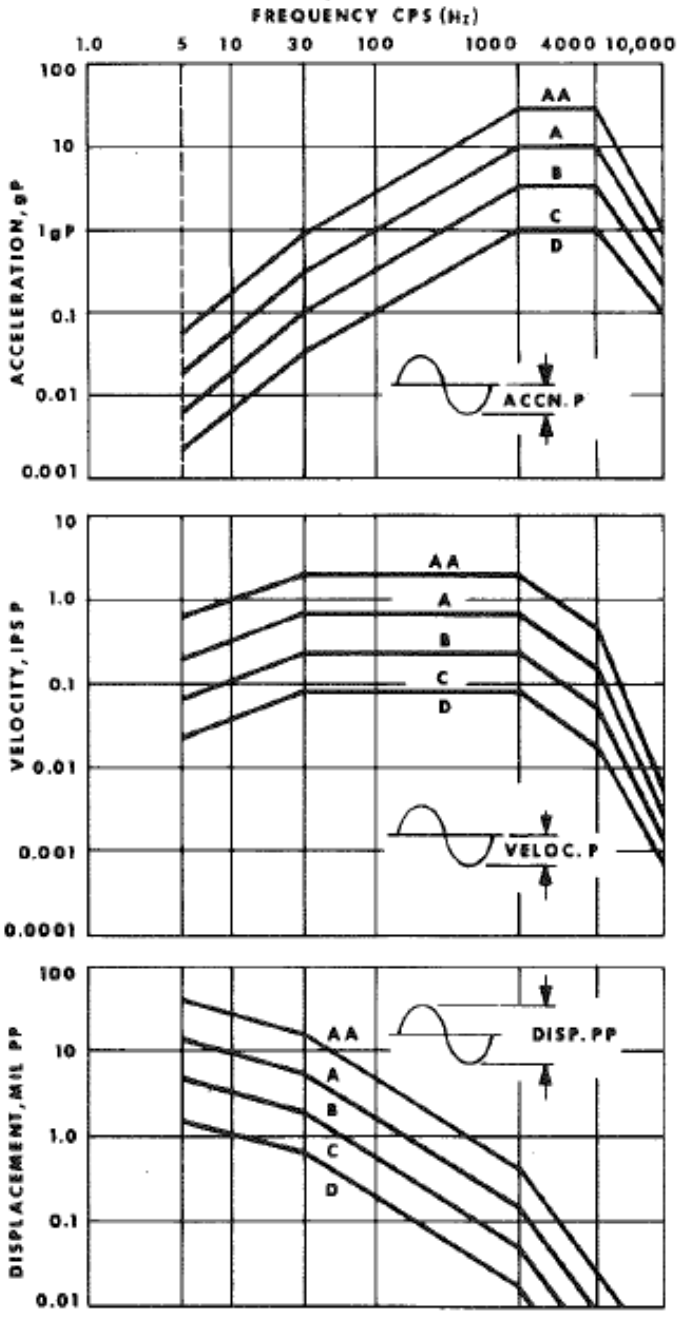

Figure 2-7 – Vibration classification charts (Seippel, 1983)

2.2.2 Harmonic motion

Vibration is classified as that which repeats itself regularly such as an unbalanced fan or the type which is very erratic. When the motion is repetitive within equal periods of time it is then defined as periodic motion of which the simplest is harmonic motion (Rao, 2004). This typically represents motion in a time wave and from this stems many definitions. The time wave is often sinusoidal as shown in Figure 2-8.

From Figure 2-8 it can be seen that a cycle is from a position of rest through to one extremity, back through the position of rest, and then to the other extremity and then finally to the position of rest again. A cycle is expressed in revolutions per minute, RPM, cycles per minute, CPM, or Hertz, Hz. Hertz is equivalent to cycles per second and thus:

$$CPM = RPM = Hz \times 60 \tag{2-3}$$

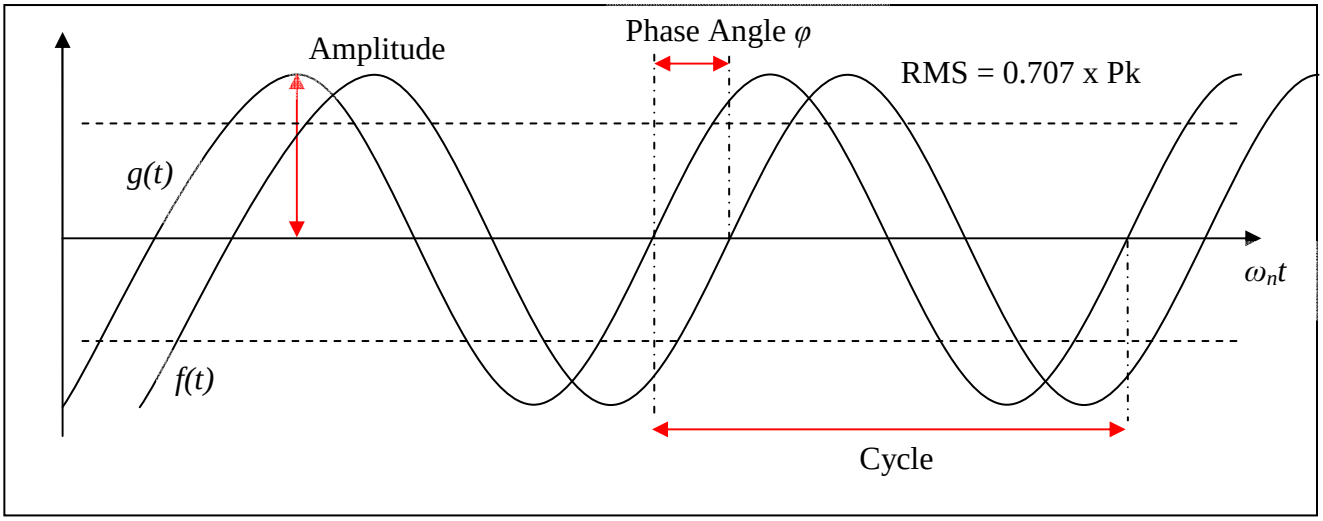

Figure 2-8 – Sinusoidal time wave

The amplitude is the maximum displacement of a body from the position of equilibrium. It is an indication of the severity of the vibration (Mobius Institute, 1999) and is denoted in displacement, mm, velocity, mm/s or acceleration, mm/s^2.

The frequency of the oscillation is the number of oscillations per unit time, f, measured in Hertz. The frequency can also be measured circularly and is called the angular frequency omega, ω, measured in radians per second.

There is another way of describing the cycle, namely the period. This is the amount of time that it takes one cycle to be completed. Period is measured in seconds and is calculated:

$$Period = 1/Frequency \tag{2-4}$$

In Figure 2-8 additionally it can be seen that there are two curves *f(t)* and *g(t).* It can be said that there is a phase difference between the two waves of phi, *Φ*, thus *f(t)* leads *g(t)* by *Φ* degrees, the phase angle.

2.2.3 Fourier transform and the frequency spectrum

Normally the time waveforms which are acquired from a data acquisition instrument are far more complex than the harmonic illustrated in Figure 2-8. An example of such a waveform is shown in Figure 2-9. The complexity of these time waveforms can be due to noise as well as the interaction between different vibrating members within the system. Time waveforms can be very useful to detect certain periodic events, such as the engagement of a broken gear tooth, but more complex systems and phenomena are difficult to determine in the time domain.

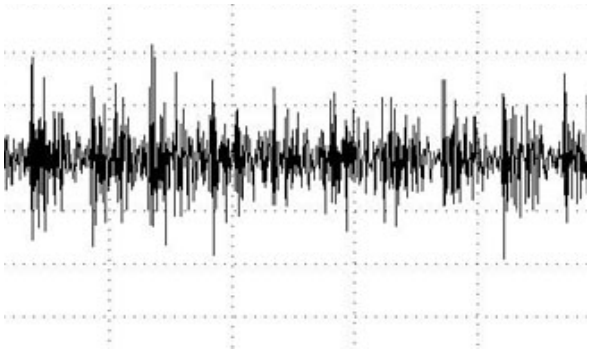

Figure 2-9 – Time waveform output (Mobius Institute, 1999)

Due to the inability to analyse complex signals in the time waveform, alternative signal processing techniques could be used. In the following sections different methods of signal processing will be discussed along with the mathematical derivation of some of these techniques.

Fourier Series

Consider the periodic function *f(t)* in Figure 2-10. It has an amplitude of *A* and a period of τ where the function varies linearly from zero to *A* in time τ and then returns abruptly to zero, and repeats itself again.

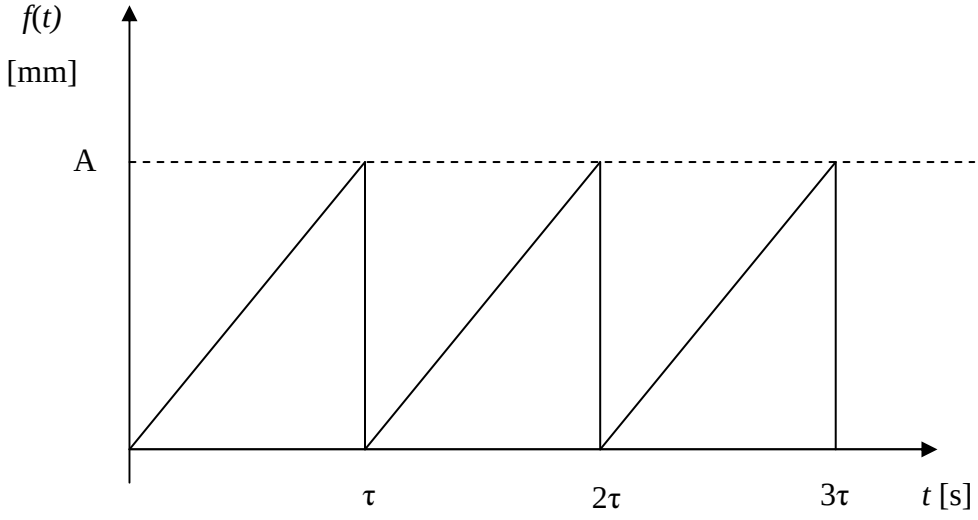

Figure 2-10 – Periodic function *f(t)*

As per Goldman (1948) the fundamental principle that the Fourier series is based upon is that any function *f(t)* defined in an interval from $-\pi$ to π can be expanded in a series of trigonometric functions.

It can be proven that if *f(t)* has a finite number of discontinuities, and a finite number of maxima and minima in the prescribed interval, and that equation (2-5) is finite, then a Fourier expansion is always possible, i.e. it is not required for the function to be expressed as a single equation in the interval for the expansion to be possible (Goldman, 1948).

$$\int_{-\pi}^{\pi} |f(t)| dt \tag{2-5}$$

The Fourier series can also be expressed as

$$f(t) = \frac{a_0}{2} + \sum_{n=1}^{\infty} (a_n \cos(nwt) + b_n \sin(nwt)) \tag{2-6}$$

where ω is the fundamental angular frequency in radians per second and can be expressed as $\omega = 2\pi/\tau$ where τ is the period over which *f(t)* exists. The series of sines and cosines on the right are known as the Fourier series and the a_n and b_n are constants. Thus the basic function of a Fourier series is that periodic signals can be expressed as a summation of sinusoidal components (Randall, 2011).

Additionally, by means of mathematical derivation not intended for the scope of this study, the coefficients can be found by

$$a_n = \frac{2}{\tau} \int_0^{\tau} f(t) \cos(n\omega t) dt \tag{2-7}$$

$$b_n = \frac{2}{\tau}\int_0^{\tau} f(t)\sin(n\omega t)dt \tag{2-8}$$

Thus Equation (2-6) shows that any periodic function can be represented as a sum of harmonic functions. Additionally, even a non-periodic function can be treated as a periodic function having an infinite period (Rao, 2004).

The harmonic functions shown in Equation (2-6) are called the harmonics of order *n* of the period function *f(t)* displayed in Figure 2-10. These harmonics can be plotted as vertical lines on a diagram of amplitude versus frequency (frequency spectrum) (Rao, 2004).

This spectrum, by means of the Fourier transform, displays a time wave form on a graph according to frequencies and amplitudes. To illustrate this point the time waveform, Figure 2-11, which is very difficult to interpret, can be re-displayed as a neat frequency spectrum as shown in Figure 2-12.

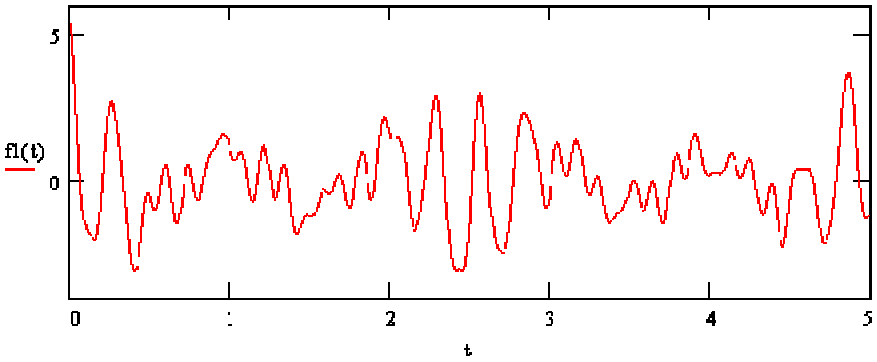

Figure 2-11 – Complex time waveform

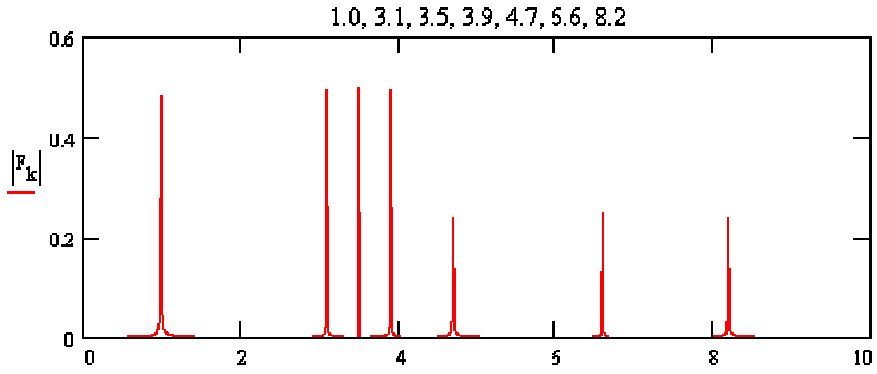

Figure 2-12 – Spectrum derived from time waveform in Figure 2-11

From this illustration it can be seen that a complex waveform can be simplified by applying the FFT and viewing the waveform in the frequency domain. However, not all vibration signals are as clear as the afore-mentioned, but the tool is advantageous to use for periodic signals.

Vibration may be classified as either deterministic or random. Deterministic signals are predictable by mathematical relationships, while random signals are expressed in terms of probabilities and statistics (Norton & Karczub, 2003). Deterministic, continuous signals may be transient in nature and thus it is beneficial to analyse the amount of energy in a transient signal. The power is the energy associated with the wave per unit time and thus the Power Spectral Densities are yielded for continuous signals (Norton & Karczub, 2003).

The Fourier transform holds true for functions that decay to zero. However, stationary random signals do not decay to zero and thus by analysing the correlation function of the Fourier transform this problem is overcome. To explain this in detail is not within the project scope, but it can be said that the auto-spectral density of a random signal can be expressed as a function of frequency. Additionally, the area under an auto-spectrum is the mean square value of the signal (Norton & Karczub, 2003). One of these forms is widely referred to as the Power Spectral Density (PSD). Otherwise explained, the power

spectrum is the power distribution with frequency of a stochastic process of the FFT. PSD's are often used in frequency analysis of discrete data. It can clearly establish the frequency composition of the data over a large frequency range and can be a powerful tool to use. The PSD is defined by applying a FFT to the data and then displaying the result as (Valentim, 1998):

$$PSD_{xx}(\omega) = \frac{a^2 + b^2}{\Delta f} \tag{2-9}$$

$$\Delta f = \frac{1}{T} = \frac{f_s}{N} \tag{2-10}$$

where Δf is the frequency line resolution [Hz],
T is the total acquisition time [s],
N is the total number of samples [ ].

There is, however, one negative and this is the relationship between bias and variance of the signal. The bias occurs due to truncation of the N^{th} point producing a smeared estimate resulting in spectral leakage. When the N^{th} point is increased, however, the error as a result of the negative effect of noise shown in the standard deviation does not get influenced by the number of samples and thus inconsistent results can be produced (Attivissimo, et al., 1995).

2.3 Condition Monitoring Fundamentals

Vibration amplitude is used as a measure of condition monitoring. It is effective to use as every machine, even ones in good condition, have inherent vibration. Many of the vibrations that machines experience are due to the periodic events that occur within the

machine such as rotation of shafts and meshing of gear teeth. Vibration can also occur due to actions such as pumping of fluids (Randall, 2011). Although there are many different methods for detecting a machine's health the two most used methods are vibration analysis and lubrication analysis. This is so because both of these methods allow the interior of a machine to be "observed" in order to diagnose. They are also both non-destructive.

The advantage of vibration monitoring over other detection methods is that it reacts immediately to change. This makes it both useful for intermittent monitoring as well as continuous monitoring. Vibration analysis is also likely to point to the exact fault. With wear particle analysis for example, if a bearing is wearing, the metal debris will be found in the oil after some time but this will not always exactly indicate which bearing is wearing if multiple components are made of the same material (Randall, 2011). Additionally vibration measurement can be very convenient. Sensors can be mounted permanently to machines where costs and space allow and processing instructions can be applied to the data to simplify analysis and only flag concerns out of the ordinary.

In machine condition monitoring most attention is given to monitoring bearing conditions for two reasons. Firstly, it is one of the most common components within machines and secondly, it has a limited lifespan and is often subjected to poor handling and installation practices (Norton & Karczub, 2003). Additionally, bearing failure has very severe consequences within rotating machinery and could result in a breakdown if not a catastrophic failure of a component of machine.

A variety of methods of vibration condition monitoring exists. The scope of this project does not allow for detailed explanation of this, but it can be said that it is not just the data sampling that is important, but how the data is viewed, filtered and analysed. Some instruments simply give an overall vibration level which has been conveniently broken down into a good and bad categorization by the International Organisation for Standardisation (ISO). Other methods include trending over a period of time to detect a

change from normal, and yet other methods will require analysis and data inputs to detect exactly what type of fault is present and which signature vibration frequency is found. With the correct instrumentation and knowledge this type of analysis can direct you to the exact component which is failing. Conversely, it is very important to understand the criteria that affect the results of the readings taken with appropriate equipment because when they are interpreted incorrectly or misused results can be very daunting and misleading and mostly unclear. This will not aid any monitoring of equipment.

2.3.1 Data sampling

Before any measurement can take place it is first necessary to determine how the sensor will be mounted onto the machine or object which requires measurement.

Mounting

Factors which will be considered in the type of mounting are safety, accessibility, application and if permanent mounting requirements exist or not. There are four possible ways of attaching an accelerometer namely adhesive mounting, magnet mounting, stud mounting or using a hand held device such as a probe. Each type of mounting has its own inherent effect on resonance which could magnify the vibration that is actually occurring (Mobius Institute, 1999). Refer to Figure 2-13 which shows the effect that the type of mounting has on the sensitivity of the reading at different frequency levels.

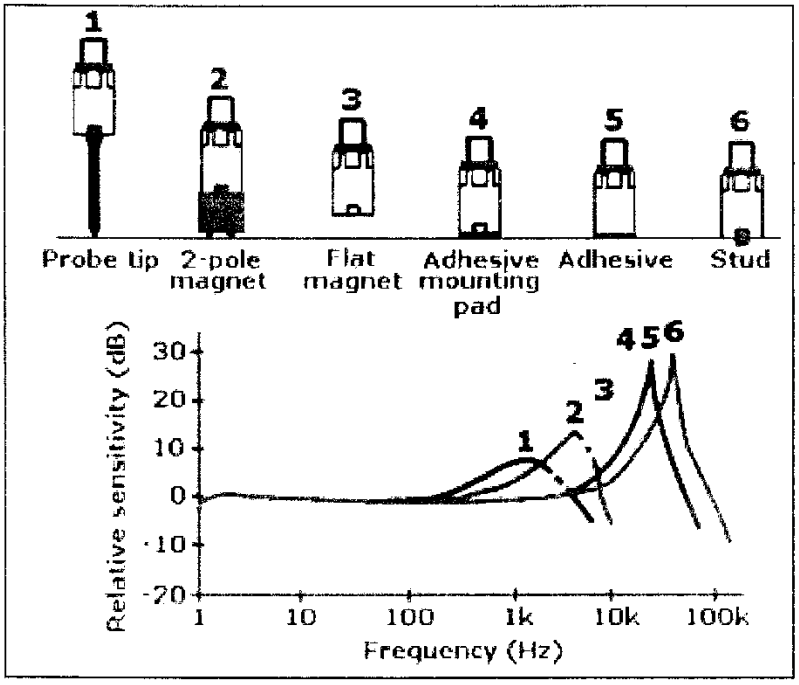

Figure 2-13 – Frequency response of different mounting styles (Mobius Institute, 1999)

The most stable method of mounting that least affects the measurements of the accelerometer is stud mounting. It is the one type of mounting which has the highest probability of operating effectively within the rated range of the accelerometer. When mounting via the stud method the sensor should be mounted onto a block or screw which is attached to the machine on a paint free smooth surface which is spot faced to a size larger than that of the sensor footprint area. It is important to take care when mounting accelerometers as incorrect mounting will result in incorrect readings. Additionally factors such as mounting by means of glue could act as a damper and could further decrease the amplitude of vibration measured. In a testing environment it is not always practical to stud mount and permanently fix the accelerometer and thus Figure 2-13 should be considered to ensure that results are not affected too much by the mounting method.

Repeatability

It is very important when taking vibration readings that repeatability in the readings are obtained or else the differences noted between the different vibration measurements are not noteworthy. In a research application this is of particular importance as an attempt is made to determine the upper and lower limits of acceptable vibrations. Thus, to ensure that maximum repeatability is achieved, the following points must be considered:

- The speed of the rotating machine must be constant
- The position of the sensor must be consistent between measurements and, where it changes, it must be clearly noted so that the difference in location can be understood in relation to the difference in reading
- The sensor must be mounted correctly and not be loose
- The same sensor should be used every time
- The sampling rates should be the same and if not, the difference should be so noted.

Sampling Rate

The definition of the sampling rate is the number of samples which are captured in a second i.e. if 1000 samples are taken in a one second period then the sampling rate is 1000 samples per second or 1000 hertz. It is important to note that the sensor records these samples at a set rate and the data is then re-constructed back into a waveform and the time domain is created. When the sampling rate is too slow in comparison to the frequency of the wave much important information is lost. To avoid this loss of data the sampling should thus take place at a rate which is greater than the frequency of the waveform. The Nyquist theory defines that the sampling rate should be greater than twice the expected frequency of the application and then minimal important information should be lost. The maximum frequency expected, is referred to as F_{max} and typically in a data acquisition application the sample rate and the total number of samples can be controlled.

Aliasing is the phenomenon that occurs when high frequency signals are sampled too slowly and they are represented as lower frequencies after the data has been captured. The risk with aliasing is that there is no way of knowing after the data has been converted from the analogue signal to the digital signal that this has occurred and thus great care must be taken when sampling of data is done. To prevent this phenomenon from occurring, a low pass filter can be applied when the signal is still in the analogue form. The general rule is that no frequencies will be contained that are greater than half the sampling frequency (Bruel & Kjaer, 1980). This is based on the Nyquist cut-off frequency as previously mentioned (Norton & Karczub, 2003).

The amount of data collected post anti-aliasing is known as the signal bandwidth. If the Nyquist principal is applied, then the bandwidth will always be at least twice as small as the sampling frequency. It is also known that a filter with a bandwidth of B Hz, takes approximately the inverse of the bandwidth in time to respond to an applied signal. Thus the analysed signal must hold true to the relationship that the bandwidth multiplied by the duration of the signal processed, T, must be greater than unity.

$$BT \geq 1 \tag{2-11}$$

If a signal therefore lasts T seconds the most ideal bandwidth is $1/T$ Hz. Additionally the user should wait $1/B$ before measurement commences (Norton & Karczub, 2003).

The resolution of the system is defined by the individual record length T and the difference between it and the next reading, i.e. $1/T$ (Norton & Karczub, 2003) where N is the number of samples.

$$B_e = \frac{1}{T} = \frac{1}{\Delta N} \tag{2-12}$$

It is important to understand the above concepts as when deciding on the hardware required for acquisition in the application this should be understood.

2.3.2 Data acquisition hardware

Various types of data acquisition means exist and most of these are transducers, which are devices that convert one type of energy into another, e.g. vibration into electric voltage or current. Two common varieties will be discussed.

Velocity Pickup

It is a transducer used for monitoring vibration of rotating machinery. They are manufactured differently for vertical or horizontal operation due to the way in which they operate and the effect that gravity has on them. They are sensitive to directional mounting as well as the size of the mounting surface and are easily dampened by glue mounting. The specified sensitivity range is applicable within the given frequency range. Velocity pickups have internal moving components that are subject to fatigue. This requires them to be calibrated and verified on an annual basis. Disadvantages are that they are relatively large compared to alternative transducers, sensitive to input frequency, have a narrow frequency response and have moving parts. Additionally, they are sensitive to magnetic fields and temperature (Scheffer, 2010). They are considered to be less accurate due to their relatively low signal to noise ratio. These sensors are only used occasionally (Mobius Institute, 1999) and are not readily available.

Accelerometer

A more popular sensor for rotating machinery is the light, rugged accelerometer that has a wide frequency response. They are most commonly used in condition monitoring applications. They operate by converting mechanical energy into a voltage signal, i.e. they are inertial instruments. Internal Electronic Piezoelectric (IEPE) utilize a piezoelectric crystal which is placed under a load. This then vibrates and the crystal is

compressed and a charge is produced. An amplifier is then used to convert the charge within the crystal to an output voltage and by Newton's second law an acceleration is determined from the force required to create the charge (Mobius Institute, 1999). These IEPE accelerometers are very commonly used and have a good operating range. Variable capacitance accelerometers are used when low frequency responses' are required. These particular types of accelerometers provide a high level of sensitivity at low level frequencies and are very desirable for measuring low frequency vibration, motion and steady state acceleration. They are DC responding which means they have a wide bandwidth and the frequency response operates down to zero hertz (Endevco Corporation, 2012).

Accelerometers are used in high-frequency vibration measurements as they are one of the only transducer types which have adequate response at these frequencies (Seippel, 1983). An accelerometer cannot be calibrated and it has no moving parts, thus no periodic adjustment is required. Care should be taken as high temperature and shock can damage the internal components. Settling time is required due to the amplifier in the sensor. It takes a few seconds to stabilize and if this is not taken into account before the readings are taken then the data collected will be affected by a voltage ramp due to this stabilizing.

Accelerometers are available in different sensitivities. These are specified in mV/g and the sensitivity required, depends entirely on the application of the accelerometer. For example in a very noisy large machine application a sensitivity of approximately 10mV/g to 100mV/g is most probably appropriate. In a low speed, low vibration application a high sensitivity accelerometer, 1V/g, would be suitable (Mobius Institute, 1999). Thus, due to the sensitivity, an accelerometer is normally selected once the desired frequency range is known and the optimal range can be used.

Amplifiers with Analogue to Digital Converter

Data acquisition hardware must be chosen carefully with knowledge before the purchase that it is able to fulfill the requirements that the testing will involve. In order to make this

decision it is important to understand on what basis the Analogue to digital converters are specified. The sampling rate that is expected should be understood before the time of acquisition to determine if the data acquisition instrument can provide the correct master sampling rate and then reduce this to the bandwidth required. The equipment's ability to deal with aliasing and have anti-aliasing routines built into the logic should also be understood. Additional considerations would be the bits that the hardware has. Modern good quality instruments are able to sample at a resolution of 24 bits. It is also important to understand what sensor types the equipment is compatible with and further understand what output the amplifier provides and how the data will be further analysed once the data is retrieved in an electronic output.

2.3.3 Signal processing techniques

Windowing

When a sample of data is collected it is not possible to know when the vibration is at the beginning of its cycle or in the middle of it. Thus the time period chosen over which to take vibration samples does not necessarily correspond with a complete cycle and thus the beginning and the end of the data will not match up completely as can be expected. This could cause broadening of the peaks by the addition of sideband frequencies that do not actually exist in the signal (Mobius Institute, 1999) and thus this scenario is not ideal. To ensure that the data is not modified the application of windows is used in the data analysis phase. These tools modulate the signal to have an amplitude of approximately zero at the beginning and the end of the data taken and thus various cycles match up on zero amplitude trailing and leading edges. Windows typically do not change the frequency information but do change the spectral peaks and amplitude levels of the data collected (Mobius Institute, 1999). By applying a window to the data the effects of only having a finite sample length is minimized. The windows are affected by applying a weighting function forcing the data to zero at the ends. This weighting can be applied in

different manners yielding different results (Norton & Karczub, 2003). Window Hanning is one of the most common windows found and used in vibration software.

Time Synchronous Averaging

The background noise in an application is often so great that it is difficult to analyse the periodic signal in question. At such times, time synchronous averaging is a good technique to use to reduce the noise in the system and in so doing separate noise from the actual signal (Randall, 2011). This is done by averaging a series of signals corresponding to one period or revolution of a signal which is described as:

$$y_a(t) = \frac{1}{N}\sum_{n=0}^{N-1} y(t + nT) \tag{2-13}$$

where N is the number of samples and T is the periodic time, at time t.

The signal is phase averaged over the time period signaled by a trigger, such as a tachometer. The synchronous signals will average to their mean value and the noise within the signal should average to zero (Norton & Karczub, 2003). Thus only the signal remains.

Filtering

After the anti-aliasing filters are applied as part of most good hardware acquisition instruments' standard routine, the user is able to further apply digital filters after the acquisition takes place. Some instruments allow this filtering to be selected from the initial data acquisition. This filtering takes all the signal that is present and either high pass or low pass filters the remaining frequencies out. This means that when using a low pass filter set at 1000Hz that all frequencies above 1000Hz will not be present in the signal when it is analysed. In theory this filtering does not happen as accurately as that because it is a transfer function with a certain response mechanism. Figure 2-14 shows graphically how this transfer function occurs. In this representation a low pass filter with

a cut off frequency of 500Hz is specified on a sampling frequency of 1200Hz. In this particular software a particular number of poles can be specified which makes the slope of the filter transfer function steeper. It can be seen that approximately 40% of 600Hz frequencies and higher are still let through.

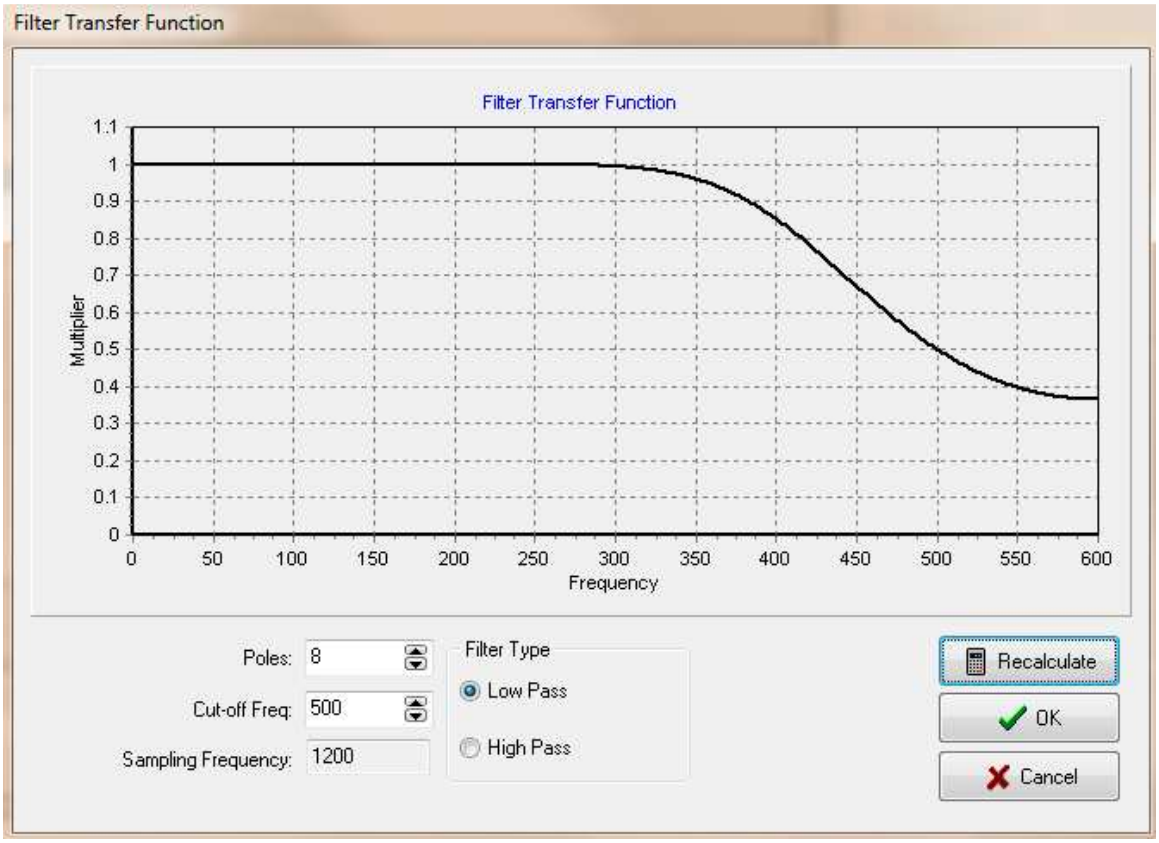

Figure 2-14 – Illustration of filter transfer function (CMS software)

Fault Detection and Alarm Limits

In the context of this research it would be important to distinguish good bearings from nicked bearings. In such cases an alarm limit would trigger an exception message which would tell the end user that there is some further investigation required on a particular bearing as it is faulty. To accurately set limits a baseline of an acceptable bearing vibration is required. To accurately set a baseline of what defines a normal running

condition, many repeatable tests are required to establish this level. Limits could then be set at given amplitude across a wide range of frequency bands to define a good baseline.

Additionally the band or frequency range can be set up in such a way that the total power in the band is measured. Thus if the power level is outside the set point the alarm is triggered (Mobius Institute, 1999). To further increase the accuracy of the limits multiple triggers can be defined. This can range from the width of a peak, the maximum limit allowable, minimum limit allowable and offset from the normal. In theory, if the frequencies that are limited are directly proportional to running speed, then they could be adapted for increased running speed as well.

2.3.4 Machine component vibration signatures

As mentioned above vibration analysis aids to identify the problem to very close proximity of the actual root cause. This is possible, because different vibrating components have their own unique vibration signature as defined by the theory e.g. characteristic frequencies of bearing defects or gear mesh frequency. With analysis of the system vibrations the exact components can be detected if faulty. For the purpose of this report only the particular frequencies that might be found in the study will be discussed in later sections, but a brief explanation of the concepts will be explained.

2.3.5 Current situation at Timken

The assembly of AP bearings at Timken is as follows: The assembled cones are placed into a cup with a spacer separating the two cones. Since this is a manual process, and could potentially be challenging when the bearings are large sizes (e.g. class GG which has a seven inch bore with an approximate total mass of 70kg), it is reasonable to consider that cup nicks and other damage may occur during this assembly stage.

At this stage of assembly the bearings go to the Lateral Machine which measures the bench end-play of the bearings. This is done by securing the cup to a fixture and then applying a vertical force in the upwards direction and then in the downwards direction, while simultaneously spinning the bearing. The action ensures that the rollers are seated against the large rib of the cone, which is the correct running position.

The seating occurs at approximately 300lbs force (1.3kN) to 400lbs force (1.8kN) and then the two cones are pushed together at a force of 850lbs force (3.8kN). When considering the included angle of the cup it means that a maximum radial force of 0.655kN can be experienced in the Lateral Machine. The function of the Lateral Machine is to measure the lateral clearance, bench end-play, within the assembly. The manner in which this is adjusted is by the addition of different spacer sizes to either decrease or increase the lateral clearance within the bearing assembly. To ensure that the correct bench end-play is achieved the operator gets an opportunity to replace the inserted spacer with different width spacers. In this process the upper cone and cup is locked in the machine's upper mandrel and the lower cone and spacer are released for spacer change. The Lateral Machine and its tooling are shown in Figure 2-15.

In normal bearing application the mounting arrangement of the bearing and the forces of the system in which it operates will force the bearing to have what is termed a "loaded zone". This is the arc (normally about 120 degrees) in which the bearings see the full load of the application. When they enter this loaded area they undergo maximum contact with the raceway and when they leave this area they are free to "rattle" within the cage boundaries and do not carry any load. This is relevant as the theoretical bearing frequencies which can be calculated in all the various methods as discussed in Section 3.2.1 are dependent in part on the bearing operating in the loaded zone.

Figure 2-15 – Lateral Machine and tooling

In the Lateral Machine the bearing is not placed under radial load but the rollers are only loaded enough to be seated on the raceways correctly to determine the actual bench end-play. Additionally, it should be noted that the bench end-play during measurement on the Lateral Machine has a larger value than end-play measured when the bearing is mounted in its intended application. This reduction is due to the interference fit of the bearing components and the shaft or housing in which it is mounted. The implication is that in the Lateral Machine the bearing has no load zone, as the rollers are equally loaded around the circumference of the bearing, and the bearing internal clearance is much more than in the mounted application in which it will operate. It is likely that this will result in different measured characteristic defect frequencies as those calculated using the theory.

2.3.6 Inherent vibrations in the Lateral Machine

The Lateral Machine is rotated with a cyclonic speed reduction motor. The information and data parameters associated with it are discussed in Appendix A and are presented in Table 4-5. When the signals are analysed these frequencies will be noted to see if they are present or not. It is also possible that the defect frequencies of the bearings can excite the frequencies of the machine.

2.4 Bearing Vibrations

Noise in bearings could result from surface damage, surface-and geometric inaccuracies, bearing element elasticity, internal clearance, wear, lubricant viscosity and housing design and stiffness. Thus radially loaded bearings that are considered to be geometrically ‘perfect’, will generate vibrations.

Tandon and Choudhury (1997) explain that vibrations are due to the nature of the rolling elements in the load zone changing position constantly during a rotation cycle, and that

only a finite number of rolling elements are in contact with the races. This gives rise to periodic variation in the total bearing stiffness. This variation generates vibrations known as varying compliance vibrations (Tandon & Choudhury, 1999). Additionally, when the races are assumed as continuous systems, then the changing direction of the contact forces which are applied by the rolling elements can cause ring-mode or flexural vibration of the races.

A used bearing which does not display any signs of damage on the races or rolling elements, however, will produce greater amplitude in vibrations than a new bearing. This is due to overall wear, increasing the internal clearance and thus resulting in overall displacement of elastic elements. This leads to higher impact velocities within the system causing greater amplitudes (Chambers & Bunting, 1981).

During the early stages of bearing failure the metal to metal contact within the bearing produces stress waves. These short duration events are characterized by sharp peaks in the vibration signal (Pineyro, et al., 2000).

Chambers and Bunting (1981) have clearly defined different types of vibrations which are summarised as follows:

Sources of acoustic energy in roller bearings are considered with a ‘pristine’ bearing packed with the correct amount of grease and rotating at design speed and load. This type of bearing is far from quiet and produces a wide range of noise throughout a wide frequency bandwidth. This is due to the following (Chambers & Bunting, 1981):

- As the rollers enter and leave the load zone throughout rotation, sliding friction and jerking motion exists. Also sideways motion of the roller exists, resulting in contact between the rollers and cage. Due to the elastic nature of the components as they are loaded and the bearing geometry changes, the force on the components vary in magnitude due to their varying sizes and this causes the components to

vibrate at a frequency equal to a rolling element passing a fixed point on the outer race.

- Although much is done to prevent contamination within a bearing, it is possible for dirt to enter the assembly. When the dirt contacts the rolling elements it creates an impact and stress waves occur. This impact can reach ultrasonic frequency ranges. Contamination can also be present within a bearing due to its own wearing components which have sheared off.
- Worn bearings also have a greater noise emission than new bearings due to their wear patterns allowing greater displacement within the system and thus higher impact velocities.

2.4.1 Theoretical bearing frequencies

Rolling contact bearings such as the tapered roller bearing around which this research project is centered have line contact and bear both radial and axial load due to the taper (Norton & Karczub, 2003). Thus each type and size of bearing produces its own frequency when rotated. There are four main sources of vibrations present in rotating bearings (Chambers & Bunting, 1981). These are:

A. Rotating element passage frequencies

These are discrete frequencies dependent on the number of impacts per unit time, and on bearing geometry and relative angular speed of the inner to the outer race. There are eleven types of frequencies. Some exist due to relative running speeds of the components and not due to defective parts. Some of these frequencies are defined below.

Tandon, and Chodhury (1997) takes the effective taper into consideration and defines the standard bearing vibrations as follows:

Cage Frequency:

$$f_c = \frac{f_a}{2}\left(1 - \frac{d}{D}\cos\alpha\right) \tag{2-14}$$

Ball Spinning Frequency:

$$f_b = \frac{Df_a}{2d}\left(1 - \frac{d^2}{D}\cos^2\alpha\right) \tag{2-15}$$

Outer Race Defect Frequency:

$$f_o = nf_c \tag{2-16}$$

Inner Race Defect Frequency:

$$f_i = n(f_0 - f_c) \tag{2-17}$$

Rolling Element Defect Frequency:

$$f_r = 2f_b \tag{2-18}$$

where

n = number of rollers in the bearing (single row) [-],
f_a = angular frequency of bearing rotation [s^{-1}],
d = roller element diameter [m],
D = pitch diameter of bearing [m],

α = cup included angle [rad].

Subscripts:

o = outer race

i = inner race

c = cage

b = roller or ball

B. Bearing Element Resonant frequencies (Chambers & Bunting, 1981)

This refers to the frequencies of the bearing components at which they are naturally resonant. The formulae for radial and flexural modes of vibration are given below:

In plane flexural modes:

$$f_{r_i} = \frac{N(N^2-1)}{\sqrt{N^2+1}} \frac{1}{2\pi a^2} \sqrt{\frac{EI}{m}} \tag{2-19}$$

Transverse flexural modes:

$$f_{r_t} = \frac{N(N^2-1)}{\sqrt{N^2+1+\sigma}} \frac{1}{2\pi a^2} \sqrt{\frac{EI}{m}} \tag{2-20}$$

Radial Mode

$$f_{r_r} = \frac{1}{2\pi a} \sqrt{\frac{E}{\rho}} \tag{2-21}$$

where

E = Young's Modulus [Pa],

ρ = Density [kg/m^3],

σ = Poisson's Ratio [ ],

N = number associated with mode order e.g. 2, 3 … [-],

a = radius of neutral axis [m],

$I = \frac{bh^3}{12}$, moment of inertia of assumed bearing shape [m^4],

b = lateral dimension of the bearing, width [m],

h = ½ (OD – ID), height [m],

$m = \rho A$ [kg/m],

$A = bh$ [m^2].

These frequencies could possibly be detected through impact tests when the bearing is stationary to understand its signature and if the frequencies would be present in frequency range to be analysed (Norton & Karczub, 2003).

C. Shock Pulse frequencies

This occurs when one element irregularity impacts another element. This results in short duration stress-waves, resulting in frequencies extending well into the ultrasonic range. Some condition monitoring equipment make use of these high frequencies and the energy associated with the shock pulse to detect bearing defects.

D. Acoustic Emission

As with shock pulse frequencies, similar short duration stress-waves are produced when bearing material undergoes non-elastic change, e.g. during fatigue crack growth. The frequencies that result are very high (in the kilo hertz to mega hertz range) and can often assist in identifying early and advanced damage (Norton & Karczub, 2003).

Chambers and Bunting (1981) discuss the transmissibility of acoustics through the various interfaces within a bearing assembly. The transmissibility is said to depend on the contact pressure between the two surfaces and the frequency of the acoustic signal. The attenuation of the defect will increase with the frequency. Chambers and Bunting (1981) point out, however, that the loaded region of a bearing has large contact pressure between the elements with a thin film of lubricant in between them acting as an acoustic couplant. This serves to improve the transmissibility of the vibration energy and thus frequency signal. It is important to understand that the transmissibility of an interface greatly depends on the contact pressure between the surfaces and thus dependent on the loading of a bearing when the frequency signal is measured.

It is also important to note that the amount of grease that a bearing already has in it will influence the vibration results achieved (Chambers & Bunting, 1981). Although at the stage of the Lateral Machine the bearings have no grease in and are only lightly lubricated with low viscosity honing oil meaning that the vibrations should not be damped too much as a result of the oil. Care needs to be taken to understand if 'equations' for typical bearing frequencies are given, based on output frequencies achieved with an average complement of grease installed.

Distributed and Local Defects

The presence of any defect on either the races or rolling elements cause a significant increase in vibration within the rotating system. When balls or rollers or races are damaged and roughness exists on the running surfaces then high frequency transient vibrations will be produced as a bearing rotates (Chambers & Bunting, 1981).

Defects are categorized as distributed or local (Tandon & Choudhury, 1999). Distributed defects could be surface roughness, waviness, misaligned races and off-sizing of rolling elements. Roughness and waviness, surface defects, are considered with regard to the

Hertzian contact width of the rolling element as compared to the output wavelength of the defect. Where the wavelength is of the order of the contact width or less, it is termed as roughness and if it is longer than the contact width, it is termed waviness (Tandon & Choudhury, 1999). All of the distributed defects are due to manufacture error, poor installation or abrasive wear. The presence of the distributed defects increases the vibration levels. This is due to the variation in contact force between the rolling elements and the races (Tandon & Choudhury, 1999).

Localized defects include spalls, pits or cracks on the rolling surfaces. These are not typically associated with poor installation. Although vibration analysis has been used extensively to classify bearing failure, the non-stationary characteristics defined above are more predictable. However, non-linear factors that also disguise these vibration signals are the changes in loads, clearance and friction within the bearing (Wang, et al., 2008).

Additionally it has been identified that the biggest difficulty with detecting damage in bearings is due to the signature frequencies spread across a large frequency band and they can also easily be buried in noise. Additionally within a system there are normally other components giving off their own distinct vibrations (Pineyro, et al., 2000). The problems associated with detecting their vibrations are as a result of the machines in which they are mounted and the complexity of such. The background noise normally makes it difficult to detect using time domain studies commonly used in vibration analysis, such as overall RMS detection, crest factor and kurtosis. Typically, methods such as spectral analysis and power spectrum are used for the detection of defects on bearings which will be further explained (Norton & Karczub, 2003).

High Frequency Sensing

When a defect on a member of a bearing makes contact with one of the other members under load an impulsive vibration is created. The duration of this impulse is very short in comparison to the time taken between impulses. Consequently the energy is filtered into

very low amplitudes over a wide range of frequencies due to the short duration of the impulse. This wide distribution of energy then makes it difficult to detect the bearing damage with a conventional frequency spectrum. A resonance is normally excited within the system. This resonance occurs at higher frequency than other machine elements and has larger amplitude. Some of this energy associated with the resonance is concentrated in a narrow band making it easier to detect. This impulse is referred to as the Characteristic Defect Frequency and occurs at approximately equal intervals due to the periodic nature of a bearing (McFadden & Smith, 1984). Piezoelectric sensors, such as accelerometers, are typically used for sensing such high vibrations as they have a good response at such frequencies. The characteristic defect frequency can be isolated by applying a band pass filter around the resonant frequency or by envelope detection. Both of these methods remove the damping frequencies associated with the resonance and ideally only the characteristic defect frequencies remain. The frequency range of the resonance typically lies between 10kHz and 50kHz. Typically, these resonant frequencies cannot be calculated very accurately and this is due to the many factors arising from the actual fit of the bearing in the shaft and housing. The sensor should also ideally be fixed very securely as especially at high frequencies the inaccuracy can vary greatly if it is not properly secured.

The location of the sensor with respect to the defect is also very important. As shown in McFadden and Smith (1984), when the sensor is close to the defect the amplitude is great, however, 180 degrees away from the sensor the amplitude is lower. At 90 degrees to the sensor the impact was at its lowest. The direction which is best for the sensor is also dependent on whether the type of bearing which is being assessed is able to carry axial, radial or a combination of loading directions. For example, a roller bearing (with no taper) must have its sensor mounted with its axis perpendicular to the rollers as it can only transmit a radial load. Best consistent results were achieved when the sensor was in the loaded zone of the bearing. This is because the line of contact for the vibration to travel is the smallest at this point and thus the strongest signal.

Bearing Failure in Condition Monitoring Trending

When a bearing defect is detected the bearing deterioration normally happens in stages shown in Figure 2-16 parts (a) and (b). The first indication that the bearing is failing occurs when high frequency stress waves and noise energy occurs. With time these frequencies increase in amplitude. When the damage to the rotating component becomes evident in the lower frequency ranges then the ball pass frequencies are being recognized. This means that there is physical damage on the actual rotating components. If the bearing is left to run then the amplitude of these frequencies will increase until finally the bearing is so loose that a noise bed is created and a general amount of rattling is seen in the vibration spectrum in the last figure. At this point the bearing cannot be repaired and should probably be replaced (Mobius Institute, 1999).

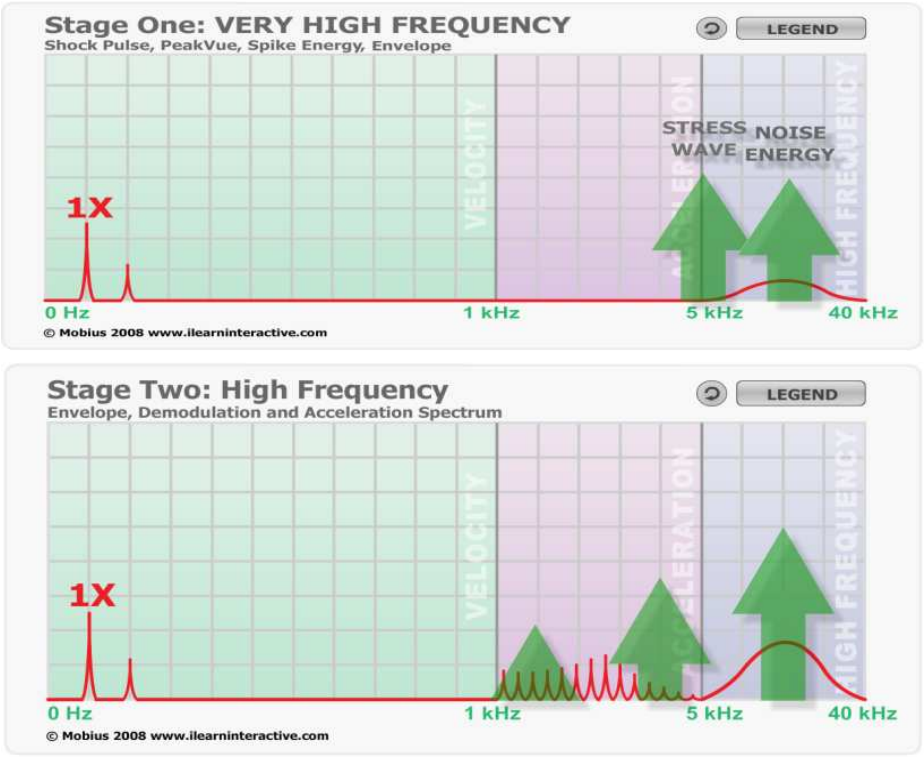

Figure 2-16 (a) – Stage one to four (top to bottom) of bearing failure in vibration analysis (Mobius Institute, 1999)

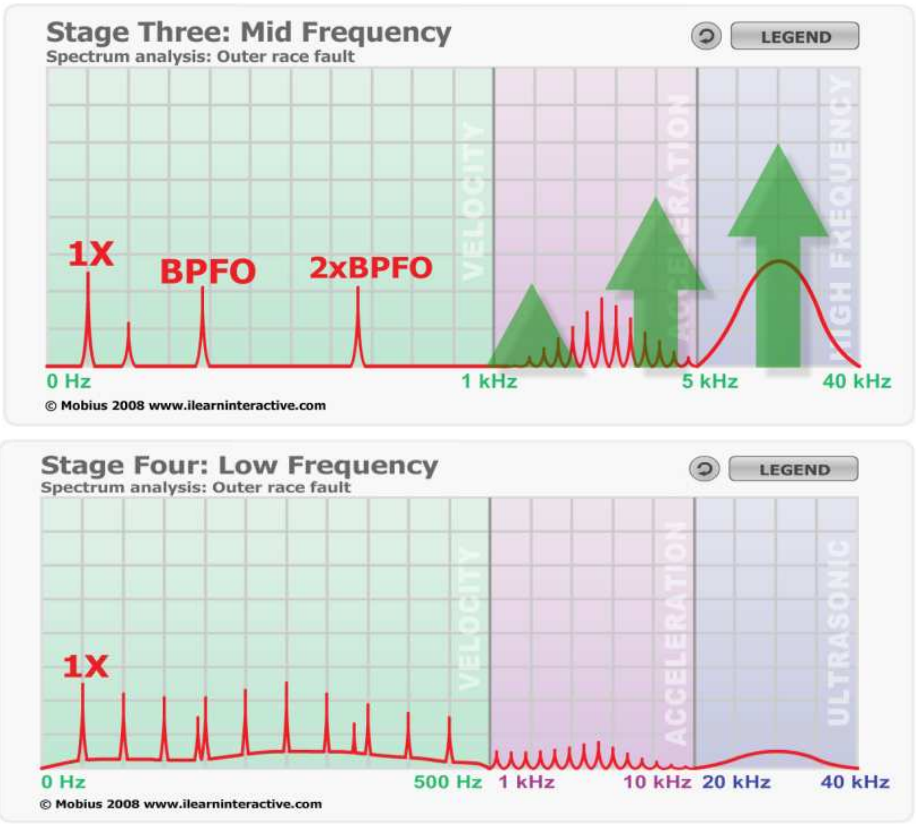

Figure 2-16 (b) – Stage one to four (top to bottom) of bearing failure in vibration analysis (Mobius Institute, 1999)

2.5 Applications of Condition Monitoring in Bearings

In industrial applications bearing faults are predicted using condition monitoring techniques. Often trending is adopted in industry to emphasize the difference between a good bearing and a bearing which is deteriorating over time. This is evident due to the increase in amplitudes of vibration as well as the increased presence of expected defect

frequencies as described in Section 2.4.1. In the case studies, however, the bearings are normally rotating at high speeds and are subjected to application loading. The bearings are also mounted and have normal clearances as per a mounted bearing design.

Mechefske and Mathew (1992) measure a slow rotating single row cylindrical bearing with damage. A vibration signal was measured with a fault present 1mm deep x 2mm wide groove, cut across the full width of a bearing outer race. It was rotating at a slow 60rpm and a load was maintained on the bearing of 23kN. In this instance the vibration signal of the fault gave a clearly periodic short impact vibration caused by the rollers contacting the fault. This vibration is in line with the outer race ball pass frequency as described in Section 2.4. In the study they completed, the fault was detectable by use of a parametric model. This was used so that various different frequency spectra can be analysed due to the slow rotation of the sampled specimen.

Tandon & Choudhury (1997) showed that a deep groove ball bearing with normal mounted clearance and an outer race defect present excited the expected ball pass outer frequency. The frequencies were present at different loadings of 20kg and 60kg, and the amplitudes of vibration at these frequencies were significantly less than when the load was decreased (Figure 2-17).

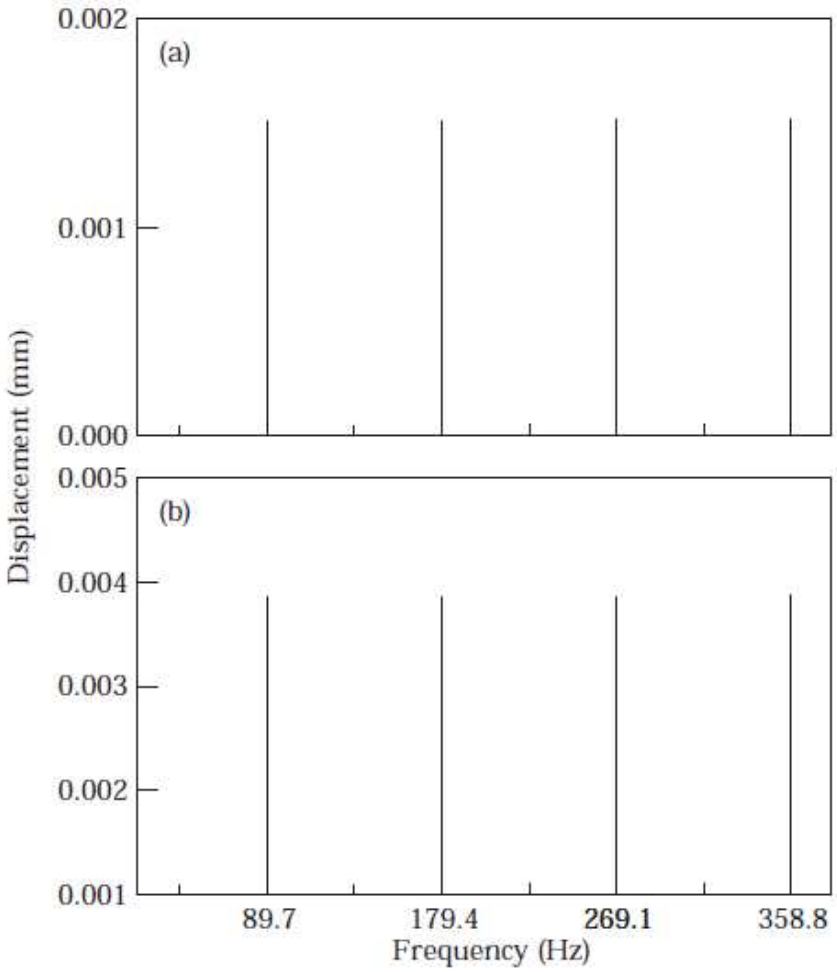

Figure 2-17 – Frequency spectrum for an outer race defect of load (a) 20kg and (b) 60kg (Tandon & Choudhury, 1997)

From the case studies it is apparent that although the bearing defect frequencies can be used quite accurately in certain applications, there are however a few criteria that must be fulfilled. In both case studies bearing loading and speed was shown to have an impact on the results. When the speed was low special models were used to analyse the vibration signal output.

2.6 Previous Research of Cup Nick Detection at Timken

Timken Rail Services in Northampton, UK experienced several customer complaints regarding noisy bearings. Most of the customer complaints were on class F bearings (ID of 6.1880" and OD of 9.9250"). The root cause has been proven to be nicks on the cup race. Subsequently the Timken Rail Services team investigated means by which to detect nicks on this size bearing. The Timken Noise, Vibration and Harshness (NVH) department conducted various tests to establish whether nicks can be detected. Testing equipment chosen was the Lateral Machine as suggested with the proposed study. Its rotational speed was constant at 138RPM. The cup remained fixed and both cones rotated. The measurement duration was approximately 15 seconds. The load was applied first on the lower and then on the upper cone.

An accelerometer 736T was used with a weight of 10 grams, a sensitivity of 10.3mV/m/s^2 and specified for low frequencies (0Hz to 500Hz). The method of mounting was with a magnet directly onto the cup outer diameter onto which the accelerometer was glued.

Tests were performed on two part numbers with and without nicks. Of the specimens with nicks some were artificially made with a hammer and others were from customer returns. The geometrical characteristics of the bearings influencing the defect frequencies were the same for all the part numbers (sizes) studied and included the semi-included cup and cone angle and the number of rollers.

The spectrum of signal processing was measured with the following parameters (Koch, 2009):

- 0-500 Hz
- 800 Lines (d_f = 625mHz)
- Window Hanning
- Overlap of 40%

- 14 second duration
- Sampling frequency f_e = 1280Hz

Signal processing techniques used for the experiment were spectral analysis as it was used on smaller bearings in production in Timken facilities and the software was available for use.

The key in using spectral analysis was to define a threshold which could define the comparison between pieces with and without defects. It was found that in samples with nicks the main vibration peaks existed on the cup defect sound harmonic of 47.5Hz. An additional high level was found at 11.88Hz (half of the fundamental cup defect frequency). On a cup with no nicks peaks were exhibited in the vicinity of 100Hz (Koch, 2009).

Based on the above findings the NVH team in Europe suggested that a threshold, based on cup defect frequencies, would be (Koch, 2009):

- 11-13Hz : 3mm/s^2
- 23-25Hz : 3mm/s^2
- 46-49Hz : 3mm/s^2
- 69-73Hz : 7mm/s^2
- 92-98Hz : none
- Harmonics 5 and 6: 10mm/s^2
- Harmonics 7-10: 20mm/s^2
- Harmonics 11-15: 40mm/s^2

A value over the limit in these defined frequency ranges determined the criteria to reject the bearing. It was still recommended that a visual inspection of each rejected bearing should be done. The values listed above were obtained from a very limited sample size.

The NVH team concluded that tests have shown some rejection and acceptance criteria ranges for two part numbers. Further study would be needed on other parts. The testing that is to be performed as part of the current research would extend this research to an additional class. Further work needs to be done to understand if the cycle time of the Lateral Machine is sufficient to give enough information. They also recommended that alterations to the current Bearing Signature Analysis software would need to be done.

Based on the above tests performed by the NVH department, the TRS UK team decided to implement a similar solution in the production line to understand if the theory holds true and that nicked bearings are detectable. They acquired a Pocket VibrA Ultra acquisition instrument from C-Cubed and used it with the C-Trend Analysis software. The hardware sampled between 0 Hz and 15 kHz and the resolution was up to 0.3Hz. The software was able to predict where the bearing frequencies would occur based on the physical geometry as well as the rotating speed of the Lateral Machine. The Lateral Machine that the UK team used for the testing was an older style Lateral Machine which had a gearbox in it with gear mesh frequencies, which had to be characterized.

The results of the testing were not very conclusive. They ran the system for a period of three months on the production line with varied success. Sometimes the nicked bearings showed lower amplitudes than the non-nicked bearings when analysed in the normal frequency domain by means of an FFT. The results were taken in the first half of the Lateral Machine cycle and then the computation was performed during the second phase of the cycle. They only used one accelerometer with a sensitivity of 25mV/g and magnetically mounted it on the track of the cup.

The team has subsequently discontinued any further testing and is, at this stage, not pursuing a solution. Their recommendations have been to use two accelerometers on both the lower and upper raceway rather than measuring on the track position of the cup. They were also concerned that their gears within the machine caused most of the noise.

In Chapter 2 the fundamentals concerning the AP bearing and the nomenclature of the parts which will be used throughout the report were reviewed. Basic bearing fundamentals have been explained to show how the theory is used to calculate the expected frequencies within a system, knowing the operating speed and geometry of the bearing under consideration. Case studies were reviewed in which bearing fault detection was conducted revealing speed and loading played a role. The work done within the Timken facility in the United Kingdom on detection of cup nicks was explained and it was shown that there were a few testing processes used which can be improved, and that more extensive vibrational analysis must be done to fully determine if the results that they have achieved were repeatable.

3 MATERIALS AND METHODS

In this chapter consideration will be given to the type of testing equipment and data analysis packages that will be used. It will also cover different data acquisition settings including sampling and filtering, and how the Power Spectrum Density method will be used within the data analysis. The bearings that will be used within the investigation will be detailed including the severity and size of the nicks associated with each bearing.

3.1 Testing Equipment

The following equipment will be used in the research:

3.1.1 Testing Facility

The Lateral Machine will be used to conduct the testing in the Benoni, South Africa Timken facility. As discussed in Section 2.3.5 the Lateral Machine cycles through an upward and then downward motion to measure the lateral clearance within the bearing assembly. In order to minimize the variability within the data acquisition testing and to ensure that both raceways are seated as much as possible within this machine motion, the testing will only be completed in the second phase of the Lateral Machine cycle. The duration of the rotation in the second phase will be extended for increased sampling time by means of a machine override connected to a key switch installed for the purpose of testing.

Figure 3-1 shows a bearing in the Lateral Machine in the testing position. The cup locks are holding the cup in position and securing it against the upper part of the machine. The lower shaft is holding the cone in position and the upper cone is rotating the whole

assembly by means of a driven shaft on the top mandrel. The accelerometer is mounted on the upper raceway and not in the track.

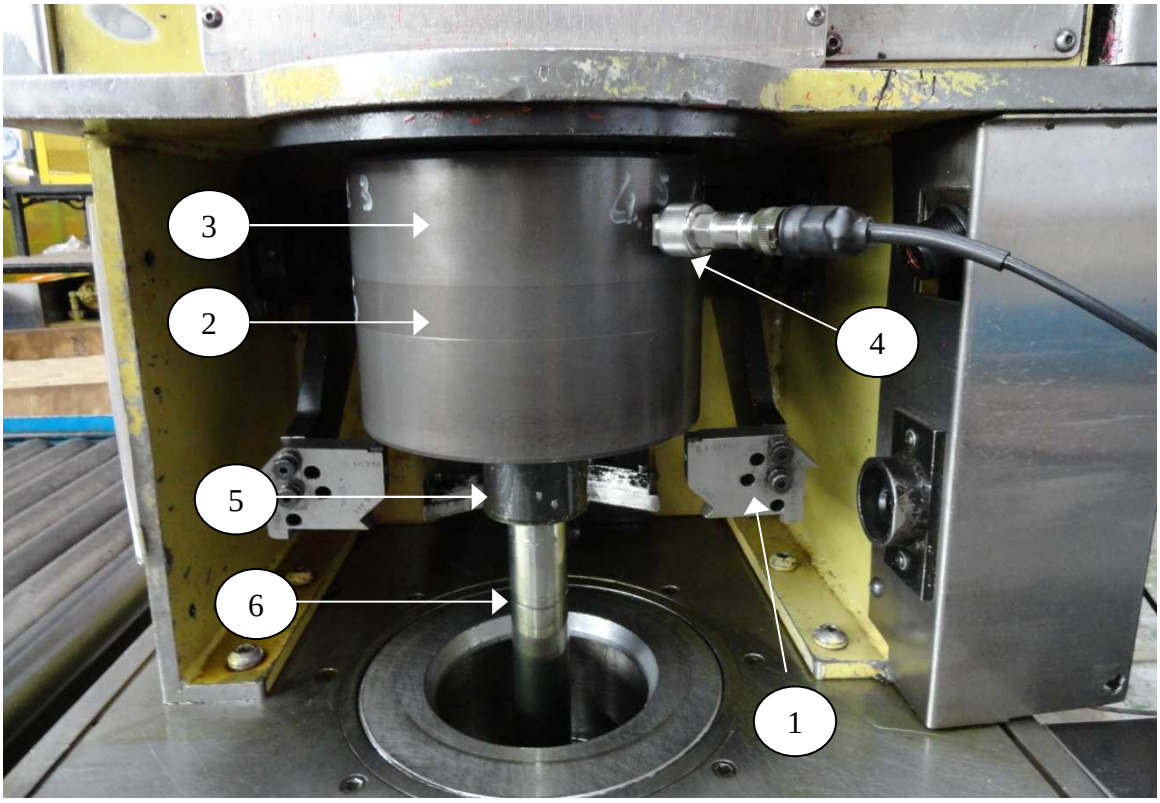

1. Cup Lock
2. Track Location of Cup
3. Upper Race Location of Cup
4. Accelerometer mounted Magnetically
5. Upper Collar of Lower Shaft
6. Lower Shaft (non-Rotating)

Figure 3-1 – Testing equipment configuration

3.1.2 Data acquisition instrument and software

An instrument from National Instruments, OROS and HBM was considered. When price, sampling rate, future flexibility with regard to input sensors and software programs were

considered the HBM QuantumX MX440A Universal Amplifier was chosen. It is able to master sample data at 19.2 kHz and applies a non-adjustable anti-aliasing filter to 3.2 kHz bandwidth. It has a 24 bit resolution. This is recorded per channel with four electrically independent channels (See Appendix B). Although this equipment was not the cheapest in its class, it appeared to have the most functionality when in later stages alternative types of sensors were to be used, other than accelerometers and velocity pickups. The software which is supported for the signal analysis, the HBM nCode GlyphXE, was used as part of the analysing tools. Additionally Matlab was used to plot information and Continuous Monitoring System (CMS) software (courtesy of TLC Engineering) was also used to plot information and calculate FFT's and PSD's.

3.1.3 Data acquisition sensor

Due to the potentially large range of frequencies expected as a result of the low bearing signature frequencies of at low rotational speeds, with the possible high frequency peaks which could be generated from a bearing defect, it was difficult to narrow the amplitude range of the sensor down. Thus, based on what was discussed in the literature survey, it was decided that, due to the overall performance of accelerometers at varying frequencies as well as their robust design and ease of availability, that an accelerometer would be used. Additionally, it was decided that it would be suitable to use an accelerometer for initial tests with a broad frequency spectrum capability as it could cope with the expected frequencies within a relative measure of accuracy. The IEPE accelerometer chosen was an IMI ICP Accelerometer with a sensitivity of 96mV/g. Additionally, a variable capacitance accelerometer, which is able to measure with greater sensitivity at low ranges was used to detect lower frequencies. This accelerometer was an Endevco Microtron 7290A-2-100 with a sensitivity of 20mV/g.

3.1.4 Sensor mounting

As discussed previously in the literature review it is not ideal to have sensors mounted by magnet or glue as there is a loss in the transmitted vibration as such methods have a dampening effect on the vibration measured at certain frequencies, as shown in Figure 2-13. However, in this particular application and for testing purposes it is not possible to stud mount the sensor as the bearings are changed and the tooling does not allow for that. If, however, the results show that the location of the sensor has an effect, and that it is feasible to implement the testing in a production environment, then further investigation can be done to consider permanent mounting of the sensor to extend into the exact, correct, permanently mounted location. A curved magnet was used which allows the accelerometer to be attached to the outside diameter of the cups (for the IMI sensor) and adhesive[1] mounting was used for the Endevco accelerometer.

3.1.5 Data analysis

During the course of the testing and data analysis phase of the project, different methods of data analysis were explored. Time domain analysis was conducted in Matlab, CMS and Glyph XE. FFT analysis was also done in these programs. Additionally, more complex analysis techniques were used, such as Power Spectral Density (PSD) in CMS.

Data capturing was conducted with and without filtering and by applying different types of low pass filters in order to determine the best method.

[1] Rapid setting anaerobic ‘superglue’ was used. While this would not be feasible in a production environment it served as a useful comparison in cases where both instruments were used simultaneously.

3.2 Preparation of Test Pieces

In order to conclusively and accurately derive information from the testing to be performed it was important that the bearings that were being tested were understood and documented well. Cups that had nicks were to be chosen from the production line, where available. If cups with nicks did not exist they were deliberately made by simulating an incorrect bearing assembly procedure, or by using a hammer. Additionally, cups were chosen that were considered as non-nicked samples in order to determine the frequencies and amplitudes of vibration against which nicked bearings would be compared.

In the following section particular nicked bearings, with photos and measurements are described.

3.2.1 Class D bearings

The most common part number run in the South African production facility is a class D cup and cone, and thus these were the main size of bearing used during testing, based on availability. A variety of class D bearings were tested to establish if results were bearing dependent, or if they were repeatable. The bearing naming convention given was D1, D2 etc, where the numeral represents only a sequential number denoting the bearing number. Non-nicked production bearings were denoted by their serial number. The testing and results in the remainder of the report will be referred to by these numbers.

The profiles of the nicks were traced on a contour profile tracing machine. This is a machine that measures accurate change in height and depth of a surface and plots this variation against the horizontal distance traversed by the needle. The cups were placed on the tracing machine so that the nicks were measured across the centre of the nick i.e. the

deepest area. Each bearing was visually examined and the deepest and largest nicks were chosen for measurement.

Table 3-1 is a summary of the type of nicks that were measured on the bearings, and the height and depth thereof. The parameter shaded in grey indicates a bearing that is within the corporate size specification limits for nicks (The Timken Company, 2011).

Table 3-1 : Summary of nicked test bearing damage

Bearing	Roller-spaced Nicks	Raised Surface	Depth [µm]	Height [µm]	Width [mm]	Number of Nicks Top Raceway	Number of Nicks Bottom Raceway	Comments
D1	N	Y	14.487	10.026	1.17	6	3	Light nicks
D2	Y	Y	28.45	16.513	1.335	8	1	Two sets of roller-spaced
D3	Y	Y	10.64	1.46	1.52	10	4	Top raceway some depth
D4	Y	N	11.78	0	0.7366[1]	3	1	No real depth
D6	N	Y	13.21	9.088	2.311	6	3	Nicks random distribution
D7	N	N	385	0	2.083	0	1	Chip on edge of raceway

D1 Nicked bearing

This bearing has approximately six light nicks on the top raceway and approximately three light nicks randomly spaced on the bottom raceway. One of the nicks displayed has a ‘double’ appearance i.e. two small indents alongside each other as shown in Figure 3-2. Figure 3-3 shows a trace depicting the depth versus position of a nick on bearing D1. There are further examples in Appendix D. Figure 3-3 shows that there is a high spot

[1] Although the size of D4 is within corporate specification there is more than one nick in a quadrant and thus it is rejected by the specification

after the nick, as well as the depth of the nick. The X-axis denotes the distance that has been travelled and the Y-axis denotes the amount of travel of the tracing needle i.e. the height and depth of the nick.

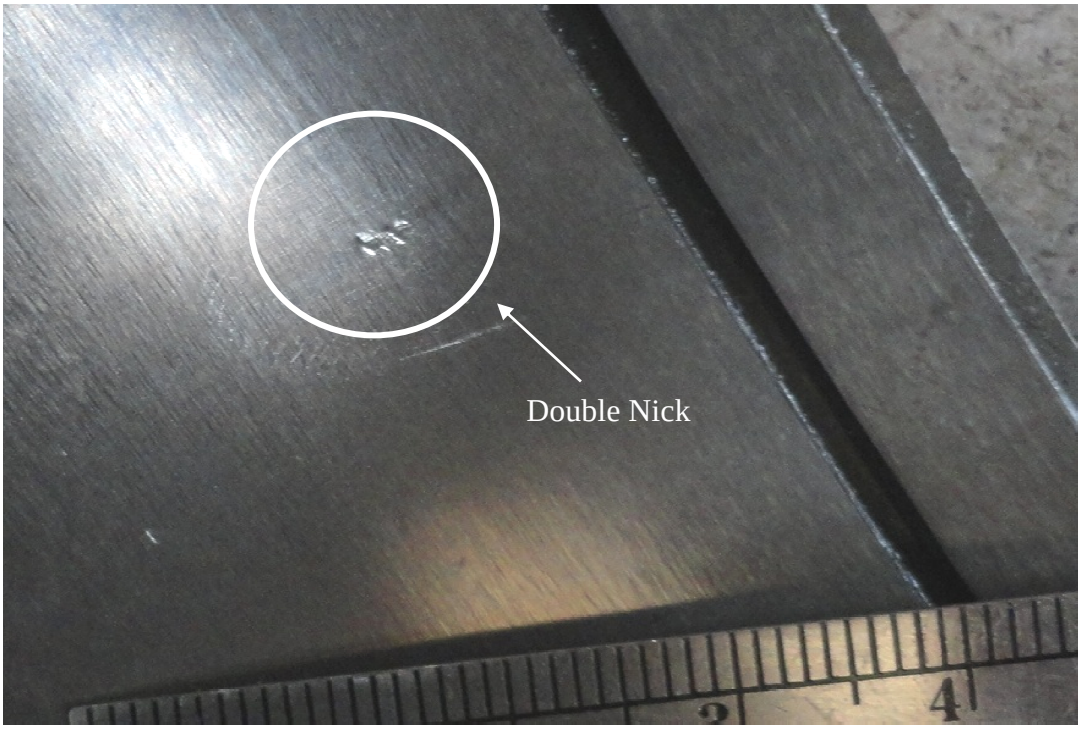

Figure 3-2 – D1 light double nick (scale in mm)

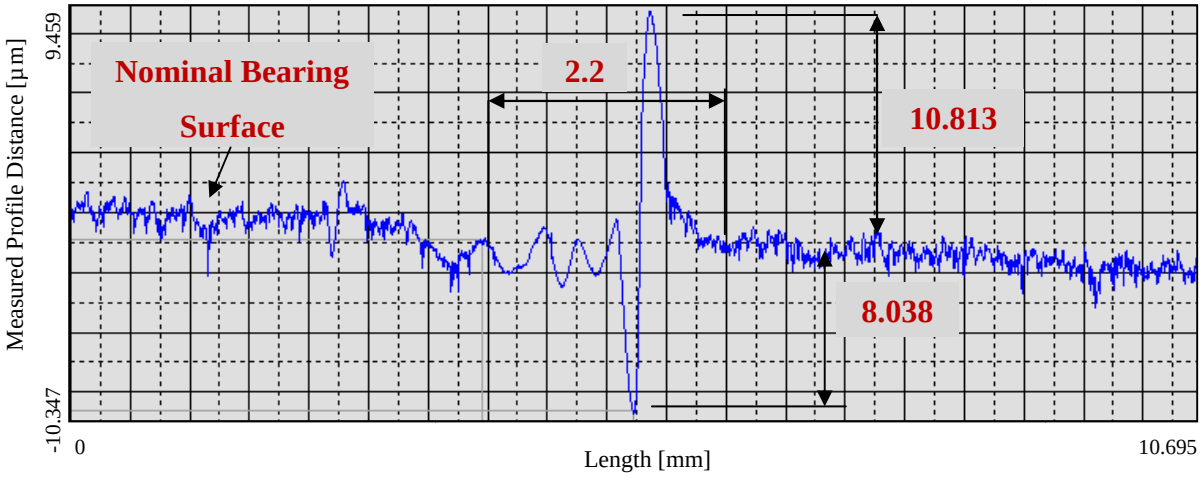

Figure 3-3 –Profile trace of D1 upper raceway nick with some depth and raised metal

D2 Nicked bearing

In this bearing the bottom race has a nick, tangible to touch and located approximately opposite to the point chosen for sensor location during testing. The upper race has multiple roller-spaced nicks each with depth as seen in Figure 3-4. They are set virtually under the sensor position when the sensor is mounted "on top of the nicks" position as will be seen later. There are two "sets" of roller-spaced nicks in this upper race. Figure 3-5 shows a profile trace of one of the roller-spaced nicks shown in the photograph. There are more profile traces of the nicks in Appendix D.

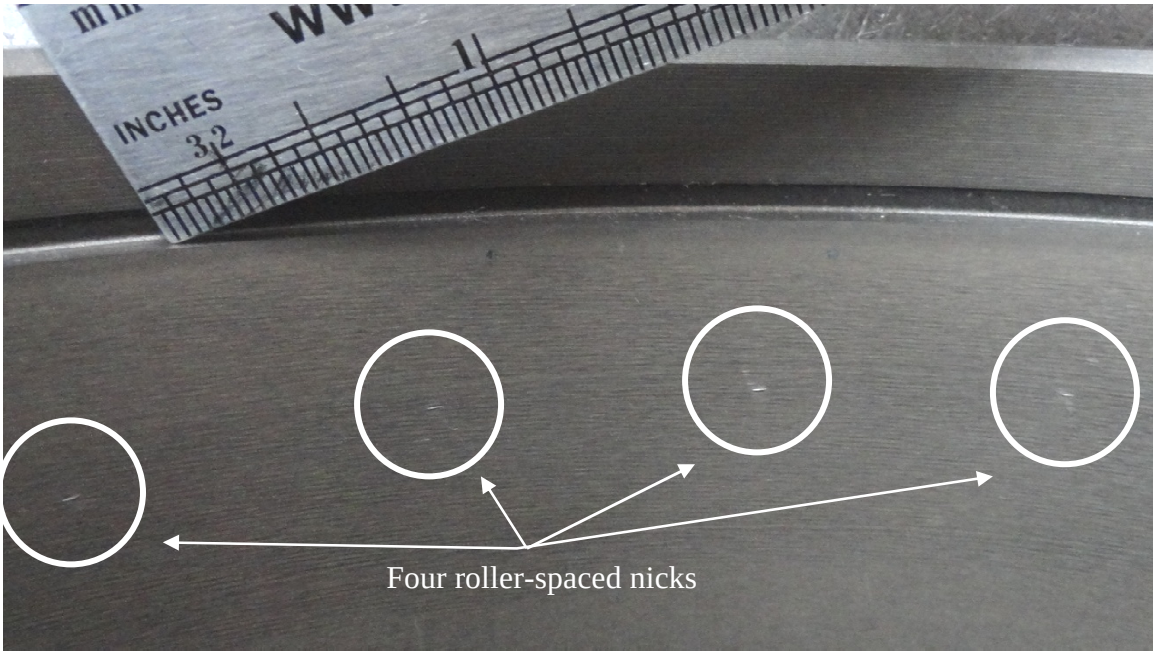

Figure 3-4 – D2 upper race roller-spaced nicks (scale in inches)

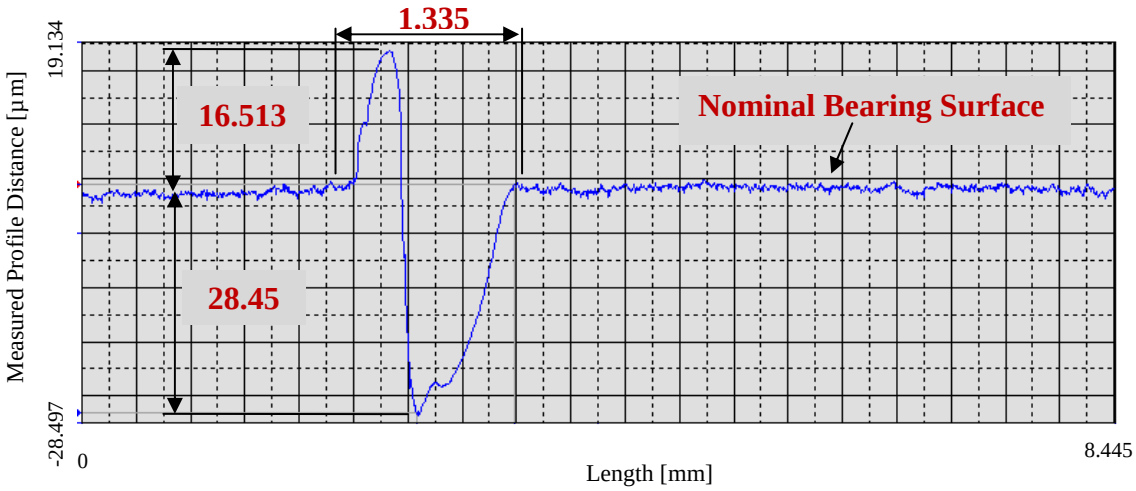

Figure 3-5 – Profile trace of deep nick on D2 (nick two of roller-spaced nicks)

D3 Nicked bearing

In this bearing the top raceway has more than ten roller-spaced nicks with considerable depth (Figure 3-6). The bottom raceway has a few nicks (approximately four) and these have some depth. Traces of the nicks are available in Appendix D.

D4 Nicked bearing

This bearing has three roller-spaced nicks which are not very deep on the upper raceway with some random shallow oddly-spaced nicks. The bottom race has some basic minor staining with a small nick with negligible depth. Traces of these nicks are shown in Appendix D.

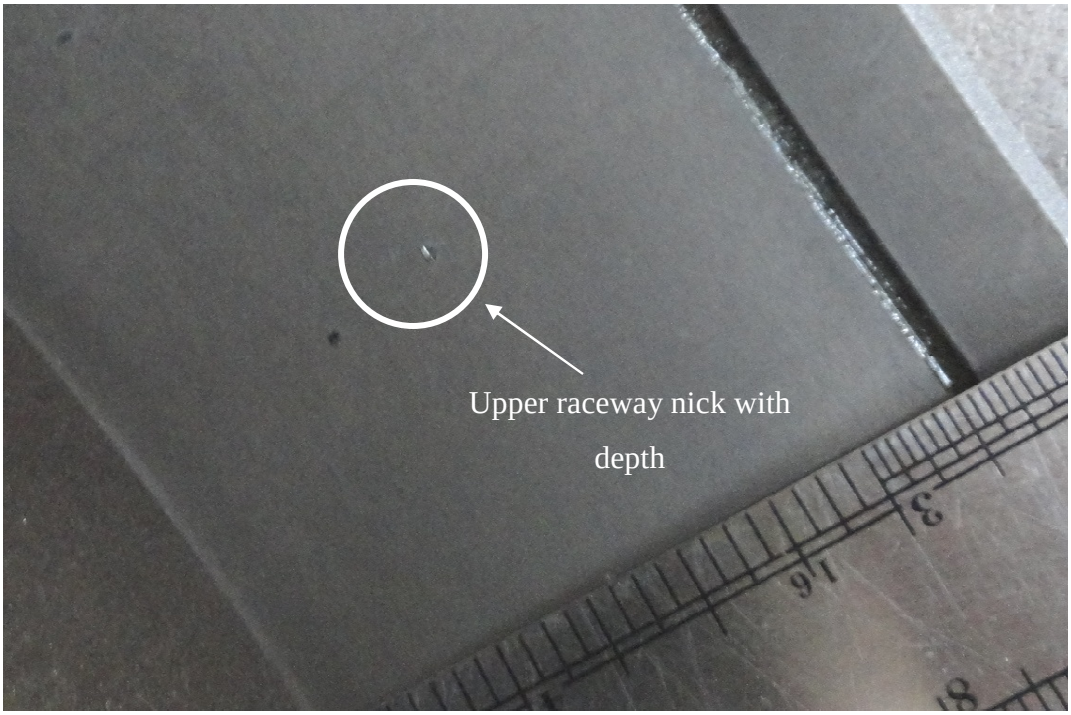

Figure 3-6 – D3 upper raceway nick with depth (scale in inches)

D5 Non-nicked bearing

This bearing is not nicked and has no visible damage on either the bottom or top raceways. Before every test it was inspected to ensure that this condition had not changed. In addition to this non-nicked bearing tested, a further seven non-nicked bearings were used throughout the testing and were always inspected for the presence of nicks. These were production bearings and thus were labeled by their serial numbers or called production bearings. They were only tested a few times and then were sent to the customers. D5 was always re-used as it was not sent on to customers and thus it is regularly mentioned.

D6 Nicked bearing

This bearing has a few nicks on the top raceway which are varied in size and depth, and are randomly distributed. The deepest nicks are located approximately 90 degrees from

where the sensor would be mounted in the track. The bottom raceway has fewer nicks and one with shallow depth but larger size, as seen in Figure 3-7. Traces of the nicks are shown in Appendix D.

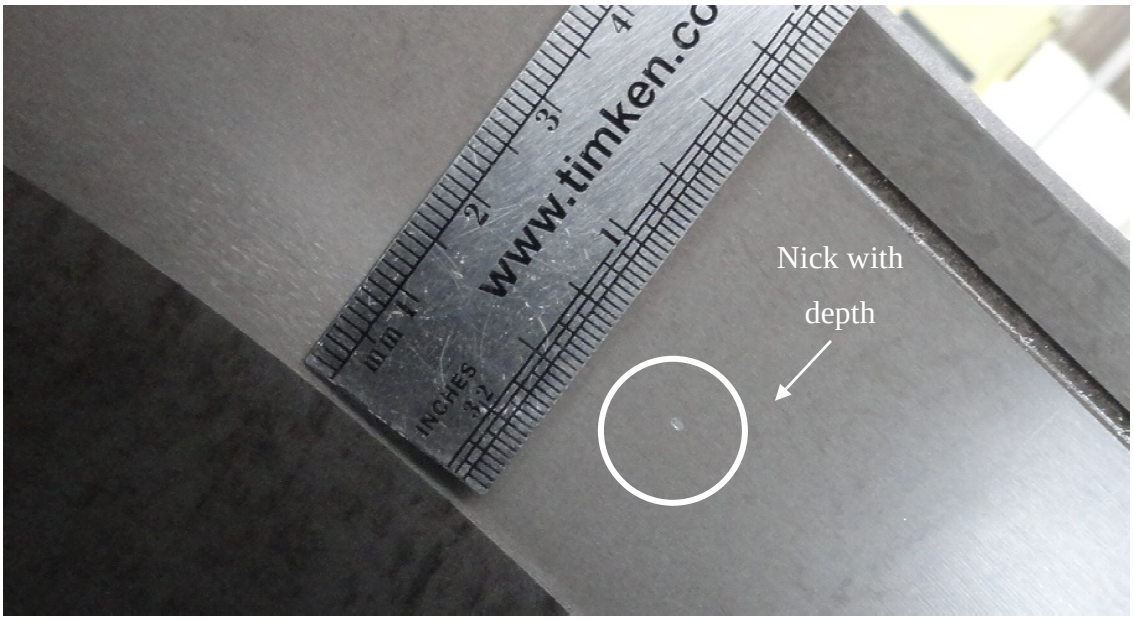

Figure 3-7 – D6 nick with depth

3.3 Proposed Testing Methodology

The testing methodology is as follows. It should be seen as a broad approach (not necessarily sequential) with intermediate evaluations made, and adjustments made to the test protocol to cover all the necessary facets of the research. As the data is gathered from the testing, an iterative approach is implemented to re-test certain parameters and understand better how they affect the results. The presentation of results is not necessarily chronological but results have been grouped according to the general parameters that were varied.

a. Establish the parameters of the bearing

i. This consists of initial testing done on one Lateral Machine and class D bearings. The testing would include simple tests on nicked and non-nicked bearings. At first the accelerometer would be mounted in a neutral position such as the centre of the double cup on the track as shown in Figure 3-1. A few tests would be conducted with the data capture program, utilizing different acquisition settings such as sampling rates and low pass filters. The accelerometer would be a general specification for fairly good performance across both low and high frequency bands. This phase of testing is to understand the frequency range present in the application.

ii. Analyse the data in the time domain to identify if any periodic waveforms are present.

iii. Convert the data to the frequency domain and identify dominant frequencies and amplitudes for non-nicked and nicked bearings.

iv. Convert the data to power spectral density and identify dominant frequencies and amplitude limits for distinguishing nicked from non-nicked bearings.

b. Establish how data acquisition variations affect the testing results

i. Further steps would be taken to understand how the settings applied within the data acquisition process affected the consistency of the results. This would include changes in sampling rate of the measurements, the use of filters, the position of the accelerometer relative to the nicks, different accelerometer sensitivities and methods of mounting of the accelerometer.

c. Establish the effect of the physical bearing parameters on vibration amplitude

i. The variation of depth, size and distribution patterns of the nicks on the outer race would be investigated and the effect of such on the vibration amplitude and frequencies determined.

ii. The variation of the bench end-play of the bearing assembly and its effect on the vibration signal will be assessed.

iii. Any other physical defects within the bearing, of which test pieces are available, can be tested to see their effect on the vibration signals.

The methodology that will be applied during the testing phase of the research has been described. It has been shown how the different physical characteristics of the nicks have been considered and how these have an effect on the research outcomes. These characteristics have been measured and defined within the test bearings to ensure that they are fully understood when the results are analysed. The settings of the equipment during testing have also been described and the impact thereof explained. Furthermore, the different acquisition parameters such as testing duration and accelerometer types used have been considered as well.

4 RESULTS

This chapter documents the findings that were established during the testing phase of the research. The theoretical bearing frequencies are calculated and documented. These are the standard bearing frequencies that would typically be associated with defects. Explanation is given into the preliminary testing that was completed and techniques that were used and not considered relevant for further discussion. Physical acquisition parameters such as the testing duration, severity and distribution of nicks in the test pieces, and location of transducer, are considered.

4.1 Theoretical Bearing Frequency Determination

The physical characteristics of the relevant local bearings are defined in Table 4-1.

Table 4-1 : Class D bearing physical characteristics[1]

Part Number	Class	Inner Diameter	Outer Diameter	d^2 Roller Diameter	D^2 Pitch Diameter	α - Half included roller centre line angle	n- Number of Rollers
		[mm]	[mm]	[mm]	[mm]	[°]	[ ]
HM127446/HM127415XD	**D**	131.750	207.962	17.6987	167.8884	9.05	23

The different methods of calculating the expected theoretical defect frequencies were explained in Section 2.4.1. These are defined in Table 4-2, sample calculations of which are found in Appendix C. These frequencies will be highlighted in the graphs to see if any particular activity or peaks coincide with these frequencies. Harmonics of the above

[1] Product knowledge in Table is available on Timken Company internal database systems
[2] Parameters d and D are calculated by bearing manufacturers and are based on average sizes of a taper

are also possible and Table 4-3 lists these for class D bearings. The rotation speed of the Lateral Machine is 135.7 RPM and the defect frequencies in Table 4-2 and Table 4-3 are based there on.

Table 4-2 : Expected defect frequencies calculated for assembled bearings at 135.7 RPM

135.7 RPM	Outer Defect Frequency	Inner Defect Frequency	Roller Defect Frequency	Ball Spin Frequency	Cage Frequency	In Plane Flexural Mode[1]	Transverse Flexural Mode[1]	Radial Flexural Mode[1]
	Hz	Hz	Hz	Hz	Hz	Hz	Hz	Hz
Class D	23.3049	28.7211	21.2246	10.6123	1.0133	1098	1069	5577

Table 4-3 : Class D bearing harmonic frequencies at 135.7 RPM

Frequency and Calculated Method		Calculated Frequency [Hz]	Harmonics [Hz]								
			0.25x	0.5x	1x	2x	3x	4x	5x	7x	9x
Tandon	Inner	28.7211	7.18	14.36	28.72	57.44	86.16	114.88	143.61	201.05	258.49
	Outer	23.3049	5.83	11.65	23.30	46.61	69.91	93.22	116.52	163.13	209.74
	Roller	21.2246	5.31	10.61	21.22	42.45	63.67	84.90	106.12	148.57	191.02

Since the rotating speed of the Lateral Machine is 135.7RPM, the fundamental frequency, which could possibly be significant due to machine excitation, is approximately 2.262Hz. The harmonics of the rotating speed are listed in Table 4-4. These Frequencies will also be monitored in the results.

The Lateral Machine has various rotating components which allow it to operate. These also need to be taken into consideration as additional frequencies that could possibly be measured. The frequencies of the bearings utilized in the speed reduction motor are given in Table 4-5.

[1] Bearing element resonant frequencies are calculated for whole assembly and are calculated for mode order N=2 per equation 2-19, 2-20 and 2-21

Table 4-4 : Frequencies associated with rotational speed of Lateral Machine

Order [ ]	Frequency [Hz]
1	2.262
2	4.524
3	6.7860
4	9.048
5	11.310
10	22.620
15	33.930
30	67.860

Table 4-5 : Rotational frequencies of bearings in reduction motor of Lateral Machine (NTN-SNR, 2012)

Bearing Part Number	Rotating Speed [RPM]	Cage Frequency [Hz]	Roller Frequency [Hz]	Outer Ring Frequency [Hz]	Inner Ring Frequency [Hz]
Slow Speed Bearings					
6306Z	136	0.87	9.3	6.97	11.16
16011	136	1.01	20.45	16.15	20.12
High Speed Bearings					
6302RSH2 and 6302Z	1500	9.13	86.18	63.95	111.03

4.2 Preliminary Results

Tests were conducted with different data acquisition settings as well as physical bearing characteristic differences. These will be discussed in detail in the relevant sections. The testing parameters were chosen in such a way as to determine the ideal combination of testing criteria in which to detect nicked bearings within the Lateral Machine operating context. In so doing thus exploring various parameters and evaluate what effect they have on the vibration signal produced. These results will be presented in the most logical manner and not in chronological order.

With initial testing completed it was difficult to achieve meaningful results. Appendix E highlights some of the steps that were followed and techniques that were tried which were not successful. An example of such a method was synchronous averaging.

Certain data packages were also used that did not provide the correct resolution in the FFT's to give spectrums which could be analysed.

It was also found that using the Microtron sensor, which had a greater sensitivity at lower frequencies, yielded better results, and the majority of the testing presented hereafter was done with this device unless stated otherwise. The use of the CMS data acquisition program (courtesy of TLC Engineering) made it easier to understand the frequencies that were present in the system and further manipulate them using filters. Matlab was used to overlay multiple bearing frequencies to accurately compare the differences between nicked and non-nicked samples.

With most of the results below it will be seen that the FFT spectrum is not used but that the PSD is used. The frequency peaks were clearer on PSD's and some of the associated noise was removed in the PSD (more so than in the FFT). In most instances the individual data was examined on the CMS data acquisition program on which manual limits could be drawn over the whole spectrum. This data was exported and it was then possible to graphically overlay multiple bearings in Matlab to see the graphs together. Certain of the spectra were calculated directly in Matlab and will be indicated as such.

Particular data acquisition parameters that were anticipated to affect the measured results include:

i. The rate at which the data was sampled.
ii. The filters that were applied during data acquisition.
iii. The type of accelerometer used.
iv. The duration of the tests.

These four factors will be discussed in more detail, showing how they affected the results.

4.2.1 Sampling rates

As is known from the theory discussed in the literature survey the sampling rate chosen for a study is very critical, as having this incorrectly set can either reduce the resolution of the data, or create a drop in resolution at the lower frequency spectrum. Based on this the tests will be presented with data sampled at 600Hz, 1200Hz, 9600Hz and 19200Hz.

600Hz Sampling Rate

Tests were completed with the sampling frequency set at 600Hz. All of these tests on nicked and non-nicked bearings are presented in Appendix F. No running frequencies of the machine at 2.262Hz and harmonics thereof were present. Figure 4-1 shows the PSD taken of nicked and non-nicked bearings sampled at 600Hz. Significant frequencies are present at 23Hz to 30Hz, 50Hz, 100Hz, 200Hz, 250Hz and 275Hz.

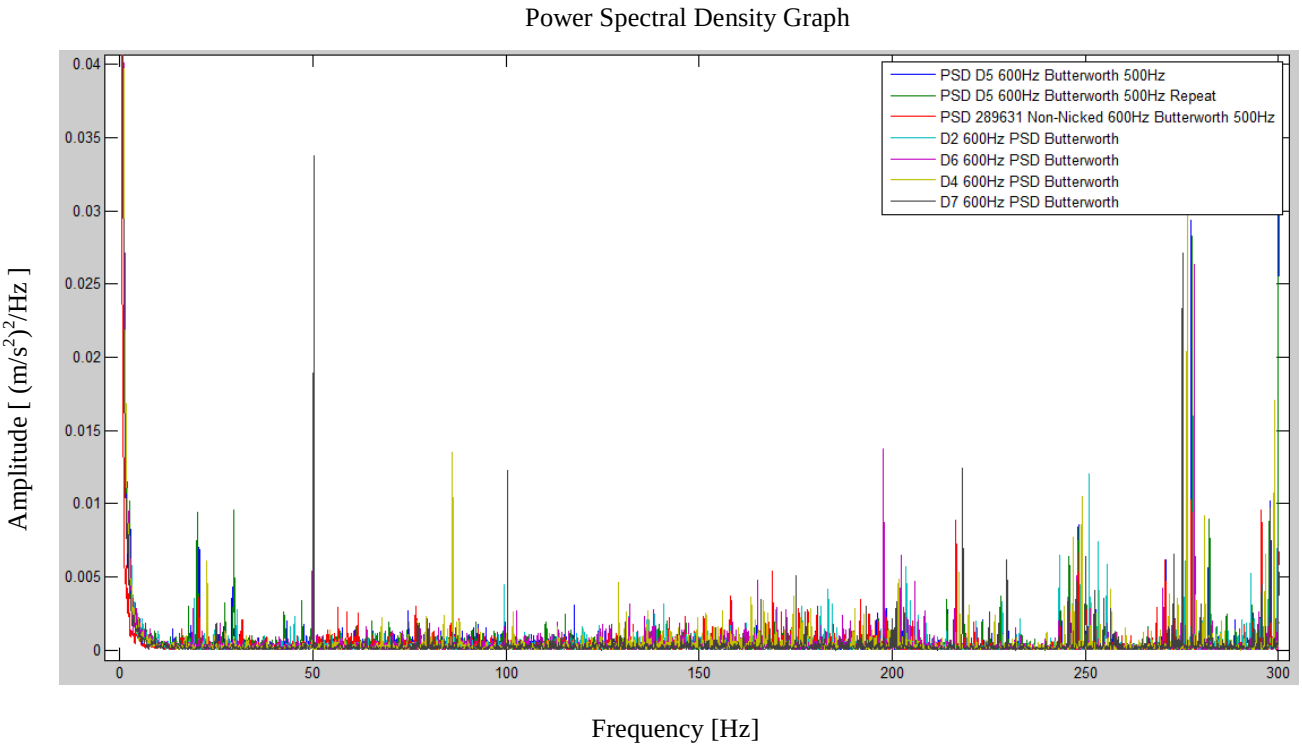

Figure 4-1 – PSD 600Hz nicked and non-nicked bearings

1200Hz Sampling Rate

For tests conducted at a sampling frequency of 1200Hz a low pass filter of 500Hz was applied. In Figure 4-2 the PSD's from CMS are overlaid in Matlab for various bearings. Figure 4-3 and Figure 4-4 are zoomed-in sections of the running-speed spaced frequencies. All of these harmonics are exactly 2.262Hz apart (these harmonics were tabulated in Table 4-4). The running speed frequency harmonics displayed between 0Hz and 100Hz are more excited in the nicked bearings than the non-nicked bearings. It can be noted that Figure 4-3 makes use of a Butterworth filter and Figure 4-4 makes use of a Bessel filter. This has been done specifically to show the results obtained with the two different filter types has remained similar and that they do not have any affect on the results.

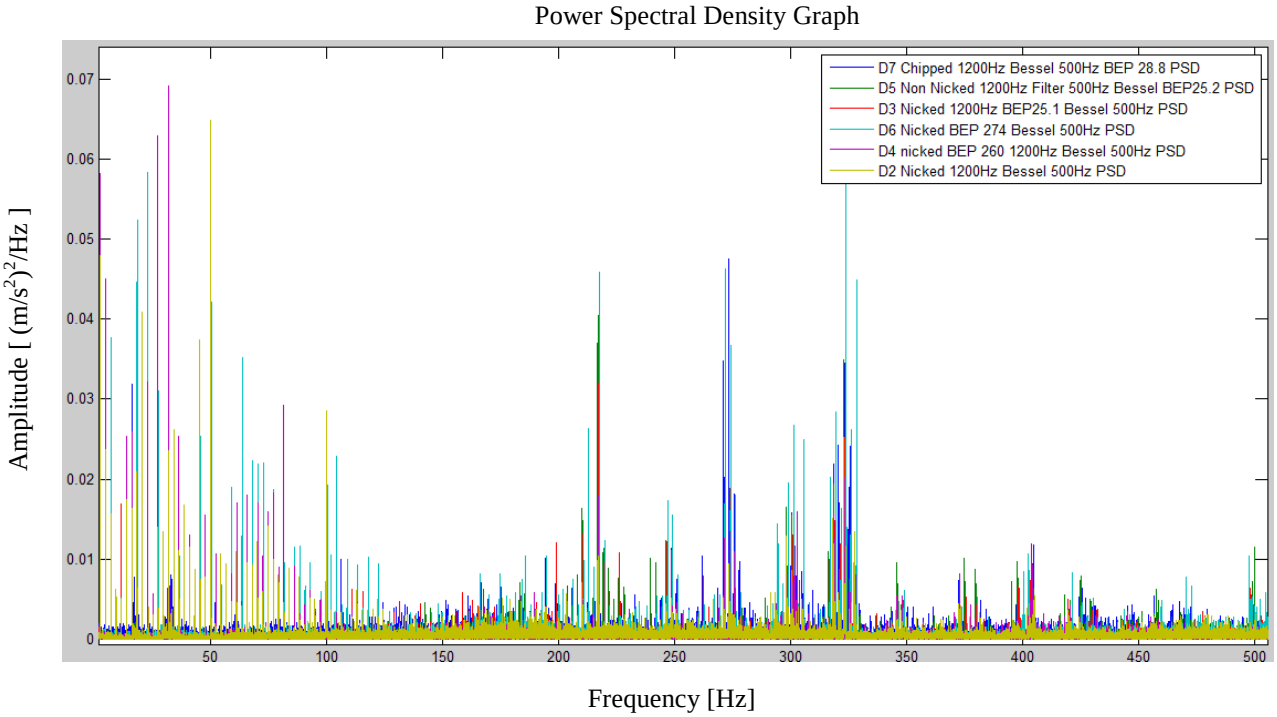

Figure 4-2 – Nicked and non-nicked bearings sampled at 1200Hz with a Bessel low Pass filter at 500Hz PSD from the CMS program

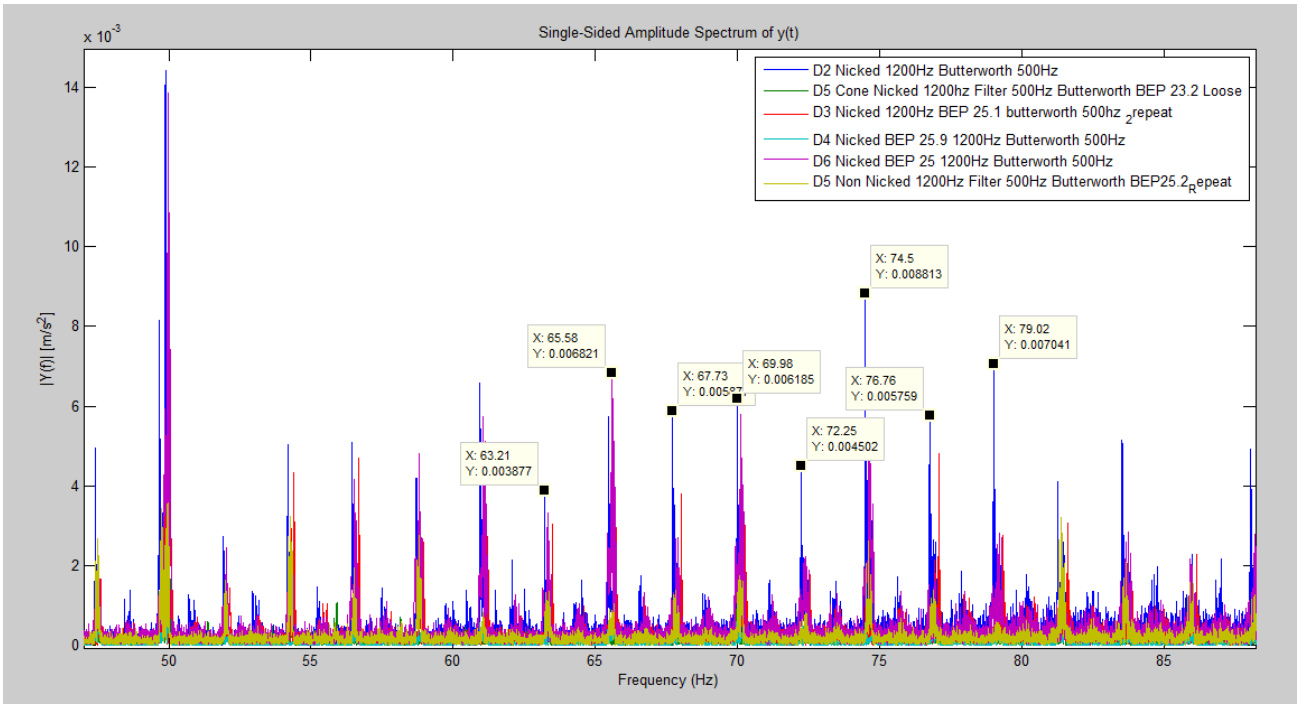

Figure 4-3 - Nicked and non-nicked 1200Hz Butterworth filter 500Hz

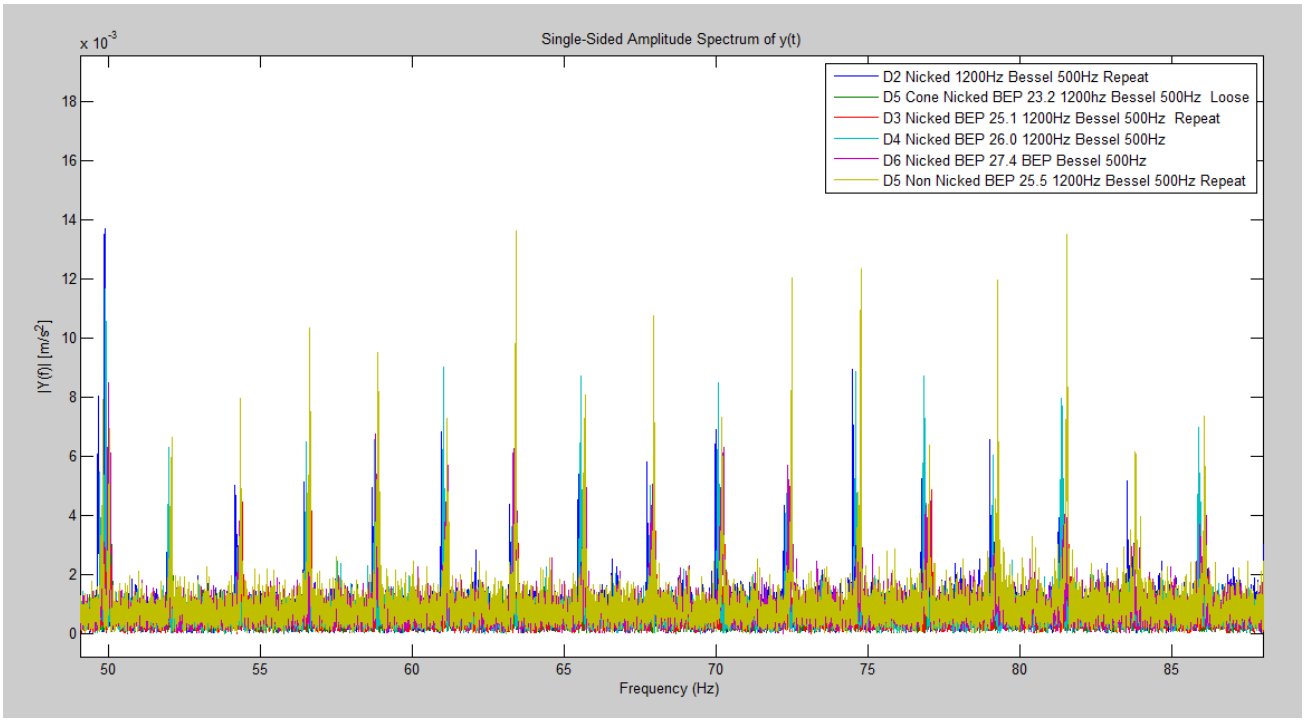

Figure 4-4 – Nicked and non-nicked 1200Hz Bessel filter 500Hz

9600Hz Sampling Rate

Data was sampled at 9600Hz with a low pass Butterworth filter of 2000Hz. When these results were analysed in the FFT spectrum the results between nicked and non-nicked bearings were not very distinct as seen in Figure 4-5. This was similar for the other sampling frequencies and as a result the PSD's were preferable to analyse rather than the FFT.

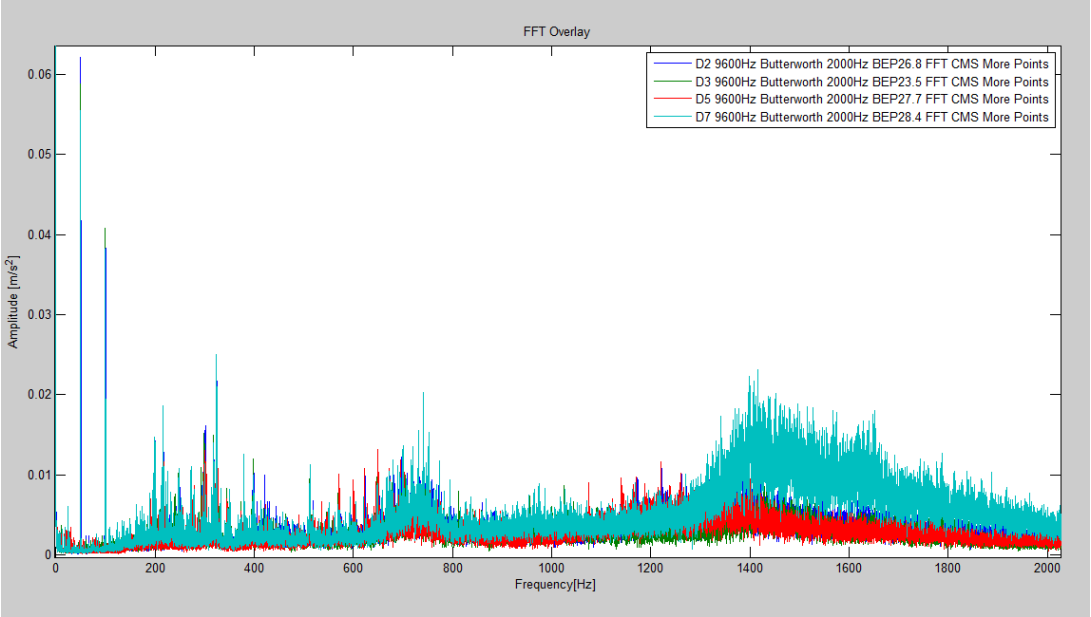

Figure 4-5 – 9600Hz Nicked and non-nicked overlay of FFT from CMS

When the results were analysed with Power Spectral Density (PSD) in Figure 4-6, trends do appear between the nicked and non-nicked bearings. Most nicked bearings have a greater frequency amplitude at 50Hz and 100Hz than the non-nicked bearing. The running frequencies are not seen as in the tests performed at 1200Hz. There are many peaks from less than 50Hz all the way to 2000Hz. This sampling rate is providing good information. The detailed sections in Figure 4-6 show that at 50Hz and 100Hz the non-nicked bearings do not have any amplitude but the nicked bearings do. Additionally, these two frequencies are repeatable, distinct and have sufficient amplitude in all the

nicked bearings. Further more in Figure 4-6 it can be seen that D7, the bearing with a chip on the edge of the raceway has a large amplitude response at approximately 1400Hz.

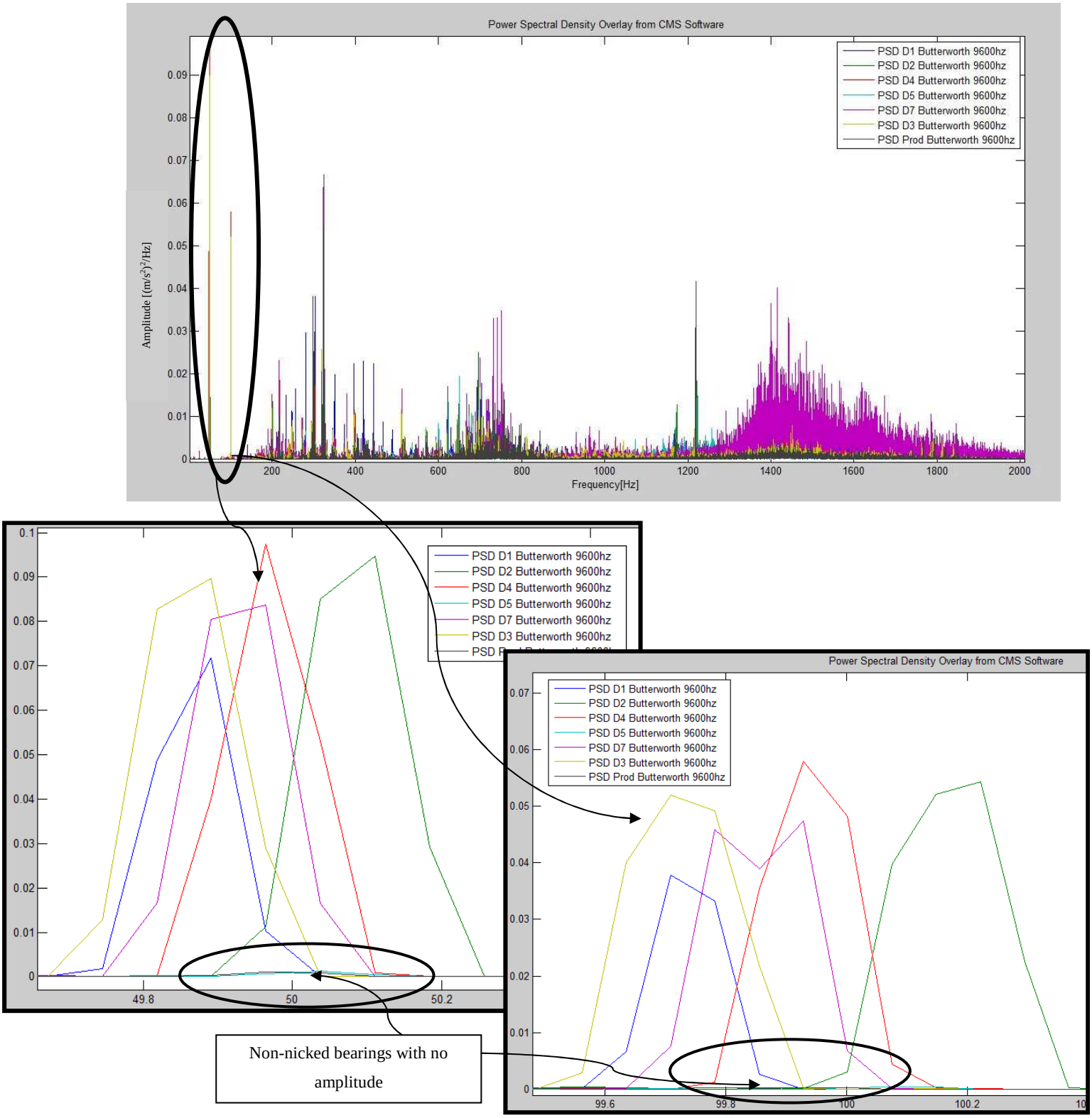

Figure 4-6 – PSD of nicked and non-nicked bearings sampled at 9600Hz FFT from CMS program

19200Hz Sampling Rate

Tests were conducted at the maximum sampling rate of 19200Hz of the MX440A data acquisition instrument. The instrument then automatically filtered the data to just under 3.2kHz ensuring that anti-aliasing filtering was done. The results of the FFT plot conducted on the CMS program are shown in Figure 4-7. The results were then also analysed using a Power Spectral Density (PSD) (see Figure 4-8).

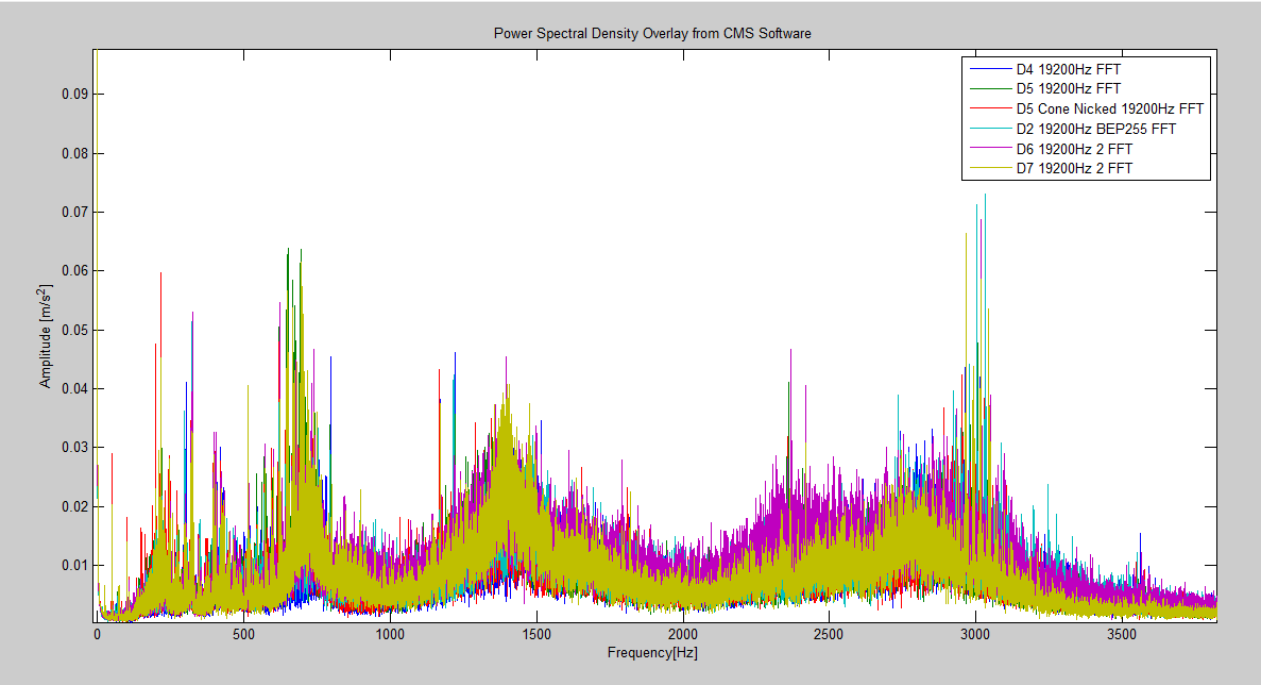

Figure 4-7 – Nicked and non-nicked bearings sampled at 19200Hz FFT from CMS program

The peaks have become slightly clearer than that shown on the FFT. On Figure 4-8 the frequencies of 50Hz and 100Hz have been highlighted to show that these are the common frequencies. However the non-nicked bearing (D5) does not have a pertinent acceleration peak when compared to the nicked bearings at 50Hz or 100Hz. There are a lot of high frequencies which are excited and these may not be so pertinent to the work examined.

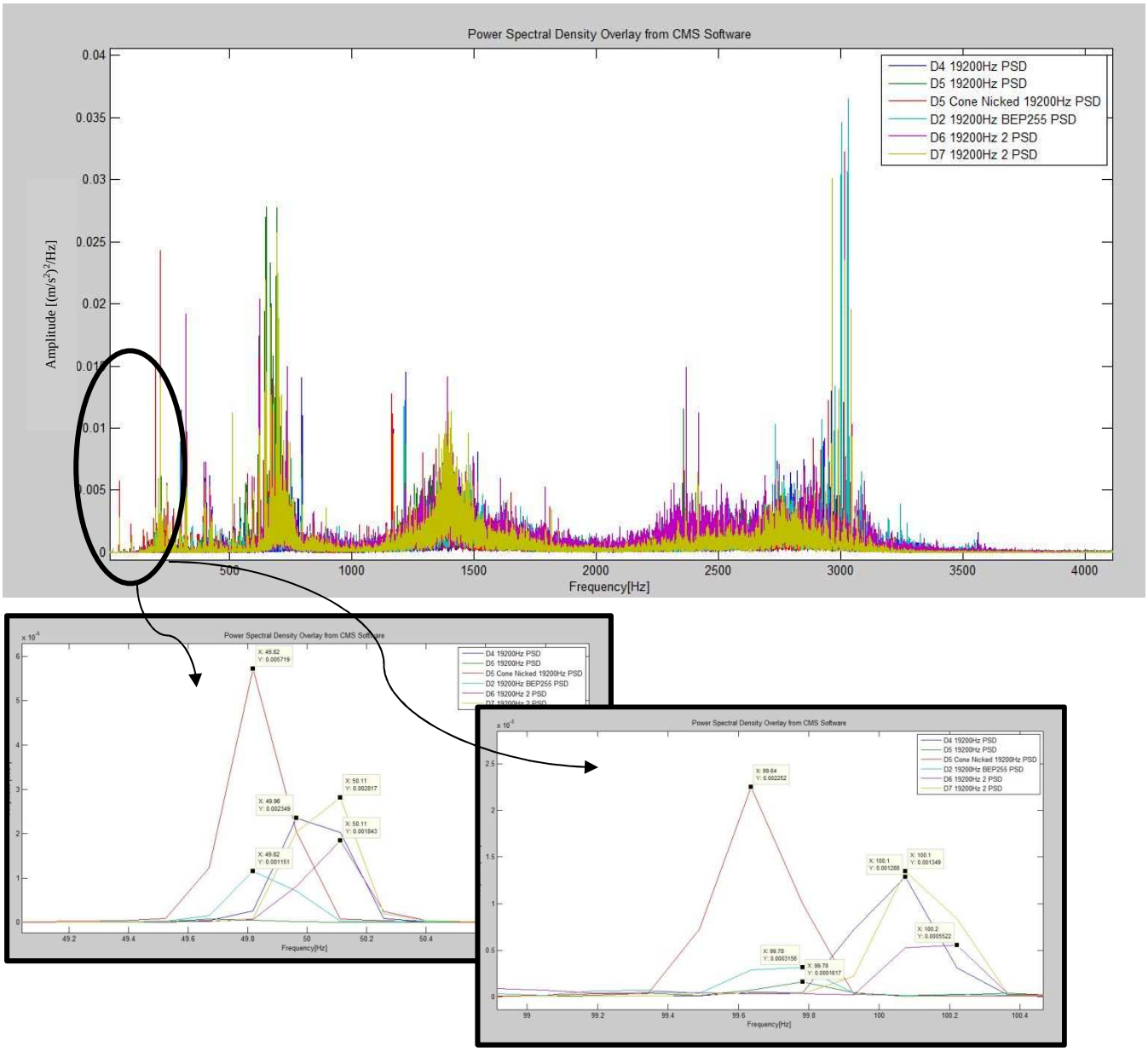

Figure 4-8 – PSD of Nicked & non-nicked bearings sampled at 19200Hz from CMS program

4.2.2 Bearing frequencies

The expected frequencies of bearing defects were calculated and defined in Table 4-2. Based on the bearing theory that a defect on an outer raceway (or any other component) will give off a distinct frequency it was expected that these frequencies would be prominent in the testing of nicked bearings. Figure 4-9, sampled at 600Hz, shows that both the nicked and the non-nicked bearings do not show peaks at the characteristic frequency of the cup outer (23.30Hz) but the non-nicked bearings do have peaks at the roller defect frequency (21.22Hz). Some of the bearings also have peaks at the inner ring defect frequency (28.72Hz). At 22.26Hz bearing D4 and production non-nicked bearing 289631, show peaks (which correspond to the 10th harmonic of running speed).

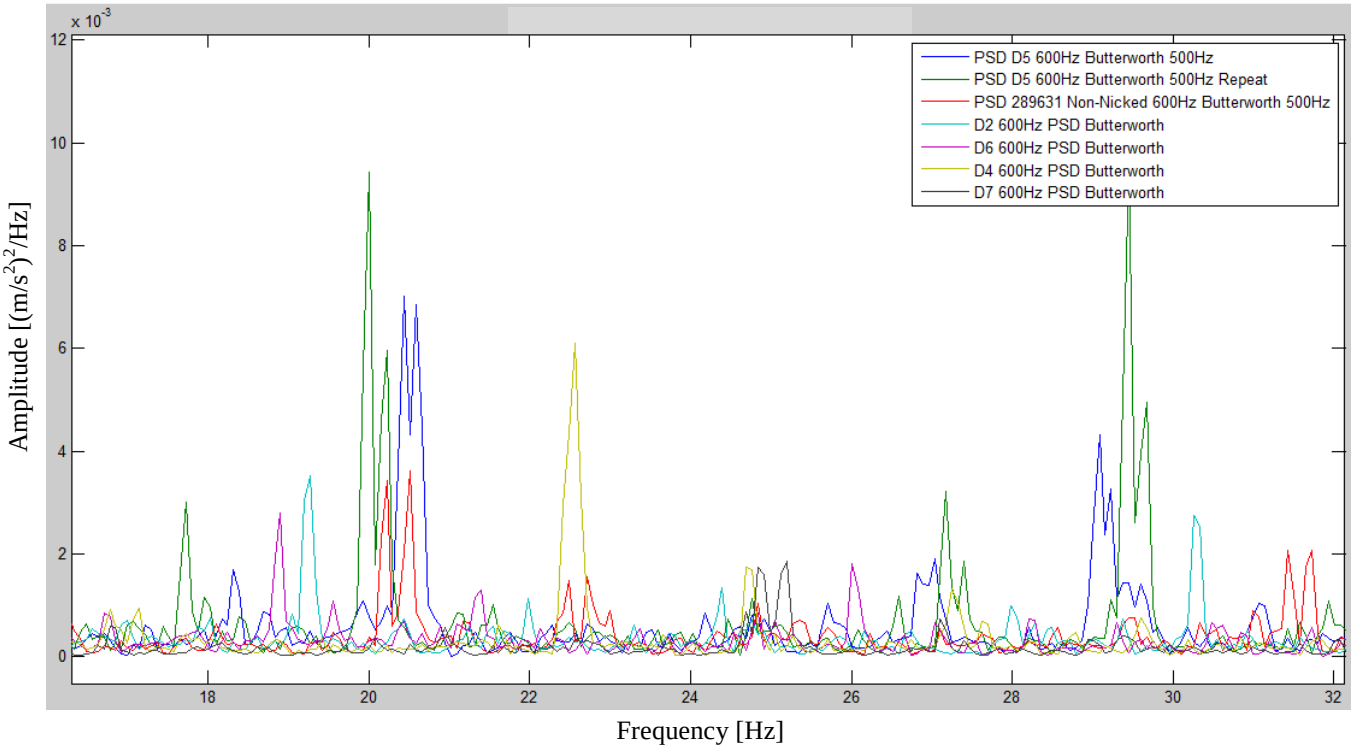

Figure 4-9 – PSD at characteristic bearing frequencies of nicked and non-nicked bearings sampled at 600Hz with a Butterworth filter set to 500Hz

Figure 4-10 shows clearly the running frequency harmonics (20.39Hz, 22.65Hz, 24.92Hz, 27.18Hz and 29.44Hz). The characteristic bearing frequencies are the frequencies in-between and these are seen again in the roller frequency (21.84Hz) and the inner ring frequency (28.27Hz). In this figure they are shown for the nicked bearing D3 and the chipped bearing, D7, which has similar amplitude. The outer race defect frequency is not shown clearly in either of the bearings.

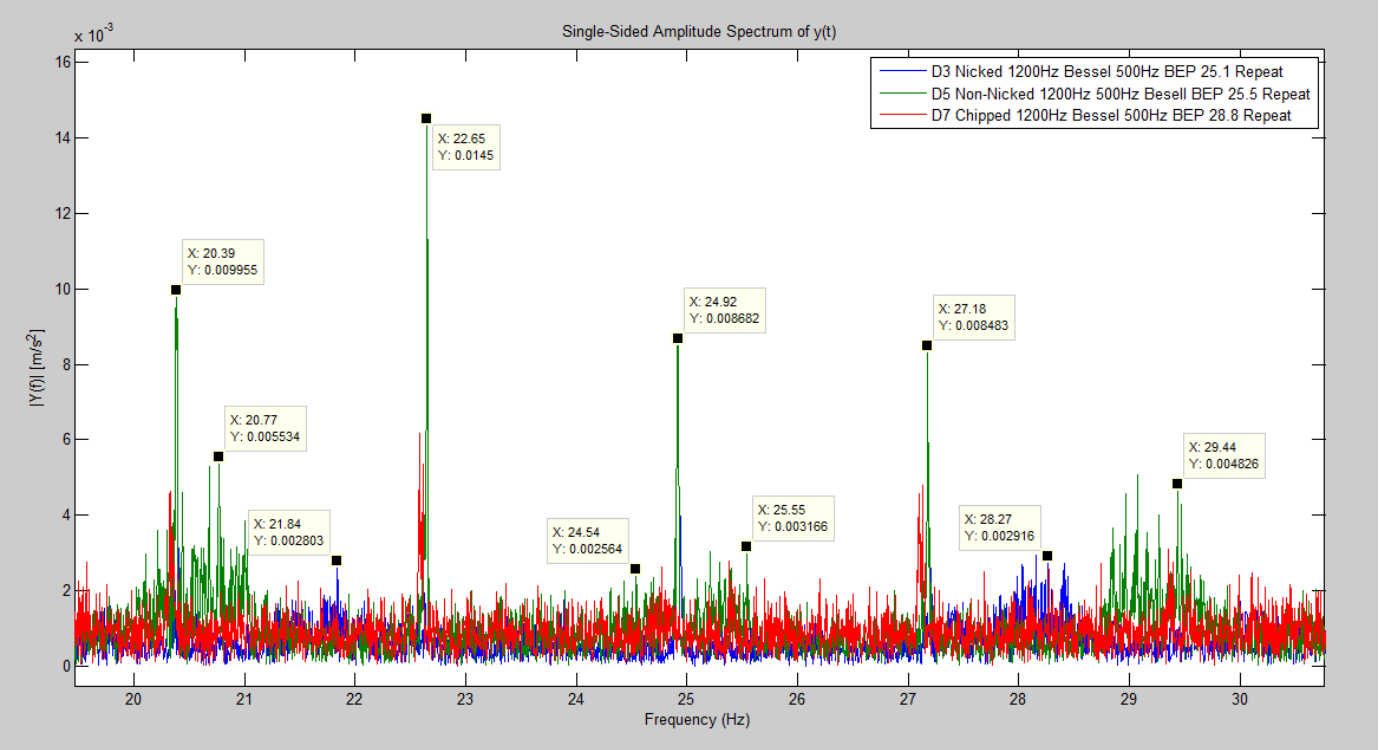

Figure 4-10 – Nicked and non-nicked 1200Hz characteristic bearing frequency

Figure 4-11 shows the zoomed-in PSD around the ball pass outer frequency as per Table 4-2. This test was sampled at 9600Hz with a Butterworth filter of 2000Hz. The ball pass outer frequency is expected at approximately 23.27Hz where it can be seen. However, the non-nicked bearings have this frequency as well (with the exception of the cone-nicked test not having this frequency). This shows that, under the loading conditions provided by the Lateral Machine, this characteristic frequency does not appear to be reliable in distinguishing between nicked and non-nicked bearings. Again, the running frequency

harmonics are seen. The roller and inner race defect frequencies are not seen in this instance.

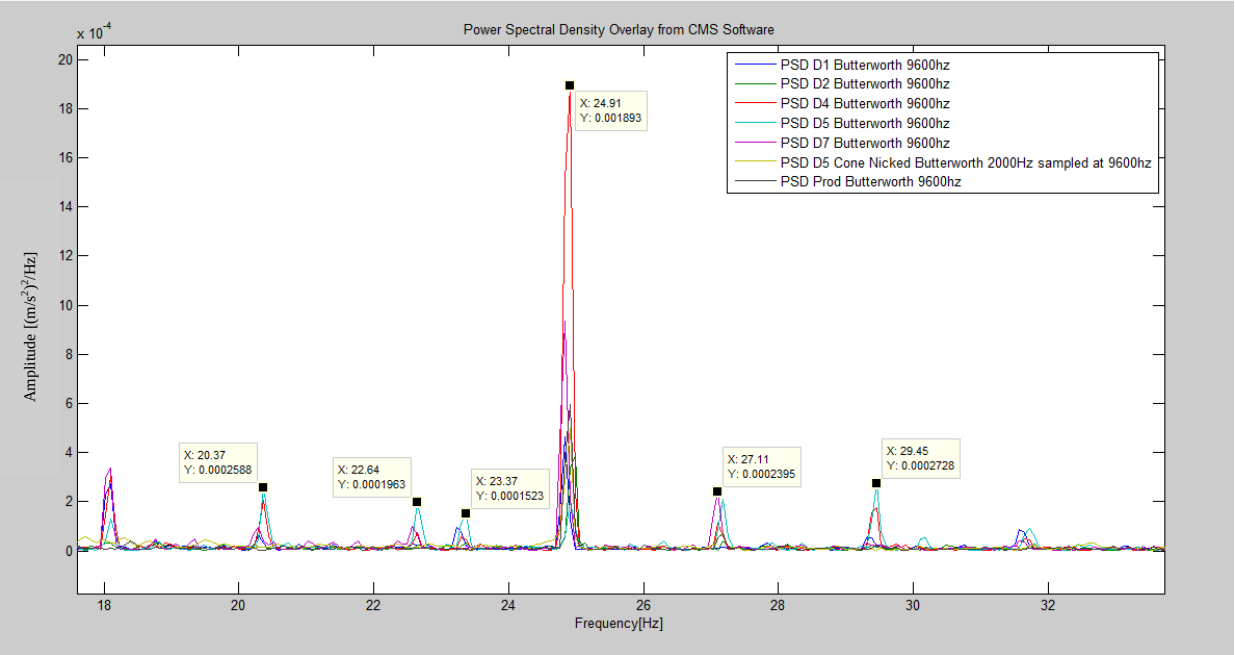

Figure 4-11 – PSD from CMS for nicked and non-nicked bearings at 9600Hz with a Butterworth filter at 2000Hz zoomed to show BPFO at 23.37Hz

Figure 4-12 shows the characteristic bearing frequencies which are visible at a sampling rate of 19200Hz. The high peaks at 24.91Hz and 27.11Hz are harmonics of the running frequency, and 23.3Hz is the outer defect frequency. This is not distinct in the resolution obtained at this sampling rate and the nicked and non-nicked frequencies are almost equally indistinct.

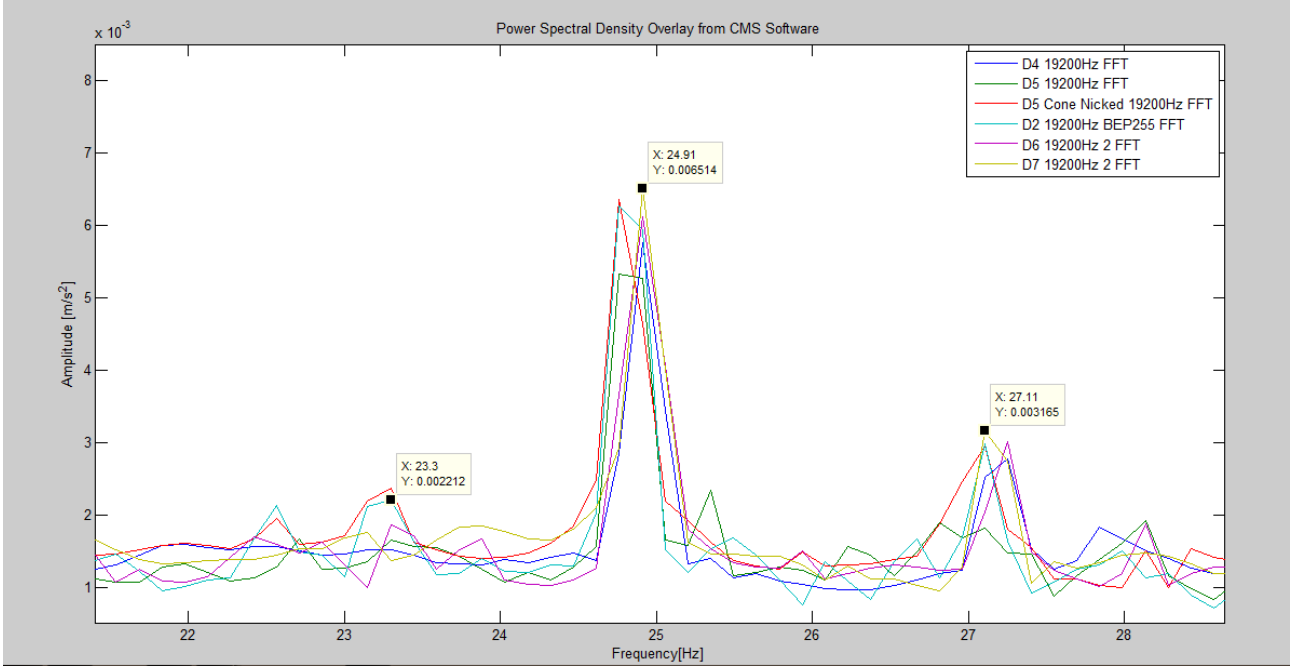

Figure 4-12 – FFT 19200Hz nicked and non-nicked with characteristic bearing frequencies

Through the various tests completed, the characteristic defect frequencies were not distinct nor were they repeatable or always visible in the nicked samples. This defect frequency is not consistently reproduced and this characteristic will not be a reliable indicator to distinguish between non-nicked (acceptable) and nicked (rejected) bearings.

What can be noted from the figures above in Section 4.2.1 is that the frequency spectra for nicked bearings do resemble the frequency spectrum for a damaged bearing in Figure 2-16 parts (a) and (b). The predominant cause of the shape of Figure 2-16 is as a result of the looseness within the bearing assembly when it suffers considerable damage. The Lateral Machine is measuring the bearings before they are installed in their intended application, and with a very large bench end-play, as compared to that when a bearing is installed and is within the mounted end-play tolerance. As a result of this it appears that the bearings are resembling a loose bearing frequency pattern. This could also explain why the bearing defect frequencies are not dominant as the bearings are not passing

through a loaded zone which is a requirement for the bearing defect frequencies to be pronounced.

4.2.3 Natural frequencies of components

The natural frequency of a cone and cup was measured[1] to determine if the measured bearing frequencies were as a result of cone or cup resonance. Figure 4-13 shows the two peaks associated with the natural frequencies at 1403Hz and 2116Hz for cones. Figure 4-14 shows the natural frequencies of a cup with peaks at 936.5Hz, 1235Hz, 2539Hz and 4463Hz. Other components were not measured as it was not practical to do so with the size of accelerometer available. The calculated frequencies in Table 4-2 are similar in range to the frequencies achieved during the testing. The calculated frequencies were for the assembly together and not for the components and thus the differences are expected.

It must be noted that the line which is visible on approximately 4400Hz on Figure 4-13 is not a frequency peak but a cursor on the graph.

[1] The natural frequency was measured by gluing an accelerometer on the components and suspending them by string and tapping them with a piece of steel. The tests were repeated and the repeatable frequencies are shown.

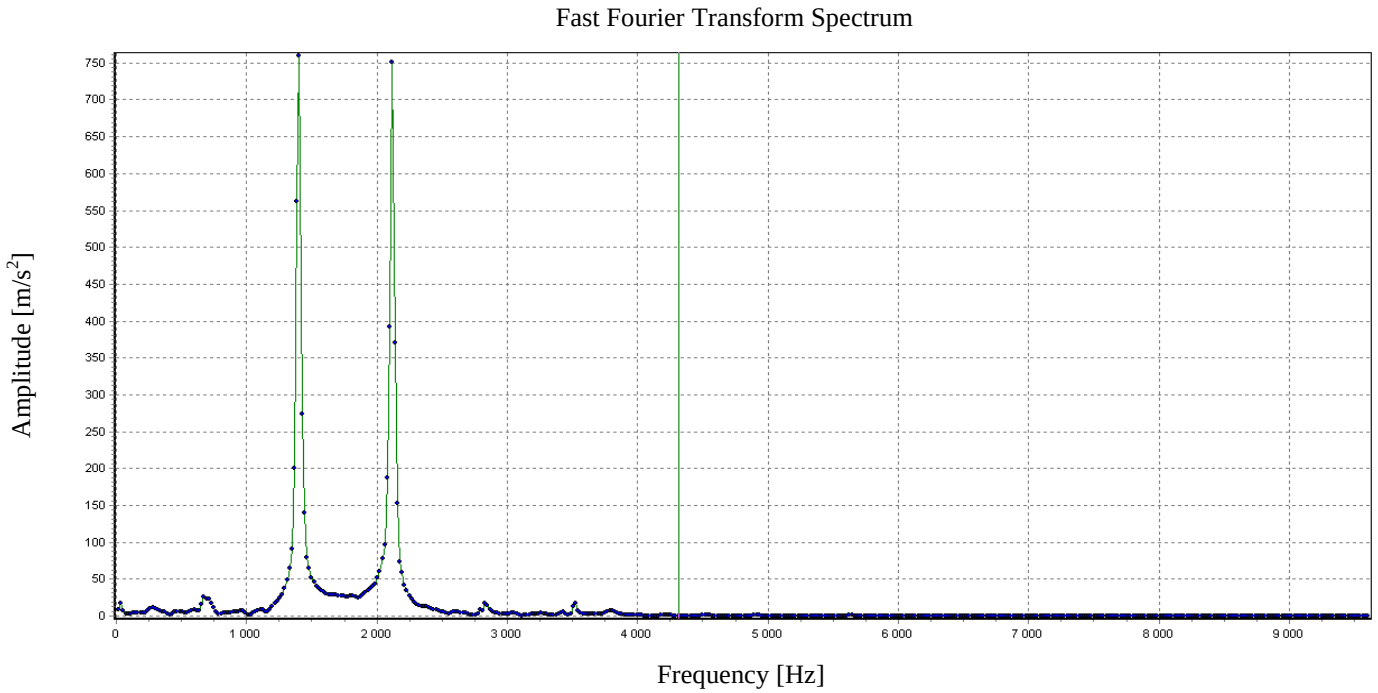

Figure 4-13 – FFT of Cone Natural Frequency (Peaks at 1403Hz and 2116Hz)

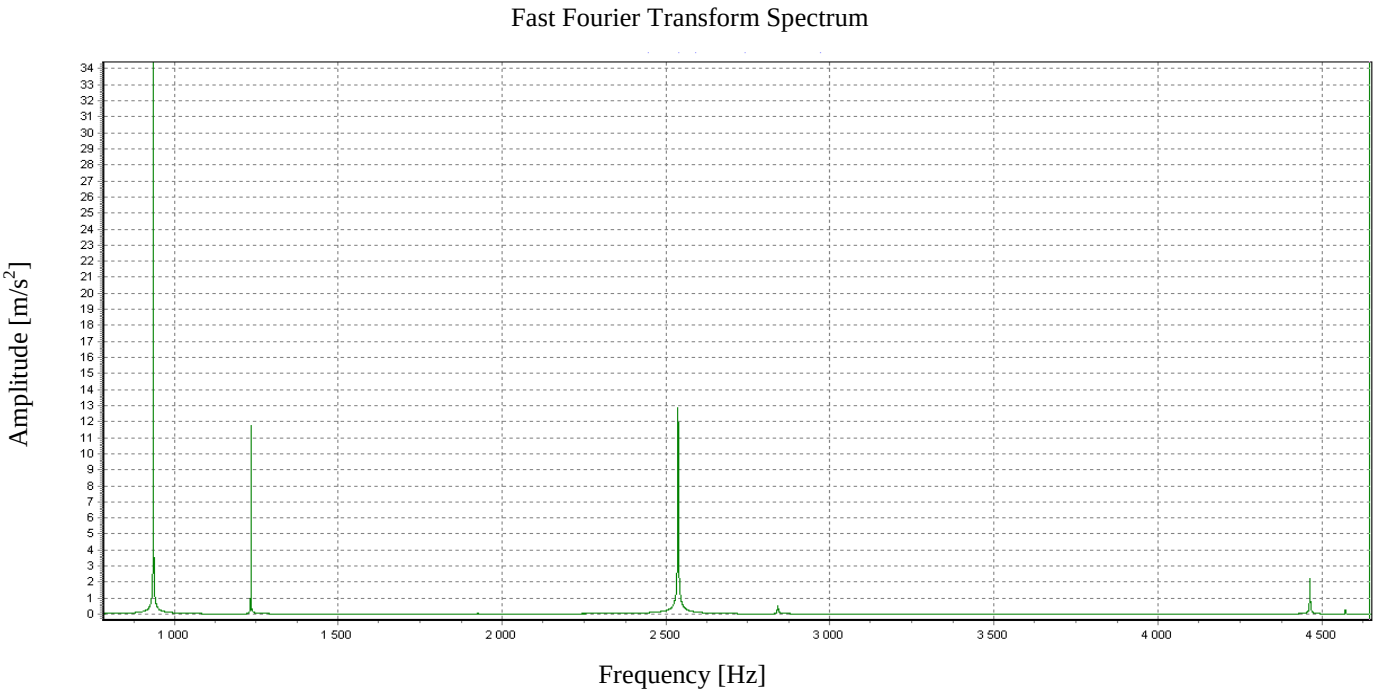

Figure 4-14 – FFT of a class D cup natural frequency (Peaks at 936.5Hz, 1235Hz, 2539Hz and 4463Hz)

4.3 Non-nicked Bearings Limits

Due to the non-repeatable results obtained from the defect frequencies as described in the previous chapter it was noted that the peaks associated with the nicked bearings were always larger than those in the non-nicked bearings, but in different parts of the frequency spectrum. Thus non-nicked bearing measurements were taken for all test parameters (at similar sampling rates) and were overlaid in Matlab. Based on the repeatability achieved, as well as the amplitudes associated with particular frequencies, that were repetitive in the testing, limits were defined for an acceptable bearing. Figure 4-15 to Figure 4-18 show the plots for each sampling frequency of non-nicked bearings. These all have a limit drawn across the frequency spectrum in blue which shows the frequency and corresponding amplitude limits for an acceptable bearing. All of the individual PSD's of the non-nicked bearings are shown in Appendix F. The limits determined in Figure 4-15 to Figure 4-18 were drawn for a sample of eight non-nicked bearings and show reasonable repeatability. The limits set were not for average amplitudes achieved but for the maximum amplitudes.

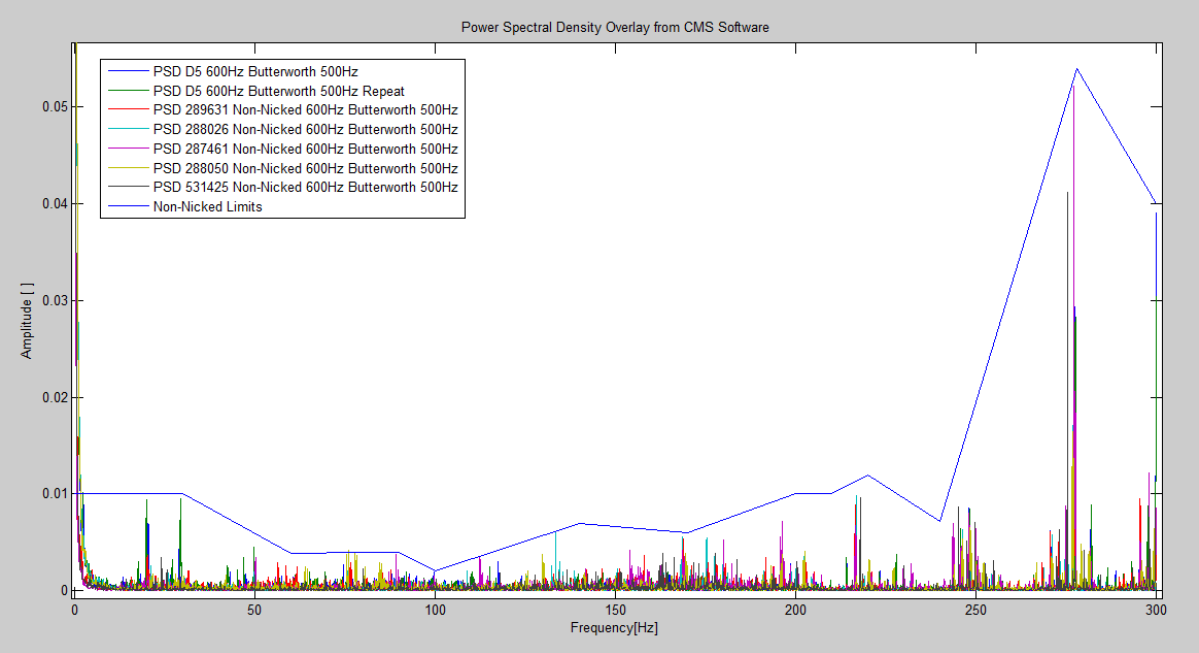

Figure 4-15 – PSD at 600Hz of non-nicked bearings with limits

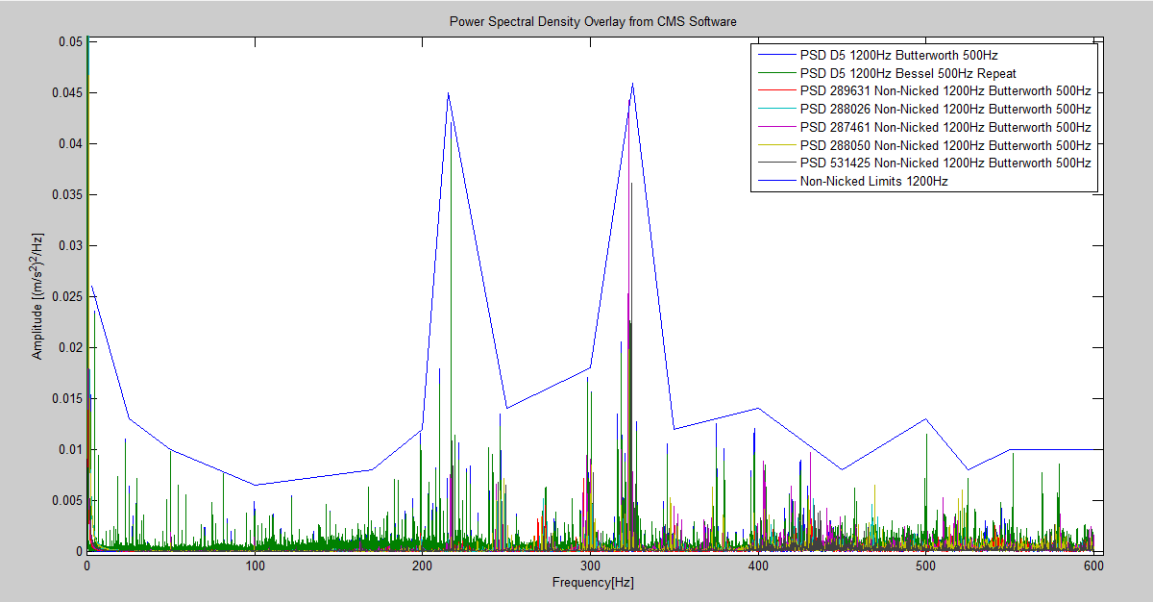

Figure 4-16 – PSD at 1200Hz of non-nicked bearings with limits

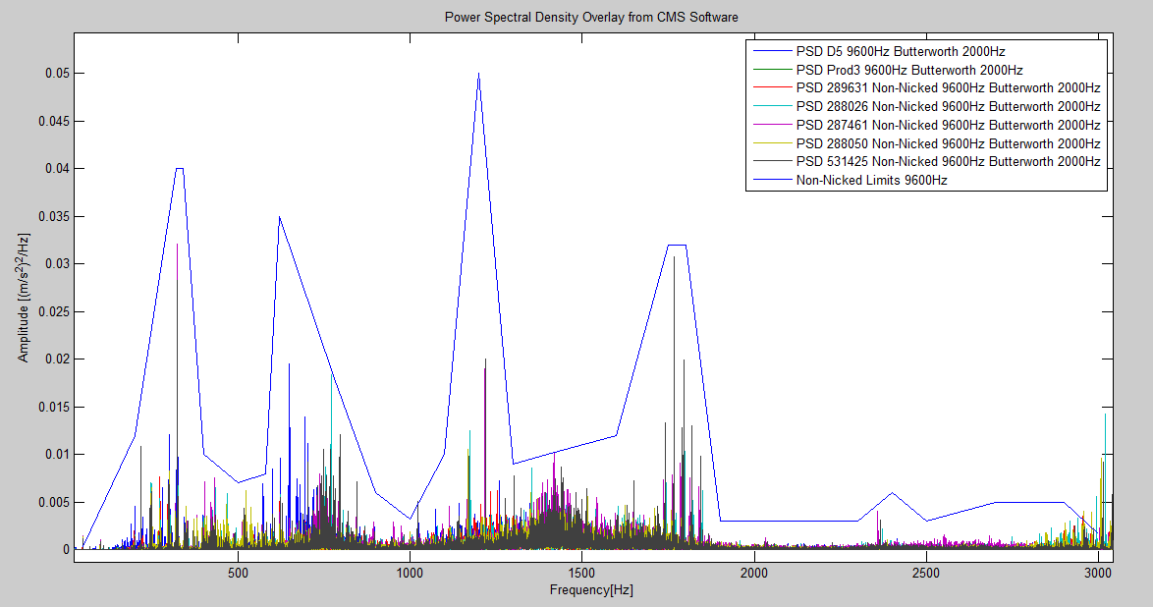

Figure 4-17 – PSD at 9600Hz of non-nicked bearings with limits

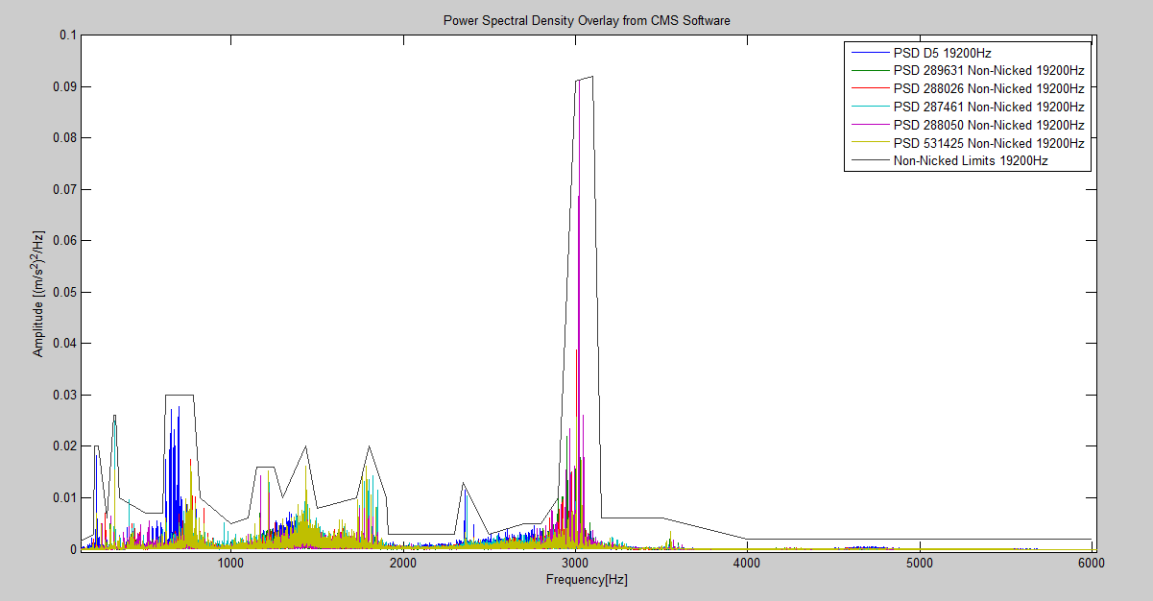

Figure 4-18 – PSD at 19200Hz of non-nicked bearings with limits

In Figure 4-17, sampled at 9600hz, frequencies up to a frequency range of 3000Hz can be seen. On Figure 4-18, sampled at 19200Hz, which has a greater range the peaks are also only defined up until 3000Hz. In Figure 4-16, sampled at 1200Hz more resolution is

available than in Figure 4-15, sampled at 600Hz. Thus in the following chapters only information from sampling frequencies 1200Hz and 9200Hz will be discussed, as these are the frequencies sampled with the Microtron accelerometer that give the most information as compared to the other two sampling frequencies. There are, however, in Appendix F, tests which show nicked and non-nicked bearing frequency plots with limits applied for all of the sampling frequencies.

4.4 Nicked Bearing Comparisons

As discussed in Section 4.3 limits have been created for all non-nicked bearings. This has been done so that nicked bearings can be measured against these limits to see if the amplitudes associated with particular frequencies for the nicked bearings are greater than those of the non-nicked bearings. In this section particular nicked bearings will be shown with their measured PSD's overlaid with the limits. These will be shown at two sampling frequencies to determine if one of the two sampling frequencies provide better information.

As mentioned in the previous sections tests at sampling frequencies of 600Hz and 19200Hz will not be shown in this section. They are available in Appendix F.

D1 Nicked bearing

Bearing D1 was only measured at 9600Hz sampling rate (see Figure 4-19). It is evident that this nicked bearing does exceed the limits as set by the non-nicked bearings sampled at 9600hz. The most prominent frequencies that are visible and exceed the limits are 50Hz, 100Hz and a range between 400Hz and 500Hz.

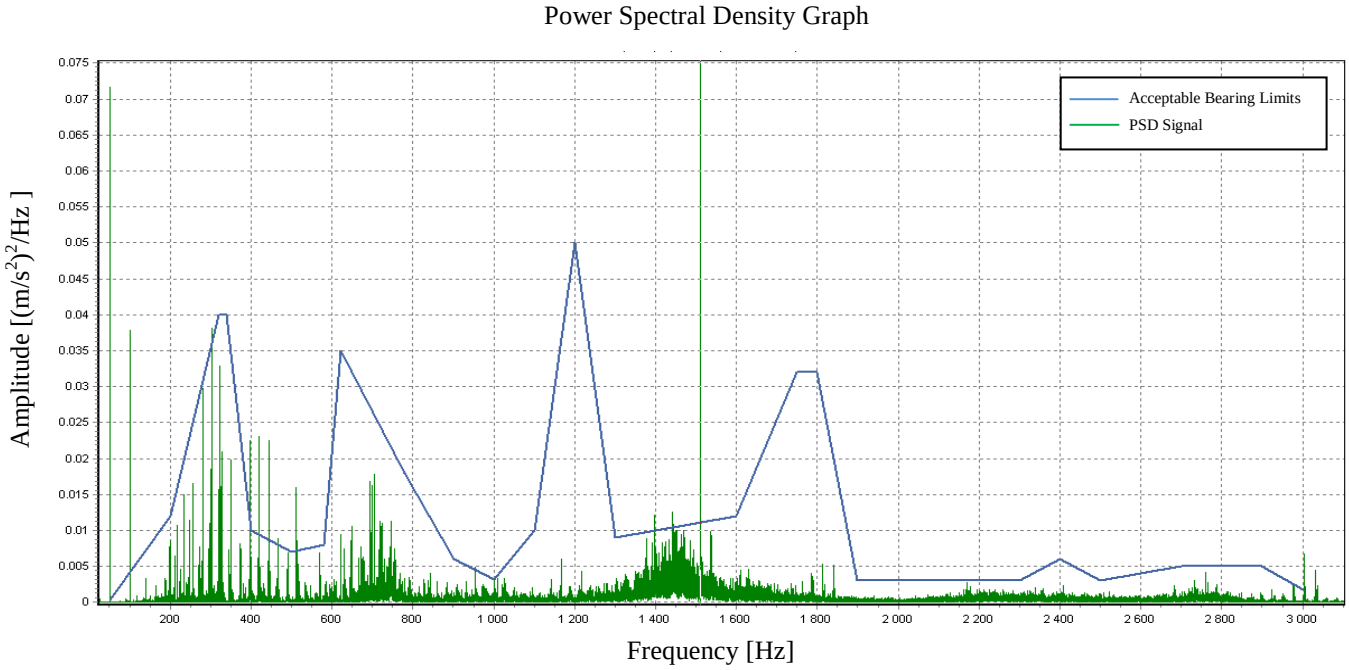

Figure 4-19 – D1 Nicked 9600Hz Butterworth 2000Hz bearing PSD from CMS software

D2 Nicked Bearing

Three sets of tests on Bearing D2 were conducted. Figure 4-20 shows bearing D2 sampled at 1200Hz, with a Butterworth filter set to 500Hz. Figure 4-21 is also sampled at 1200Hz but the filter used is a Bessel filter. In both these figures the limits, as defined by the non-nicked bearings in Figure 4-16, are exceeded, and especially at 50Hz and 100Hz frequencies. The Bessel filtered function also exceeds the limit at approximately 325Hz. Figure 4-22 shows bearing D2 sampled at 9600hz and again the limits are exceeded at 50Hz and 100Hz. It is also noted that the bearings sampled at 1200Hz have a strong frequency response at the running speed harmonics shown from 0Hz to 100Hz. In the test sampled at 9600Hz it can be seen that the frequencies around approximately 1500Hz are excited and this is very close to the natural frequency of the cup. This correlates with McFadden and Smith's (1984) theory that defects in bearings are excited through the resonance frequencies of the components.

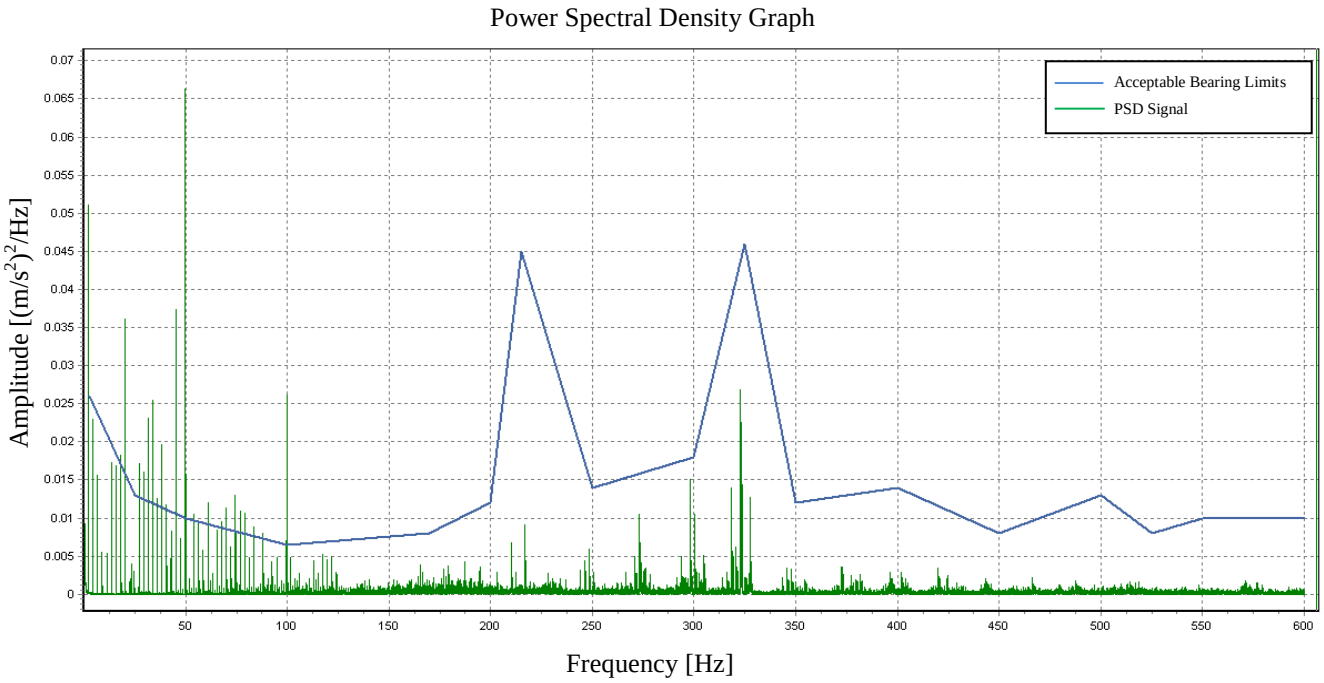

Figure 4-20 – D2 nicked 1200Hz Butterworth 500Hz PSD from CMS with D5 non-nicked bearing limit

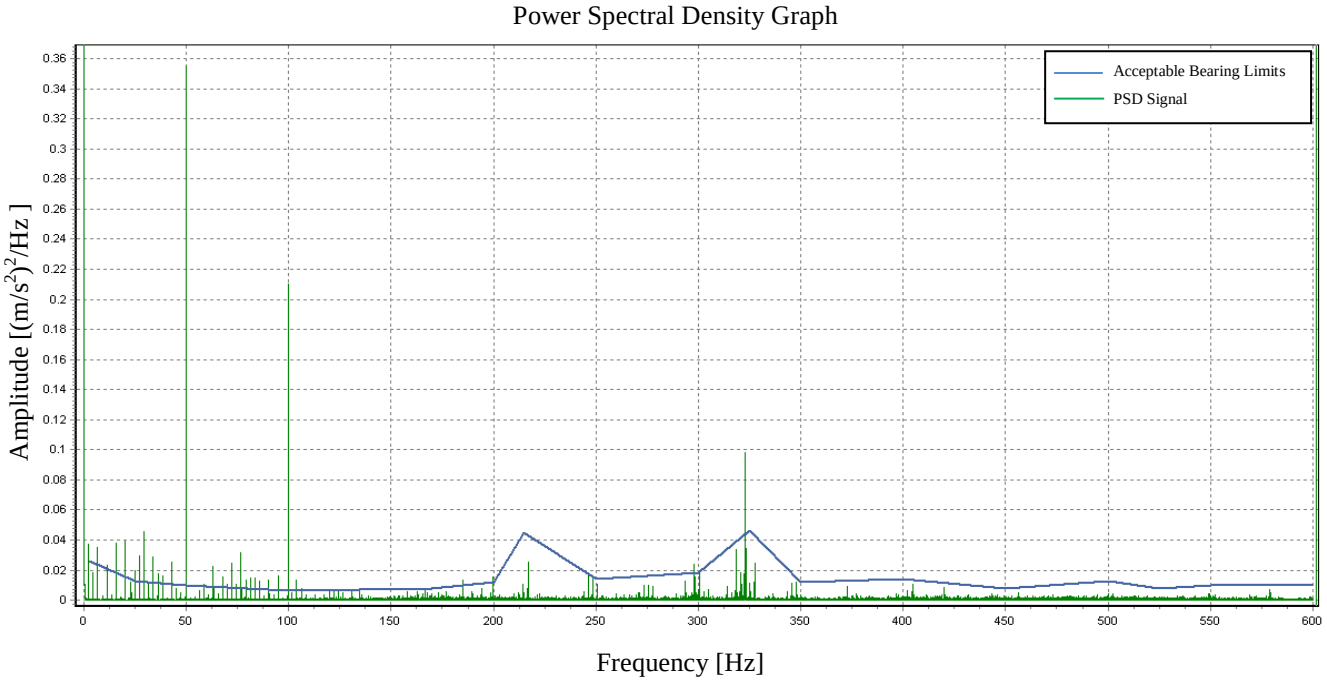

Figure 4-21 – D2 Nicked 1200Hz with 500Hz Bessel filter PSD from CMS with limits from non-nicked bearings

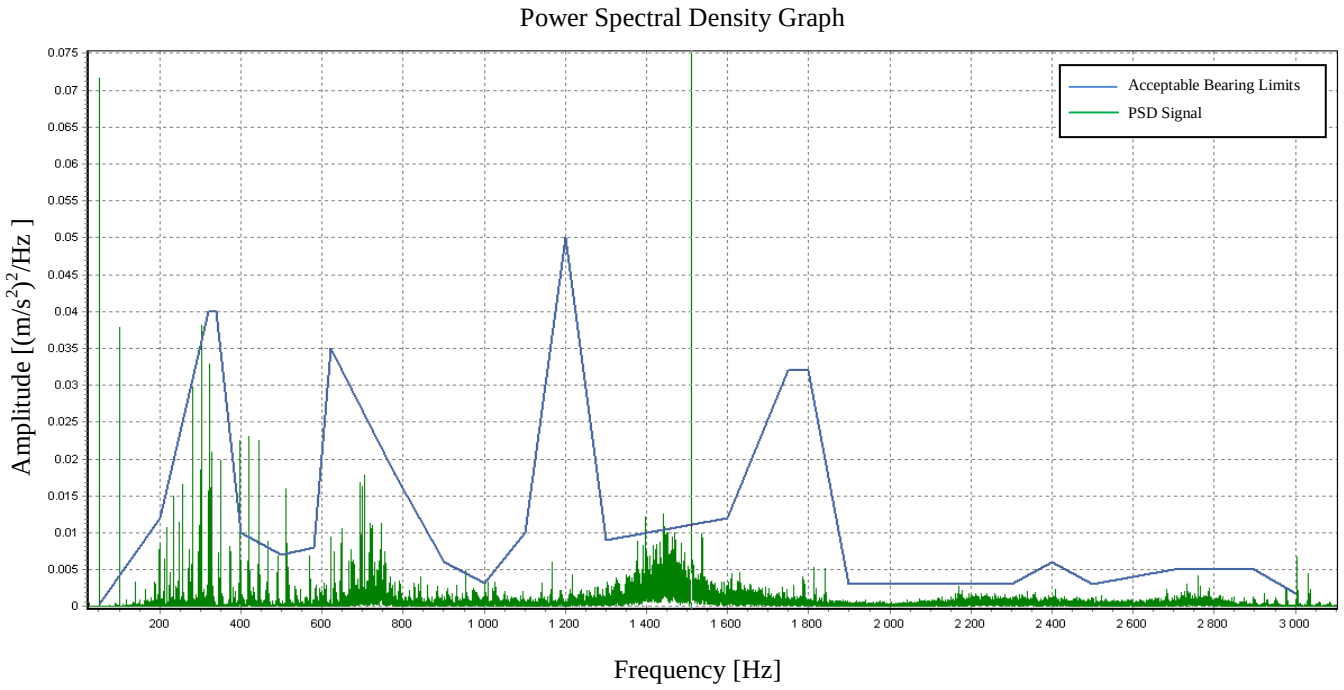

Figure 4-22 – D2 nicked 9600Hz Butterworth 2000Hz PSD from CMS software

D3 Nicked bearing

Nicked bearing D3 shows running frequencies (2.262Hz to 100Hz) in Figure 4-23 but amplitudes that do not exceed the defined limits. However, the limits are exceeded at approximately 270Hz. In Figure 4-24, sampled at 9600Hz, the limits are strongly exceeded at 50Hz and 100Hz.

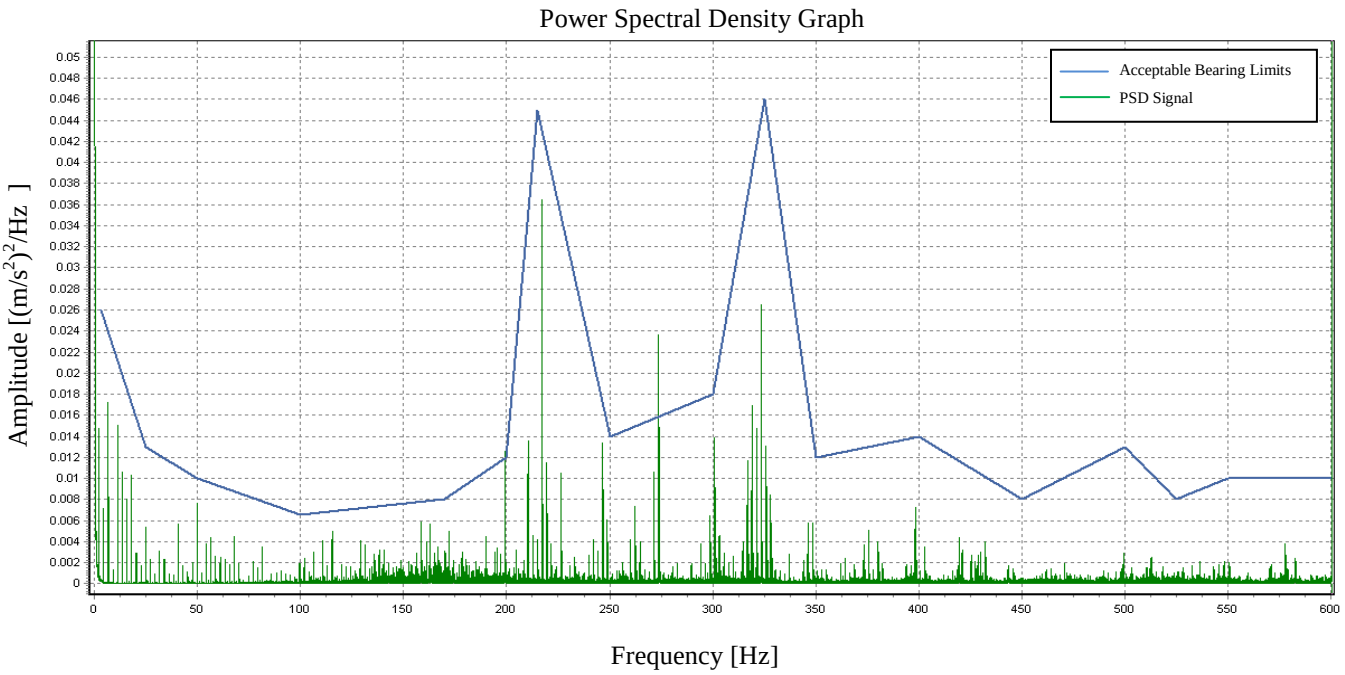

Figure 4-23 – D3 nicked 1200Hz Butterworth 500Hz BEP 25.1 PSD from CMS with limits from non-nicked D5

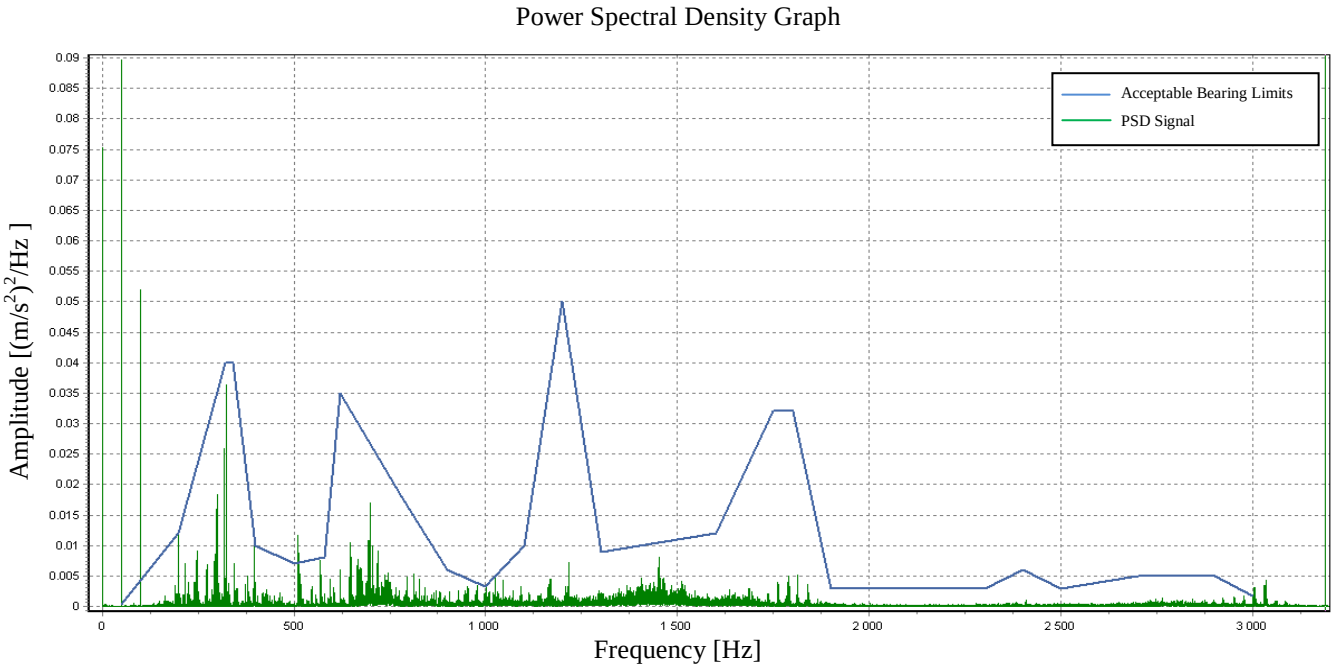

Figure 4-24 – D3 nicked PSD 9600Hz Butterworth 2000Hz from CMS software

D4 Nicked bearing

Bearing D4 shows increased amplitude in the running frequencies in Figure 4-25, and the limits are exceeded. The 50Hz and 100Hz frequencies are also prominent. In Figure 4-26, sampled at 9600Hz, the 50Hz and 100Hz frequencies are greater than the limits as well as the frequencies at approximately 200Hz.

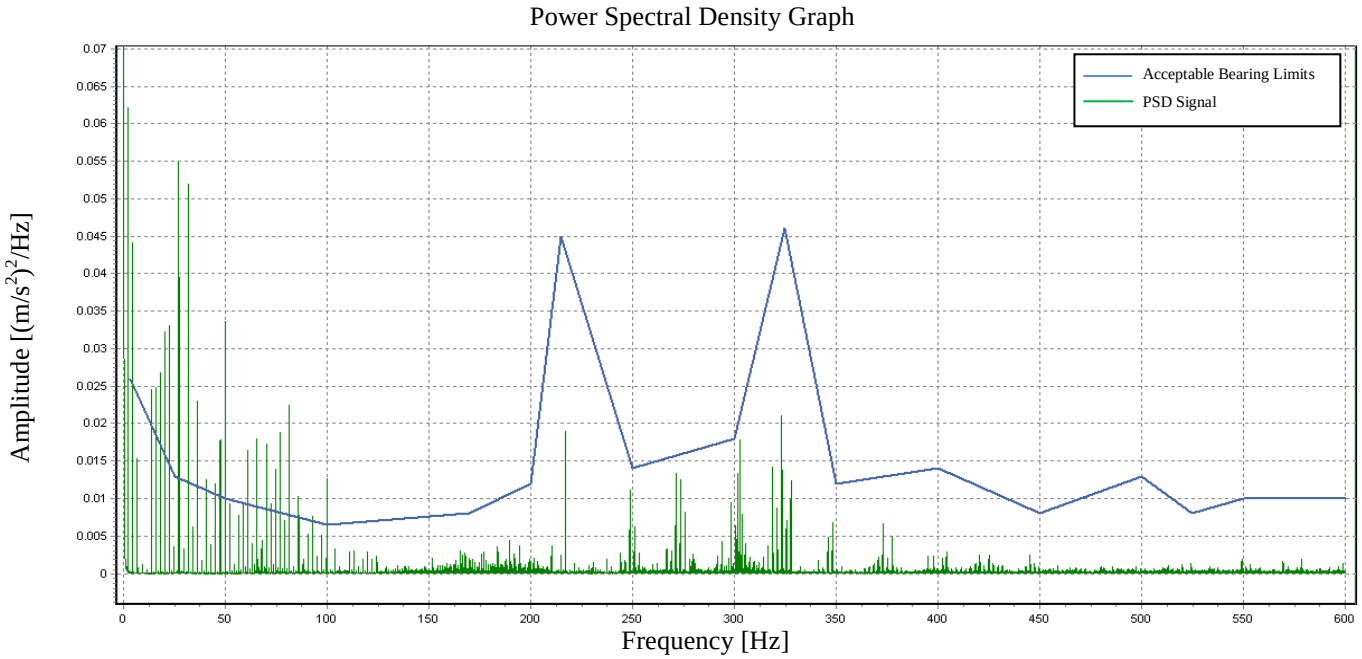

Figure 4-25 – D4 nicked 1200Hz Butterworth 500Hz filter BEP26.0 PSD from CMS with limits from non-nicked bearings

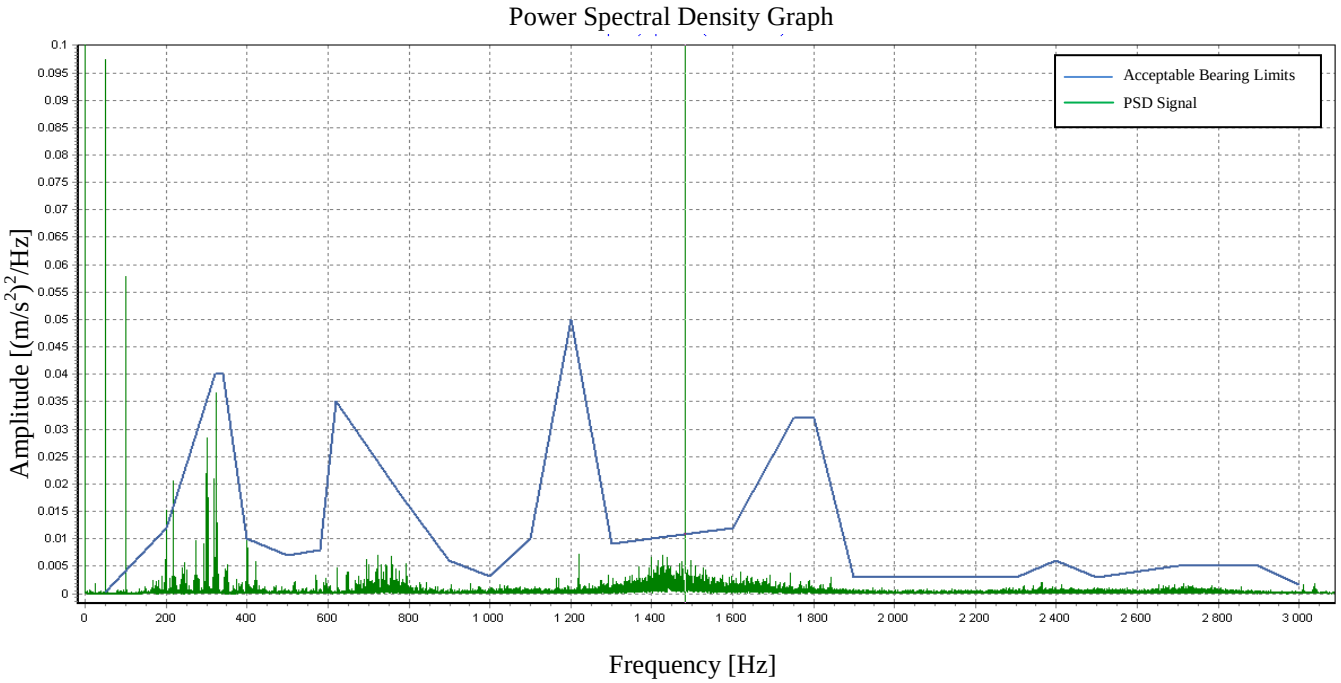

Figure 4-26 – D4 nicked PSD 9600Hz Butterworth 2000Hz from CMS software

D6 Nicked bearing

In Figure 4-27, sampled at 1200Hz, bearing D6 exceeds the limits at the running frequencies, 50Hz and 100Hz as well as at approximately 275Hz and 325Hz frequencies. In Figure 4-28, sampled at 9600Hz, the limits are exceeded at 50Hz, 100Hz, 200Hz, 320Hz and 400Hz. Again, the amplitudes are increased around the resonance frequency of the cup at 1500Hz.

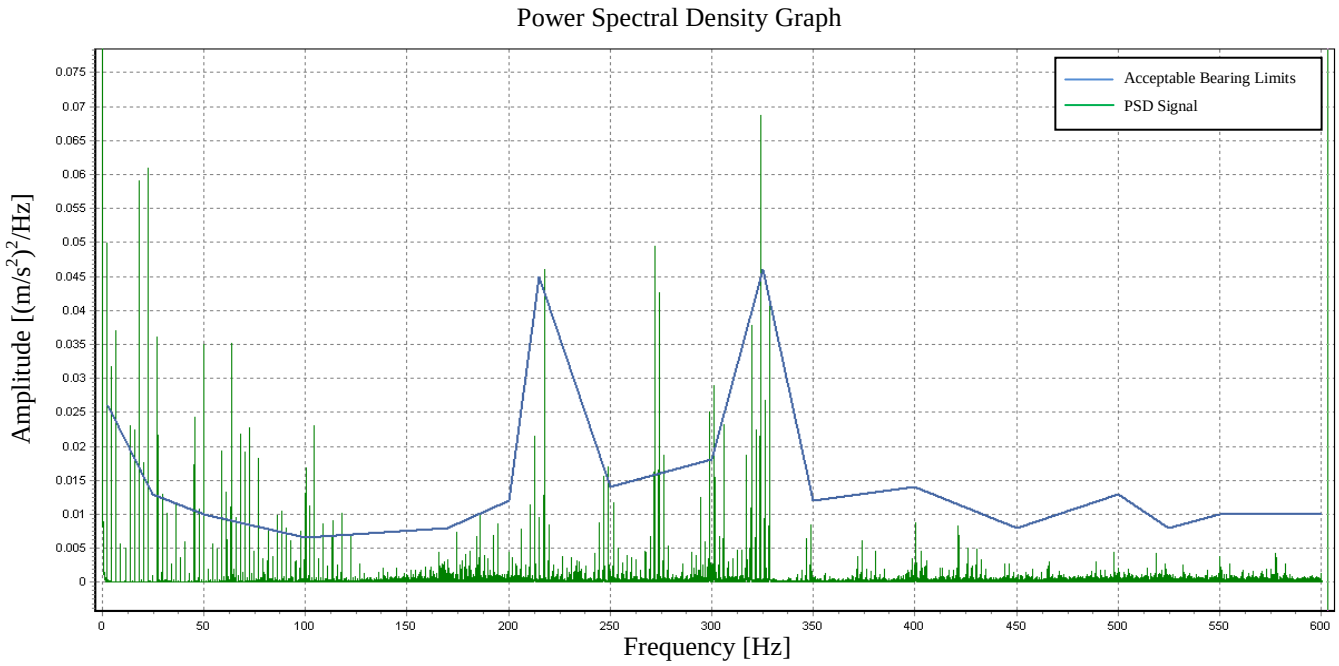

Figure 4-27 – D6 nicked 1200Hz Butterworth filter 500Hz BEP27.4 PSD from CMS with limits from non-nicked bearings

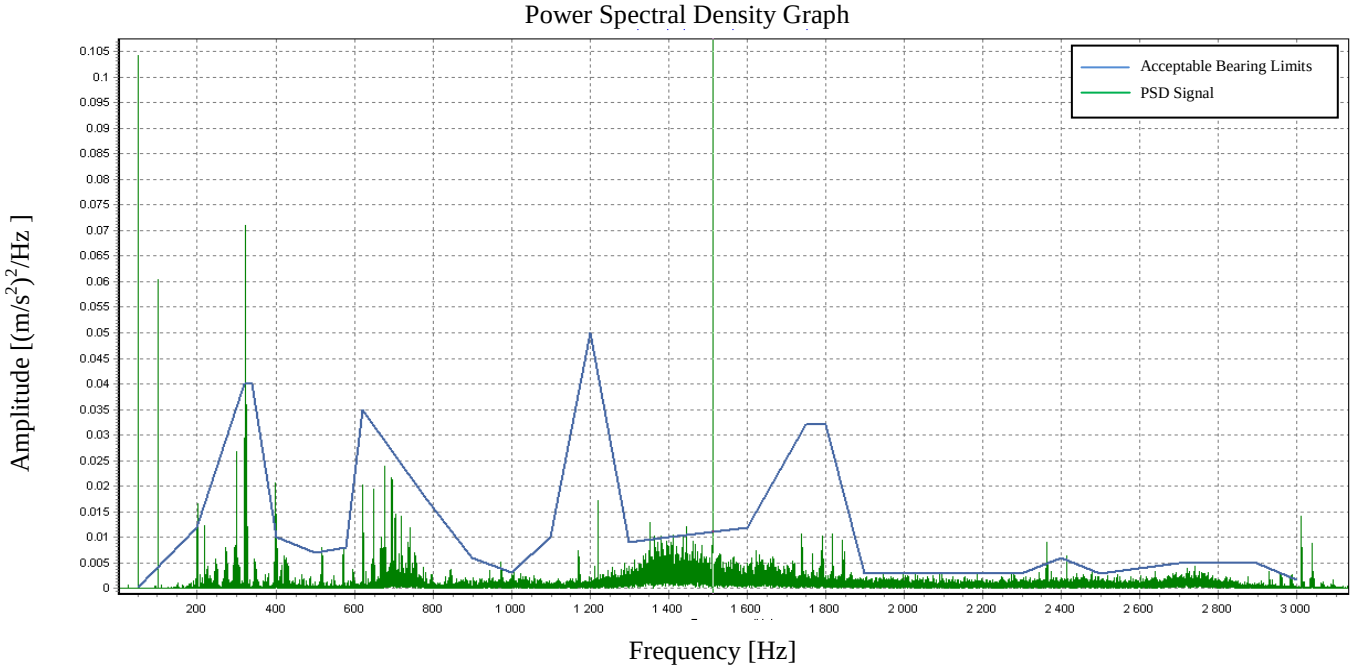

Figure 4-28 – D6 nicked PSD 9600Hz Butterworth 2000Hz from CMS software

D7 Nicked bearing

Bearing D7 is the chipped bearing where most of the defect is out of the running position of the roller i.e. the chip is on the edge of the raceway. In Figure 4-29 the limits are greatly exceeded at a few running frequencies as well as at 270Hz. At a sampling rate of 9600Hz, Figure 4-30, the limits are exceeded at various positions including the 50Hz and 100Hz location as well as by the natural frequency of the cup around 1500Hz. At approximately 320Hz, 500Hz and 700Hz the limits are also exceeded.

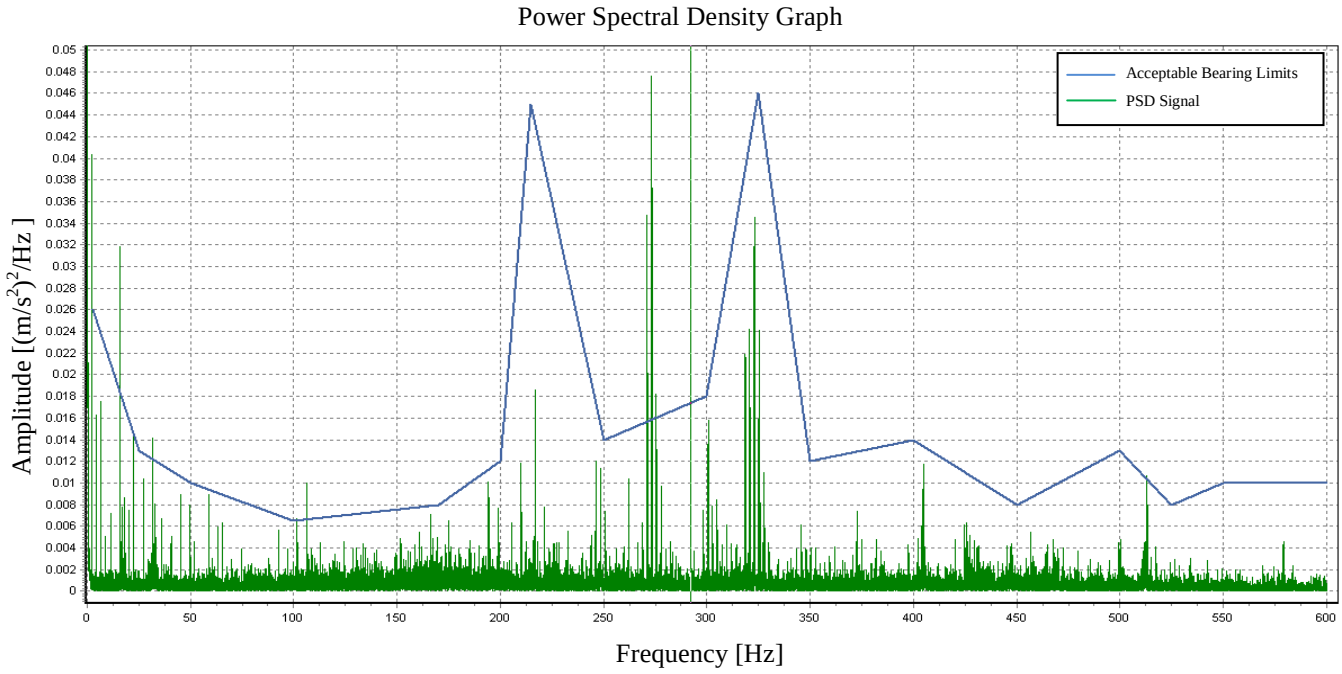

Figure 4-29 – D7 Chipped 1200Hz Bessel filter 500Hz BEP 28.8 PSD from CMS with limits from D5 non-nicked bearing

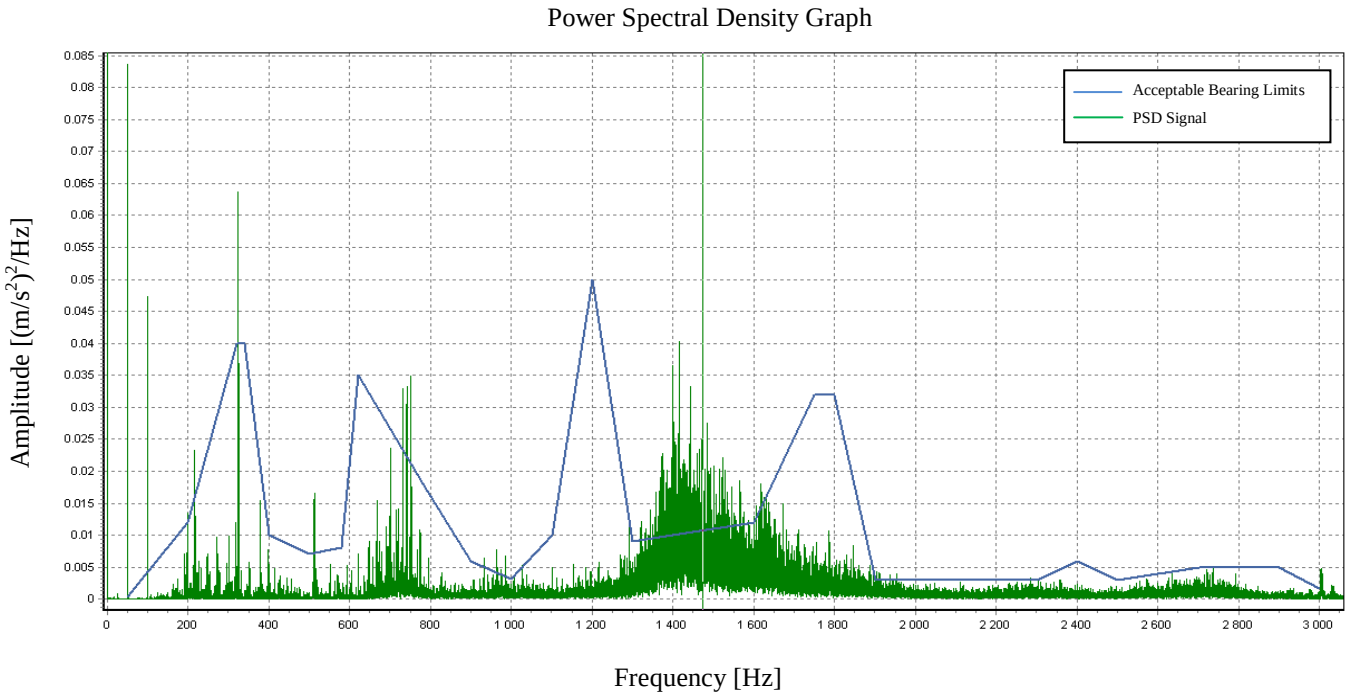

Figure 4-30 – D7 nicked PSD 9600Hz Butterworth 2000Hz from CMS software

Table 4-6 is a summary of the frequencies with high amplitudes in each of the bearings sampled at 1200Hz. The X denotes the frequency range in which the amplitudes peak and if the phenomena of running speed is present or not. The additional samples taken of non-nicked bearings which are in Appendix F are not tabulated above. These however do have similar peaks to D5 (the non-nicked bearing).

Table 4-6 : Results tabulation of 1200Hz nicked and non-nicked frequencies

	Non-nicked	**Nicked**				
	D5	D2[1]	D3	D4	D6	D7
50Hz & 100Hz		X		X	X	
Running Speed		X	X	X	X	X
200Hz - 250Hz	X				X	X
250Hz - 300Hz			X		X	X
300Hz - 350Hz	X				X	X

[1] Shaded cells are Bearings with Roller-spaced Nicks

Table 4-7 shows a summary of all of the bearings' PSD's sampled at 9600Hz and the characteristic frequencies noted in these figures. The non-nicked bearings which were tested for repeatability purposes and are in Appendix F are not included in the table.

Table 4-7 : Results tabulation of nicked and non-nicked frequencies at 9600Hz

	Non-nicked		**Nicked**					
	Production	D5	D1	D2[1]	D3	D4	D6	D7
50Hz & 100Hz			X[2]	X	X	X	X	X
Running Speed			X					
200Hz - 300Hz						X		X
600Hz - 800Hz	X	X		X				X
1200Hz	X							
1400Hz – 1600Hz			X				X	X

Table 4-8 shows a summary of the frequency peaks seen in the PSD of bearings sampled at 19200Hz. This shows that there are frequencies which are not triggered by the non-nicked bearings and which make the nicked bearings unique from the non-nicked samples. These figures are in Appendix F and the difference between the nicked and the non-nicked bearings are not that great, although they are there.

Table 4-8 : Tabulated frequency results of nicked and non-nicked bearings at 19200Hz

	Non-nicked	**Nicked**				
	D5	D2	D4	D6	D7	D5 Cone Nicked
50Hz & 100Hz			X	X	X	X
Running Speed						
200Hz - 300Hz	X	X	X	X		X
600Hz - 800Hz	X					X
1200Hz		X	X			X
1400Hz – 1600Hz				X	X	
2000Hz – 3000Hz		X	X	X	X	

[1] Shaded Cells are Bearings With Roller-spaced Nicks
[2] X denotes that the characteristic is present

For the sampling rates of 9600Hz and 1200Hz, when the limits were applied to the nicked bearings in the above figures, it can be seen that the nicked bearings exceed the limits in every case. This shows that, with further testing and refinement of the limits, nicked bearings are distinuishable from non-nicked bearings based on the principle that they are not only examined in one particular frequency band, but that examination occurs across a wide range of frequencies. As shown in Appendix E the limits for the bearings sampled at 600Hz and 19200Hz show that nicked and non-nicked bearings are also detectable at this sampling rate. However the difference between the nicked and the non-nicked samples is not great and thus these sampling rates should preferably not be used. The advantage of sampling at 9600Hz over 1200Hz is that the natural frequency of the bearing components become visible in the frequency spectrum and the nicked samples seem to excite these frequencies more than the non-nicked samples. This is in-line with the material presented on bearing resonance calculations in Section 2.4.1.

4.5 Physical Acquisition Parameters

4.5.1 Testing duration

It was considered that the duration of the testing could possibly result in different findings. At the early stages of testing only the standard time of the Lateral Machine was used, which was approximately 14 seconds for both the upward and downward motion of the machine. It was then decided to increase the testing duration to a maximum of 200 seconds, with intervals shorter in duration than that as well. The testing was also only done in the second half of the Lateral Machine cycle which is when the downward force is applied.

Measurements sampled at 1200Hz were truncated to 50 second sample lengths in order to determine if the limits would still be followed as per the full 200 second test duration. In all test cases the amplitudes varied slightly for the same frequencies but did not alter the outcome. This was checked with nicked and non-nicked bearings of which two examples are shown in Figure 4-31.

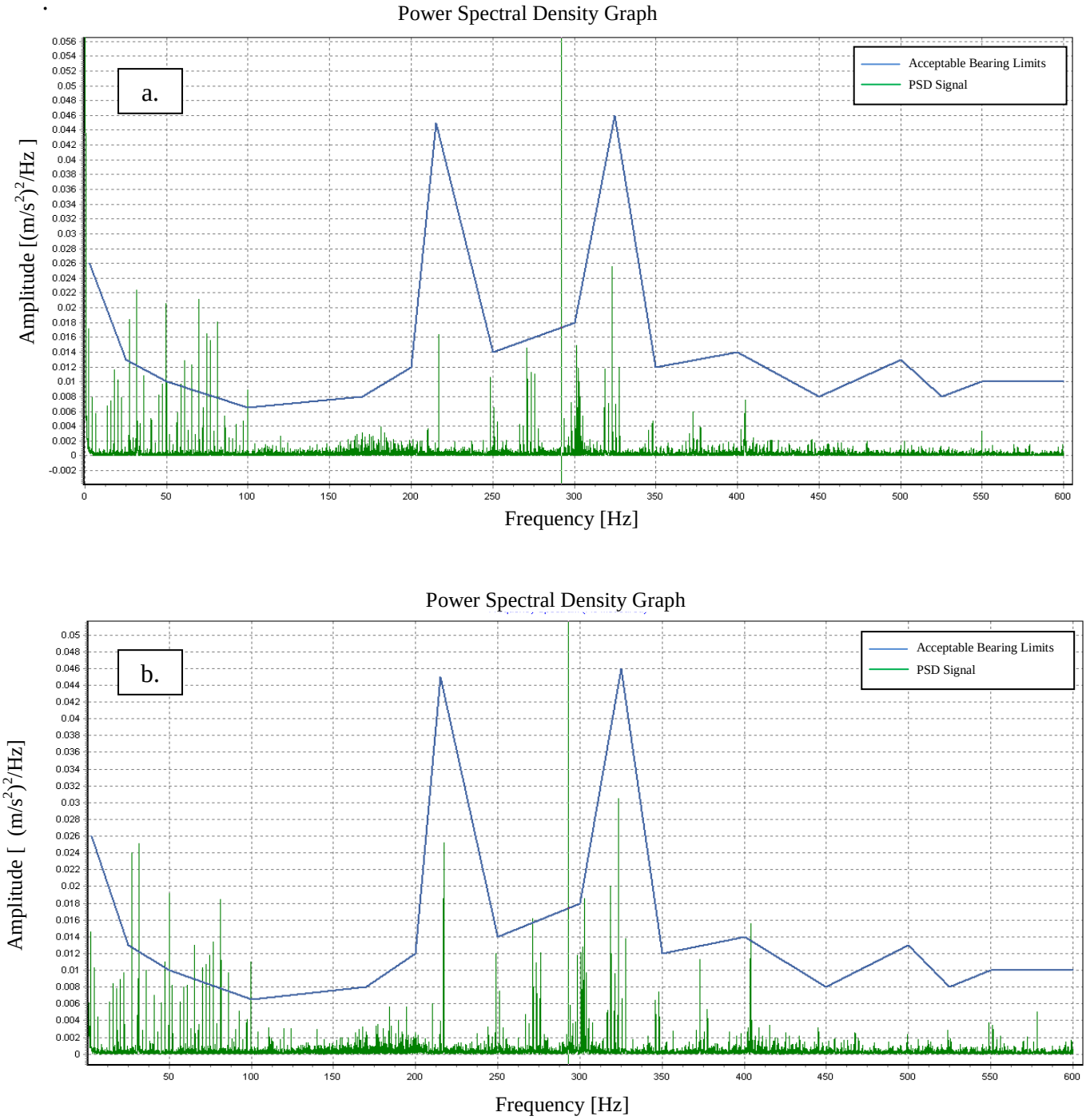

Figure 4-31 – D4 nicked bearing 1200Hz Bessel 500hz PSD from CMS with D5 non-nicked Limits a. 0 – 50 seconds and b. 100 – 150 seconds

Tests of nicked bearing D2 were taken and different time duration intervals were captured from one signal of long duration. At first testing was performed at 10s, 20s, 40s and 80s intervals as seen in Figure 4-32. These plots contain the PSD's of the same data acquisition signal but truncated for the various lengths as described. The limits were still exceeded as per the long interval test with slight changes in amplitude between the different durations.

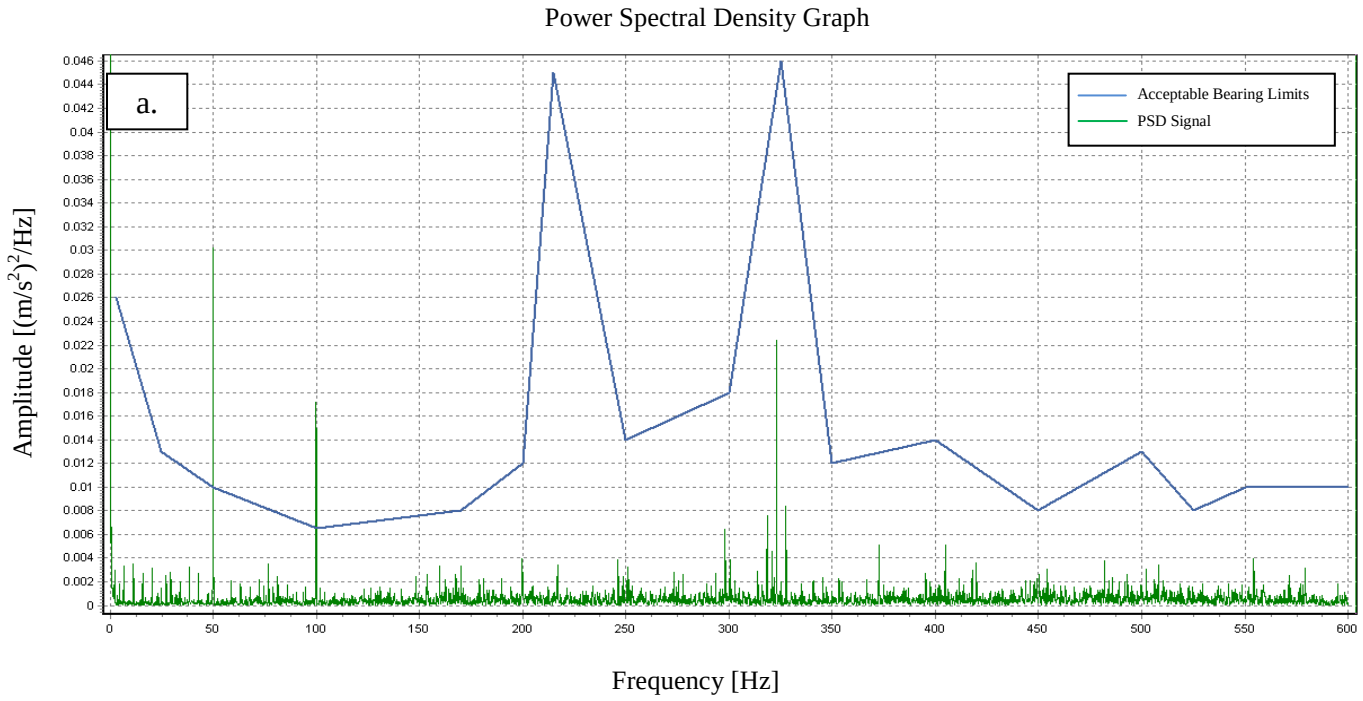

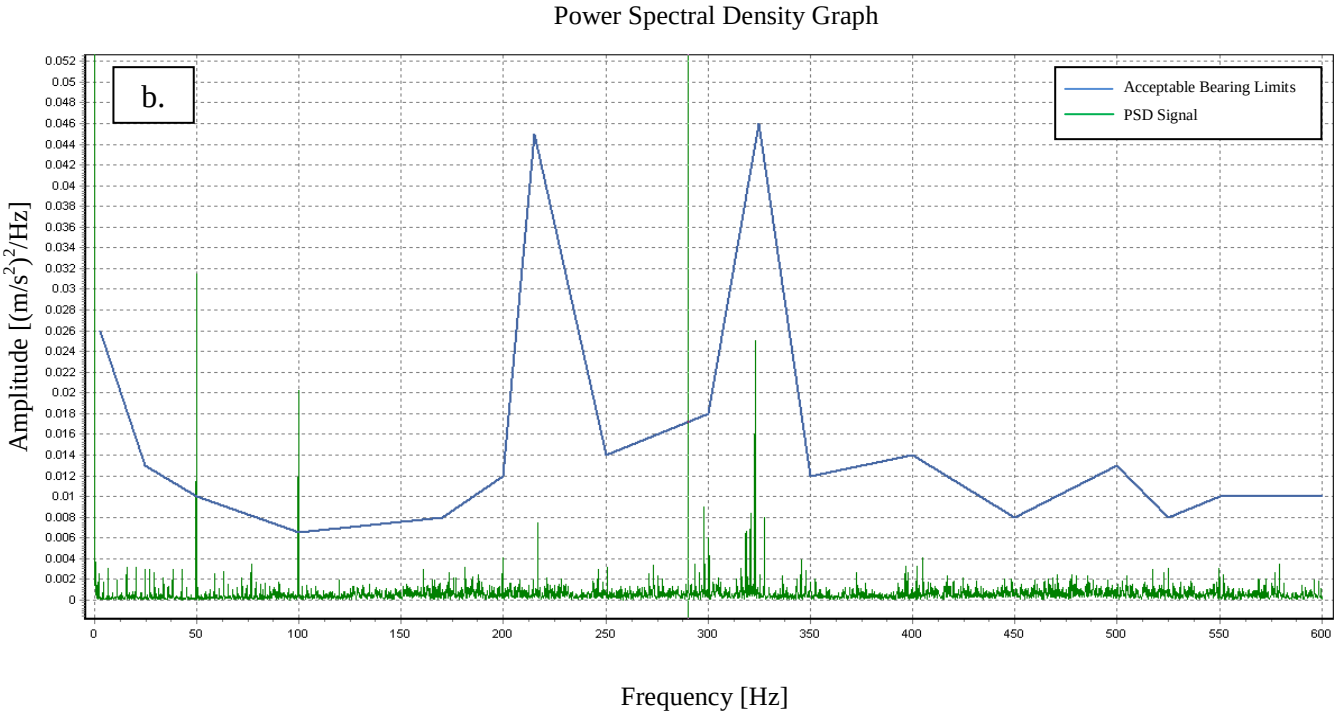

Figure 4-32 - D2 Nicked 1200Hz Bessel 500Hz filter PSD from CMS with D5 non-nicked Limits a. 0-10 Seconds b. 10-30 Seconds

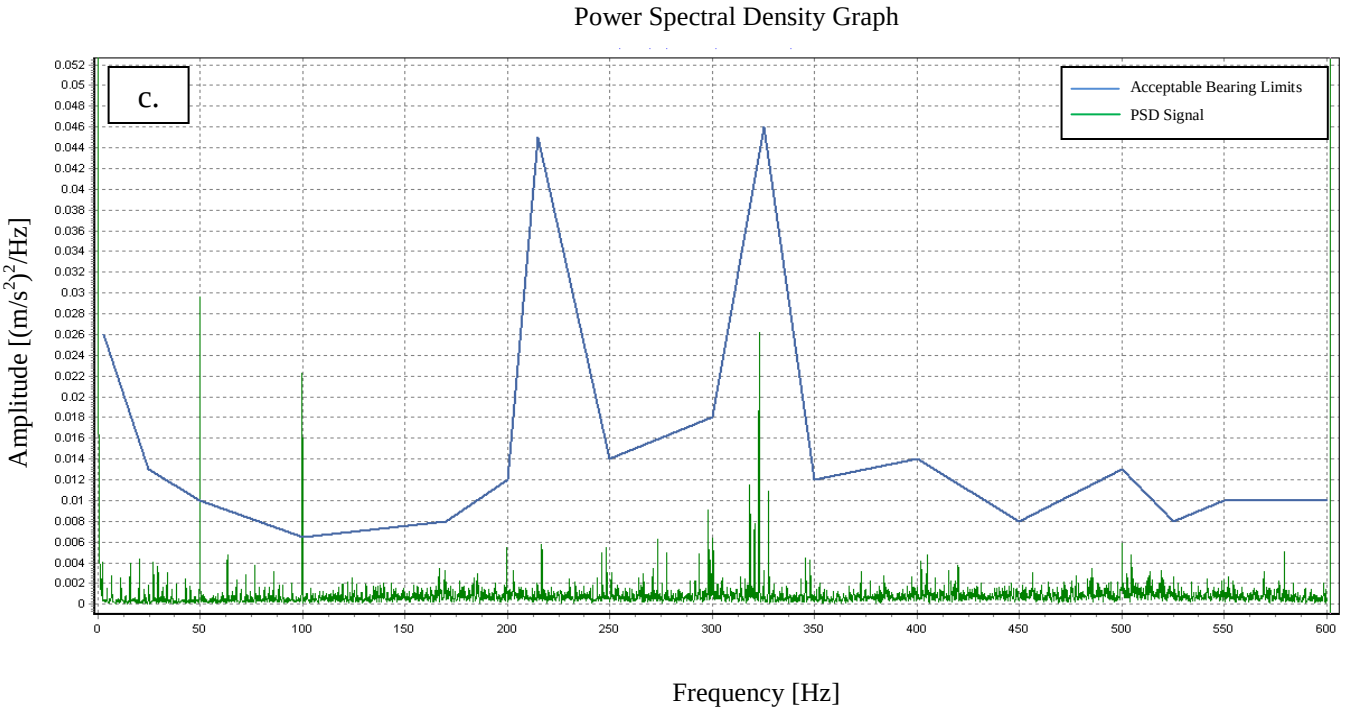

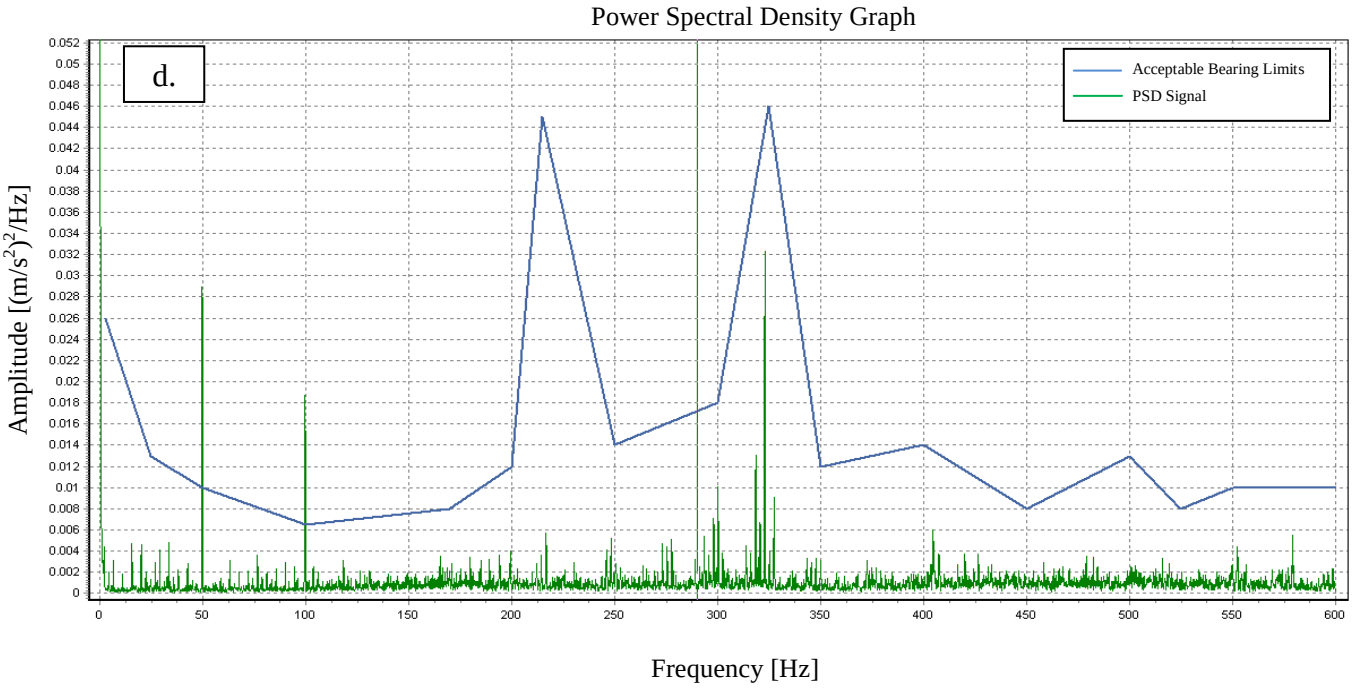

Figure 4-32 – D2 Nicked 1200Hz Bessel 500Hz filter PSD from CMS with D5 non-nicked Limits c. 40-80 Seconds d. 80-130 Seconds

4.5.2 Accelerometer type

Tests were done at 9600Hz filtered at 2000Hz with a Bessel Low pass filter. This was done with an IMI accelerometer with decreased sensitivity as compared with the Microtron accelerometer (used for all the other tests where the accelerometer type is not mentioned). Due to its decreased sensitivity as it is not a capacitance type accelerometer it has a greater range and can be regarded as a more general purpose accelerometer.

Figure 4-33 shows the results of the IMI accelerometer with the original limits drawn from the Microtron accelerometer. The results show that the IMI accelerometer is more sensitive in the higher frequencies and that the 50Hz and 100Hz frequencies are no longer visible on the nicked bearing, D6.

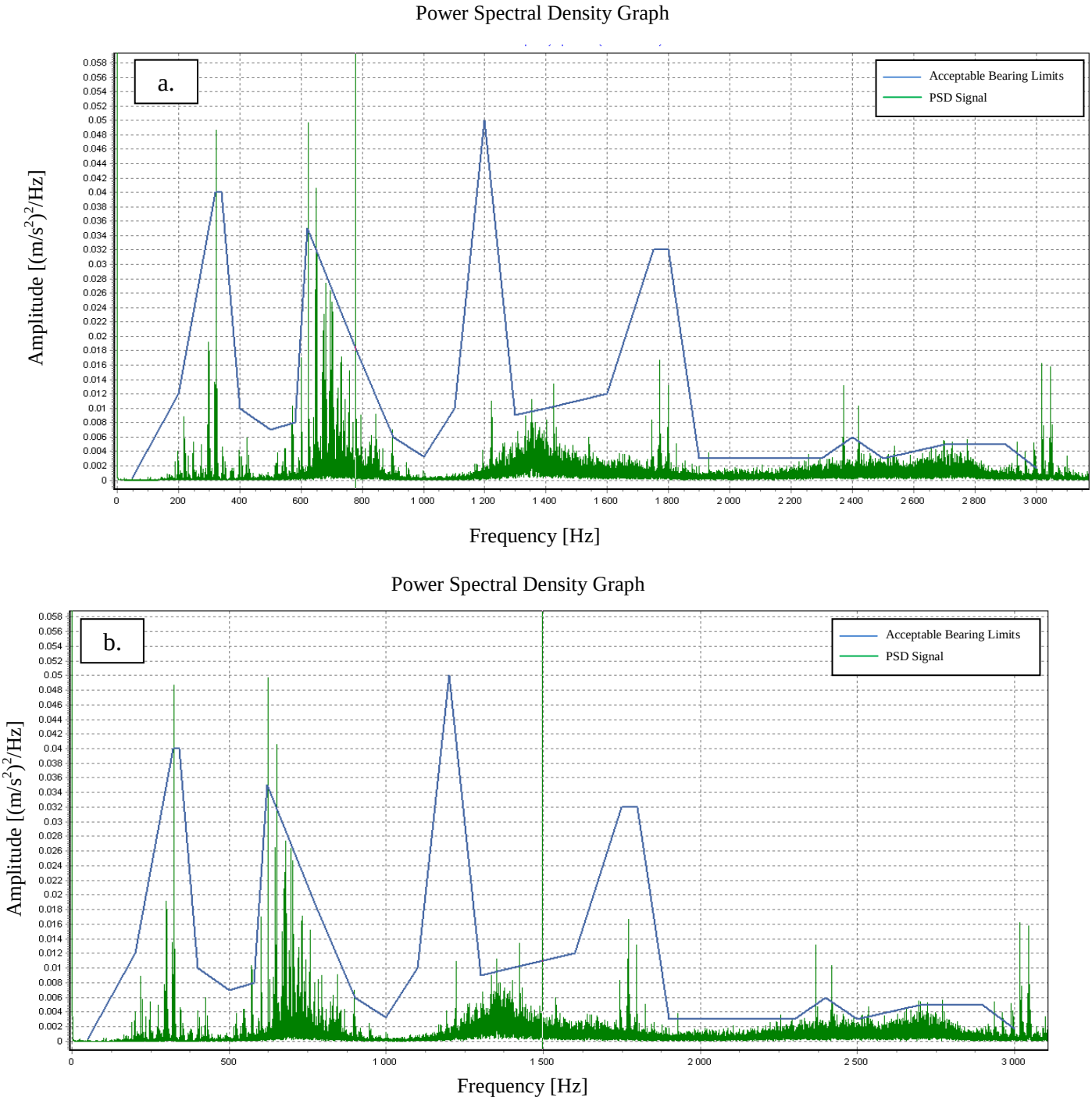

Figure 4-33 – 9600Hz at 2000Hz Bessel filter with IMI accelerometer PSD in CMS with limits from non-nicked production with Microtron accelerometer

a. D5 non-nicked and b. D6 nicked

The IMI accelerometer was also tested on more bearings and limits were created for the non-nicked D5 IMI PSD. These are shown in Figure 4-34 to Figure 4-38. In these PSD's it can again be seen that in every nicked bearing the limits are exceeded. It is clear from these figures that with the correct accelerometer at the correct sampling frequencies, that the limits are indicative of nicks. The frequencies that are excited in these results sampled at 19.2kHz are greater than the frequencies that are excited when sampled at lower frequencies but with the accelerometer that is able to accurately measure at this frequency limits can be created that are repeatable.

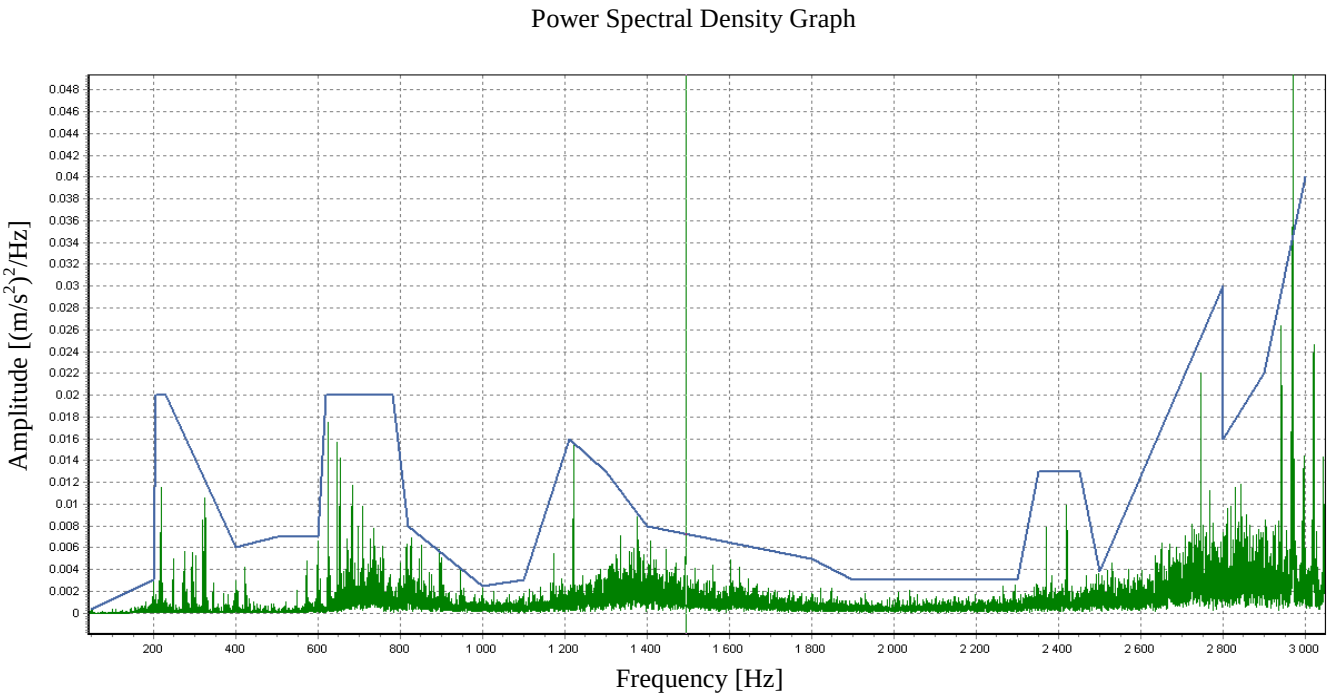

Figure 4-34 – D5 non-nicked 19200Hz IMI PSD with IMI Limits

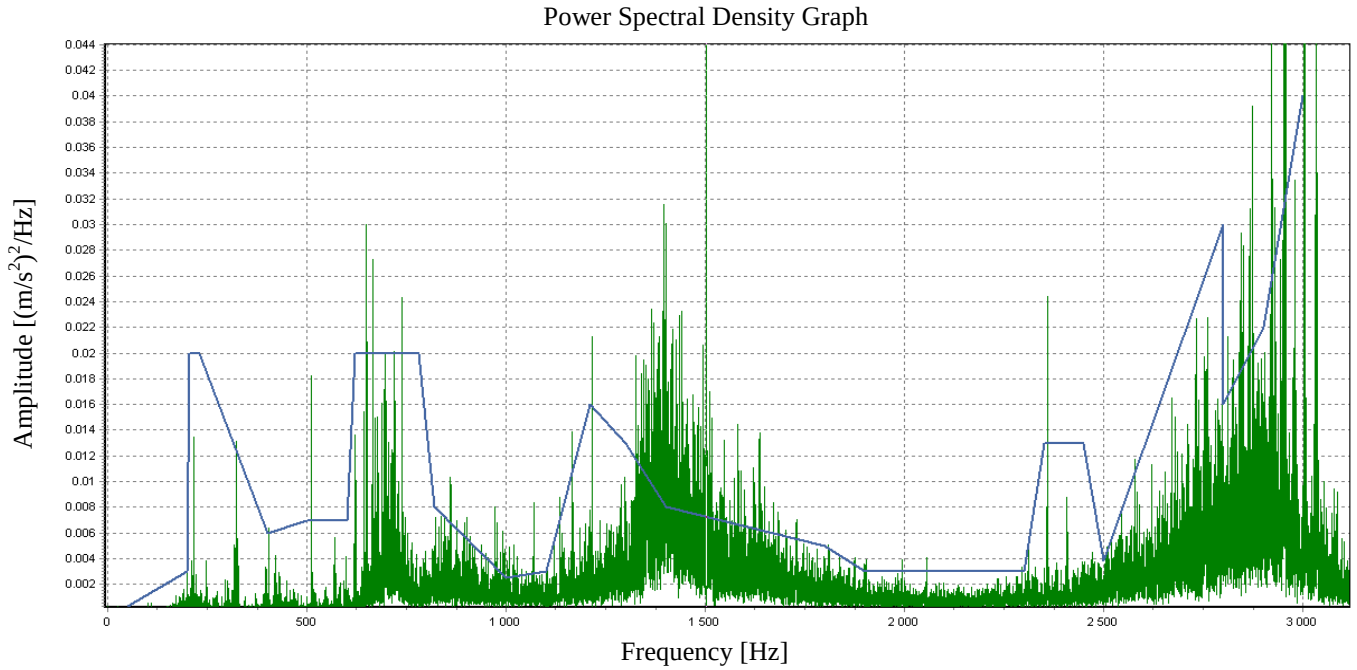

Figure 4-35 – D7 nicked 19200Hz IMI PSD with IMI limits

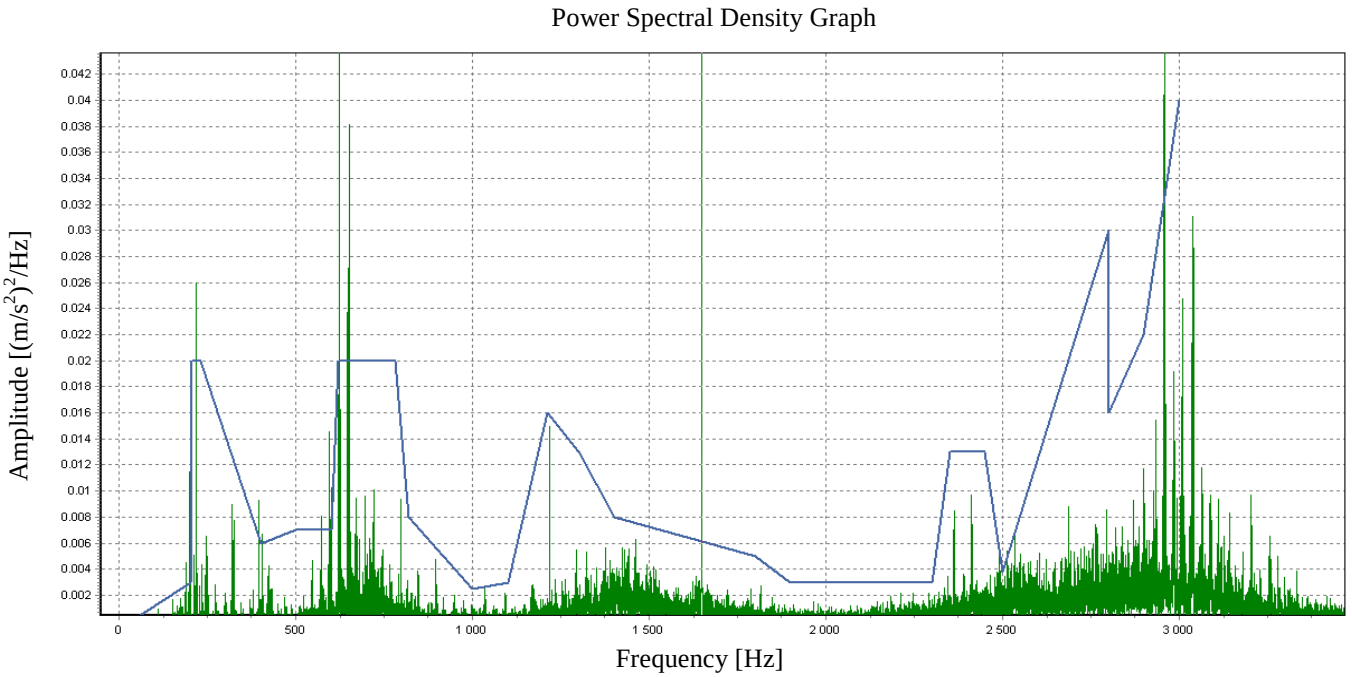

Figure 4-36 – D5 Cone-Nicked 19200Hz IMI PSD with IMI limits

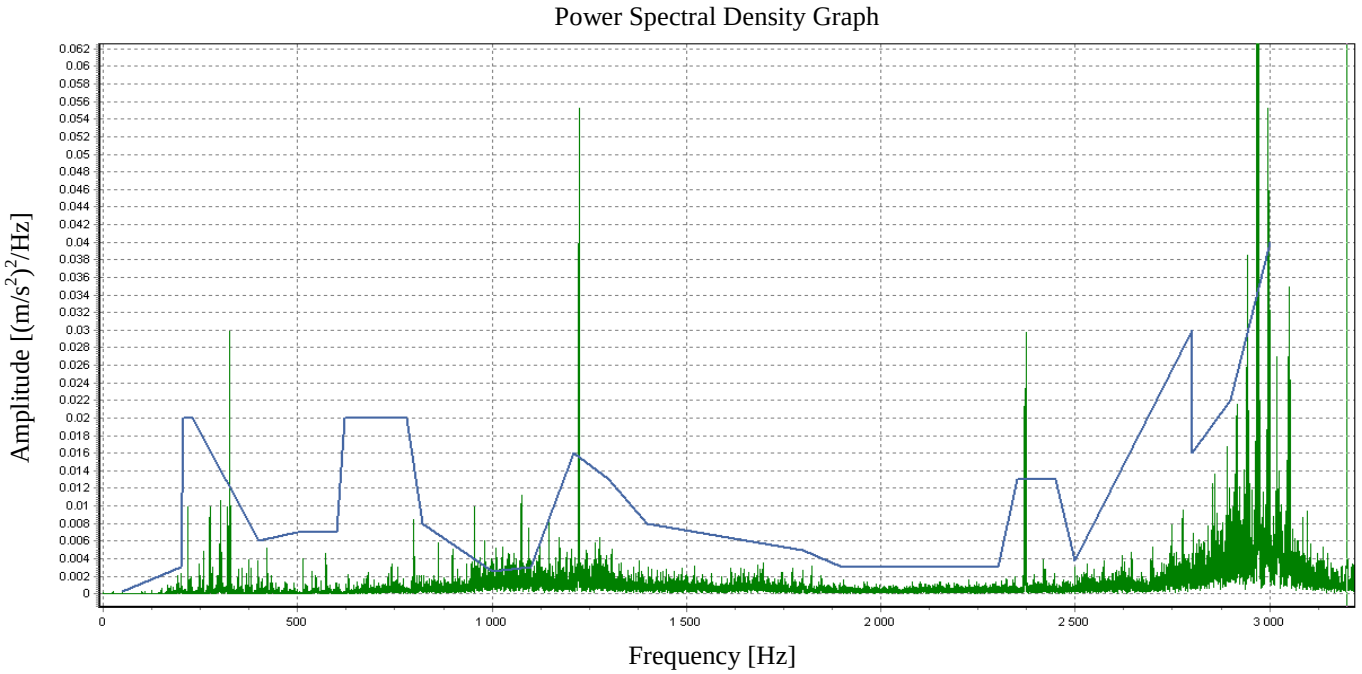

Figure 4-37 – D4 nicked 19200Hz IMI PSD with IMI limits

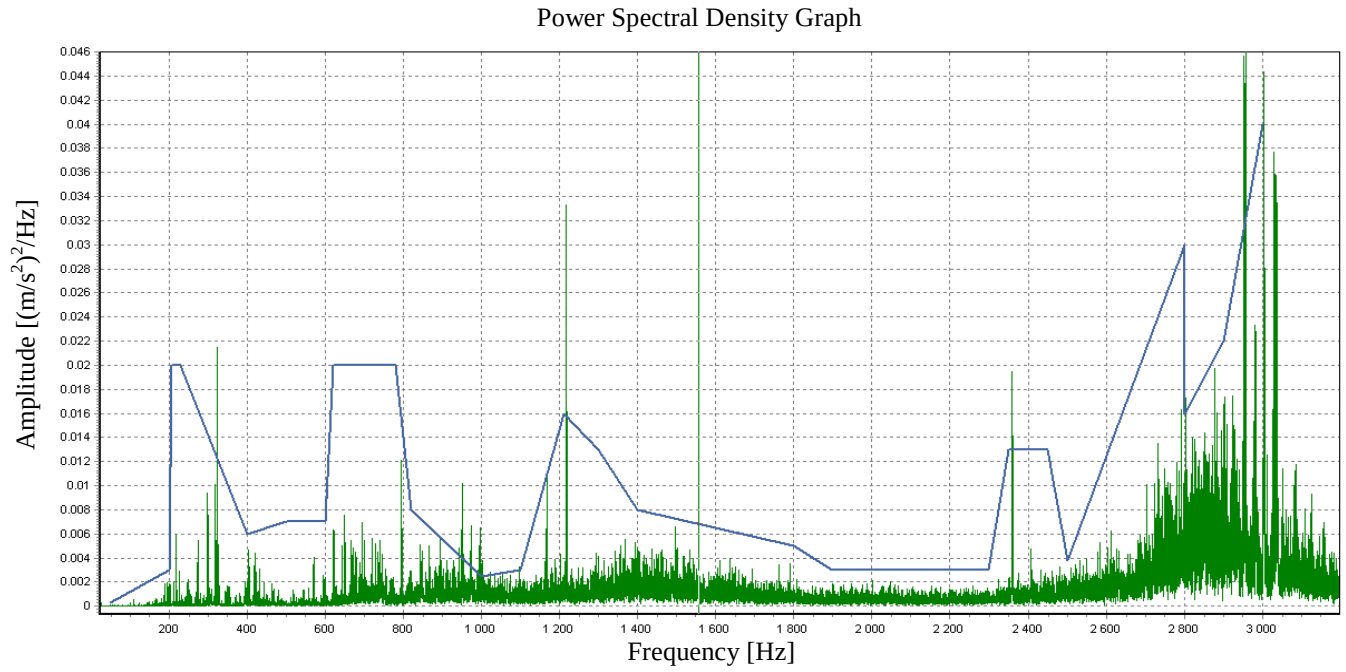

Figure 4-38 – D2 nicked 19200Hz IMI PSD with IMI limits

4.5.3 Effect of bearing bench end-play

The Lateral Machine measures the Bench End-Play (BEP) of the bearing in order to determine a spacer size for use in the particular bearing, in order to align the BEP with the Timken specifications. Each bearing class has a certain acceptable range of BEP. As BEP is a direct measure of how loose the bearing is internally this could potentially alter the vibration patterns registered during testing, due to the increased internal noise. Thus nicked and non-nicked bearings were tested at different BEP's to understand if the frequency signal was affected. Figure 4-39 shows a non-nicked bearing measured at two different BEP settings.

In Figure 4-40 the nicked bearing is shown with different results at low, medium and high BEP. The results are very similar for the two BEP's shown as the BEP's are very similar. Results were found of bearings which had greater differences in BEP and these correlated as well.

It is seen from the plots that the BEP does not have a great effect on the results of the amplitude vibrations. There are differences but the nicked bearings are still in excess of the limits set and the non-nicked bearings are within the limits for different BEP's.

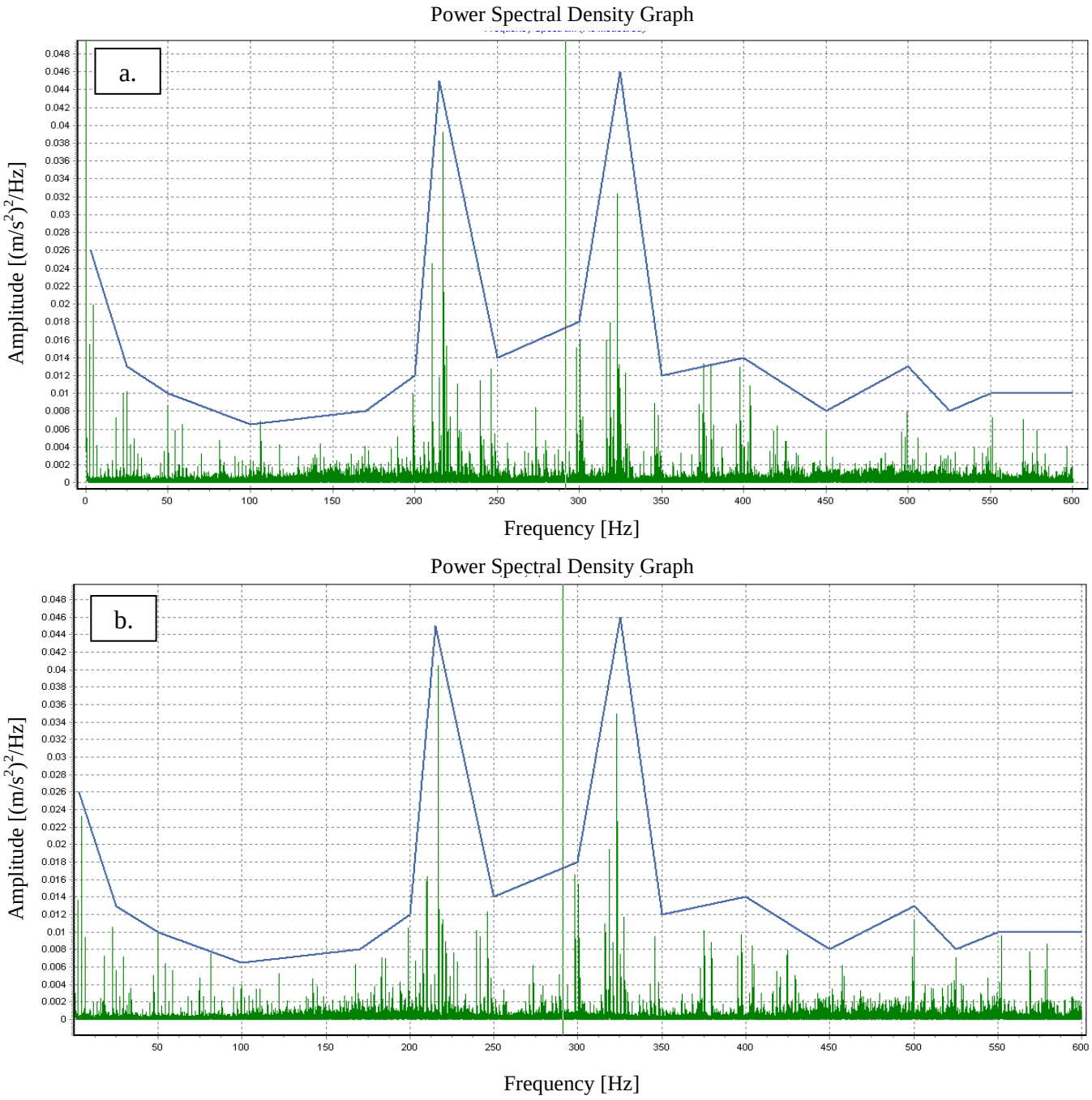

Figure 4-39 – D5 non-nicked bearing at 1200Hz BEP a. 0.0248” and b. 0.0252”

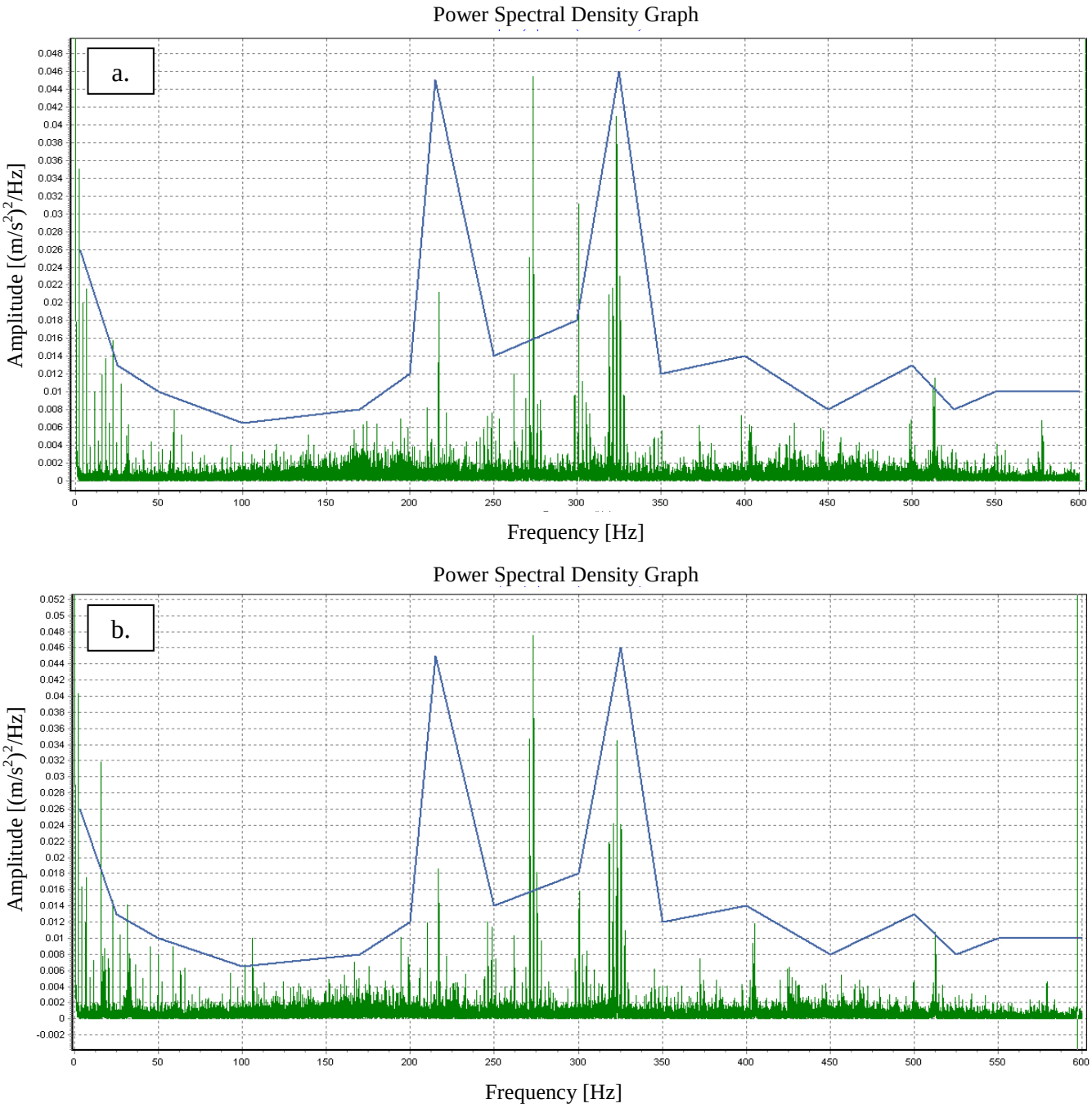

Figure 4-40 – D7 nicked bearing at BEP 0.0285” and 0.0288”

4.5.4 Location of transducer

Nick position relative to sensor

Based on the information provided by McFadden and Smith (1984) it is expected that the position of the nick relative to the sensor would be important. As discussed in the literature survey when the damage is located 90 degrees to the location of the accelerometer it is least likely to be detected and when the accelerometer is mounted directly on top of the defect the amplitude is expected to be greatest. In Figure 4-41 a PSD is shown of bearing D2 (which is a nicked bearing with quite deep nicks). For one of the tests the accelerometer was mounted at the same position as the deepest nick. This is compared to a normal test where the accelerator is mounted on the track. It can clearly be seen that the amplitudes of vibration of the bearing are higher when the accelerometer is located directly over the nick. Bearing D6 has its nick 90 degrees to the sensor position and all the results with D6 presented thus far show that it is detectable.

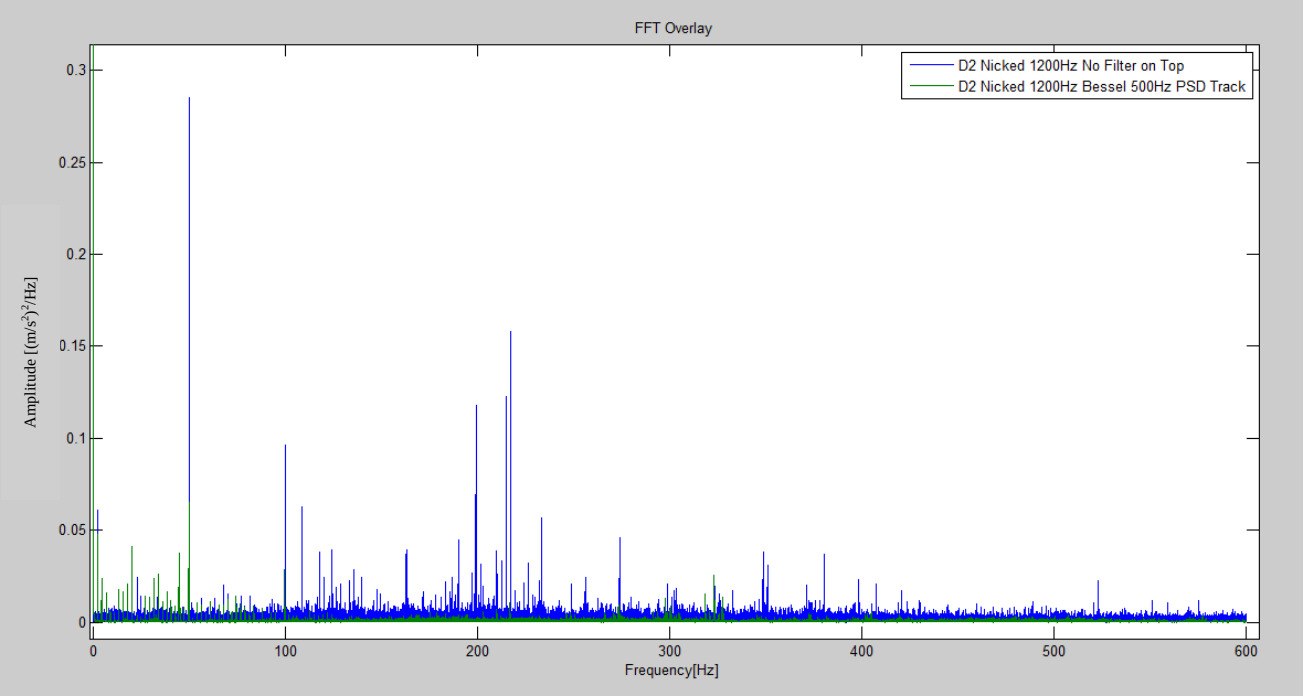

Figure 4-41 – PSD of D2 Nicked bearing with the accelerometer on top of the deepest nick and on the track of the cup

Accelerometer position during testing

Tests were performed with the IMI accelerometer magnetically mounted to different parts of the machine. This is important, as, if this research were to be implemented in a production line, it is not ideal that the accelerometer mounting is the responsibility of the operator. If it is possible to distinguish acceptable bearings from nicked bearings by mounting the sensor on the machine then a solution for production is potentially possible. For this particular test the accelerometer was mounted to the left cup lock, the lower mandrel, as well as the "upper' collar of the lower mandrel. The locations described are labeled in Figure 3-1. The PSD's of the tests conducted on the Cup lock are shown in Figure 4-42 through Figure 4-45.

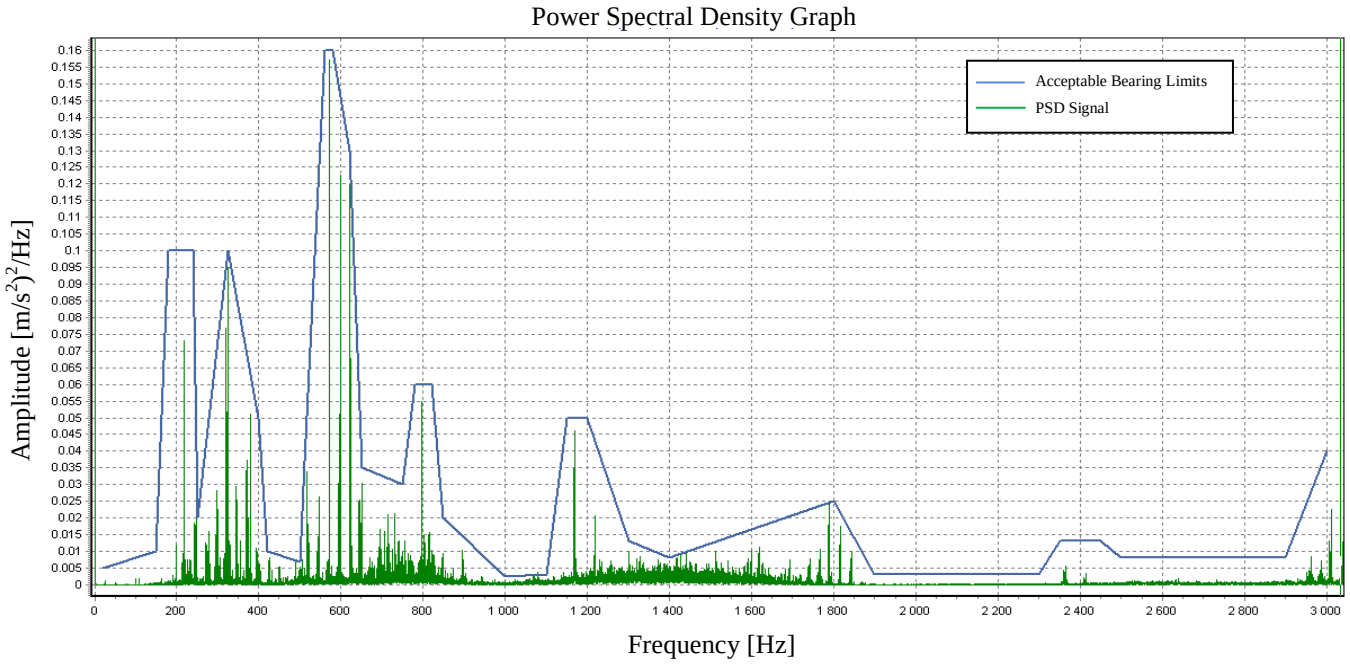

Figure 4-42 – D5 non-nicked 9600Hz Butterworth 2000Hz PSD IMI left cup lock from CMS

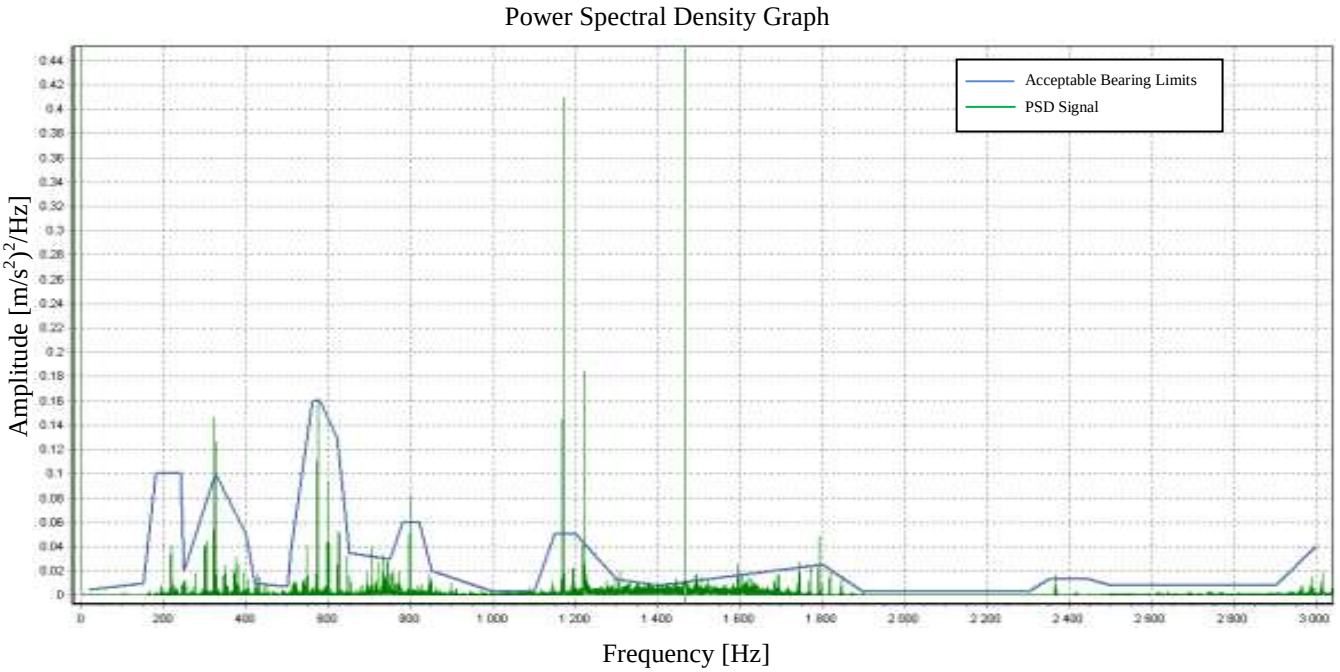

Figure 4-43 – D4 Nicked 9600Hz Butterworth 2000Hz PSD IMI left cup lock from CMS

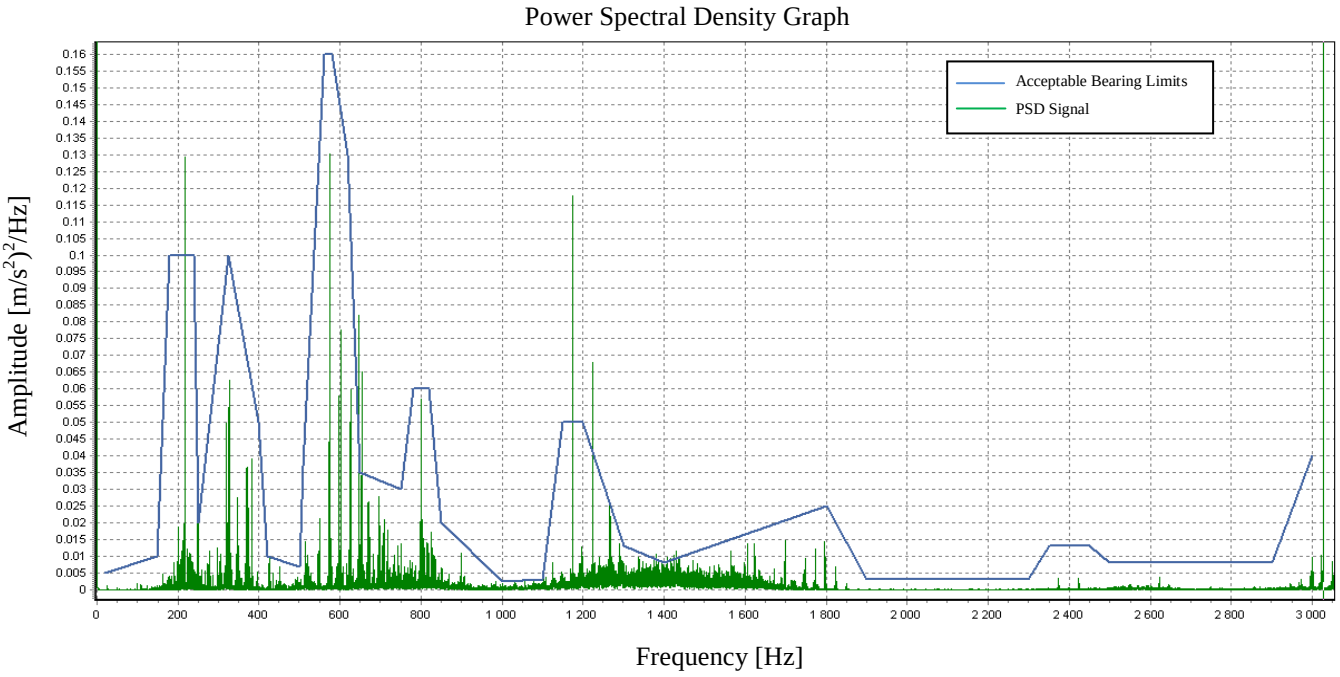

Figure 4-44 – D7 Nicked 9600Hz Butterworth 2000Hz PSD IMI left cup lock from CMS

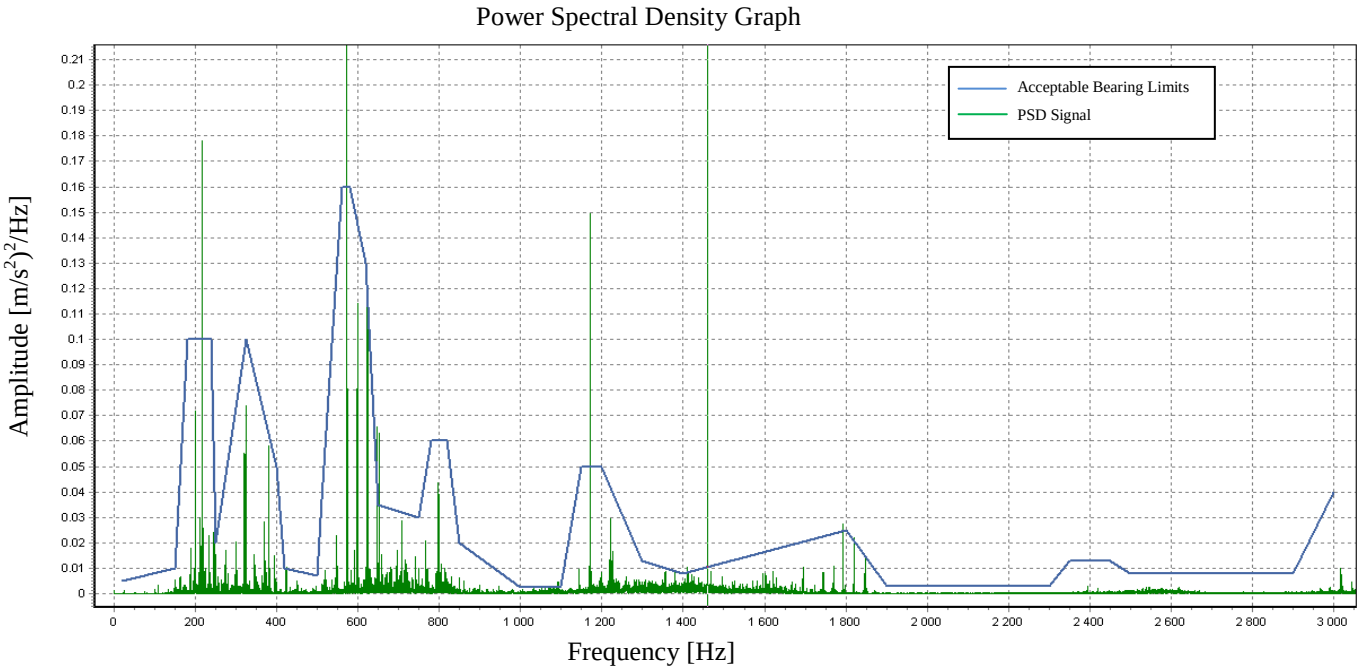

Figure 4-45 – D5 cone-nicked 9600Hz Butterworth 2000Hz PSD IMI left cup lock from CMS

From the results it can be seen that other frequencies are present to the ones seen previously on the bearing but what is important is that the frequencies are repeatable and by creating limits it is also possible to distinguish the non-nicked bearings from the nicked bearings.

Tests were also performed by placing the IMI accelerometer on the lower non-rotating shaft. This shaft is connected to the pneumatic cylinder which provides the upward force in the bearing assembly. By seating the cone against the upper rotating elements the lower cone also rotates. Figure 4-46 through Figure 4-49 show the PSD's of the tests with limits of the non-nicked bearing on the lower shaft.

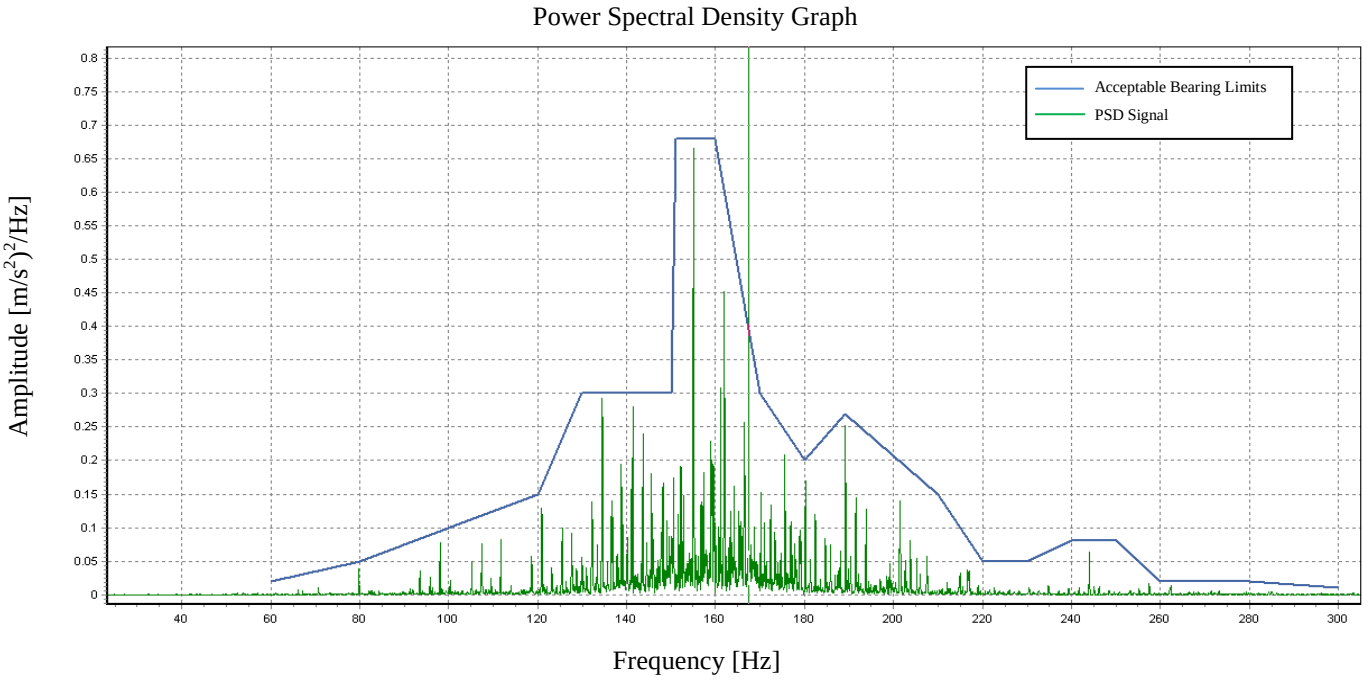

Figure 4-46 – D5 non-nicked 9600Hz Butterworth 2000Hz filter IMI accelerometer PSD on lower shaft from CMS program with limits from D5 non-nicked

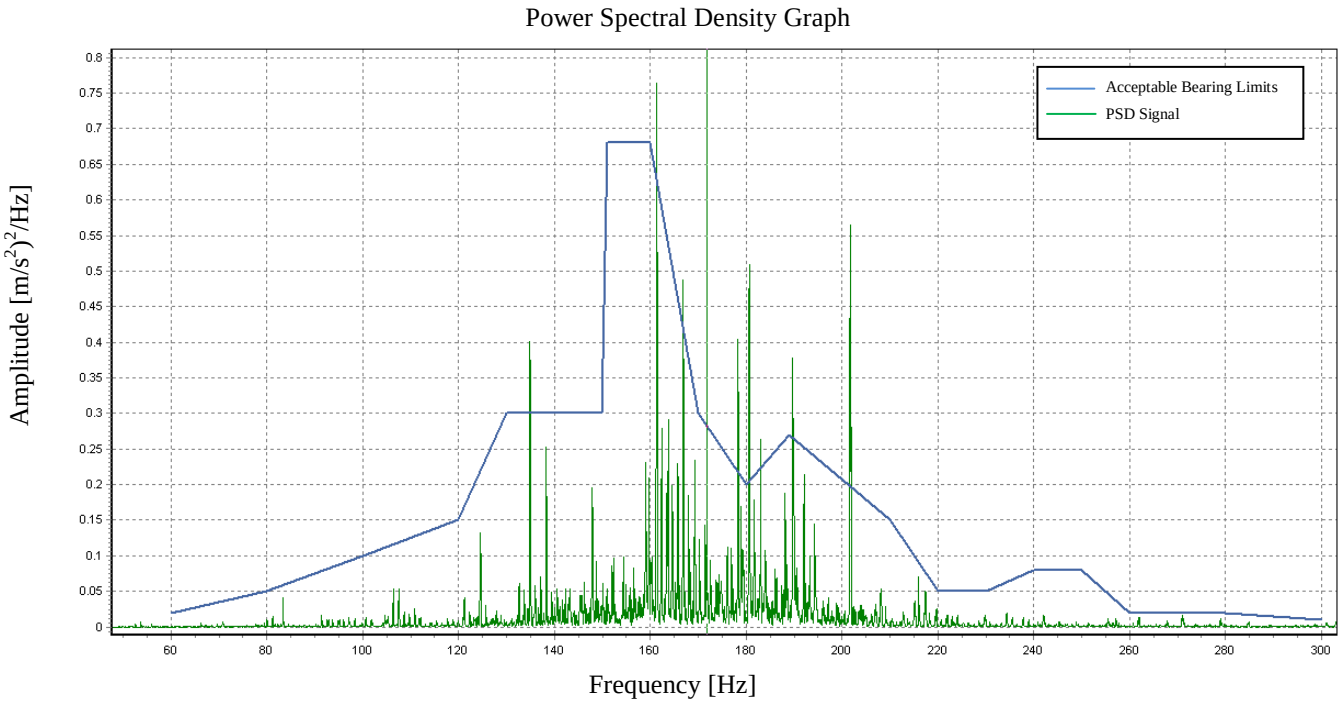

Figure 4-47 – D4 9600hz Butterworth 2000Hz IMI accelerometer on lower shaft PSD from CMS software with D5 non-nicked lower shaft limits

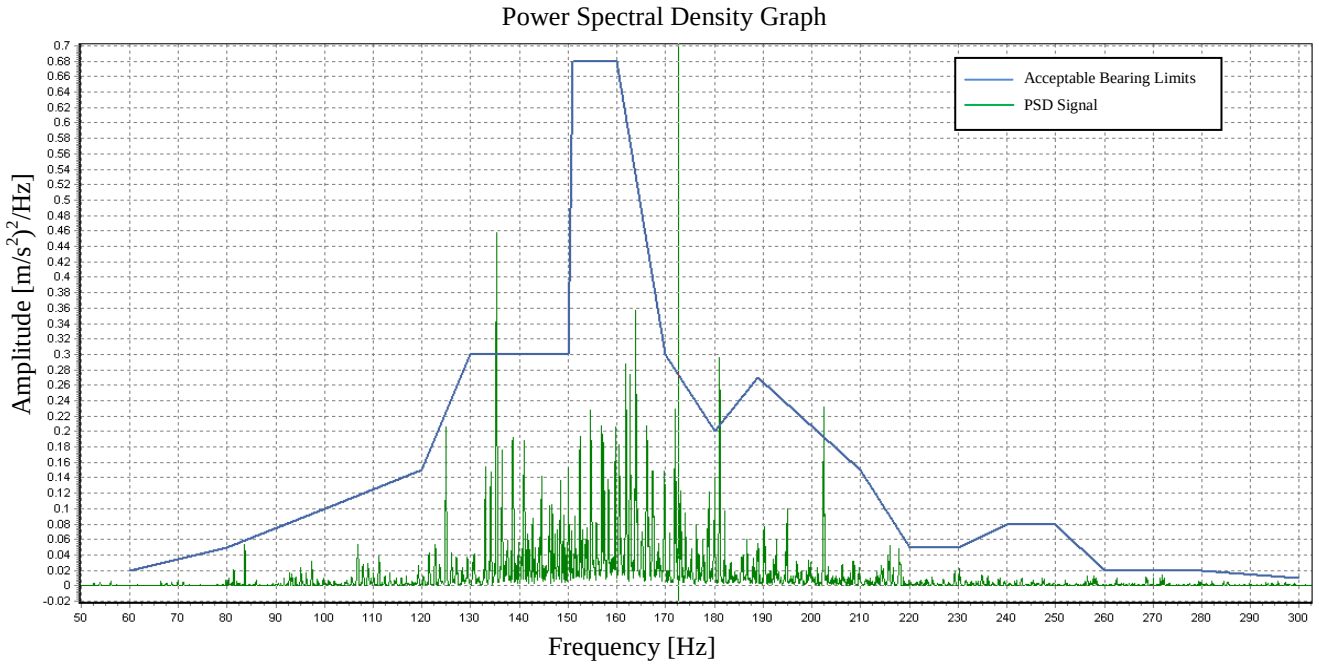

Figure 4-48 – D7 9600Hz Butterworth 2000Hz filter IMI on lower shaft PSD from CMS with limits from D5 non-nicked

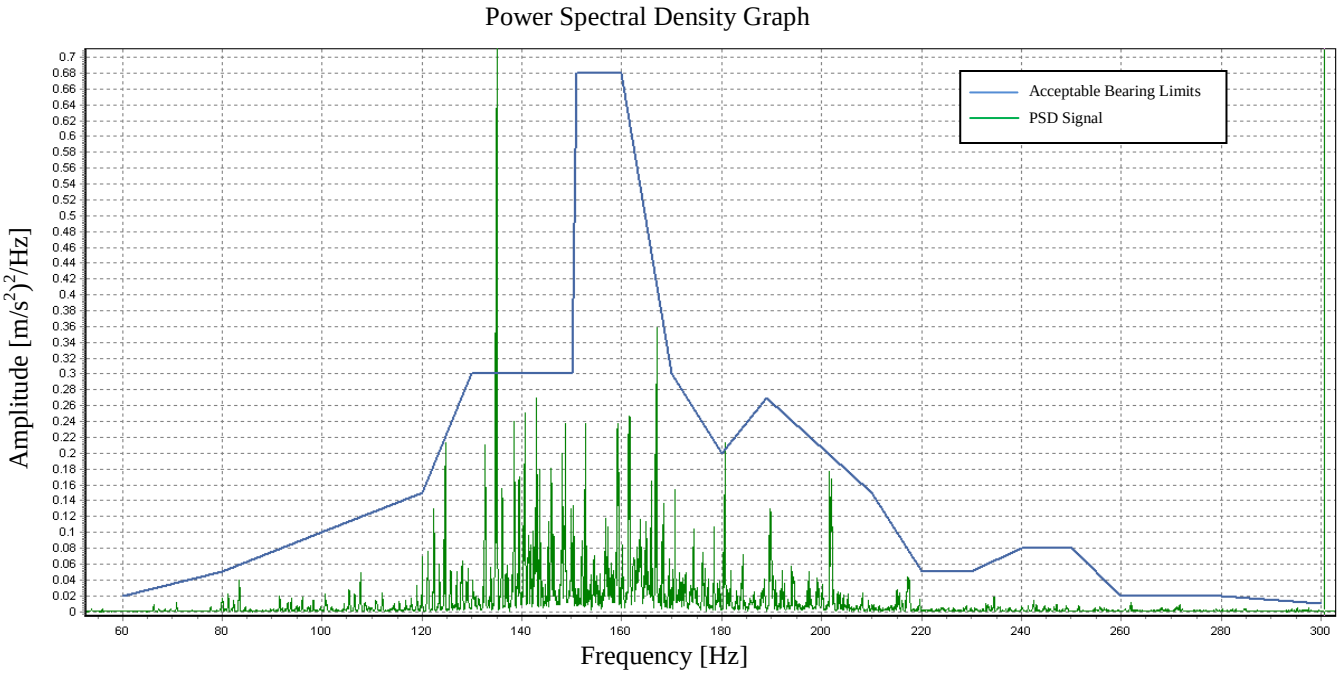

Figure 4-49 – D5 cone-nicked 9600Hz Butterworth 2000Hz filter IMI lower shaft PSD from CMS with D5 non-nicked limits

From the figures it can be seen that limits are created for the non-nicked bearings but the nicked bearing frequencies do not seem to be distinguishable from the non-nicked bearings.

4.6 Vibration Associated With Defects Other Than Cup Nicks

4.6.1 Cone nicks

Although the scope of the project did not include the testing of any other defects besides cup nicks, a nicked cone was available and it was then subsequently tested within bearing D5, which is a cup and bearing assembly with no nicks. Below is the PSD of this test, Figure 4-50. It can be seen that the nicked cone is not less noisy than the nicked bearings. There are one or two vibrations which are more distinct than with the cup-nicked product. Detailed extractions are given at 50Hz and 100Hz showing that the amplitudes of the nicked cone are not as high as the nicked bearings at these frequencies.

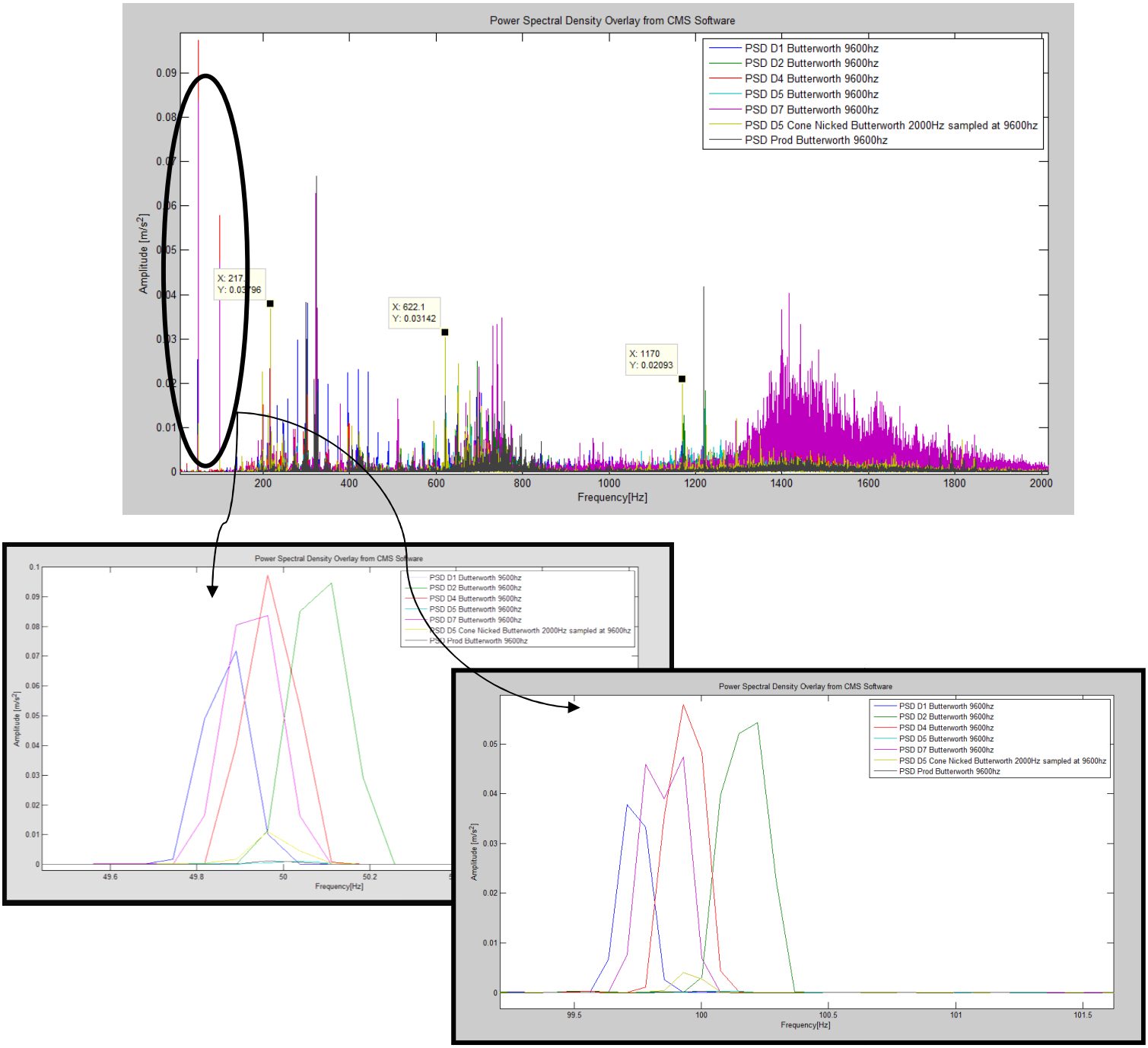

Figure 4-50 – PSD of D5 with nicked-cone at 9600Hz with Butterworth 2000Hz from CMS overlaid in Matlab

However in Figure 4-51the limit of the non-nicked production bearing PSD shown above are imposed onto the PSD of the cone nick and it is clear that the limits were correctly triggered at approximately 50Hz, 200Hz and 600Hz to 800Hz

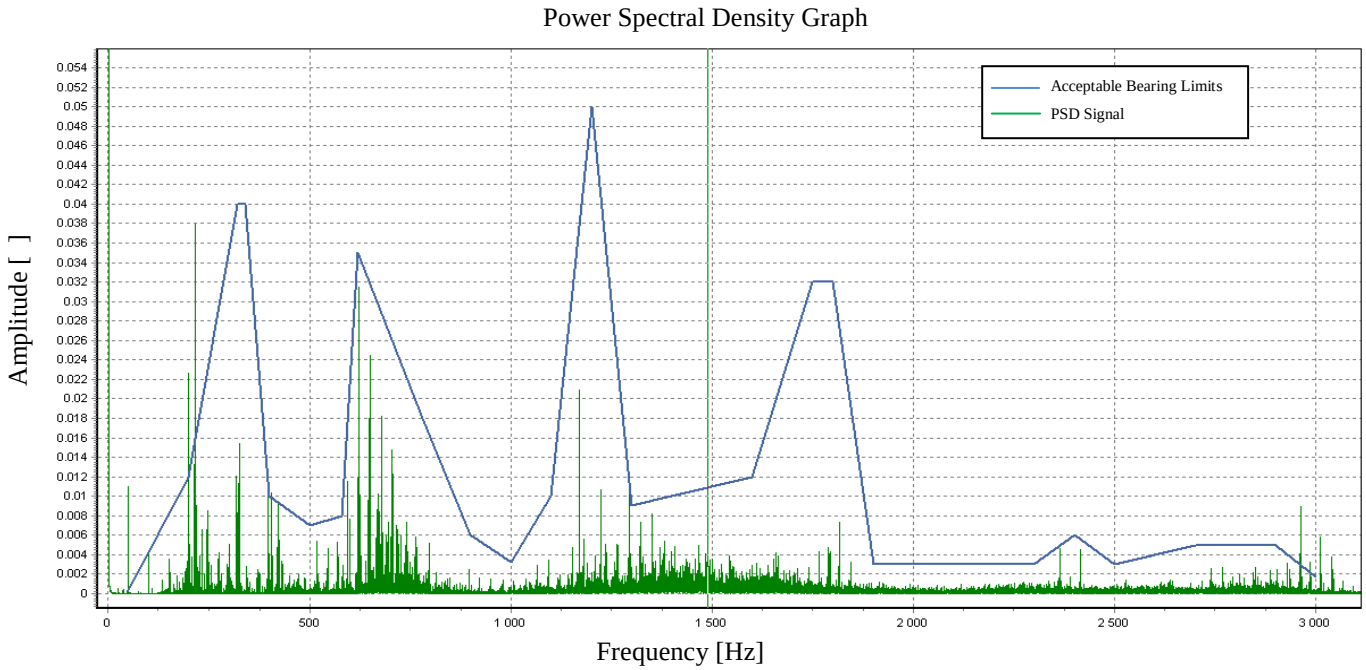

Figure 4-51 – D5 Cone nicked 9600Hz Butterworth 2000Hz PSD with limits from non-nicked production bearing in CMS

In Figure 4-52 high amplitude smearing can be seen between 100Hz and 150Hz. This is an interesting observation as after this test was performed it was realized that the incorrect tooling was used in the Lateral Machine and the smearing was created due to the contact tolerances being too tight between the inner ring and the rotating tooling. This is an added observation to show that the analysis techniques can be used for error proof verification within the production line as well.

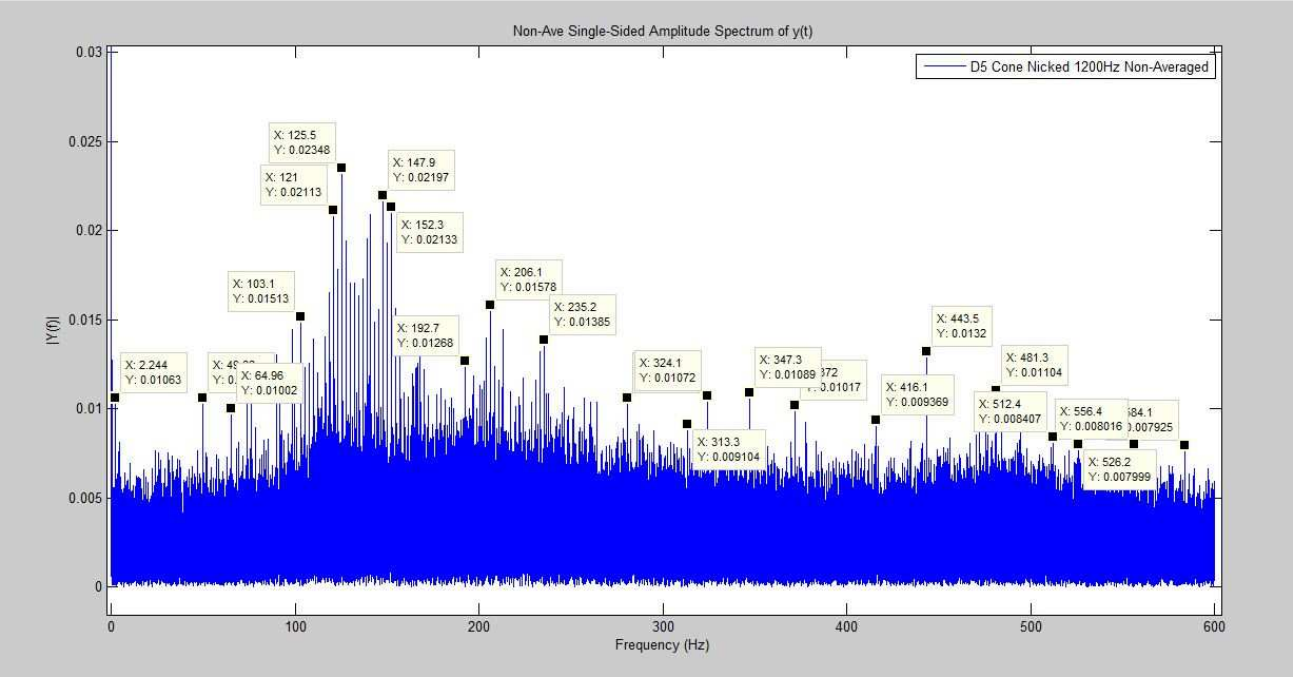

Figure 4-52 – FFT of D5 (non-cup-nicked) with a nicked cone at 1200Hz no filter with incorrect tooling

In this chapter many graphical results were given of the various testing runs that were conducted during the testing phase. The results were grouped by themes. In this chapter the repeatability of non-nicked bearing vibrations were established and the limits defined over a wide range of frequencies against which nicked bearings could be assessed. These limits were then transposed onto the PSD's of nicked bearings and it was shown that the nicked bearings exceeded these limits in all cases. Data was presented for different acquisition parameters such as testing duration and the effect that parameters such as bench end-play, type of sensor, and location of sensor. This indicated that it is possible to define limits in which acceptable bearing vibration amplitudes fall within. The nicked bearings' amplitude of vibrations are in excess of these limits. The different parameters described above do have an impact on the limits set for acceptable bearings and thus these are dependent on the data acquisition settings.

5 DISCUSSION

The main objective of the research was to evaluate the feasibility of detecting cup nicks when bearings were tested in the Lateral Machine. The cup nick is a very small defect on the cup raceway which sometimes has a high spot associated with it. These nicks are most easily created within the assembly process when the cone is incorrectly inserted into the cup by the operators. Testing was completed on one Lateral Machine with nicked and non-nicked bearings. The nicked specimens were analysed for the quantity, distribution and severity of nicks. Some of the nicks were traced on a contour tracing machine to measure their depth and height of the high spots. An accelerometer was mounted to the outside diameter of the cup and the Lateral Machine cycled through its process with an extended time duration on the second phase of the cycle i.e. when the bearing was pushed downwards. Two different types of accelerometers were used and the testing was described as such. The data was analysed in both the FFT as well as the PSD spectra, with the latter yielding better results.

5.1 Preliminary Testing

From Table 3-1 and with the knowledge of the corporate Timken specification on nicks (The Timken Company, 2011) it was seen that the size of the nick measured in bearing D4 was smaller than the maximum allowed size. It did however have roller-spaced nicks which were not acceptable (as there should not be more than one nick in a quadrant). Thus all the bearings that have been considered that have nicks present should have been rejected. The specification also makes mention that no nicks with raised metal are allowed. It was clear that the bearings with raised metal nicks had vibration amplitude's in excess of the limits set for acceptable bearings, and thus the nicks within the required size range and type (as per the corporate standard) have been detected.

The initial testing was not successful. The sampling frequencies were mainly too low and the analysis took place when the Lateral Machine was completing both cycles (cylinder pushing upwards and then cylinder pushing downwards). The motion of the Lateral Machine is seen in Appendix E, Figure E-2. With the low sampling rates it was difficult to maintain the required resolution in the FFT that was needed to analyse the results. The IMI sensor was also used which did not have such high sensitivity at low frequencies.

As a general observation it was noted in Figure 4-5, and all the other FFT's showing the full frequency spectrum, that the results appeared similar to a bearing's failure in its different stages (as shown in Figure 2-16). This is probably due to the fact that in the Lateral Machine the bearing is not mounted (as it would be in application) and it has large internal clearances and thus is loose. In reality, the last stages of bearing failure, when analysed for vibration, also have this looseness as the bearings are worn out and have large internal clearances, and loose and irregularly worn components.

5.1.1 Low pass filters

As explored in Chapter 3 it was seen that the HBM data acquisition unit was master sampling at 19.2 kHz and then the anti-aliasing filter would filter the data to a bandwidth of 3.2 kHz in the analogue domain. Thus all filters that are referred to in this context are filters applied by the user and these are filters in the digital domain. Filters were applied to a 2.5 to 5 times ratio where possible. Both Bessel and Butterworth filters were used in the testing and it was found that there was not a distinct difference between the results yielded from both methods. This was shown in Figure 4-3 and Figure 4-4.

5.1.2 Power spectrum density

The bearings were sampled and the results converted using Fast Fourier Transforms (FFT's). It was found that the FFT's had a large amount of noise and this was not helpful in analysing trends between nicked and non-nicked bearings. This analysis was used to distinguish nicked from non-nicked bearings. There was no distinct frequency in all of the sampling rates that was unique only to nicked bearings and did not appear in the non-nicked specimens. Additionally, when a pattern was observed there was always one bearing that broke the pattern and then the theory was not accurate.

Much of the data was analysed firstly in the FFT domain. With the correct filters applied and the windows in the FFT set to Hanning and 30% overlap, there was still sufficient noise in the system to not always clearly define the peaks. To illustrate this point note must be taken of Figure 4-5 (which is the FFT) and Figure 4-6 (which is the PSD) of the same data set. Both were achieved with a window Hanning, 30% overlap and a resolution step of 0.073Hz. The difference is that in the PSD the frequencies with energy become very distinct and the frequencies without that particular energy, seen on the FFT, die away.

As a result of this the data was analysed making use of the Power Spectral Density (PSD) method. When the non-nicked bearings were analysed with a PSD, the peaks were quite clear and it was possible to create limits on the PSD in which the acceptable bearings vibration amplitudes were contained. When nicked bearings were analysed against the defined limits they were seen to exceed the limits and were thus able to be distinguished from non-nicked bearings.

Therefore PSD's were shown to be more effective in discerning nicked from non-nicked bearings.

5.1.3 Sampling rates

With different sampling rates used, resolution and information was either lost in the lower frequencies or was not available in the higher frequencies. As a result of this it was important to determine at what sampling rate the best results would be achieved for detecting cup nicks, and what the differences would be between sampling at high rates or low rates. In order to do this, sampling was started at 600Hz and increased to 19200Hz as a maximum rate. As per anti-aliasing principles and the Nyquist theorem the samples were filtered correctly with the digital filter after the anti-aliasing filters were applied by the acquisition hardware. Because of the slow rotating frequency of the Lateral Machine, the expected bearing frequencies for defects were between 20Hz and 30Hz. It would then seem reasonable that sampling at 600Hz maximum should be more than sufficient. However, the spectrum was analysed at a high sampling rate first in order to understand the range of all the frequencies present in the vibration signature.

When comparing Figure 4-25, bearing D4 sampled at 1200Hz and filtered with a Bessel low pass filter at 500Hz, with Figure 4-26, where bearing D4 was sampled at 9.6 kHz and filtered to 2kHz, there were frequencies below 50Hz which lost clarity in the latter case. Some of the frequencies not present at the higher sampled test set are the running speed harmonics of the inner ring and motor i.e. 135 RPM. Additionally, when considering Figure F-9, bearing D4 sampled at 600Hz with a 500Hz filter frequency applied, it can be seen that the running frequencies are not present, and that fewer peaks exist in the system. Conversely Figure F-26, bearing D4 sampled at 19200Hz, has many high frequency components and less resolution in the low frequencies. It was therefore decided that the testing would be concentrated around 1200Hz and 9600Hz sampling rates as these yielded the most distinct amplitude and frequency differences between nicked and non-nicked bearings.

5.1.4 Bearing frequencies

As discussed in the literature survey and shown in sample calculations (Appendix C) and Section 4.1, bearings portray specific frequencies, associated with the rotational speed of the components, based on the rotational speed of the shaft. When analyzing the bearing frequencies that were supposed to be present based on calculations shown in Table 4-2, these were all present for nicked and non-nicked bearings. This is shown in Figure 4-9 for 600Hz, Figure 4-10 for 1200Hz, Figure 4-11 for 9600Hz and Figure 4-12 for 19200Hz. These figures were zoomed to the outer raceway defect frequency, based on the size of the bearing, as well as the rotational speed of the bearing. It was expected that this would be a distinguishing factor to detect cup nicks; however, it was shown that both the nicked and the non-nicked bearings have a vibration peak at this frequency, as well as the other defect frequencies such as inner and roller defect frequencies. Additionally, in other tests the frequencies that should have been excited by either the roller, inner or outer defect had not been excited. There are various ways to interpret this, but the most important point is that the bench end-play of the bearing is far greater than it would be in a mounted application. Since in the Lateral Machine test there is ample clearance within the bearing, the rollers are not forced as hard into the outer race as they would be in practice, and there is a large amount of lateral end-play within the bearing. Additionally, due to the design of the Lateral Machine, it is known that there is no significant radial loading, and that the force applied to the bearing is almost 100% axial force, i.e. a full 360 degree evenly distributed load. However, in practice the force would be applied mostly in the radial direction with a lower axial component, and the bearing would be under its full loading; thus the rollers would drive hard into the raceway as they pass in and out of the load zone. As discussed in the literature survey the outer and inner race defect frequencies are largely excited due to the rollers passing into the load zone and then out of it again. This phenomenon does not occur in the Lateral Machine.

5.1.5 Natural frequencies of components

It does appear from the discussion on the visible results that the noise being generated by the nick within the bearing system is exciting the amplitudes of alternative frequencies. There are frequencies that are carrying greater amplitude, e.g. 50Hz and 100Hz which are not directly calculated from expected bearing frequencies, but definitely reflect the severity of the nick in the nicked bearings and under the correct testing conditions. In Section 3.2.1 it was mentioned that Chambers and Bunting (1981) showed that acoustics are transmitted through various bearing interfaces and are dependent on contact pressure between the two surfaces. Although the bearing is not in a loaded zone there is contact pressure as the rollers are seated and the Lateral Machine is applying a constant pressure so the frequencies that are unique between nicked and non-nicked bearings could be transmitted acoustics. McFadden and Smith (1984) showed that the presence of defects could be transmitted to the resonant frequencies of the bearing components. Figure 4-13 and Figure 4-14 were plots of the natural frequencies measured of the cone and cup respectively. These frequencies were in the order of the excitation experienced with the samples taken at 9600Hz and 19200Hz and thus this theory is plausible. In nicked bearings the frequencies in the range of the natural frequencies were definitely more excited than in the non-nicked bearings. This explains the high frequencies experienced in a system in which relatively low frequencies are expected.

5.2 Non-nicked bearing limits

The reason limits were created was because there were not distinct frequencies in nicked bearings that were not present in non-nicked bearings. It was noticed that sometimes the amplitude of vibration of nicked bearings was greater in the lower frequency spectrum and sometimes it was larger than non-nicked bearings in the higher frequency spectrum. By applying limits it was possible to deal with both scenarios. In Section 6.2 non-nicked

bearing vibration amplitudes at different sampling frequencies were presented. It was shown that the non-nicked bearings had repeatable frequency patterns with correspondence in amplitudes. Limits were created for all frequencies based on non-nicked bearings. The vibration response of nicked bearings was overlaid on a graph with the limits drawn across the frequency spectrum. Where limits were exceeded by nicked bearings it indicated a faulty bearing. These limits thus signified the frequency band in which a bearing, measured with a particular transducer, was deemed to be acceptable on a particular Lateral Machine. The limits are seen in Figure 4-15 for 600Hz, Figure 4-16 for 1200Hz, Figure 4-17 for 9600Hz and Figure 4-18 for 19200Hz sampling rates.

5.3 Nicked bearing comparison

The nicked bearings were analysed using PSD's with the limits created for the non-nicked bearings and it was determined whether they exceeded the limits in one of the frequency bands.

The variety of tests were sampled at 19200Hz, 9200Hz and 1200Hz and 600Hz and the limits are shown in the Section 4.4 and in Appendix F. In each of these four sampling rates the nicked bearings were distinguishable from the non-nicked bearings, based on the reject limits determined from the non-nicked specimens.

With the tests conducted at 19200Hz the limits were not clearly triggered at 50Hz and 100Hz but rather by sporadically increased amplitudes at 300Hz, 1200Hz, 2400Hz and 3000Hz, as summarised in Table 4-8. As mentioned the resolution was lost in the lower frequency ranges when the sampling rate was too high and thus the 50Hz, 100Hz and rotating speed harmonics were not clear.

In the 9600Hz tests all of the limits were exceeded at 50Hz and 100Hz. The limits were also exceeded between 1250Hz and 1700Hz (range of natural frequencies) by some

bearings, e.g. D7 the chipped bearing, significantly exceeded the limits, while D6, D2, D3 and D1 exceeded the limits slightly, and some more than others.

With the tests sampled at 1200Hz with the 500Hz Bessel filter the nicked bearings very clearly excited the running speed and its harmonics more than the non-nicked bearing did. Additionally, most bearings except for D7 excited the 50Hz and 100Hz frequencies. This could possibly be due to the fact that D7 is not nicked (as nicks are typically in the middle of the raceway) but rather chipped on the extreme outside of the cup raceway, i.e. the rollers' line of contact at this part in the raceway was very limited. Some bearings excited the 240Hz to 270Hz range and D7 and D6 highly excite the 300Hz range frequencies. The summarised Table 4-6 clearly shows which bearing excited which frequencies.

The tests analysed at 600Hz had relatively clear resolution at lower frequencies but the difference between nicked and non-nicked bearings was not very distinct. The amplitudes were generally quite low on most peaks.

It was possible to create good limits for all sampling rates but it was noted that the difference between nicked and non-nicked bearing amplitudes for 600Hz and 19200Hz was quite small and thus these frequencies were possibly not considered ideal.

5.4 Physical Acquisition Parameters

5.4.1 Testing duration

At the beginning of the testing the decision was made to increase the testing duration. Most of the tests for 1200Hz sampling rates were performed over a duration of 200

seconds. For the tests sampled at 9600Hz the tests were a duration of 50 seconds and for the tests sampled at 19200Hz the tests were a duration of 26 seconds. The normal Lateral Machine cycle only has a total cycle time (including the upper cone seated and the lower cone seated) of about 14 seconds. The time in the second phase of the machine was extended to have longer duration during testing. In Figure 4-31, a 200 second test was taken and only samples of 50 seconds were analysed using a PSD. These were performed for a nicked bearing and the PSD was analysed in comparison to the non-nicked bearing limits. In both the 50 second duration tests the nick was detectable when compared to the defined limits. Figure 4-32 shows a nicked bearing and in this example the test duration was broken down from a 200 second interval into different duration lengths with the shortest duration being 10 seconds. In all of the different test durations the nicks were visible as the amplitudes were greater than those defined by the limits. The amplitudes from test to test had a slight variation but this was to be expected. Therefore, considering the potential to conduct such tests on the Lateral Machine in future it would be feasible to conduct shorter tests without significantly altering the Lateral machine cycle times.

5.4.2 Accelerometer type

Two sensors were used during the testing and these were defined in Chapter 3 and noted with the results in Chapter 4. The Microtron accelerometer had a greater sensitivity at lower frequencies due to it being a capacitance type accelerometer. The IMI accelerometer is less suited to measure at lower freqeuencies and gave greater amplitudes at intermediate frequency ranges. Almost all tests were done with the Microtron accelerometer unless otherwise stated. This was done as the key frequencies were expected at a low frequency range, due to the theoretical calculations made (based on the running speed of the Lateral Machine). In all instances the Microtron was attached to the cup outer surface by the use of adhesive and the IMI accelerometer was always mounted by means of a curved magnet. As per Figure 2-13 the magnetic mounting should be less accurate than the adhesive mounting. It must be noted however from the relationship plot

that at low frequencies (less than 1000Hz) the relationship between the different mounting methods makes little difference. It could, however, become evident when the frequencies are greater than 1000Hz.

When considering tests taken at a sampling rate of 9600Hz with the IMI accelerometer reference was made to Figure 4-33. The limits in this figure were not defined based on an IMI accelerometer, but based on the readings taken from the Microtron. It is clear that the frequencies at a lower frequency range, 0Hz to 300Hz, did not have the same amplitudes as compared with the Microtron.

When looking at spectra from the IMI accelerometer it is clear in the 19200Hz tests, Figure 4-34 to Figure 4-38, that there are larger amplitudes at the higher frequencies than what is achieved by testing with a Microtron accelerometer. As a result of this it was observed that the IMI accelerometer had elevated amplitudes in the upper and middle frequency bands as compared to the Microtron. Thus it was necessary to define a limit set based on the type of accelerometer being used i.e. one for the IMI accelerometer and another for the Microtron accelerometer in the various test protocols. IMI limits are seen on the nicked and non-nicked bearings from Figure 4-34 to Figure 4-38. In these figures the limits have been defined for the non-nicked D5 bearing, measured with the IMI accelerometer. These limits were then applied to the nicked bearings (D5 Cone nicked, D4, D2 and D7). Analyses of these figures confirm that none of the lower frequency reject limits exist as with the 9600Hz samples. The 50Hz and 100Hz are barely visible and even absent on some bearings. The lowest reject limits are on approximately 250Hz and not in every bearing. All the nicked bearings portray a peak between 600Hz and 700Hz and also various peaks much higher in frequency, e.g. 1200Hz, 2400Hz and 3000Hz. The fact that these are so much higher than the information displayed in the 9600Hz tests is a combination of the type of accelerometer used, as well as the higher sampling rate. Again it is noted that with a limit set, across the usable frequency range, the nicks were detectable.

The nicked bearings sometimes excited different frequency bands. The ability to set limits across the full frequency range of the PSD existed in the software. Thus even though the excited frequencies in various nicked bearings differ from those expected from the theoretical requirements, and the frequencies excited by the nicked bearings were not always exactly the same, it was possible to define limits across the full frequency range of the PSD. When a bearing was thus nicked these limits were exceeded at various frequencies. This amplitude of frequencies greater than the amplitudes of the set limits showed that the bearing was suspect and that it needed to be examined before passing the unit to a customer.

The use of the limits across the full PSD spectrum is very powerful in the application within the production environment. This means that a “good signature” of a bearing can be defined and any deviations from such a pre-defined signature during a vibration analysis routine can detect that there is something out of the ordinary and that the bearing needs to be investigated. The basis of this evaluation means that in future work the detection of good versus bad bearings can be automated. It would be worthwhile to select an accelerometer that is sensitive across all the expected frequencies, though.

5.4.3 Size, distribution and spacing of nicks

Although tests were not done specifically to see if a larger nick size made a difference to the results it could be deduced from the tests completed. It was known that the nicks on D4 are not as deep and numerous in quantity and thus the deepest and worst nicked bearings would be D2, D3 and D6. D7 has a very large chip but the chip is located towards the edge of the lower raceway of the cup, and this chip was mostly out of the line contact of the rollers. As per the summary in Table 3-1 the bearings which have roller-spaced nicks are D2, D3 and D4. Of these three bearings the ones with the greatest depth are D2 and D3 while D4 is relatively shallow.

When analysing the results obtained from the PSD's it shows that the bearings exciting the most running frequency harmonics were D2, D4 and D6 while D7 was less severe and D1 had even less. It is definitely clear that when the nicks are deeper and more of them occur on the bearings, the greater the running speed harmonics resonate. The running speed harmonics also do not seem to be dependent on the roller-spaced nicks as D4 is not very deep and has this phenomenon. D6 does exhibit running spaced frequencies too and it does not have roller-spaced nicks but is deeply nicked.

Table 3-1 summarises the test bearings nicks. From this table it can be seen that the stylus does not only measure depth of the nick but also the protrusion of the metal surrounding the nick. In this table it is evident that D6 and D2 have the largest amount of protruding metal on the particular nicks that were measured. Intuitively it makes sense that when the roller passes over the high spot an impulse is created as explained in Section 2.4.1. Additionally, when the results are observed at the different sampling rates it can be seen that the amplitudes of vibration that are present in the D2 and D6 bearing are particularly high. When considering bearing D7, it can be seen that there are no high spots and that there is deformation and removed metal from the raceway. It has also been mentioned that the defect occurs close enough to the edge of the raceway that it should be outside of the line contact area. Thus it could be concluded that when there is a small void of metal up to a certain point there is negligible vibration as a result of such. However, when the void of metal becomes great enough then it can become detectable as shown with bearing D7. Additionally, when a high spot exists, then the frequency is excited more than without the high spot.

5.4.4 Bearing bench end-play

The effect that different bench end-plays (BEP's) has on the vibration analysis has been illustrated in Figure 4-39 and Figure 4-40. From the tests completed it appeared as though the results were not greatly affected as a consequence of different BEP readings. Intuitively, it is expected that the BEP would have an impact because with increasing

BEP the internal clearance of the bearing is increased, which would result in vibration associated with looseness. . When the tests were conducted the Lateral Machine had already completed its measurement and the bearing was only being held at a constant lateral position and was being rotated. Thus the effect of various BEP values was negated slightly as the whole assembly was being pushed upwards. Additionally, in order to obtain a good BEP value on the Lateral Machine, the bearings have a tolerance which is normally between 0.023" to 0.029", i.e. there is only 0.006" difference between upper and lower specification. Thus with a bearing within specification on the Lateral Machine the vibrational tests are possible and should not be affected by the variation between upper and lower specification of BEP. The difference within this tolerance band should not vary the expected amplitude of vibration measurement results.

5.4.5 Location of transducer

Nick Position Relative to Sensor

The full range of tests were not conducted with the accelerometers specifically mounted on the nicks or opposite the nicks, unless it was stated as such. With the accelerometer mounted on the track position both nicks in the lower and upper bearings were detectable. As stated in Section 3.2.1, McFadden does say that a race defect is most detectable when the accelerometer is located on top of it, which is in line with the testing observations. He then shows that at 180 degrees from the nick it is less detectable and least detectable at 90 degrees from the nick. Bearing D6 has its deepest nick 90 degrees from the sensor location and it was still detectable. Additionally Figure 4-41 shows that the amplitude is slightly greater for the tests done where the accelerometer was directly on top of the nick, and that the results were similar for tests done with the accelerometer in the track. All tests were performed with the accelerometer mounted in the track.

Mounting Position

As part of the scope of the project an investigation was done to understand if the distinct frequencies present in nicked bearings, and not in non-nicked bearings, could be monitored from a location on the Lateral Machine remote from the bearing. The advantage of finding a result that is distinguishable in a part which is not a bearing component is that it can be permanently set up in the production line to usefully distinguish bad from good bearings, without being dependent on an operator to mount an accelerometer.

a. Cup Lock

Results of tests performed with the IMI accelerometer on the left cup lock of the machine are shown in Figure 4-42 to Figure 4-45. In these figures the frequency pattern occurring at the cup lock was quite different from that which was seen on the bearing itself. The cup lock holds the cup stationary and locked against the upper mandrel to ensure that the cup does not move. The only movement allowed, is the slight movements of the cup lock arms which must be controlled and verified by maintenance and the operators on a periodic basis. The vibration that was thus experienced from the cone rotating within the stationary cup was transferred through the cup onto the cup locks, where the accelerometer could measure it.

From these results it is apparent that when the PSD of the cup locks was taken in the CMS program (and limits were applied to a non-nicked bearing) and various nicked bearings were then subjected to the same limits, that in each case the nicked bearing had exceeded these limits in some way. The amplitudes experienced in the cup locks were much greater than those in the cup outer. The frequencies distinguishing nicked and non-nicked were between 200Hz and 300Hz, 600Hz and 1200Hz. In these frequencies it was noted that they were not present in the non-nicked bearing, but that the amplitudes were considerably greater in the nicked bearings and thus the limits were exceeded.

b. Lower Shaft

The tests that were performed with the IMI accelerometer magnetically mounted to the lower shaft are shown in Figure 4-46 to Figure 4-48. As with the cup lock example the PSD's of the tests were taken and then the limit region was set for the non-nicked bearings. The nicked bearings did exceed these set limits but the amount by which they were exceeded was not substantial. Additionally, the frequency response was much less than with the sensor mounted onto the bearing outer race or onto the cup locks, and only frequencies in the range 30Hz to 300Hz are visible.

5.5 Vibration Associated with Defects other than Cup Nicks

One bearing with no cup nicks (D5) was tested and had one cone nick assembly inserted into the bearing. This was tested in the upper raceway of the cup while the sensor was mounted in the track position, as per all the other standard tests.

The results are shown in Section 4.6.1 and it appears that the cone nick is detectable. When detecting the defect, based on a limit defined from a non-nicked bearing frequency spectrum, the nicked cone was detectable.

However, the defect was not detectable at the 50Hz and 100Hz frequencies in which the cup nicked raceways were so clearly noticeable. The frequencies that were noticeable were between 600Hz and 800Hz and also the 217Hz frequency band.

5.6 Comment on Timken UK NVH Report

The Timken UK (TRS) facility did not have success with their nick detection system in the production line. It is important to understand why this happened as it could provide

valuable information to the future recommendations of the proposal of detecting cup nicks on the production line, whether it is at the Lateral Machine or if a stand-alone testing facility is designed and implemented at the end of the lubrication process.

The main differences between the results of the TRS UK study and results from this research project are as follows:

- The measurement duration was much less in the UK. It was done for the first half of the duration of the Lateral Machine cycle which means measurements were taken between 5 seconds and 7 seconds
- The testing was done in the first half of the Lateral Machine cycle which means that the lower cone was seated and the upper cone's rollers were disengaged. Thus there was rattling occuring in the upper cone's rollers.
- The type of Lateral Machine was different compared with the local one. It was one of the first generation machines which had a gearbox instead of a reduction motor. There must have thus been more gear mesh frequencies introduced into the system.
- The analyzing software was looking for the difference within the FFT results and not the PSD results as was done locally. Additionally, the maximum resolution that the data capturing system could provide was 0.3Hz vs. the 0.009Hz obtainable with the local data acquisition system.
- The maximum sampling rate of the acquisition instrument was 15 kHz which means that the maximum frequency which can be considered without having aliasing concerns was between 2500Hz and 3000Hz, and low frequencies were not clearly distinguished.
- The software was looking for bearing defect frequency limits which were not apparent in the local testing.
- The magnet was applied by an operator and perhaps care was not taken where the sensor was mounted.
- The UK tests spanned a period of 3 months, within a production line, and thus had a much larger sample from which to determine whether the results really were

repeatable or not, and from which representative amplitude limits could be averaged.

From the above points it is difficult to pinpoint exactly what made the UK results seem unsuccessful and the South African results successful. The biggest difference could be the accuracy and resolution with which the data was sampled locally as well as at which part of the Lateral Machine cycle the data was captured in. Tests in this research were not done at such a short duration to understand if that would make a difference as well. The main concern would be that in such a short time, with the operator applying the accelerometer to the bearing, that it is possible that the accelerometer was not given enough settling time.

The associates from the UK believe that as part of their possible future testing, if ever, that they would consider using two accelerometers mounted on each raceway. They would also try to investigate if they could use a newer technology Lateral Machine on which to conduct the testing.

5.7 Research Questions

Considering the research questions that were asked at the commencement of the research project the following paragraphs will aim to address these.

Based on the research completed, it is believed that it is feasible to detect cup nicks in class D AP bearings. A representative sample was tested from the production line (non-nicked). Tests were also conducted with simulated nicks, and there was a difference between the non-nicked and nicked test pieces. The standard condition monitoring techniques associated with bearing defect frequency detection were not used to distinguish such differences, as both the nicked and non-nicked bearings displayed vibration amplitudes at the expected ball pass frequencies. It is believed that this is as a

result of the loading provided by the Lateral Machine. The standard vibration techniques associated with bearing fault detection are typically practiced when bearings are installed and the correct mounted end-play exists within the mounted system in the application. Additionally, the bearings are exposed to loads similar to their design load rating and mostly in a radial direction. In the Lateral Machine most of the bearing loading that occurred was in the axial direction. Most importantly, because of the design of the machine the rollers were equally loaded along the full load zone. Thus there was not clear deformation of the rollers as they entered and exited the load zone. This feature is part of the explanation as to why the repetitive ball pass frequencies were created. Thus it is believed that it is possible to detect the difference between nicked and non-nicked bearings on the Lateral Machine as per the results shown with pre-defined acceptable limits over the whole frequency range using PSD's.

The Lateral Machine, however, may not be the most ideal piece of equipment due to the characteristics described. It is recommended that more testing should be completed in high volumes on the production line and that the technique described is tested within the production environment to understand if the limits are truly repeatable.

The vibration amplitude measurement was found to correlate with the severity of the cup nicks as found on the bearing raceways. This was true in depth, raised metal and amount of nicks on the raceway. The correlation in physical nick size such as length was less noticeable than the other parameters.

Bearings were not tested when they were fully assembled i.e. once they had been lubricated with grease. The testing was completed in the Lateral Machine so that easy disassembly could occur and the defects could be clearly examinable. To fully understand the answer to this question extensive testing would be required once the bearings are lubricated. A separate test facility would need to be designed and sufficient radial loading would need to be induced.

In summary the discussions were themed to understand how the different parameters taken into consideration during data acquisition phase influenced the results achieved during data analysis. It was seen that analysing the data with the power spectral density rather than only the frequency spectrum accentuated the vibrational amplitude in such a manner that the differences between the nicked and non-nicked bearings were more distinct. It was shown that bearings of different bench end-play still showed measureable results, and that the limits prescribed for non-nicked bearings were exceeded in all cases where nicks were present on the cup raceways. Additionally, it was shown that nicks that were present on the cone raceways were also detectable. From the production and nicked sample of bearings that were analysed it has been seen that nicks are detectable when considering the whole frequency spectrum and that they are not detectable when only considering the normal bearing defect frequencies associated with the bearing geometry and rotational speed of the bearing components.

6 CONCLUSIONS

The following paragraphs summarise the conclusions as they relate to the stated objectives.

i. The system that was set up on the Lateral Machine to complete the research was to use the machine in the production environment with as little modification to the operating cycle as possible. This was done in order to apply potential solutions found in the research project directly to the Lateral Machine in a production context. The speed of the Lateral Machine was measured using a tachometer and verification was done of the repeatability of the measured vibrations. The vibration was measured with two different accelerometer sensitivities and it was found that the accelerometer with greater sensitivity (of capacitance design) that was glued onto the cup OD was the most effective. Testing was also completed to determine the effectiveness of mounting the accelerometer onto a machine component instead of on the bearing. It was possible to use the Lateral Machine in the state as used in production and testing was possible on the bearings. A stand alone non-automated method was used to detect the vibration amplitude and separate post-testing data processing had to be conducted.

ii. With the testing that was completed the frequency signature of a nick-free bearing on the Lateral Machine produced repeatable results. A number of nick-free bearings were tested to form a baseline for comparison. Depending on the data acquisition sampling rate, different frequencies were more prominent than others, based on the non-nicked bearings tested at such sampling rates. This baseline was repeatable. It was noted that non-nicked bearings did depict the signal of the outer defect frequency as well as the roller and inner defect frequencies. This is attributed to the frequency being accurate when defects

pass in and out of the load zone of a bearing which is not the case on the Lateral Machine i.e. the frequencies are not representative of defects on any of these components. The differences between nicked and non-nicked bearings were most clearly seen in a power spectral density spectrum (PSD) which depicts the energy associated with frequencies, rather than just the frequency spectrum derived from an FFT. It was possible to create limits across the frequency spectrum of each sampling rate measured for a nick-free bearing. Other non-nicked bearings maintained repeatable results within this non-nicked limit. The vibration of the nicked bearings were then measured against these limits at the same sampling rates. In every test, these limits were exceeded by the energy present in certain frequencies within the nicked bearing specimens. This limit was exceeded due to the increased vibration amplitudes of the nicked specimens at specific frequencies. In certain frequency bands and at certain sampling rates, frequencies were excited in the nicked bearings that were not present in the non-nicked specimens. The characteristic frequencies associated with bearing defects were not beneficial in the tests. Specifically the ball pass frequency of an outer defect was present in both nicked and non-nicked bearings. The nicks did however excite frequencies that did not have relevance to the bearing geometry such as 50Hz and 100Hz, thus the energy associated with the impact of the roller across the nick was transmitted into machine running frequencies and possibly acoustics. The natural frequencies of the cone and cup did coincide with some of the frequency peaks that were excited by the nicked bearings.

iii. The different sampling parameters such as sampling rate did have a significant affect on the results measured. This was due to the lack of certain frequencies in the lower frequency range when sampled at high rates, or the lack of high range frequencies at low sampling rates. The 1200Hz sampling rate yielded very interesting running speed frequencies which were excited in amplitude by the presence of nicks, and specifically roller-spaced nicks. The 1200Hz sampling

rate did not have a high frequency range to show the effect of resonance frequencies of the bearing components. The sampling that was completed at 9600Hz did have the high resonance frequencies of the bearing components and it was clear that the presence of nicked cups did excite these frequencies. The running speed frequencies were not clear in this sampling rate but the nicked bearings did exceed the limits of non-nicked bearings at 50Hz and 100Hz. The testing duration was shown to not have a significant effect and the difference in amplitudes between nicked and non-nicked bearings sampled at 200 seconds or 10 seconds was negligible. This is good for detection in the production line as 200 seconds would have slowed the process down considerably. Conclusively, when the tests are sampled at a particular sampling rate it is important that the non-nicked acceptable limits are set per those conditions. The limits are not interchangeable between different sampling rates.

iv. There was a correlation in the results with the size of nicks detectable and the amplitude of the associated frequencies. With the approach taken to set a limit across the whole frequency spectrum of the results it was not greatly concerning if the nicks were not big enough to excite one particular frequency as much as the larger nicks did. This is because in totality another frequency band was excited and thus the baseline limits were exceeded showing the presence of a defect of some size. It was found that the severity of the nick did play a role in transposing the energy of the rollers passing over the nicked surface to the running speed frequency and its associated harmonics. In the tests done, the presence of roller-spaced nicks did not have a big impact on the results and the depth and presence of raised metal of the nicks were more noticeable. In all cases where raised metal existed in the nicks the greatest vibration amplitudes were measured. In one sample no raised metal was present but the defect was of much greater size and it also had considerable vibration peaks. A single test was performed with a cone nick and this too exceeded the baseline set by the non-

nicked bearing specimens. The cone nick was a very small, single nick and thus its identification shows that nicks of a very small size can be detected.

v. It was found that variation in bench end-play (BEP) did not have a significant affect on the results of the frequency spectrum. If it was a nicked bearing, at different BEP's, the limits were exceeded and if it was a non-nicked bearing, at different BEP's, the amplitudes were within the limits set. The tolerance for acceptable BEP's at the Lateral Machine will control this parameter and thus the BEP's should not have an affect on the ability to detect nicks in a production environment.

vi. The roller-spaced nicks did excite the running speed frequencies more than the non-roller-spaced nick test pieces. The limits were exceeded and both roller-spaced and non-roller-spaced nicks gave greater amplitudes than defined by non-nicked acceptable bearings.

vii. The accelerometers were mounted both magnetically and with adhesion. The biggest impact on the results was due to using accelerometers with different sensitivities. With a larger sensitivity certain of the low frequencies were neither distinct nor present and with the lower sensitivity instrument certain of the higher frequencies were not present. Most of the limits that were required to be exceeded to classify a bearing as non-nicked were of the lower frequency range and thus the lower frequency accelerometer was recommended. Tests were done where the sensors were mounted across a deep nick and the amplitude of such tests were greater than when the accelerometer was mounted on the track of the bearing. When, however, the accelerometer was mounted in the track it was still possible to distinguish between nicked and non-nicked test pieces. Additionally, it was found that when taking measurements in the second half of the Lateral Machine cycle, when the bottom cone is seated and the top cone is partially seated, both nicks in the top and bottom races are detectable.

Nicks were also detectable at ninety degrees to the accelerometer attachment location which theory suggests is the most difficult to detect. Tests were done with the accelerometer mounted on the cup lock as well as on the lower shaft. It was found that when the accelerometer was mounted on the cup lock that the vibration transfers to the cup lock were sufficient to give repeatable results to successfully detect cup nicks from that location. The distinguishing frequencies and amplitudes between the nicked and non-nicked bearings sampled from the lower shaft were not very distinct nor were they repeatable and this location is not recommended.

viii. As a result of the knowledge gained during this investigation and the results that have been achieved it is recommended that further work be done to develop this model for implementation within the production facility. On the Lateral Machine it has been shown that with all the inherent noise, that the frequencies from a nicked bearing are still exciting amplitudes greater than that of a non-nicked bearing, and as they result should be detectable. Further, it has been found that these frequencies are carrying through to the cup lock and thus a sensor could be mounted on this area that does not have to be handled by the operator. Further development would be needed with regard to the computational ability of software to automatically detect defects in the production line. This computation would need to be rapid enough so that it does not considerably slow down the production output. Additional consideration would also have to be given to the impact of doing the testing at the Lateral Machine or if it would be better to do it at the last station before packaging. This could then become a certificate provided to the customer with the frequency signature of the good bearing which they have acquired. This would, however, require a separate testing facility as well as the ability to detect the nicks through the dampening effect that the grease of the lubricated bearing would have. Such a testing facility should have the ability to create a loaded zone on the bearing such that the characteristic defect frequencies are detectable

in the arrangement. Further work will also include broadening the scope of the project to different modes of bearing defects and not only nicks.

7 RECOMMENDATIONS

Further work needs to be done on the South African solution to ensure that the same problems are not encountered as with the UK tests. It will only become apparent when the number of samples is considerably increased, to ensure that the results that have been achieved are repeatable, and that limits can confidently be established on good bearings which become the baseline for all tests. It will also further need to be understood at what sampling rate the repeatability is better and if the shorter testing duration is truly plausible. The importance of having the sensors mounted off the bearing components is crucial as it negates the need for the operator to mount the sensor which would affect repeatability of the results and calibration of the sensor.

Once the repeatability of the baseline is confirmed then work will need to be done to analyse the results against the baseline in real time, without slowing down the production line.

Further recommendations exist to explore using machinery with less inherent noise than the Lateral Machine. Most importantly it would be beneficial to have a machine that can create a load zone on the bearing. This could make the detection of nicks via the characteristic defect frequencies easier.

In addition, there may be other bearing defects that could be detected but research will need to be conducted to identify these defects and the affect that they may have on the bearing vibration signature.

It is recommended that further work be done on ensuring that nicks are prevented in both the production line and assembly lines. This could be achieved by incorporating an assembly jig (especially for larger bearings with heavier components). It is important that operator and inspector awareness is further driven to ensure they understand the severity

of allowing a bearing component with a nick to pass through to the customer. An assessment is also recommended on all machinery during the grinding and assembly process to ensure that nicks are not being created by them.

It will however be greatly valuable if a vibration print out of each bearing could be on record and provided to the customer to show that the bearing has been tested for vibration patterns and that it passed that requirement as well. This will further increase the quality of the product delivered to the customer as well as the traceability of the bearings provided to them. This is currently not a company requirement but this need may need to be reviewed if benefit is seen in having such a quality check in place.

8 WORKS CITED

Attivissimo, F., Savino, M. & Trotta, A., 1995. Flat-Top Smoothing of Periodograms and Frequency Averagings to Increase the Accuracy in Estimating Power Spectral Density. *Measurement,* Volume 15, pp. 15-24.

Bruel & Kjaer, 1980. *Mechanical Vibration and Shock Measurements,* K. Larsen & Son.

Chambers, J. & Bunting, K., 1981. *Bearing Vibration Monitoring.* Derby, The Timken Company.

Endevco Corporation, 2012. *Steps to Selecting the Right Accelerometer TP327,* San Juan Capistrano, California: Endevco Corporation.

Goldman, S., 1948. *Frequency Analysis Modulation and Noise.* New York: McGraw-Hill Book Company.

Koch, J.-R., 2009. *Feasibility of Detecting Nicks on Rail Bearings,* Colmar: The Timken Company.

McFadden, P. & Smith, J., 1984. Vibration Monitoring of Rolling Element Bearings by the High-Frequency Resonance Technique - Review. *Tribology International,* 17(1), pp. 3-10.

Mechefske, C. & Mathew, J., 1992. Fault Detection and Diagnosis in Low Speed Rolling Element Bearings Part I: The Use of Parameteric Spectra. *Mechanical Systems and Signal Processing,* 6(4), pp. 297-307.

Mobius Institute, 1999. *Vibration Training Course Category I.* Johanesburg: Vibration Institute of South Africa.

Norton, M. & Karczub, D., 2003. *Fundamentals of Noise and Vibration Analysis for Engineers.* Second Edition. Cambridge: Cambridge Univeristy Press.

NTN-SNR, 2012 [Online] Available at: https://www.ntn-snr.com/catalogue/fr/en-en/index.cfm?page=/catalogue/home/industry [Accessed 15 October 2012].

Pineyro, J., Klempnow, A. & Lescano, V., 2000. Effectiveness of new spectral tools in the anomaly detection of rolling element bearings. *Journal of Alloys and Compounds,* Volume 310, pp. 276-279.

Randall, R. B., 2011. *Vibration-Based Condition Monitoring Industrial, Aerospace and Automotive Applications.* West Sussex: John Wiley and Sons.

Rao, S., 2004. *Mechanical Vibrations.* Fourth Edition ed. New Jersey: Pearson Prentice Hall.

Scheffer, C., 2010. *Practical Machinery Vibration Analysis and Predictive Maintenance.* Version 1.03 ed. Johannesburg: IDC Technologies.

Seippel, R., 1983. *Transducers, Sensors and Detectors.* Reston: Reston Publishing Prentice-Hall.

Sumitomo Machinery Corporation of America, 2012. *SM-CYCLO Speed Reducers, Gearmotors and Brakemotors Manual 04.601.60.001,* Sumitomo Machinery Corporation.

Sumitomo Machinery Corportation of America, 2011. *Cyclo 6000 Gearmotors Catalog 04.601.50.007*.

Tandon, N. & Choudhury, A., 1997. An Analytical Model for the Prediction of the Vibration Response of Rolling Element Bearings due to a Localized Defect. *Journal of Sound and Vibration,* 205(3), pp. 275-292.

Tandon, N. & Choudhury, A., 1999. A Review of Vibration and Acoustic Measurement Methods for the Detection of Defects in Rolling Element Bearings. *Tribology International,* Volume 32, pp. 469-480.

The Timken Company, 1990. *AP Bearings for Industrial Applications Catalogue.* Canton: Order Number 10.

The Timken Company, 1990. *Timken Bearing Damage Analysis with Lubrication Reference Guide.* Canton: Order Number 5892.

The Timken Company, 2011. *Corporate Standard 10.25 Nicks on Finished Tapered, Cylindrical and Spherical Bearing Surfaces.* Canton: The Timken Company.

Valentim, L., 1998. *CMS Program Version 4.0.8.0,* Johannesburg: TLC Engineering Solutions.

Wang, G. et al., 2008. Fault identification and classification of rolling element bearing bsed on time-varying autoregressive spectrum. *Mechanical Systems and Signal Processing,* Volume 22, pp. 934-947.

9 BIBLIOGRAPHY

Adams, M. J., 2001. *Rotating Machinery Vibration from Analysis to Troubleshooting.* Marcel Dekker Inc.

Childers, G. D., 1978. *Modern Spectrum Analysis.* Florida: Institute of Electrical and Electronics Engineers Press.

de Silva, C. W., 2007. *Vibration Fundamentals and Practice.* Second Edition. Florida: CRC Press.

Dong, G. & Chen, J., 2012. Noise Resistant Time Frequency Analysis and Application in Fault Diagnosis of Rolling Element Bearings. *Mechanical Systems and Signal Processing,* Volume 33, pp. 212-236.

Fox, G., Martens, M. & Nixon, H., 1999. A Beraing life Prediction Method for Utilizing Progressive Functional Surface Damage Analysis from a Debris Contaminated Lubrication Environment. *The Engineering Society for Advancing Mobility Land Sea, Air and Space International.*

Li, C. & Li, S., 1995. Acoustic Emission Analysis for Bearing Condition Monitoring. *Wear 185,* pp. 67-74.

Litmann, W. & Moyer, C., n.d. Competitive Modes of Failure in Rolling Contact Fatigue. *Society of Automotive Engineers.*

Littmann, W. & Widner, R., 1966. Propogation of Contact Fatigue From Surface and Subsurface Origins. *Journal of Basic Engineering,* Volume September 1966, pp. 624-636.

Mechefske, C. & Mathew, J., 1992. Fault Detecion and Diagnosis in Low Sped Rolling Element Bearings Part II: The Use of Nearest neighbour Classification. *Mechanical Systems and Signal Processing*, 6(4), pp. 309-316.

Ragulskis, K.M., 1979. *Vibration of Bearings*, Amerind Publishing.

Sawalhi, N. & Randall, H., 2007. The Enhancement of Fault Detection and Diagnosis in Rolling Element Bearings Using Minimum Entropy Deconvolution Combined with Spectral Kurtosis. *Mechanical Systems and Signal Processing*, Volume 21, pp. 2616-2633.

Sawalhi, N. & Randall, R., 2008. Simulating Gear and Bearing Interactions in the Presence of Faults Part I. The Combined Gear Bearing Dynamic Model and the Simulation of Localised Bearing Faults. *Mechanical Systems and Signal Processing*, Volume 22, pp. 1924-1951.

Sawalhi, N. & Randall, R., 2008. Simulating Gear and Bearing Interactoins in the Presence of Faults Part II: Simulation of the Vibrations Produced by Extended Bearing Faults. *Mechanical Systems and Signal Processing*, Volume 22, pp. 1952-1966.

Sawalhi, N. & Randall, R., 2011. Vibration Response of Spalled Rollng Element Bearings: Observations, Simulations and Signal Processing Techniques to Track the Spall Size. *Mechanical Systems and Signal Processing*, Volume 25, pp. 846-870.

APPENDIX A – LATERAL MACHINE FREQUENCIES

The single reduction motor that is used in the Lateral Machine is a Sumitomo SM-Cyclo part number CNHM S 1 4097 YC 11. This is an older type of motor which has now been replaced with the 6095 series model replacing 4097 in the part number. It is a 4 pole motor which when operated at a 50Hz power supply delivers rotates a motor at 1500RPM and has an output speed of 136RPM due to its 11 times reduction ability achieved by the eccentric bearing shown as 3-04 in Figure A-1 (Sumitomo Machinery Corportation of America, 2011).

In the preceding text the vibration frequencies associated with the bearings within this motor will be defined at the input and output speed of the motor.

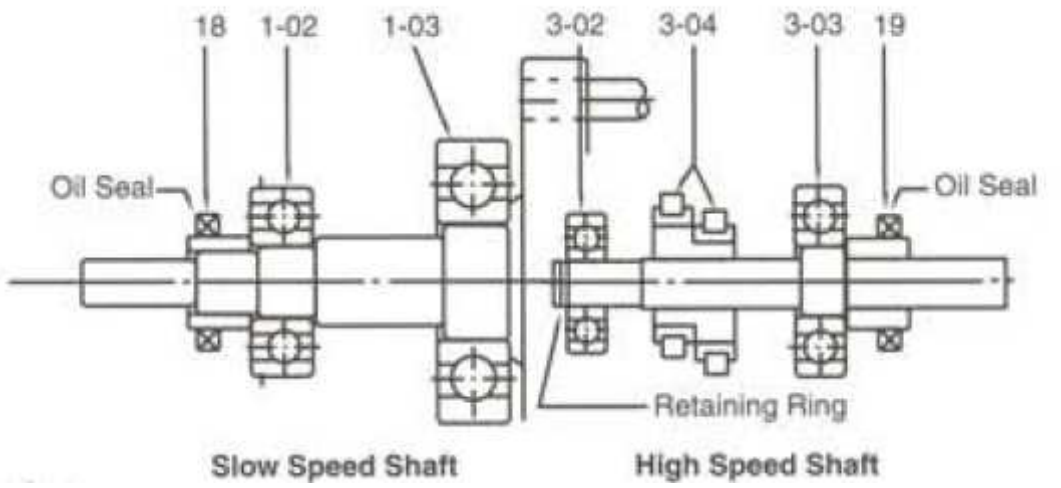

Figure A-1 – Bearing arrangement in sumitomo SM-Cyclo speed reducer (Sumitomo Machinery Corporation of America, 2012, pp. Figure A-9)

As per Figure A-1 the slow speed shaft has two bearings and the high speed shaft has two bearings as well as the eccentric bearing shown. In Figure A-2 the bearings used on

the slow speed shaft are shown and it can be seen that bearings 6306Z and 16011 are present. Similarly in Figure A-3 the bearings used on the high speed shaft are defined.

Frame Size		Slow Speed Shaft	
Single Reduction	Double Reduction	Bearing A Part #1-02	Bearing B Part #1-03
6060, 6065	6060DA, 6065DA	6204Z	6909
6070, 6075	6070DA, 6075DA	6204Z	6909
6080, 6085	–	6305Z	6009
6090, 6095	6090DA, 6095DA	6306Z	16011
6100, 6105, 610H	6100DA, 6105DA	6306Z	16011
6110, 6115	–	6307Z	6011
6120, 6125, 612H	6120DA, 6125DA, 6120DB, 6125DB	6308Z	6013
6130, 6135	6130DA, 6135DA, 6130DB, 6135DB, 6130DC, 6135DC	6211NR	6213
6140, 6145,614H	6140DA, 6145DA, 6140DB, 6145DB, 6140DC, 6145DC	22211EXNR	6213
6160, 6165	6160DA, 6165DA, 6160DB, 6165DB, 6160DC, 6165DC	3TM-6213NR[1]	6215[1]
6170, 6175	6170DA, 6175DA, 6170DB, 6175DB, 6170DC, 6175DC	6216NR[1]	6218[1]
6180, 6185	6180DA, 6185DA, 6180DB, 6185DB	6218NR[1]	6220[1]
6190, 6195	6190DA, 6195DA, 6190DB, 6195DB	6221NR[1]	6026[1]
6205	6205DA, 6205DB	22220BNRC2	6222C2
6215	6215DA, 6215DB	23022BNRC2	6224C2
6225	6225DA,6225DB	23024BNRC2	6226C2
6235	6235DA, 6235DB	23026BNRC2	NUP228C2
6245	6245DA, 6245DB	23028BNRC2	NUP230C2
6255	6255DA, 6255DB	23032BNRC2	NUP234C2
6265	6265DA	23034BNRC2	NUP236C2
6275	6275DA	23136BNXR	6340

Figure A-2 – Bearing reference for slow speed shaft (Sumitomo Machinery Corporation of America, 2012, pp. Table A-21)

Frame Size		High Speed Shaft			
Single Reduction	Double Reduction	Bearing C Part #3-02	Bearing D Part #3-03	Eccentric Part #3-04	Qty.
6060, 6065	6060DA, 6065DA, 6070DA, 6075DA	6301	6301Z	607YXX	1
6070, 6075	6090DA, 6095DA, 6100DA, 6105DA, 6120DA, 6125DA, 6130DA, 6135DA, 6140DA, 6145DA	6301	6301Z	607YXX	1
6080, 6085	–	6301SH	6302Z	6004RSH2ZZC3	1
6090, 6095	6120DB, 6125DB, 6130DB, 6135DB, 6140DB, 6145DB, 6160DA, 6165DA, 6170DA, 6175DA	6302RSH2	6302Z	Refer to Table A-22	1
6100, 6105, 610H	6130DC, 6135DC, 6140DC, 6145DC, 6160DB, 6165DB, 6170DB, 6175DB, 6180DA, 6185DA	6302RSH2	6302Z		
6110, 6115	–	6302RSH2	6302Z	611YSS, 611GSS	2
6120, 6125, 612H	6160DC, 6165DC, 6170DC, 6175DC, 6190DA, 6195DA, 6205DA	6304	6305Z	Refer to Table A-22	1
6130, 6135	6180DB, 6185DB, 6190DB, 6195DB, 6205DB, 6215DA, 6225DA	6305	6306		
6140, 6145, 614H	–	6305R	6306		
6160, 6165, 616H	6215DB, 6235DA, 6245DA	6307R	6308		
6170, 6175	6255DA, 6255DB	6406	6407	617YSX	2
6180, 6185	6235DB, 6245DB	6407	6409	618YSX	2
6190, 6195	6255DB, 6265DA, 6275DA	6408	6411	619YSX	2
6205	–	NJ310EV7	21311V1	620GXX	2
6215	–	NJ311EV16	21311V1	621GXX	2
6225	–	NJ312EV11	21312V1	622GXX	2
6235	–	NJ313EV11	21314V1	623GXX	2
6245	–	NJ314EV7	21315V1	624GXX	2
6255	–	NJ316EV1	21318V1	625GXX	2
6265	–	NJ317EV1	21318V1	626GXX	2
6275	–	NJ417	22222BL1	627GXX	2

Note: [1] For grease lubricated models, a sealed bearing should be used, which changes the following letters in the part number to those shown in bold: NR (Std.) – **ZNR;** NXR – **ZNXR;** None – add **Z**.

Figure A-3 – High speed shaft bearing selection table (Sumitomo Machinery Corporation of America, 2012, pp. Table A-21)

As seen in Figure A-3 the eccentric bearing used is found in Figure A-4. All the bearings have been looked up and the associated frequencies have been tabulated in Table 4-5.

	Frame Size					
High Speed Shaft, Motor Shaft Part #3-04	6090, 6095	6100, 6105	6120, 6125	6130, 6135	6140, 6145	6160, 6165
Intermediate Shaft Part #5-04 / Reduction Ratio	6090DA 6095DA	6100DA 6105DA	6120DA, 6125DA 6120DB, 6125DB	6130DA, 6135DA 6130DB, 6135DB 6130DC, 6135DC	6140DA, 6145DA 6140DB, 6145DB 6140DC, 6145DC	6160DA, 6165DA 6160DB, 6165DB 6160DC, 6165DC
6	60906YRX	6100608YRX	6120608YRX	61406-11YSX	61406-11YSX	6160608YRX2
8	60908-15YSX	6100608YRX	6120608YRX	61406-11YSX	61406-11YSX	6160608YRX2
11	60908-15YSX	61011-15YRX	6121115YSX	61406-11YSX	61406-11YSX	61611-15YSX
13	60908-15YSX	61011-15YRX	6121317YSX	61413-17YSX	61413-17YSX	61611-15YSX
15	60908-15YSX	61011-15YRX	6121115YSX	61413-17YSX	61413-17YSX	61611-15YSX
17	60917YSX	61017YSX	6121317YSX	61413-17YSX	61413-17YSX	61617-25YSX
21	60921YSX	61021YRX	61221YRX	6142125YSX	6142125YSX	61617-25YSX
25	6092529YSX	6102529YRX	6122529YSX	6142125YSX	6142125YSX	61617-25YSX
29	6092529YSX	6102529YRX	6122529YSX	6142935YSX	6142935YSX	6162935YSX
35	60935YSX	61035YRX	61235YRX	6142935YSX	6142935YSX	6162935YSX
43	60943YSX	61043YSX	61243YSX	61443-59YSX	61443-59YSX	6164351YSX
51	60951YRX	61051YRX	6125159YSX	61443-59YSX	61443-59YSX	6164351YSX
59	60959YSX	61059YRX	6125159YSX	61443-59YSX	61443-59YSX	61659YSX
71	60971YRX	61071YRX	6127187YSX	6147187YSX	6147187YSX	61671YRX2
87	60987YSX	61087YRX	6127187YSX	6147187YSX	6147187YSX	61687YSX
119	609119YSX	610119YSX	–	–	–	–

Figure A-4 – Eccentric bearings described as 3-04 in Figure A-1 (Sumitomo Machinery Corporation of America, 2012, pp. Table A-22)

APPENDIX B – TESTING EQUIPMENT SPECIFICATIONS

IMI Accelerometer - Sensitivity 96mV/g

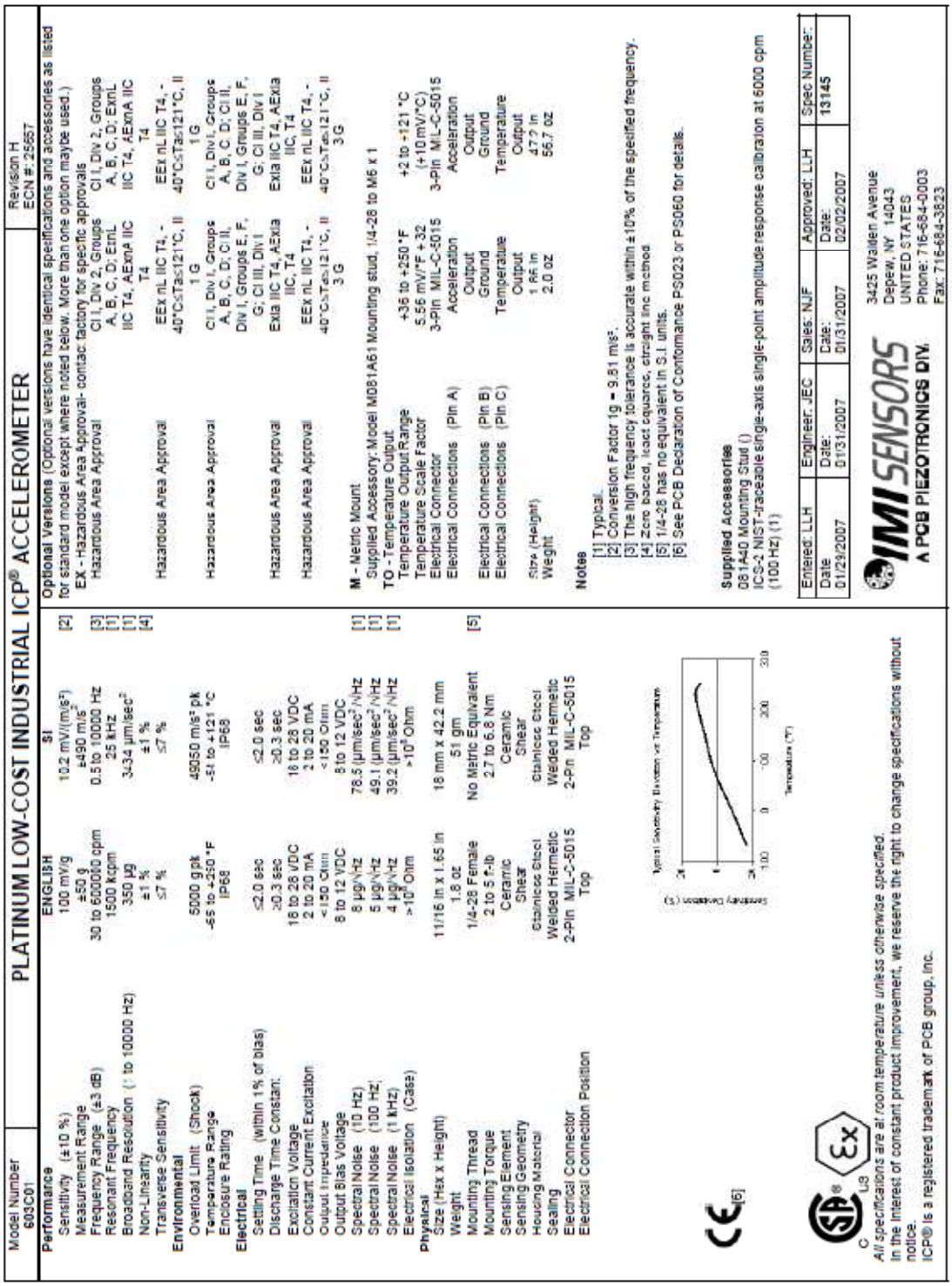

Model Number 603C01 | PLATINUM LOW-COST INDUSTRIAL ICP® ACCELEROMETER | Revision H, ECN #: 25657

Performance	ENGLISH	SI	
Sensitivity (±10 %)	100 mV/g	10.2 mV/(m/s²)	[2]
Measurement Range	±50 g	±490 m/s²	
Frequency Range (±3 dB)	0.5 to 10000 Hz	0.5 to 10000 Hz	[3]
Resonant Frequency	25 kHz	25 kHz	[1]
Broadband Resolution (1 to 10000 Hz)	350 µg	3434 µm/sec²	[1]
Non-Linearity	±1 %	±1 %	[4]
Transverse Sensitivity	≤7 %	≤7 %	
Environmental			
Overload Limit (Shock)	5000 g pk	49050 m/s² pk	
Temperature Range	-65 to +250 °F	-54 to +121 °C	
Enclosure Rating	IP68	IP68	
Electrical			
Settling Time (within 1% of bias)	≤2.0 sec	≤2.0 sec	
Discharge Time Constant	≥0.3 sec	≥0.3 sec	
Excitation Voltage	18 to 28 VDC	18 to 28 VDC	
Constant Current Excitation	2 to 20 mA	2 to 20 mA	
Output Impedance	<150 Ohm	<150 Ohm	
Output Bias Voltage	8 to 12 VDC	8 to 12 VDC	
Spectral Noise (10 Hz)	8 µg/√Hz	78.5 (µm/sec²)/√Hz	[1]
Spectral Noise (100 Hz)	5 µg/√Hz	49.1 (µm/sec²)/√Hz	[1]
Spectral Noise (1 kHz)	4 µg/√Hz	39.2 (µm/sec²)/√Hz	[1]
Electrical Isolation (Case)	>10⁸ Ohm	>10⁸ Ohm	
Physical			
Size (Hex x Height)	11/16 in x 1.65 in	18 mm x 42.2 mm	
Weight	1.8 oz	51 gm	
Mounting Thread	1/4-28 Female	No Metric Equivalent	[5]
Mounting Torque	2 to 5 ft-lb	2.7 to 6.8 Nm	
Sensing Element	Ceramic	Ceramic	
Sensing Geometry	Shear	Shear	
Housing Material	Stainless Steel	Stainless Steel	
Sealing	Welded Hermetic	Welded Hermetic	
Electrical Connector	2-Pin MIL-C-5015	2-Pin MIL-C-5015	
Electrical Connection Position	Top	Top	

Optional Versions (Optional versions have identical specifications and accessories as listed for standard model except where noted below. More than one option maybe used.)

EX - Hazardous Area Approval- contact factory for specific approvals

Hazardous Area Approval	Cl I, Div 2, Groups A, B, C, D; ExmL IIC T4, AExmA IIC T4	Cl I, Div 2, Groups A, B, C, D; ExmL IIC T4, AExmA IIC T4
Hazardous Area Approval	EEx nL IIC T4, - 40°C≤Ta≤121°C, II 1 G	EEx nL IIC T4, - 40°C≤Ta≤121°C, II 1 G
Hazardous Area Approval	Cl I, Div I, Groups A, B, C, D; Cl II, Div I, Groups E, F, G; Cl III, Div I	Cl I, Div I, Groups A, B, C, D; Cl II, Div I, Groups E, F, G; Cl III, Div I
Hazardous Area Approval	Exia IIC T4, AExia IIC, T4	Exia IIC T4, AExia IIC, T4
Hazardous Area Approval	EEx nL IIC T4, - 40°C≤Ta≤121°C, II 3 G	EEx nL IIC T4, - 40°C≤Ta≤121°C, II 3 G

M - Metric Mount

Supplied Accessory: Model M081A61 Mounting stud, 1/4-28 to M6 x 1

TO - Temperature Output

Temperature Output Range	+36 to +250 °F	+2 to +121 °C
Temperature Scale Factor	5.56 mV/°F ±32	(±10 mV/°C)
Electrical Connector	3-Pin MIL-C-5015	3-Pin MIL-C-5015
Electrical Connections (Pin A)	Acceleration	Acceleration
	Output	Output
Electrical Connections (Pin B)	Ground	Ground
Electrical Connections (Pin C)	Temperature	Temperature
	Output	Output
Size (Height)	1.66 in	47.2 in
Weight	2.0 oz	56.7 oz

Notes

[1] Typical.
[2] Conversion Factor 1g = 9.81 m/s².
[3] The high frequency tolerance is accurate within ±10% of the specified frequency.
[4] Zero based, least squares, straight line method
[5] 1/4-28 has no equivalent in S.I. units.
[6] See PCB Declaration of Conformance PS023 or PS060 for details.

Supplied Accessories

081A40 Mounting Stud ()
ICS-2 NIST-traceable single-axis single-point amplitude response calibration at 6000 cpm (100 Hz) (1)

Entered: LLH	Engineer: JEC	Sales: NJF	Approved: LLH	Spec Number:
Date: 01/29/2007	Date: 01/31/2007	Date: 01/31/2007	Date: 02/02/2007	13145

Typical Sensitivity Deviation vs Temperature

(%) Deviation from Reference

Temperature (°F)

CE [6]

C US

All specifications are at room temperature unless otherwise specified.
In the interest of constant product improvement, we reserve the right to change specifications without notice.
ICP® is a registered trademark of PCB group, Inc.

IMI SENSORS
A PCB PIEZOTRONICS DIV.

3425 Walden Avenue
Depew, NY 14043
UNITED STATES
Phone: 716-684-0003
Fax: 716-684-3823

Microtron 7290A Accelerometer – Sensitivity 20mV/g

Specifications

All values are typical at +75°F (+24°C) and 15 Vdc excitation unless otherwise stated. Calibration data, traceable to the National Institute of Standards, (NIST), is supplied.

Dynamic characteristics	Units	7290A-2	-10	-30	-50	-100	-150
Range [1]	g	±2	±10	±30	±50	±100	±150
Sensitivity	mV/g	1000 ±50	200 ±10	66 ±4	40 ±2	20 ±1	13.2 ±0.66
Frequency response (± 5%) [2]	Hz	0 to 15	0 to 500	0 to 800	0 to 1000	0 to 1000	0 to 1000
Mounted resonance frequency	Hz	1300	3000	5500	6000	6000	6000
Non-linearity and hysteresis	% FSO typ (max)	±0.20 (±0.50)	±0.20 (±0.50)	±0.20 (±0.50)	±0.20 (±0.50)	±1 (±2)	±1 (±2)
Transverse sensitivity [3]	% (max)	2	2	2	2	2	2
Zero measurand output	mV	±50	±50	±50	±50	±50	±50
Damping ratio		4.0	0.7	0.7	0.6	0.6	0.6
Damping ratio change							
From -65°F to +250°F (-55°C to +121°C)	%/°C	+0.08	+0.08	+0.08	+0.08	+0.08	+0.08
Thermal zero shift (max)							
From 32°F to 122°F (0°C to 50°C)	% FSO [4]	±1.0	±1.0	±1.0	±1.0	±1.0	±1.0
From -13°F to +167°F (-25°C to +75°C)	% FSO	±2.0	±2.0	±2.0	±2.0	±2.0	±2.0
Thermal sensitivity shift (max)							
From 32°F to 122°F (0°C to +50°C)	%	±2.0	±2.0	±2.0	±2.0	±2.0	±2.0
From -13°F to +167°F (-25°C to +75°C)	%	±3.0	±3.0	±3.0	±3.0	±3.0	±3.0
Thermal transient error per ISA RP 37.2	Equiv. g/°C	‹ 0.001	‹ 0.001	‹ 0.001	‹ 0.001	‹ 0.001	‹ 0.001
Overrange (determined by electrical clipping or mechanical stops, whichever is smaller.)							
Electrical clipping	g	-3.5/+3.8	-18/+19	-53/+57	-87/+95	-175/+190	-265/+288
Mechanical stops, typical	g	±4	±30	±90	±90	±150	±300
Recovery time	µs	‹ 10	‹ 10	‹ 10	‹ 10	‹ 10	‹ 10
Threshold (resolution) [5]	Equiv. g's	0.0005	0.0025	0.0075	0.013	0.013	0.013
Base strain sensitivity, max	Equiv. g's	0.01	0.01	0.01	0.01	0.01	0.01
Magnetic susceptibility (@ 100 gauss, 60 Hz)	Equiv. g's	‹ 0.1	‹ 0.1	‹ 0.1	‹ 0.1	‹ 0.1	‹ 0.1
Warm-up time (to within 1%)	ms	1	1	1	1	1	1

Electrical characteristics	
Excitation voltage	9.5 to 18.0 Vdc
Current drain	8.5 mA typ, 10 mA max
Output impedance/load	500 ohms max/10K ohms resistance minimum, 0.1 µF capacitance maximum
Residual noise	100 µV rms typ, 0.5 to 100 Hz
	500 µV rms typ, 0.5 Hz to 10 kHz

Physical characteristics	
Case material	Anodized aluminum alloy
Electrical connections	Integral cable, four conductor No. 28 AWG, Teflon® insulated leads, braided shield, Hyperflex™ jacket
Mounting/torque	Two holes for 4-40 or M3 mounting screws / 6 lbf-in (0.68 Nm)
Weight	12 grams without cable (cable weighs 9 grams/meter)

Environmental characteristics	
Acceleration limits (in any direction)	
Static	20 000 g
Vibration	100 g sinusoidal 20 - 2000 Hz / 40 g rms random 20 - 2000 Hz
Shock	5000 g (150 µS haversine pulse) for -2 and -10; 10 000 g (80 µS haversine pulse) for -30, -50, -100 and -150
Zero shift	0.1% FSO typical at 5000 g
Temperature	
Operating	-65°F to +250°F (-55°C to +121°C)
Storage	-100°F to +300°F (-73°C to +150°C)
Humidity/altitude	Unaffected. Unit is epoxy sealed.
ESD sensitivity	Unit meets Class 2 requirements of MIL-STD-883, Method 3015

HBM Quantum MX440A

Data Sheet

QUANTUM^X
MX440A
Universal amplifier

Special features

- 4 individually configurable inputs (electrically isolated)
- Connection of more than 12 transducers technologies
- Data rate: up to 19,200 Hz
- 24-bit A/D converter per channel for synchronous, parallel measurements
- Active low pass filter
- TEDS support
- Supply voltage (DC): 10 V ... 30 V
- Supply voltage for active transducers (DC): 5 V ... 24 V

Block diagram

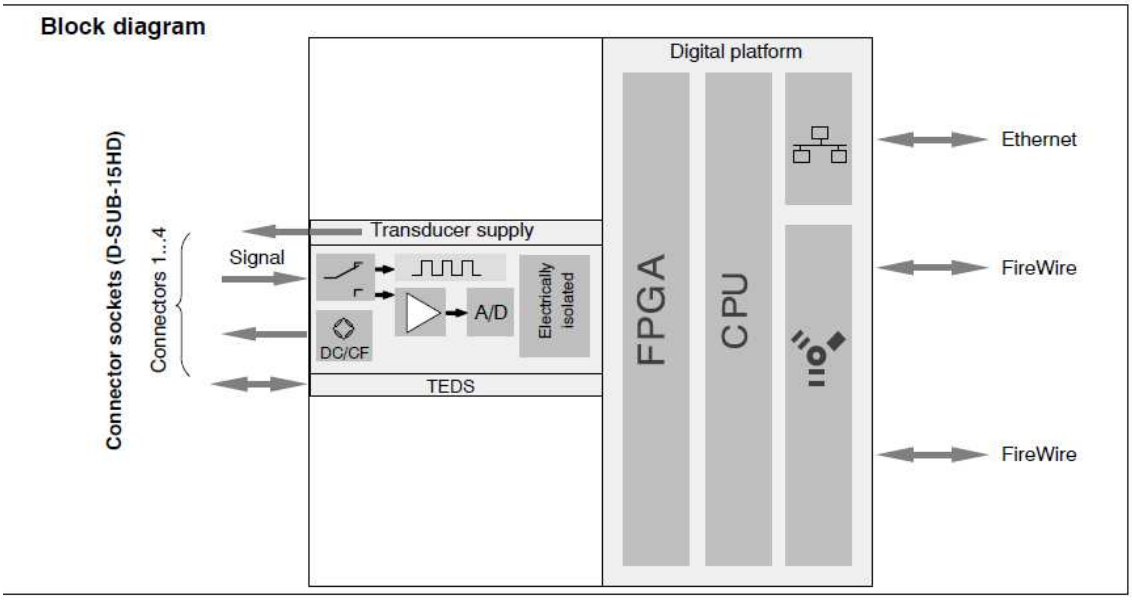

B2925-1.0 en

HBM

Specifications MX440A

General specifications		
Inputs	Number	4, electrically isolated from each other and from the supply voltage[1)]
Transducer technologies		Strain gage full and half bridge, inductive full and half bridge, piezoresistive full bridge, potentiometric transducers, three voltage ranges, current; resistance (e. g. PTC, NTC, KTY); resistance thermometer (PT100, PT1000); thermocouples (K, N, E, T, S, ...) with cold junction in the plug (1-THERMO-MXBOARD). Frequency, pulse counting, SSI, incremental rotary encoder.
A/D converter		24 Bit Delta Sigma converter
Data rate	Hz	0.1 ... 19200, adjustable for each channel
Active low-pass filter (Bessel/Butterworth, can be switched off)	Hz	0.01 ... 3200 (–3 dB)
Transducer identification (TEDS, IEEE 1451.4) max. distance of the TEDS module	 m	 100
Transducer connection		D-SUB-15HD
Supply voltage range (DC)	V	10 ... 30 (24 V nominal (rated) voltage)
Supply voltage interruption		max. 5 ms at 24 V
Power consumption without adjustable transducer excitation with adjustable transducer excitation	 W W	 < 7 < 10
Transducer Excitation (active transducers) Adjustable supply voltage (DC) Maximum output power	 V W	 5 ... 24; adjustable for each channel 0.7 each channel / a total of 2
Ethernet (data link)		10Base-T / 100Base-TX
Protocol/addressing	–	TCP/IP (direct IP address or DHCP)
Connection	–	8P8C plug (RJ-45) with twisted pair cable (CAT-5)
Max. cable length to module	m	100

FireWire (module synchronization, data link, optional supply voltage)		IEEE 1394b (HBM modules only)
Baud rate	MBaud	400 (approx. 50 MByte/s)
Max. current from module to module	A	1.5
Max. cable length between the nodes	m	5
Max. number of modules connected in series (daisy chain)	–	12 (=11 Hops)
Max. number of modules in a FireWire system (including hubs[2], backplane)	–	24
Max. number of hops[3]	–	14
Nominal (rated) temperature range	°C [°F]	–20 ... +60 [–4 ... +140]
Operating temperature range (no dewing allowed/module not dew-point proof)	°C [°F]	–20 ... +65 [–4 ... +149]
Storage temperature range	°C [°F]	–40 ... +75 [–40 ... +167]
Rel. humidity at 31 °C	%	80 (non condensing) lin. reduction to 50 % at 40 °C
Protection class (up to 2000 m height, degree of contamination 2)		III
Degree of protection		IP20 per EN 60529
Mechanical tests[4]		
Vibration (30 min)	m/s^2	50
Shock (6 ms)	m/s^2	350
EMC requirements		per EN 61326
Max. input voltage at transducer socket to ground (Pin 6)		
PIN 1, 2, 3, 4, 5, 7, 8, 10, 13, 15	V	5.5 (no transients)
PIN 14 (voltage)	V	60 (no transients)/typ. 500
Dimensions, horizontal (W x H x D)	mm	52.5 x 200 x 122 (with case protection) 44 x 174 x 119 (without case protection)
Weight, approx.	g	850

1) When the variable transducer supply is used, there is no electrical isolation from the supply voltage.
2) Hub: FireWire node or distributor
3) Hop: Transition from module to module/signal conditioning
4) Mechanical stress is tested according to European Standard EN60068–2–6 for vibrations and EN60068–2–27 for shock. The equipment is subjected to an acceleration of 50 m/s^2 in a frequency range of 5...65 Hz in all 3 axes. Duration of this vibration test: 30min per axis. The shock test is performed with a nominal acceleration of 350 m/s^2 for 6 ms, half sine pulse shape, with 3 shocks in each of the 6 possible directions.

Specifications MX440A (Continued)

Potentiometric transducer		
Accuracy class		0.1
Excitation voltage (DC)	V	2.5 (±5 %)
Transducers that can be connected		potentiometric transducers
Permissible cable length between MX440A and transducer	m	100
Measuring range	mV/V	±500
Measurement frequency range (–3 dB)	kHz	0 ... 3.2
Transducer impedance	Ω	300 ... 5000
Noise at 25 °C (peak to peak) with filter 1 Hz Bessel with filter 10 Hz Bessel with filter 100 Hz Bessel with filter 1 kHz Bessel	 µV/V µV/V µV/V µV/V	 < 40 < 100 < 200 < 700
Linearity error	%	< 0.02 of full scale
Zero drift (1 V excitation)	% / 10 K	< 0.1 of full scale
Full-scale drift (1 V excitation)	% / 10 K	< 0.1 of measurement value

APPENDIX C – SAMPLE CALCULATIONS

Sample Calculation for a class D HM127646/HM127415XD AP Bearing

The known variables are listed :

n – number of rollers is 23 (single row)
d – Roller diameter which is 17.7mm
D – pitch diameter of the bearing which is 167.9mm
$f_{a\_}$ the angular frequency of bearing rotation

The Rotational speed of the Lateral Machine is assumed to be 138RPM and thus the equivalent angular frequency is 2.3Hz

Using the Chambers formulae which do not take into consideration the included angle of the bearing the frequencies of the defects can be calculated .

Thus for a single defect on the outer race the expected frequency would be calculated as:

$$f_o = \frac{1}{2} n f_a \left(1 - \frac{d}{D}\right)$$
$$= \frac{1}{2}(23)(2.3)_a \left(1 - \frac{0.0177}{0.1679}\right)$$
$$= 23.66 Hz$$

For a single defect on the inner race the calculation would be:

$$f_i = \frac{1}{2} n f_a \left(1 + \frac{d}{D}\right)$$
$$= \frac{1}{2}(23)(2.3)\left(1 + \frac{0.0177}{0.1679}\right)$$
$$= 29.24 Hz$$

And for a single defect on the roller:

$$f_r = \frac{D}{d}\left(1 - \frac{(d)^2}{D}\right) f_a$$
$$= \frac{0.1679}{0.0177}\left(1 - \frac{(0.0177)^2}{0.1679}\right)(2.3)$$
$$= 21.575 Hz$$

Using Tandon's method of calculating the expected frequencies of the defects it can be seen that the included angles of the bearing are taken into consideration.

Cage Frequency as:

$$f_c = \frac{f_a}{2}\left(1 - \frac{d}{D}\cos\alpha\right)$$
$$= \frac{2.3}{2}\left(1 - \frac{0.0177}{0.1679}\cos(9.1)\right)$$
$$= 1.0303 Hz$$

Ball Spinning Frequency as:

$$f_b = \frac{Df_x}{2d}\left(1-\frac{d^2}{D}\cos^2\alpha\right)$$
$$=\frac{(0.1679)(2.3)}{2(0.0177)}\left(1-\frac{(0.0177)^2}{(0.1679)}\cos^2(9.1)\right)$$
$$=10.791Hz$$

And outer race defect frequency is

$$f_o = nf_c$$
$$=(23)(1.0303)$$
$$=23.70Hz$$

Inner race defect frequency is

$$f_i = n(f_a - f_c)$$
$$=23(2.3-1.0303)$$
$$=29.20Hz$$

Rolling Element defect frequency

$$f_r = nf_b$$
$$=23(10.791)$$
$$=21.58Hz$$

APPENDIX D – MEASUREMENT OF NICKS

Measurements were taken of nicks across the broadest section of the nick with a contour tracing machine. This machine is able with a very fine needle to probe into the depth of the nick and thus measure its width and overall height. Figure D-1 to Figure D-15 are screen shots of the measurement values in both metric and imperial units. They are presented so that the reader can become familiar with the nick's geometry in the pieces used. It is clear from the figures that nicks either are like scratches or have raised metal on either side of the nick.

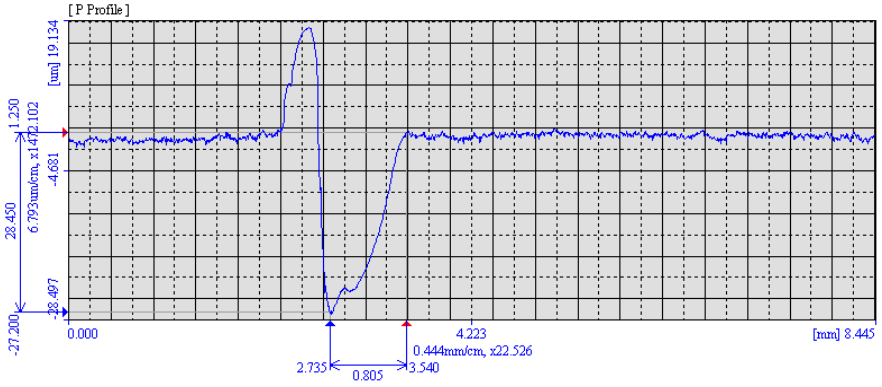

Figure D-1 –Bearing D2 upper raceway – one of four roller-spaced nicks

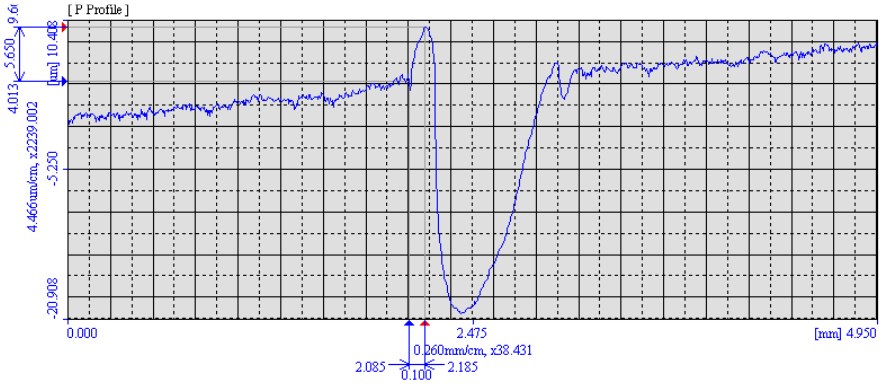

Figure D-2 – Bearing D2 upper raceway – one of four roller-spaced nicks

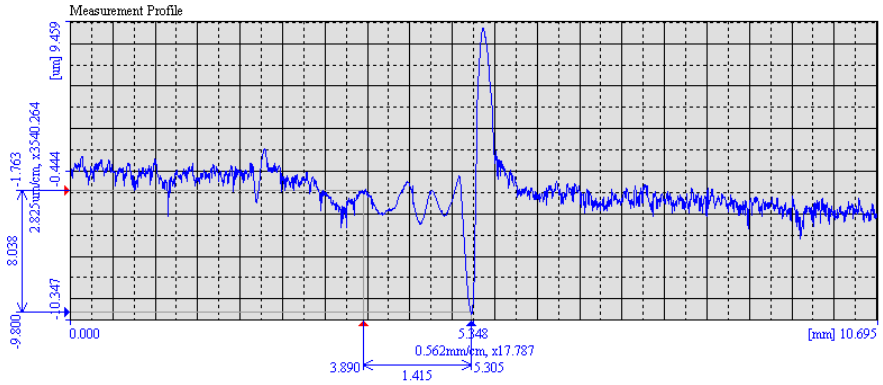

Figure D-3 – Bearing D1 nicks from upper raceway random nicks

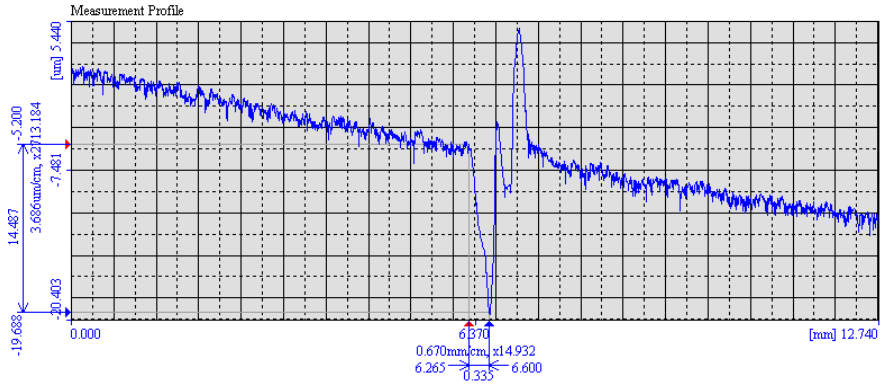

Figure D-4 – Bearing D1 upper raceway random nicks

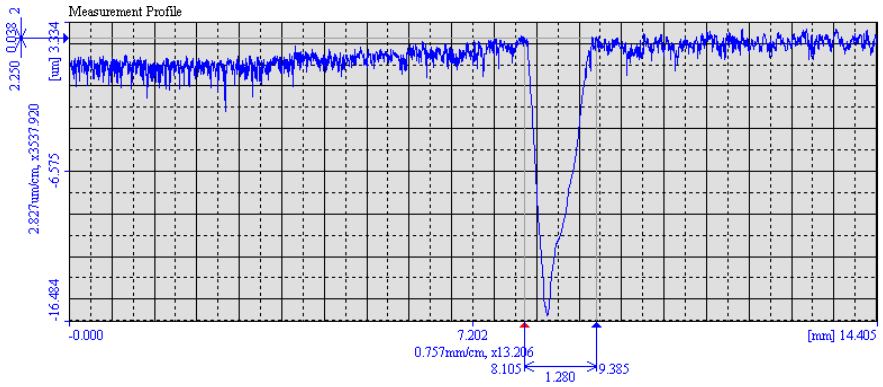

Figure D-5 – Bearing D1 nick, not so deep visually and hardly high spot to touch

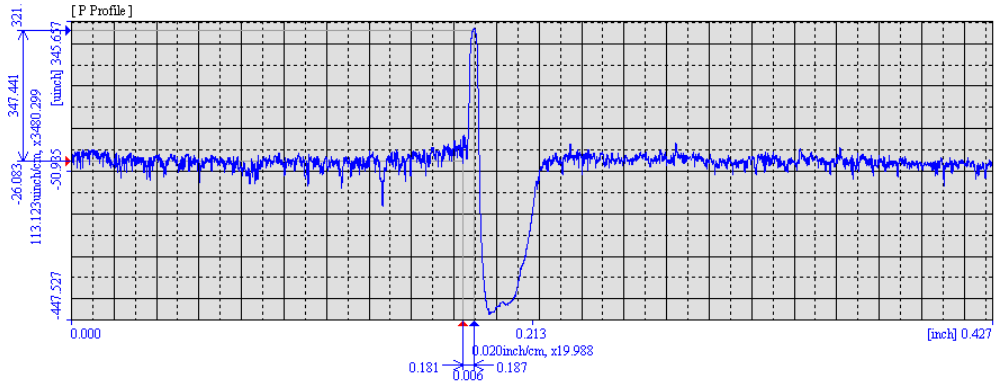

Figure D-6 – Bearing D6 lower raceway nick

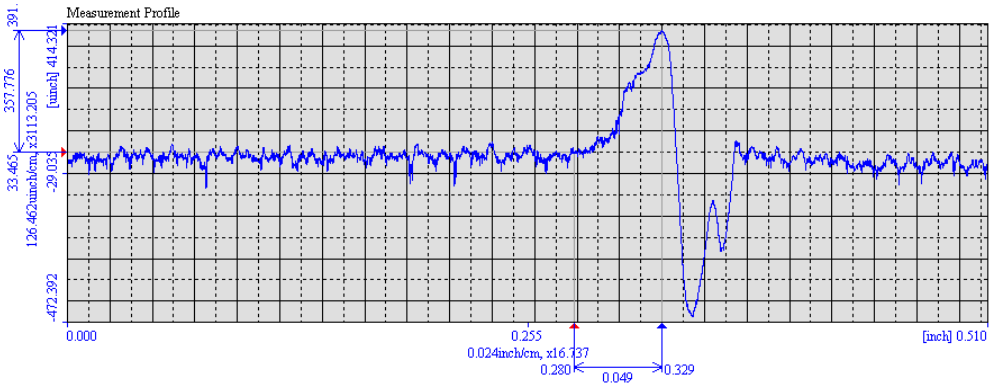

Figure D-7 – Bearing D6 upper raceway nick with visible depth

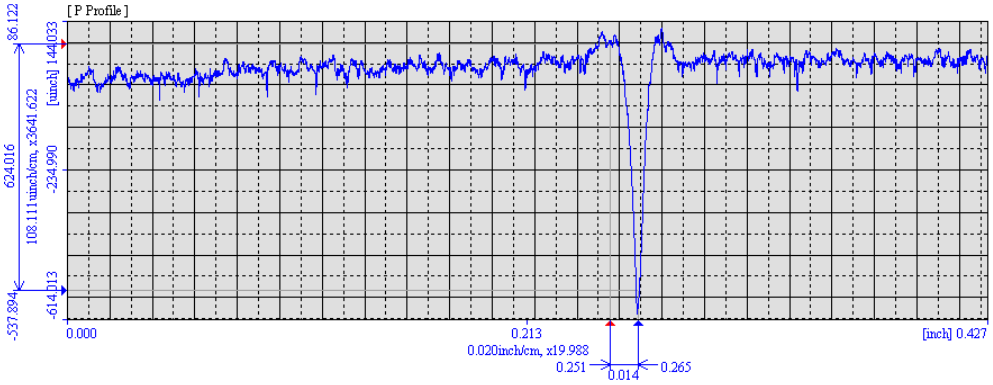

Figure D-8 – Bearing D6 upper raceway scratch type nick

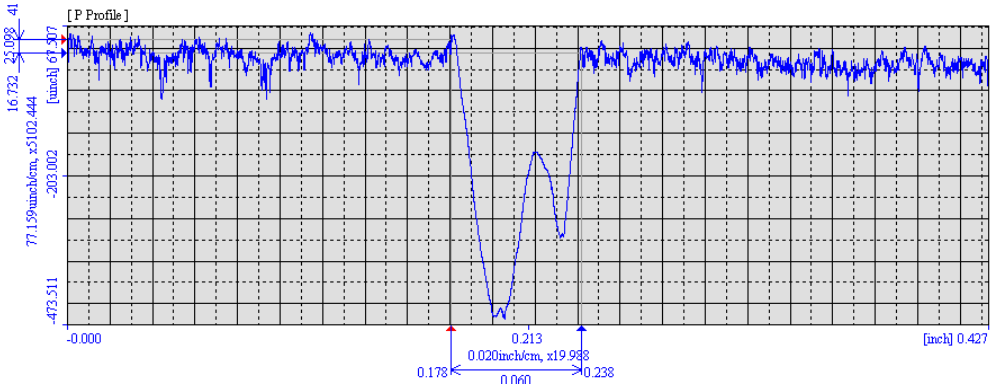

Figure D-9 – Bearing D3 nick upper raceway - deep

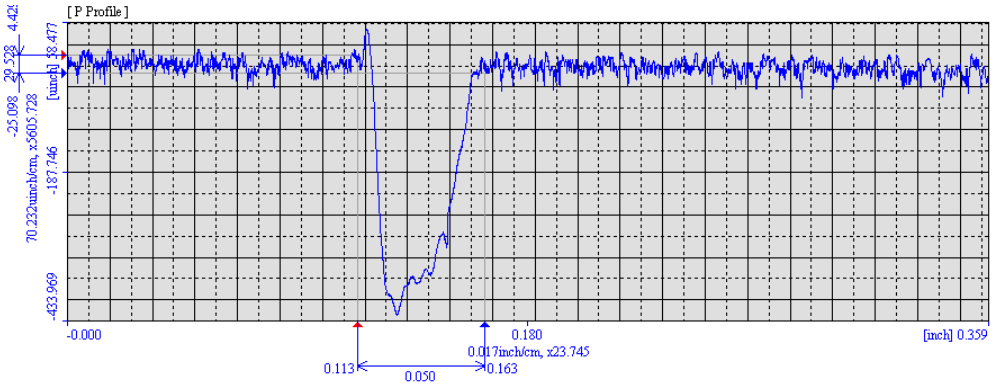

Figure D-10 – Bearing D3 upper raceway one of roller-spaced nicks

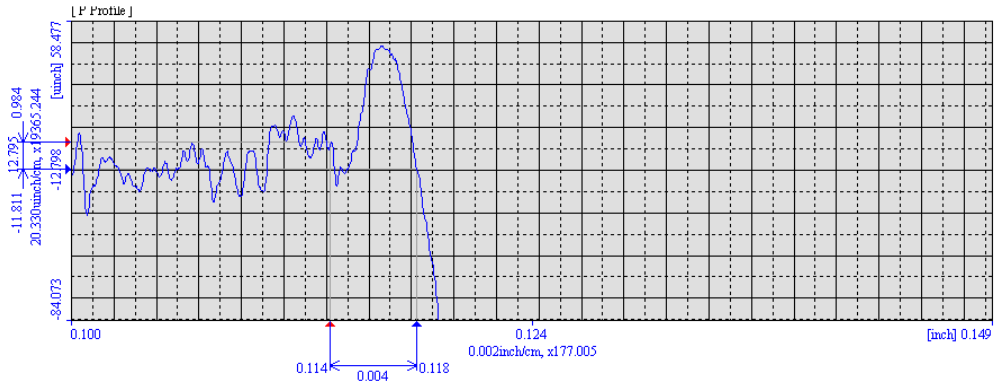

Figure D-11 – Bearing D3 upper raceway one of roller-spaced nicks – zoomed area of Figure D-10

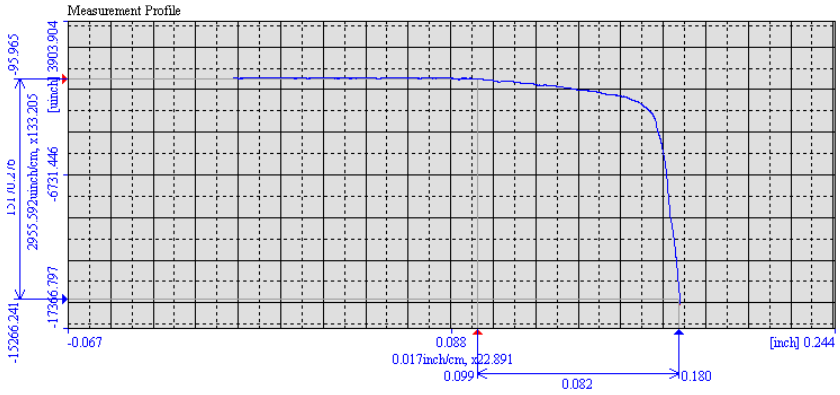

Figure D-12 – Bearing D7 chipped edge of raceway

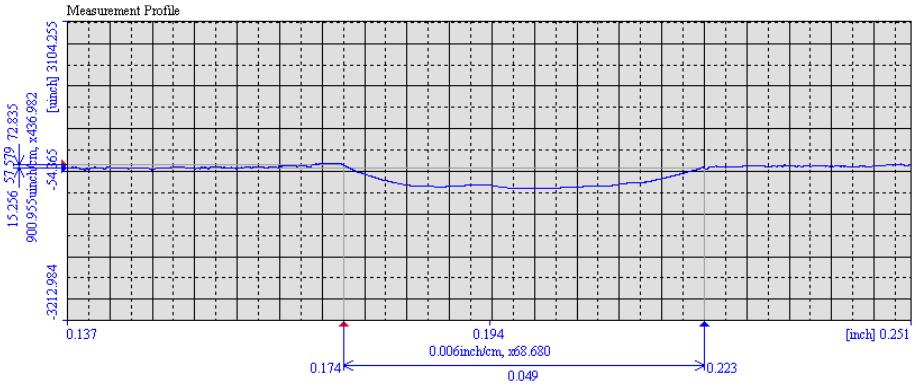

Figure D-13 – Bearing D4 lower raceway – large shallow nick

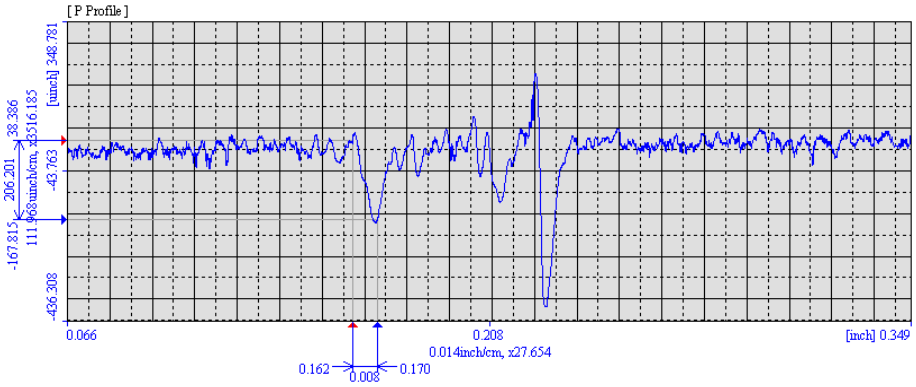

Figure D-14 – Bearing D4 upper raceway – one of roller-spaced nicks

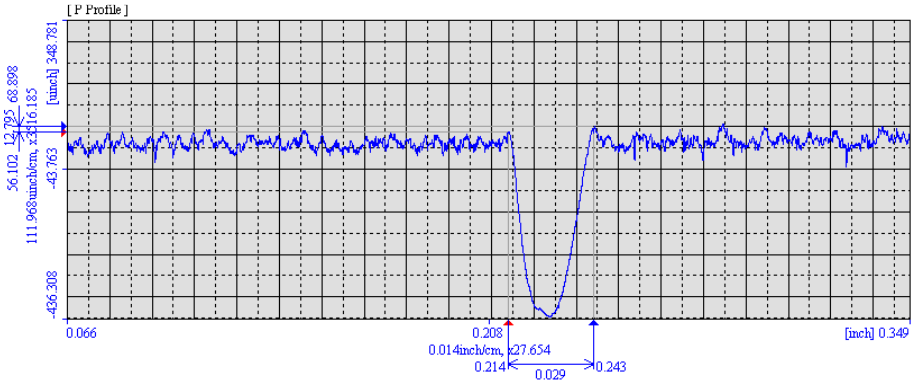

Figure D-15 – Bearing D4 upper raceway – nick with depth outside of roller-spaced area

APPENDIX E – PRELIMINARY TESTING INFORMATION

Basic testing was performed with an accelerometer mounted magnetically on the track of the cup OD. The testing was performed on the Line 1 Lateral Machine during the normal Lateral Machine cycle at various sampling frequencies.

The results are seen in Figure E-1. This shows a class D bearing sampled at 600 Hz for 15 seconds. The duration of the cycle shows high amplitude signal, low amplitude signal and then the rotation of the bearing stops. This change in amplitude during the testing represents the motion of the Lateral Machine as described in Section 2.3.5

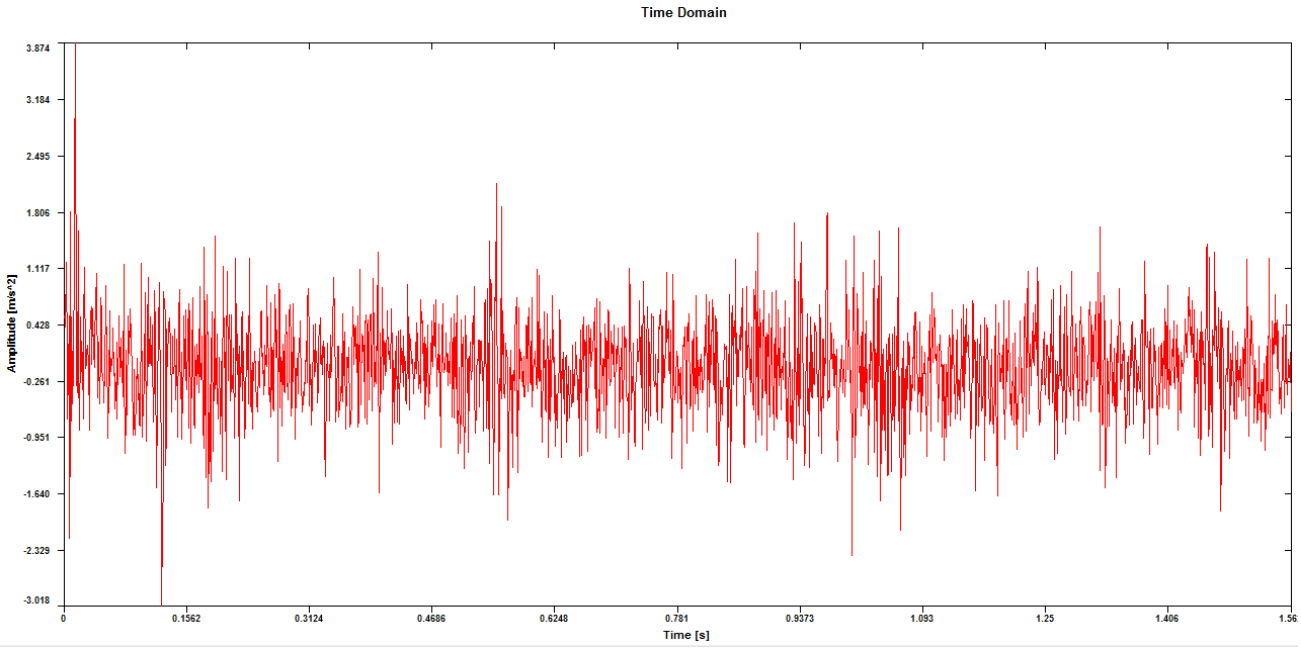

Figure E-1 – Raw time domain plot [D2, 1200Hz]

Many of these tests were done with various sized bearings, bearings that had nicks and ones that did not. The data was analysed using the HBM software and the FFT's were done to see if any distinct patterns were visible as shown in Figure E-2. The figure

depicts D5 which is a non-nicked bearing and D2 which is a nicked bearing. Many different versions of the same FFT's were compiled with no real distinct information retrieved from any.

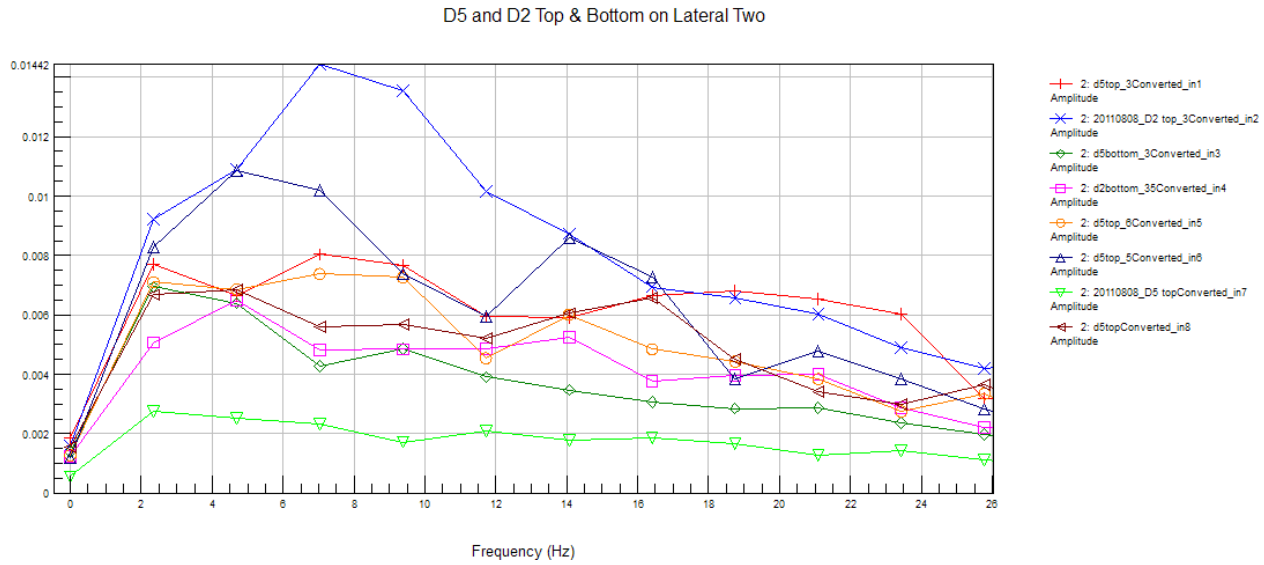

Figure E-2 – D2 top and bottom on Lateral Machine one and two

The FFT's were analysed in normal scale as well as logarithmic scale to understand if there were any differences. Additionally the signals were broken into 'first half" and 'second half' depending on if the Lateral Machine was in the first or second part of its cycle to see if there was any distinctive noise that could be removed in that process (Figure E-3). Still no favorable results were visible.

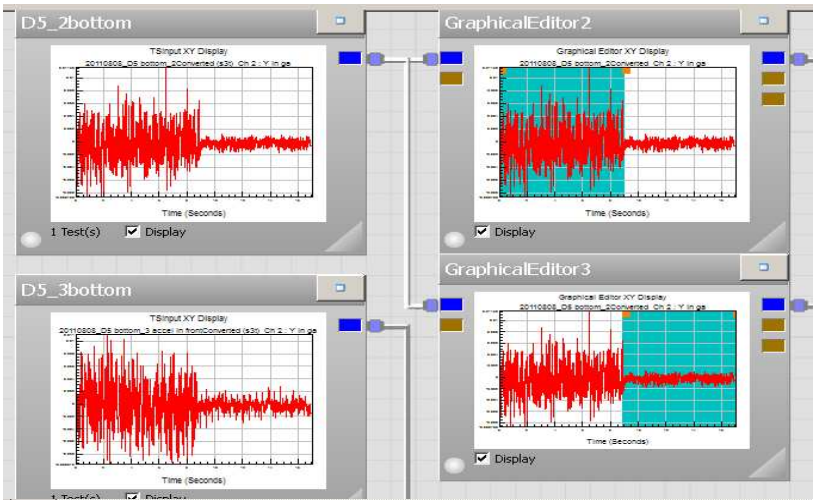

Figure E-3 – Figure depicting removal of signal during data Analysis

Sampling Rates

It was then considered that the resolution of the testing is not necessarily ideal and that sampling at 2400Hz was too fast and possibly that information was being lost in the acquisition process. Further testing was done of nicked and non-nicked bearings at different sampling rates to see if any more distinct frequencies were visible. Figure E-4 represents one bearing at multiple sampling rates. Although it can be seen that resolution is missing there are no definitive peaks visible in either logarithmic or normal scale.

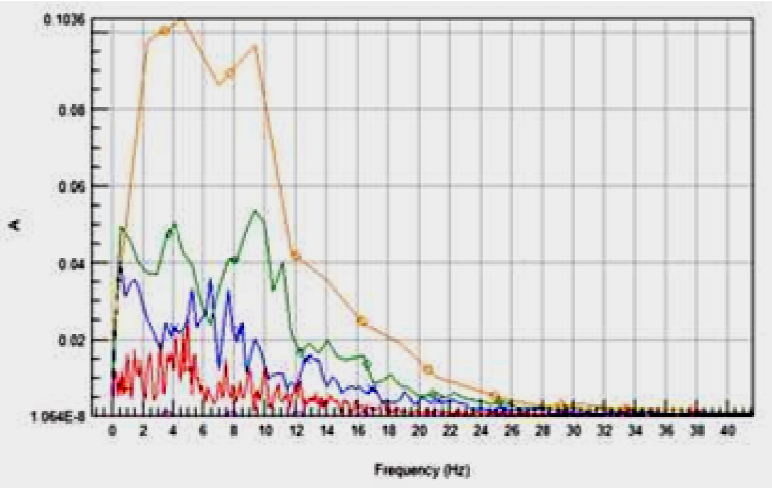

Figure E-4 – FFT of same bearing at different sampling frequencies

Testing Duration

At this stage all the tests were done for the standard Lateral Machine interval which is a period of approximately thirteen seconds in which valuable data is captured for analysis. Based on this short span of information and all of the inherent noise that seemed to be present within the Lateral Machine it was decided that time synchronous averaging should be tried as per the explanation in Section 2.3.3. In order to do this the amount of revolutions must be significantly greater than is allowed in 13 seconds and thus the time of the experiment was increased to approximately 200 seconds.

Synchronous Averaging

To reduce variation further until basic results were achieved, the decision was made to extend the timing of the Lateral Machine in the "second phase" of the rotation cycle, i.e. when the rollers are seated in the lower cone and the rollers are almost seated in the upper cone and thus there is less rattling of rollers within the cages. A tachometer was used to denote a revolution of the bearing and it was found that the bearings were rotating at a 135.5RPM. All the rotations were overlaid on each other and averaged in the hope that the noise would tend to zero and that the distinct frequencies would tend to their mean value.

At first the results seemed to be very successful. In Figure E-5 nicked and non-nicked bearings sampled at 600Hz were averaged in the time domain and then the FFT was plotted. It can be seen that D1, a nicked bearing, showed clear peaks which was not portrayed in the other bearings.

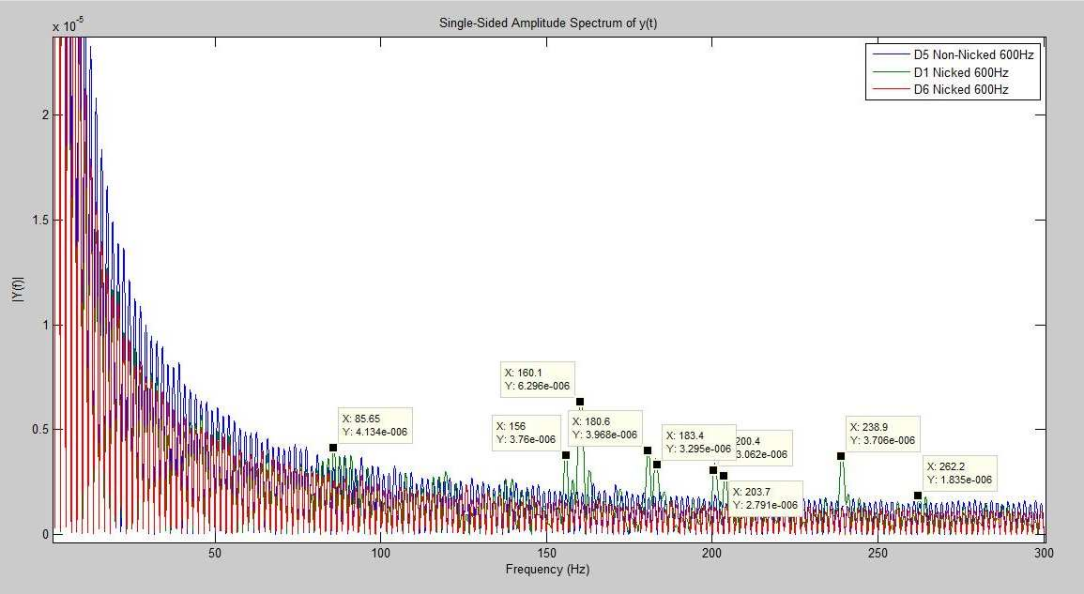

Figure E-5– Non-nicked Data 1 (D5), nicked Data 2(D6) and nicked Data 3 (D1)

Further work was done to understand if any results were achievable without completing synchronous averaging on the longer tests that had more samples. Figure E-6 shows this.

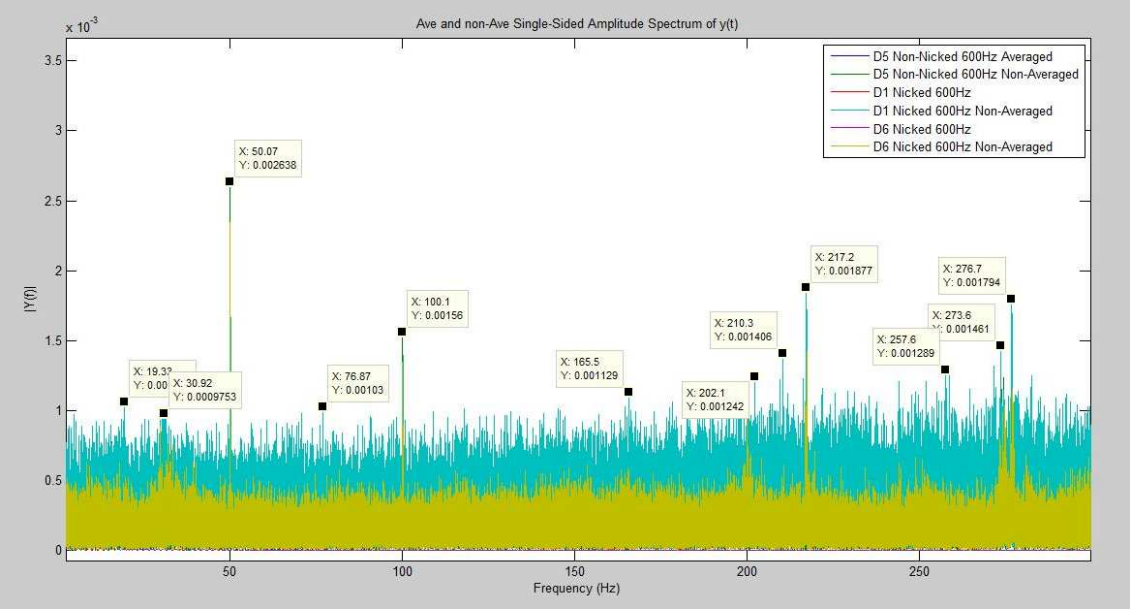

Figure E-6 – Average and non-average FFT's D5, D1 and D6 at 1200Hz

It then became apparent with more testing completed and synchronized averaged that the results of the time averaging was not very successful and that more of the distinct peaks were tending to zero and not their mean. So much data was lost that the analysis became meaningless. Figure E-7 shows the averaged values which are almost not visible in comparison to the non averaged values.

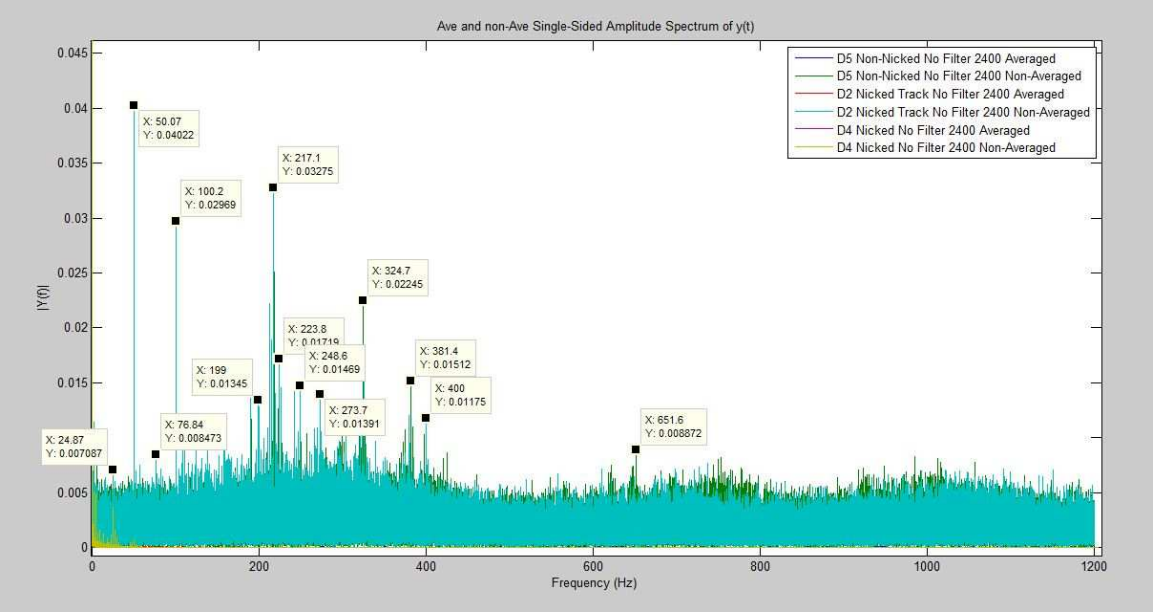

Figure E-7 – FFT of synchronized average results and non-averaged results of data 1 and 2 non-nicked D5, data 3 and 4 Nicked D2 and data 5 and 6 nicked D4

APPENDIX F – ADDITIONAL TESTING

Repeatability testing has been completed on non-nicked bearings to show that the limits defined for various sampling rates hold true and are applicable. In this appendix tests of 600Hz (nicked and non-nicked), 1200Hz (non-nicked), 9600Hz (non-nicked) and 19.2kHz (nicked and non-nicked) are presented.

i. 600Hz sampling rate nicked and non-nicked tests

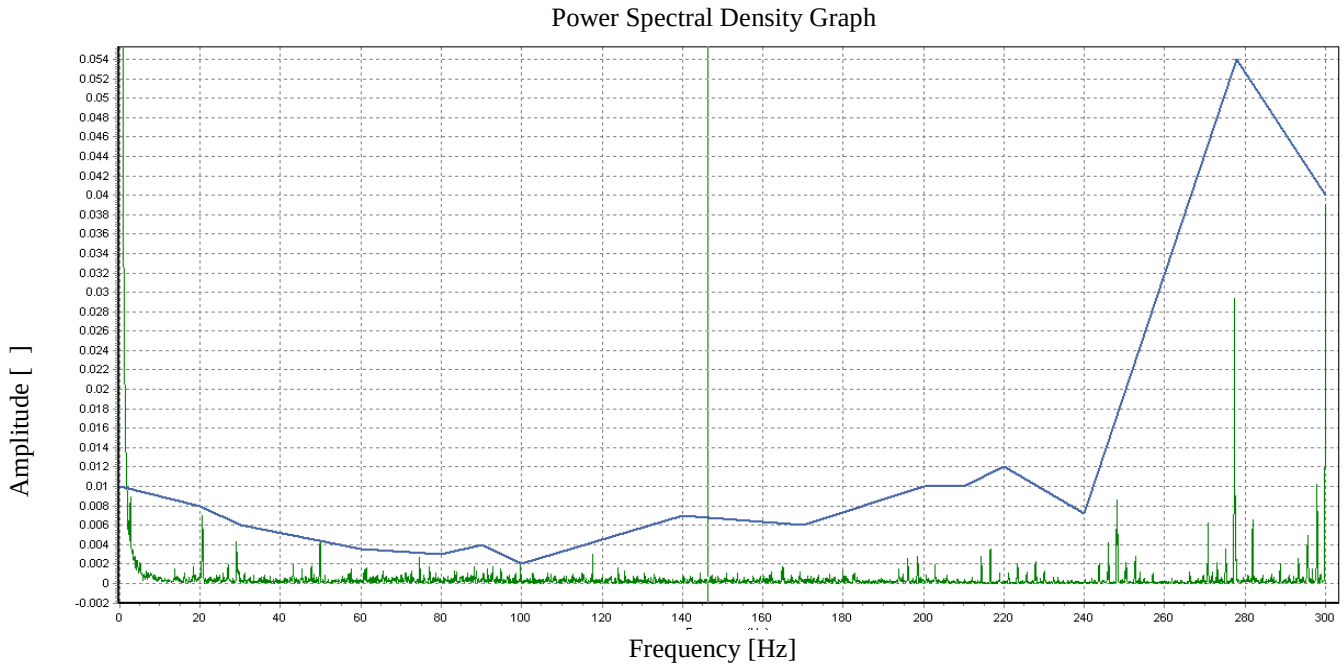

Figure F-1– D5 non-nicked 600Hz Butterworth 500Hz PSD

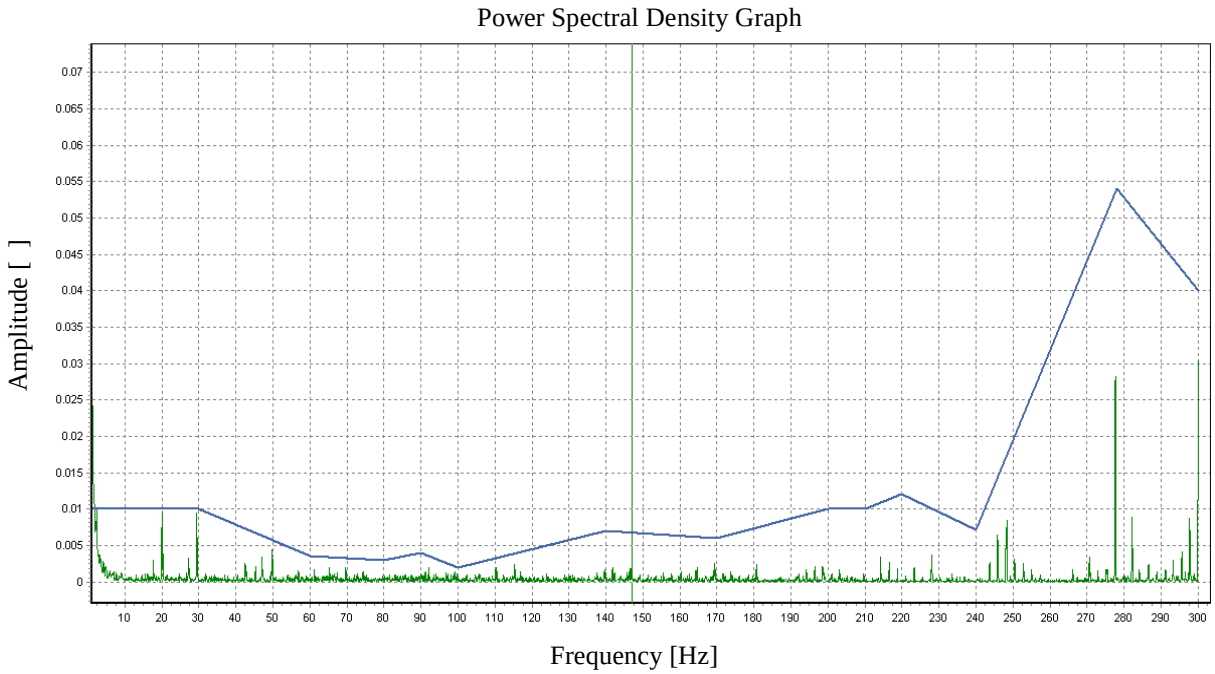

Figure F-2- D5 non-nicked repeat test 600Hz Butterworth 500Hz PSD

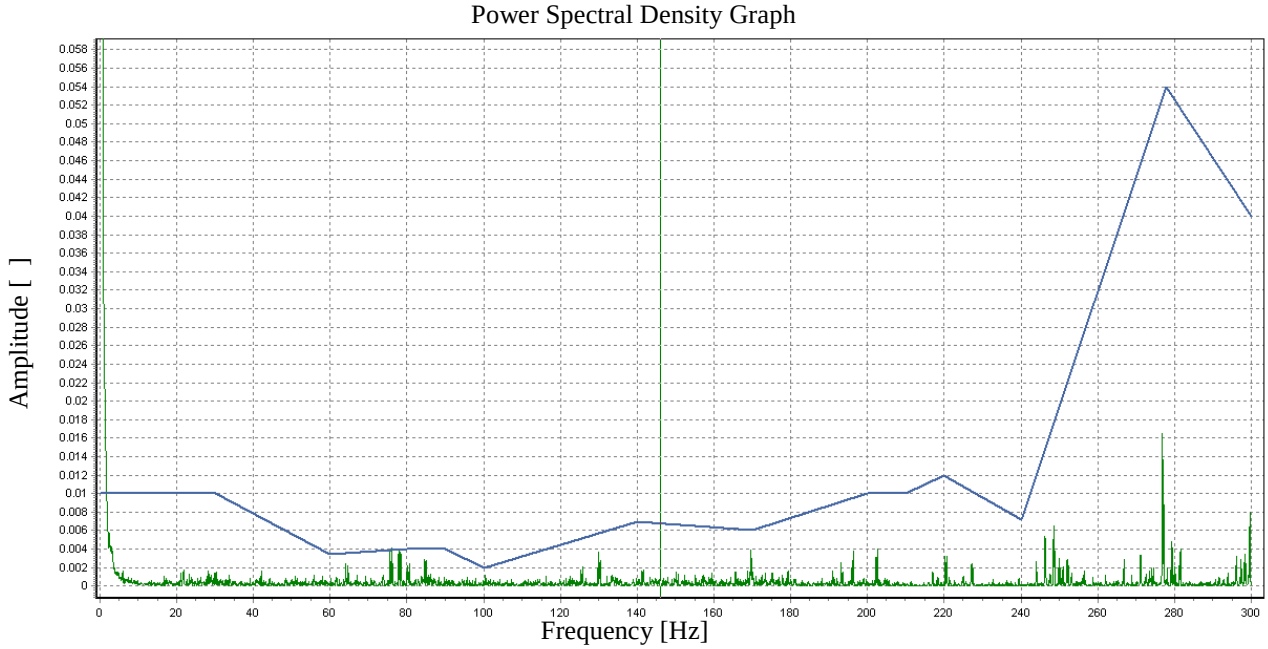

Figure F-3– Production 531425 non-nicked test 600Hz Butterworth 500Hz PSD

Power Spectral Density Graph

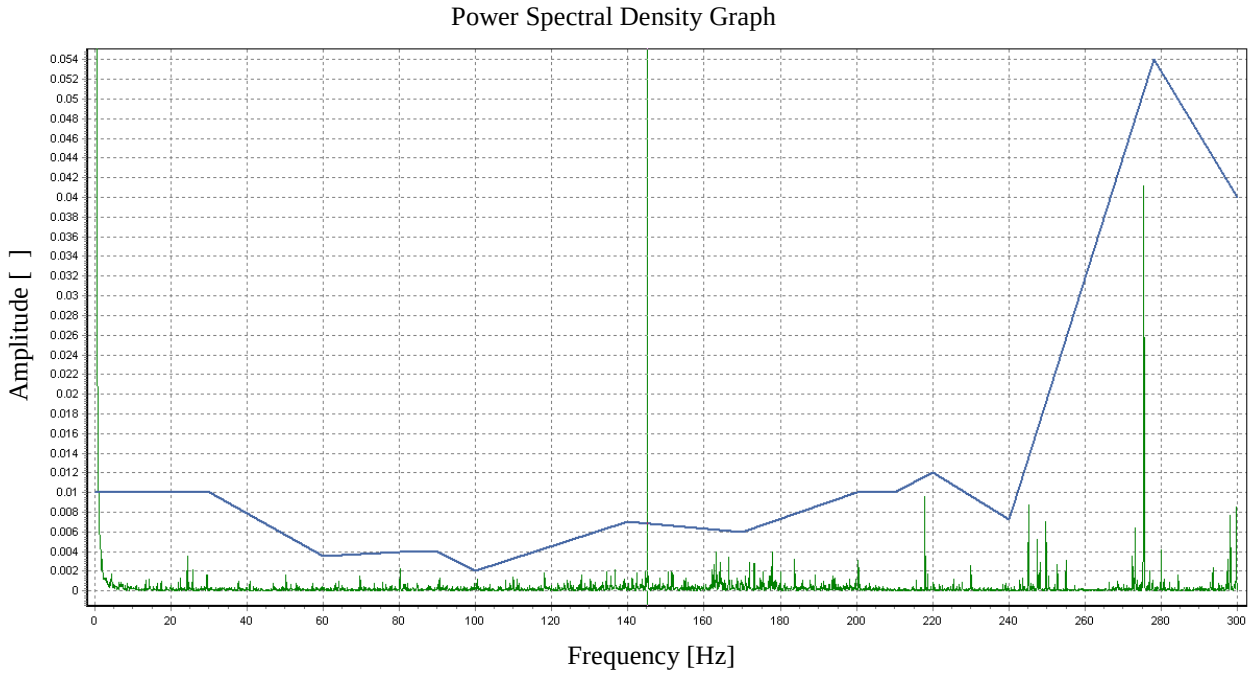

Figure F-4– Production 288050 non-nicked test 600Hz Butterworth 500Hz PSD

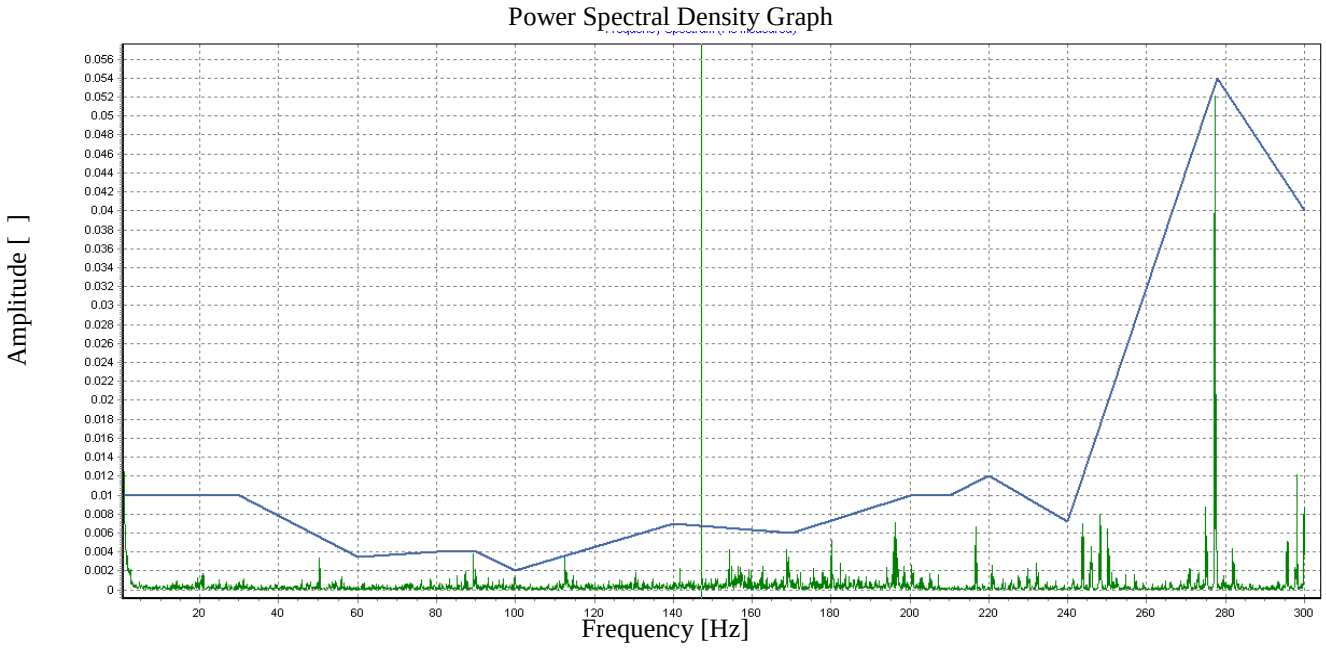

Figure F-5- Production 287461 non-nicked test 600Hz Butterworth 500Hz PSD

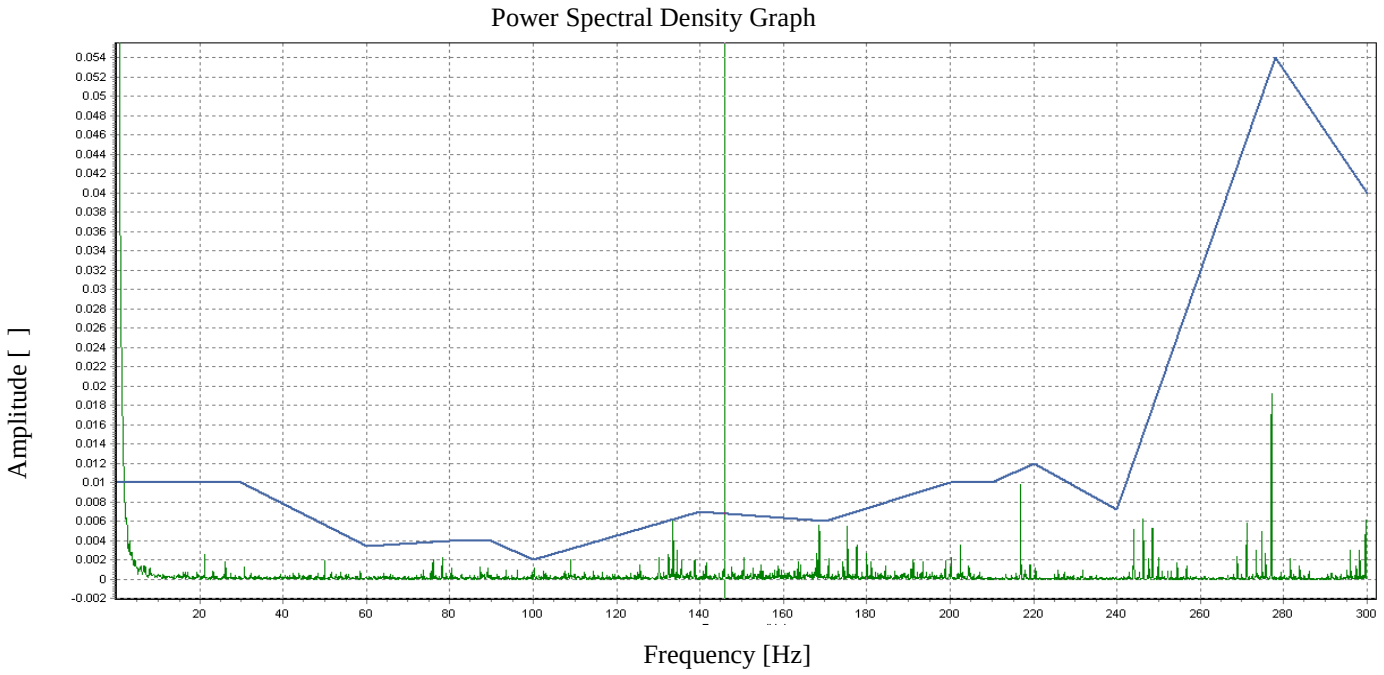

Figure F-6 - Production 288026 non-nicked test 600Hz Butterworth 500Hz PSD

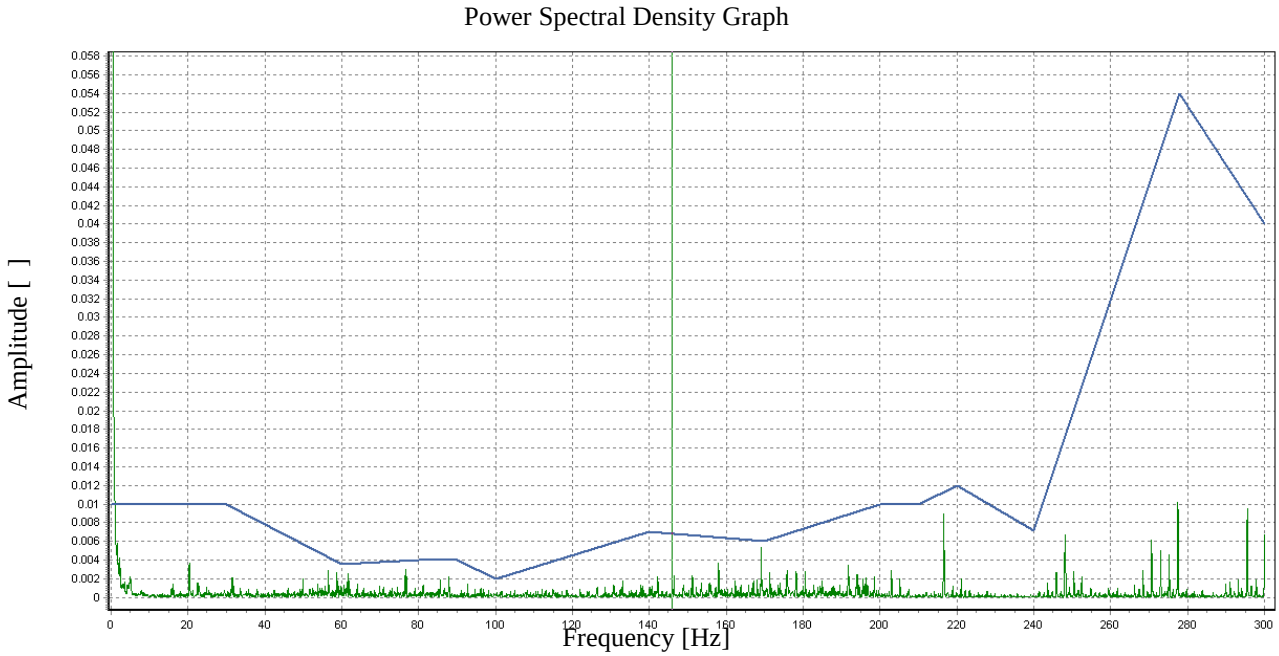

Figure F-7- Production 289631 non-nicked test 600Hz Butterworth 500Hz PSD

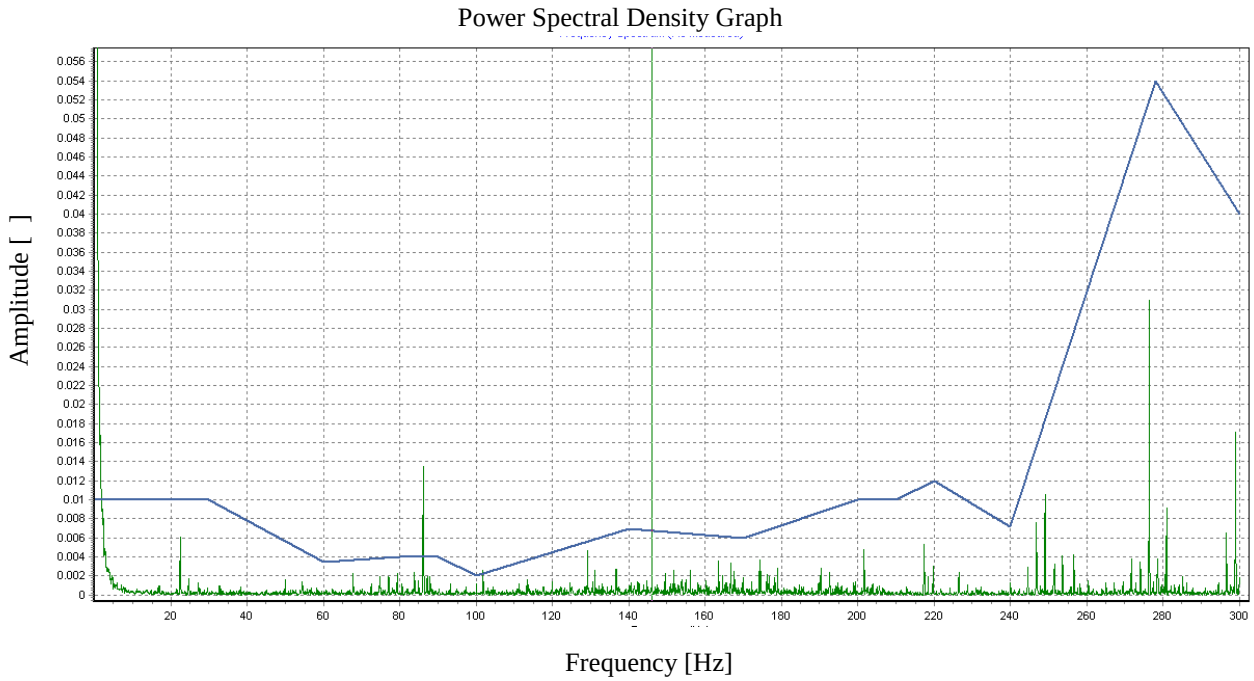

Figure F-8– D7 nicked bearing 600Hz Butterworth 500Hz PSD

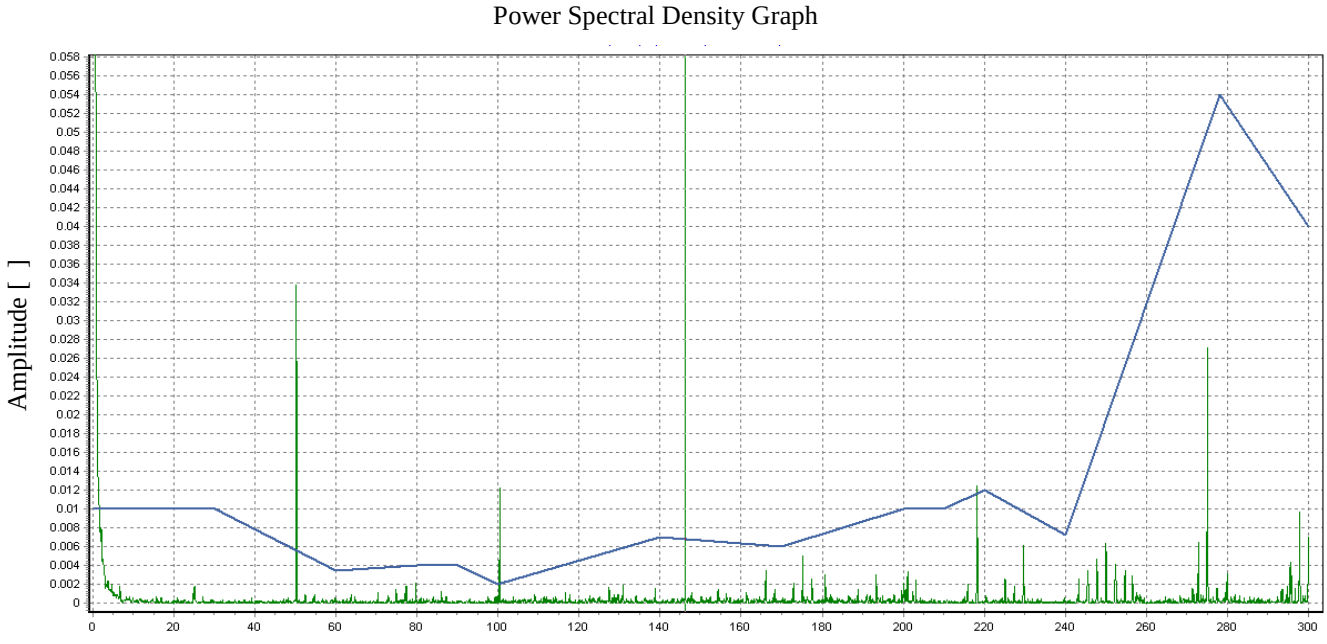

Figure F-9– D4 nicked bearing 600Hz Butterworth 500Hz PSD

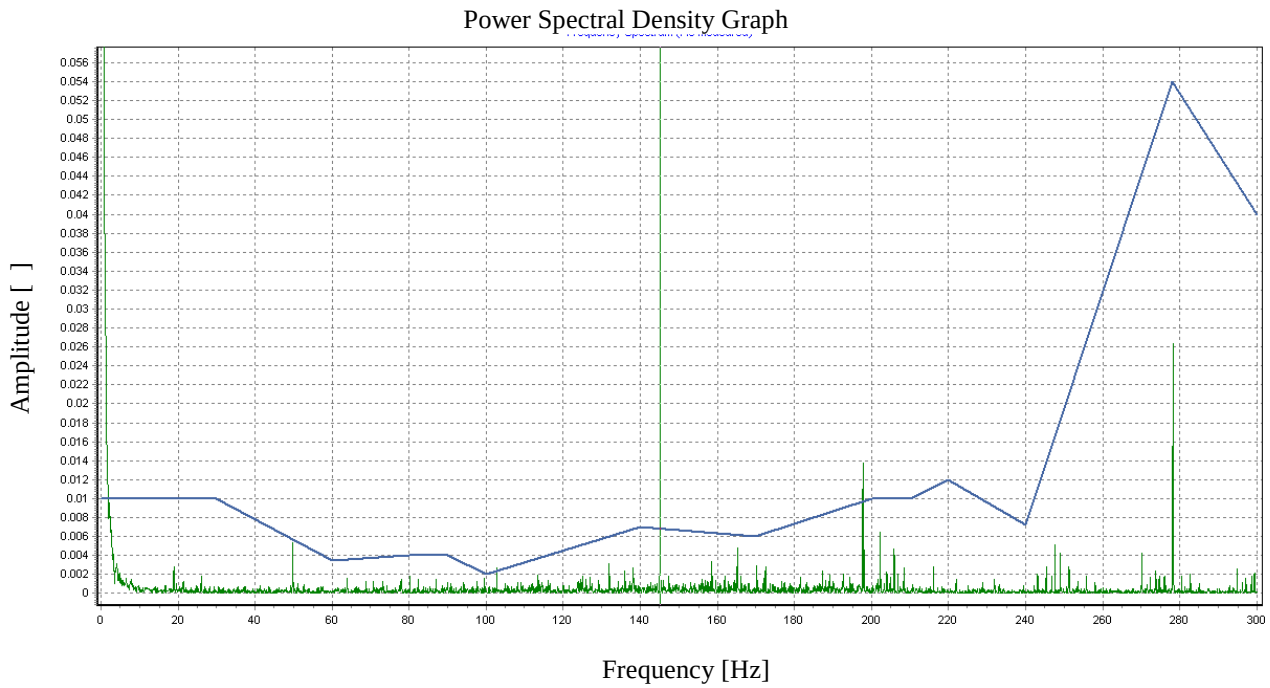

Figure F-10– D6 nicked bearing 600Hz Butterworth 500Hz PSD

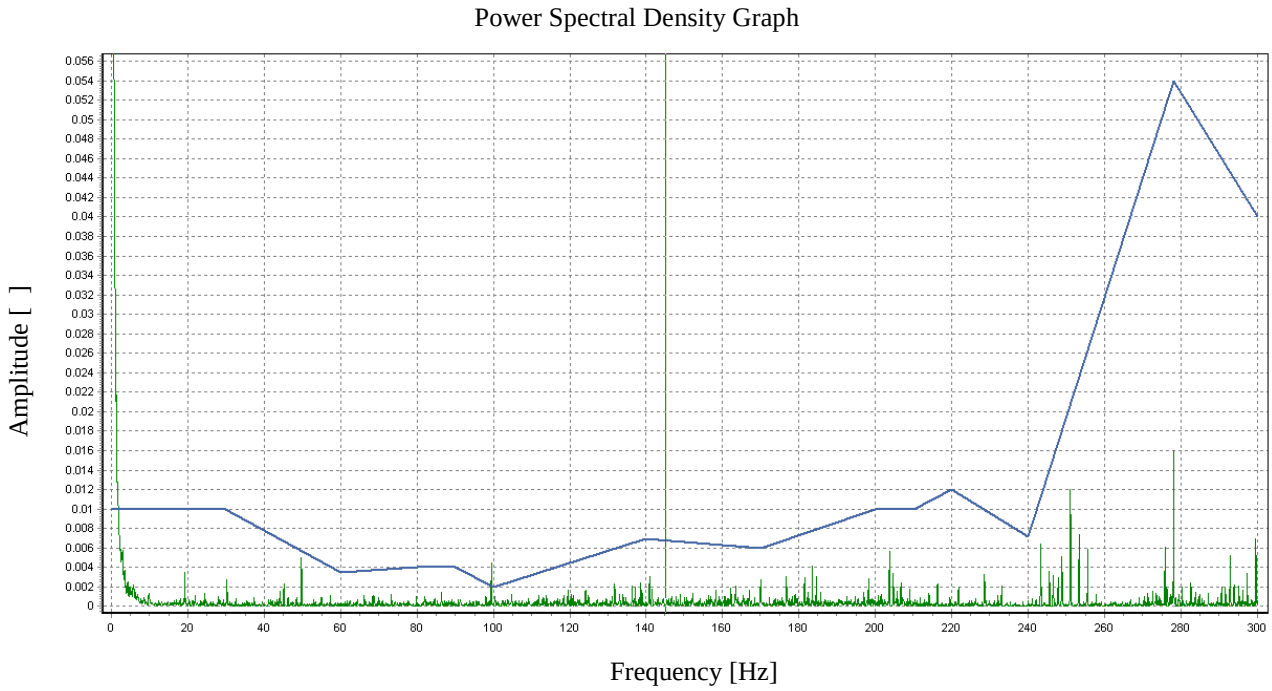

Figure F-11– D2 nicked bearing 600Hz Butterworth 500Hz PSD

ii. Repeatability 1200Hz sampling rate non-nicked bearings

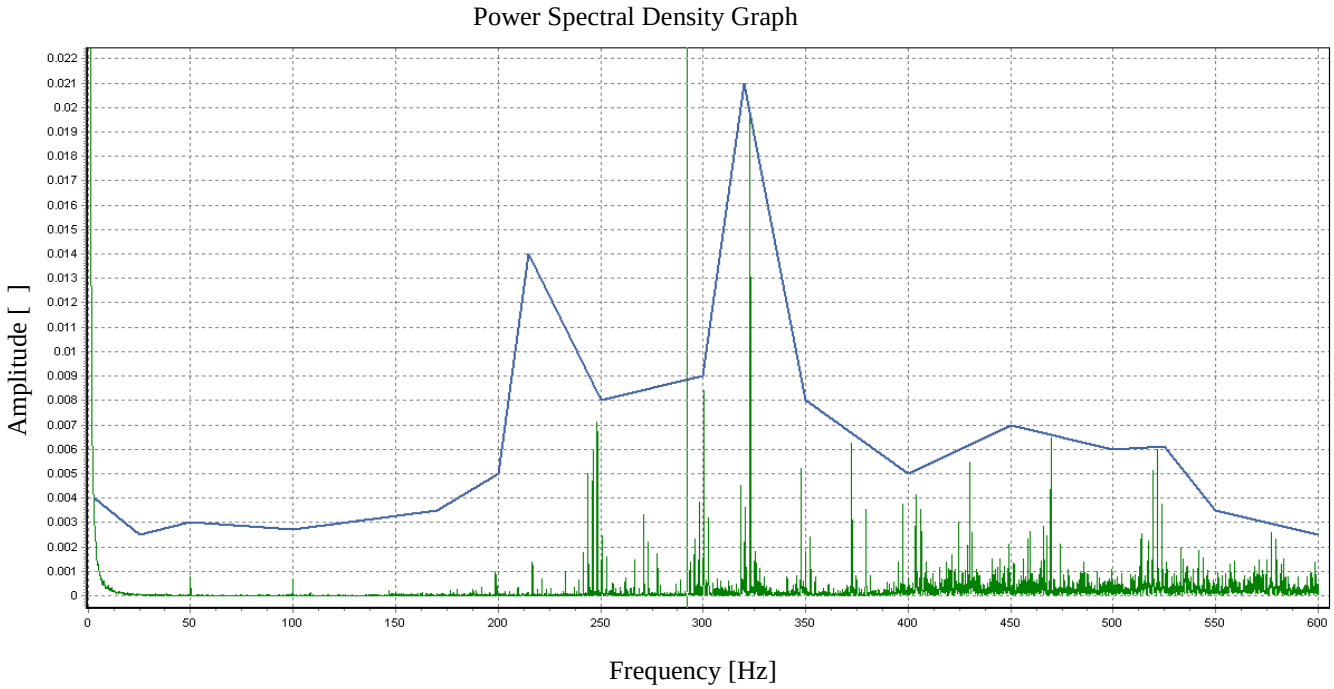

Figure F-12 – Production 531425 non-nicked 1200Hz PSD with 500Hz Butterworth filter

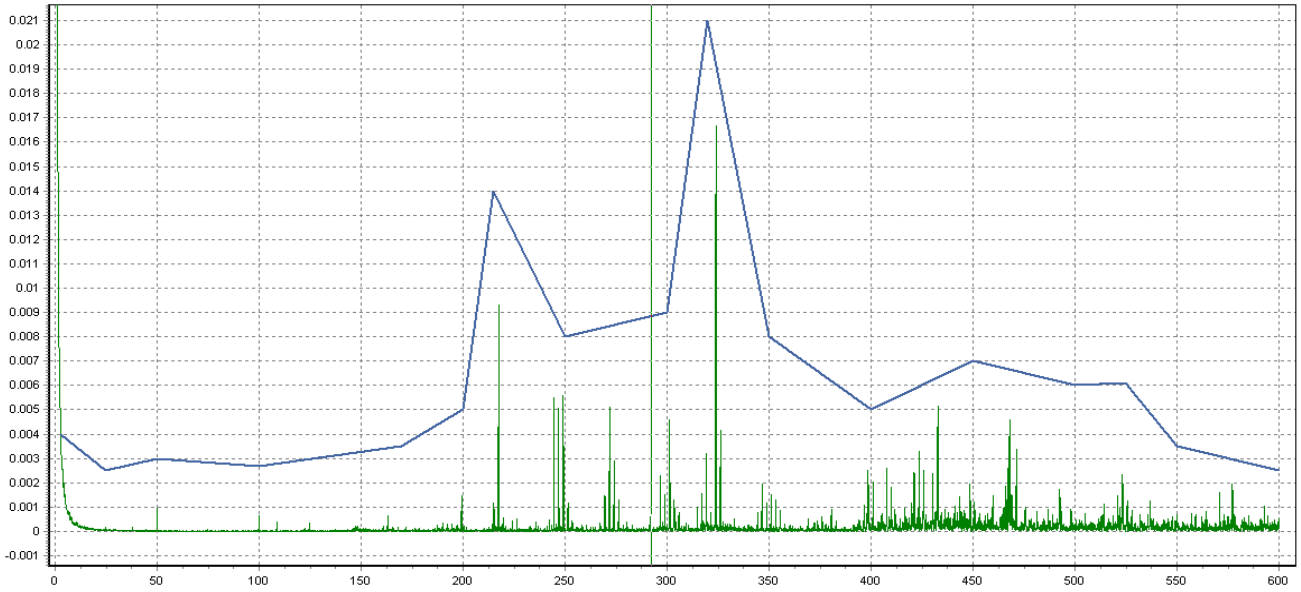

Figure F-13 – Production 288026 non-nicked bearing 1200Hz PSD with 500Hz Butteworth Filter

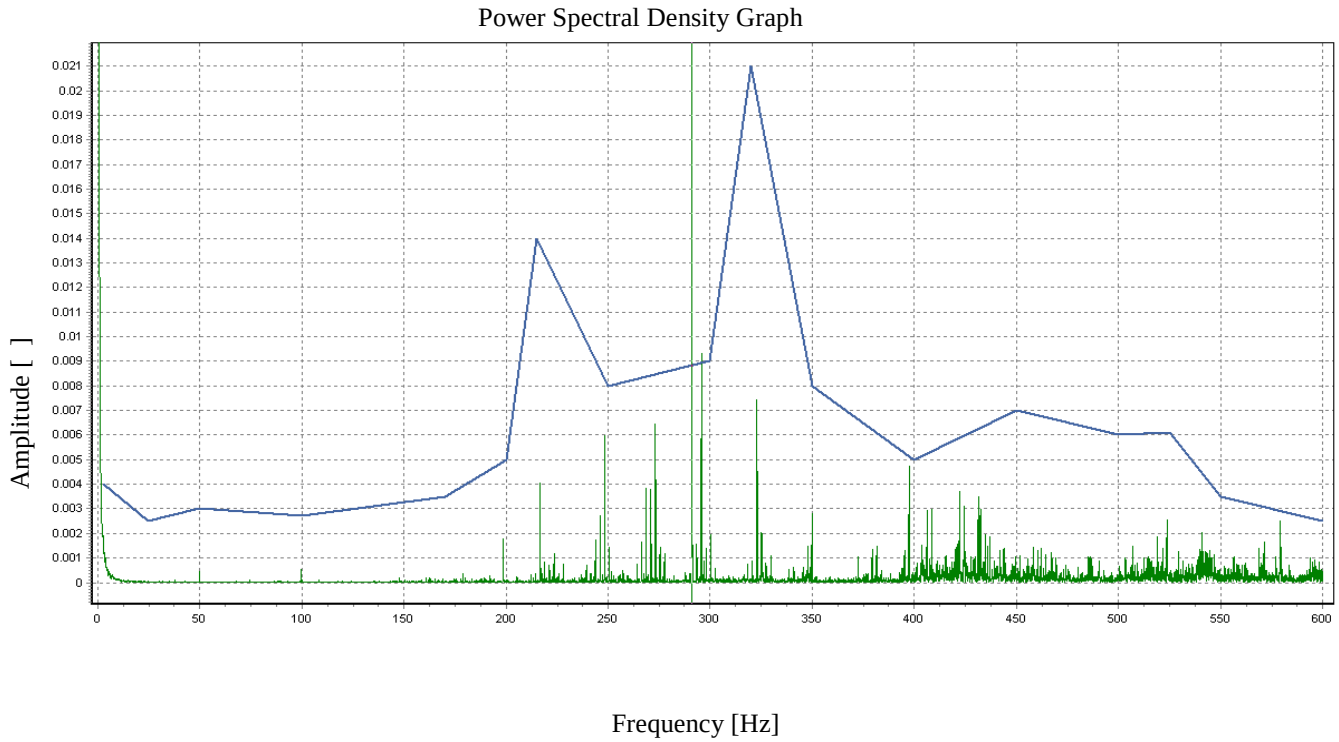

Figure F-14 – Production 289631 non-nicked 1200Hz PSD with 500Hz Butterworth Filter

iii. Repeatability 9600Hz sampling rate non-nicked tests

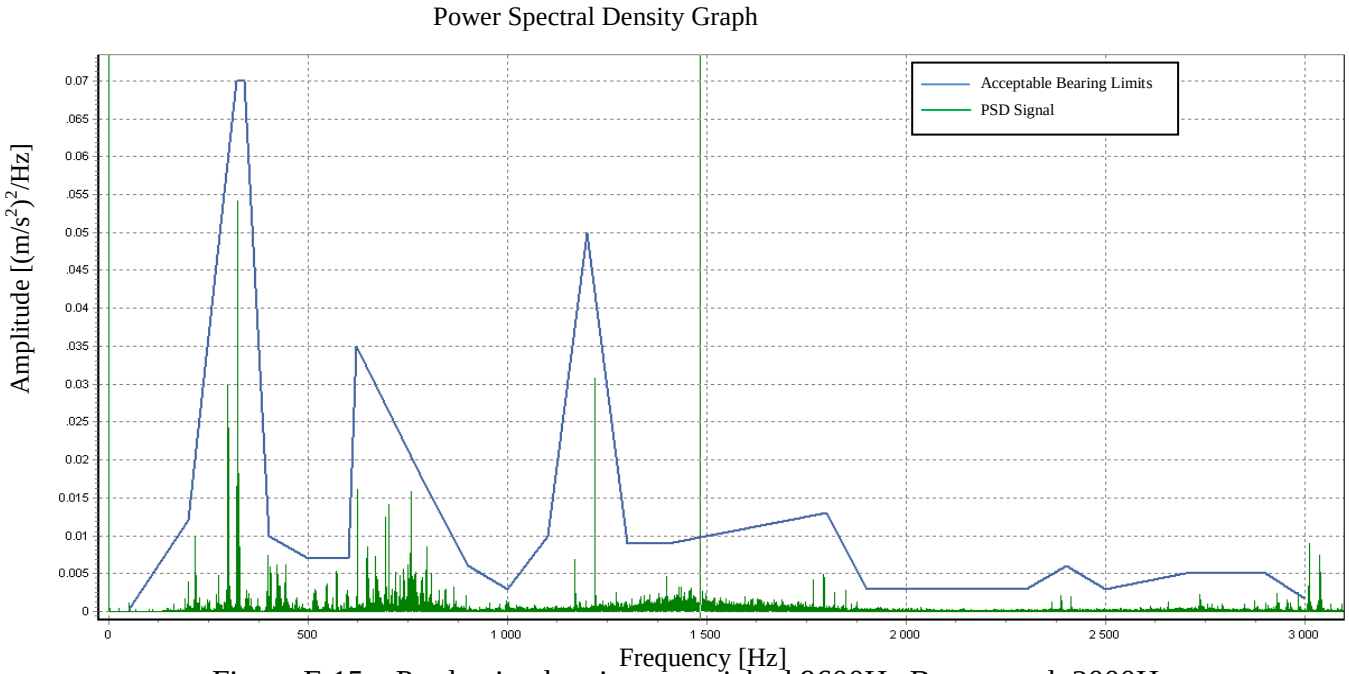

Figure F-15 – Production bearing non-nicked 9600Hz Butterworth 2000Hz PSD from CMS software

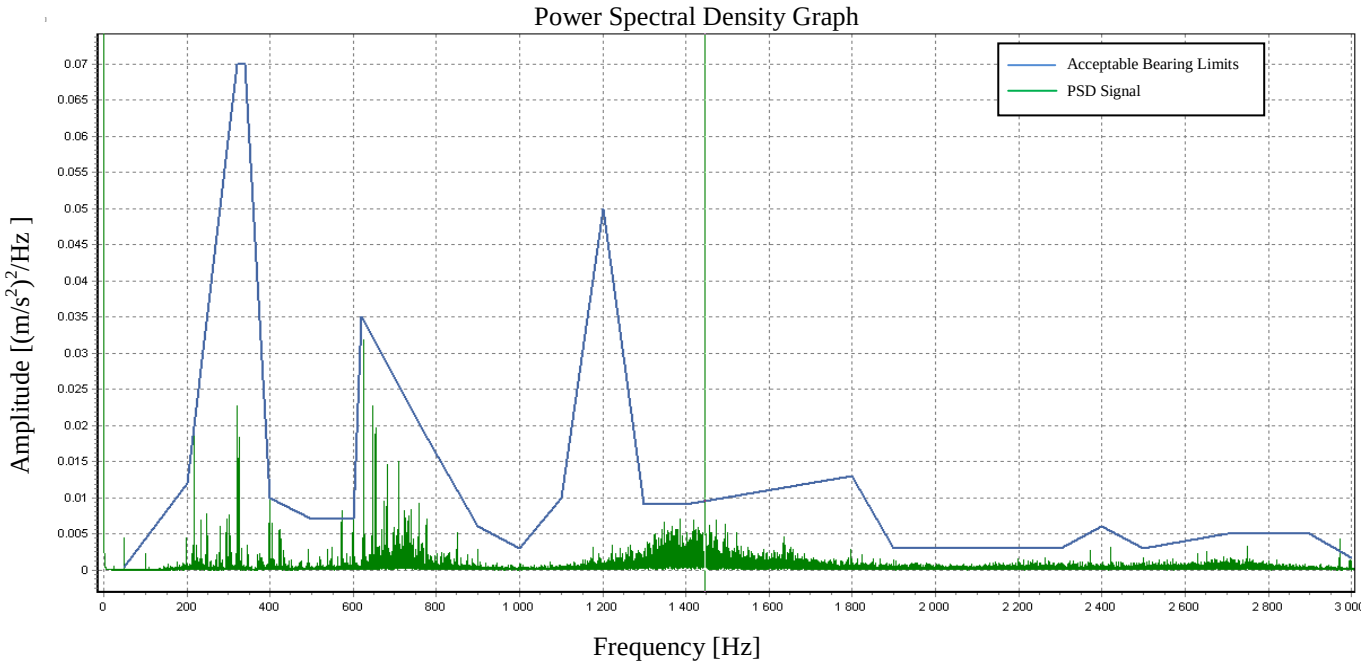

Figure F-16 – D5 non-nicked 9600Hz Butterworth 2000Hz PSD from CMS software

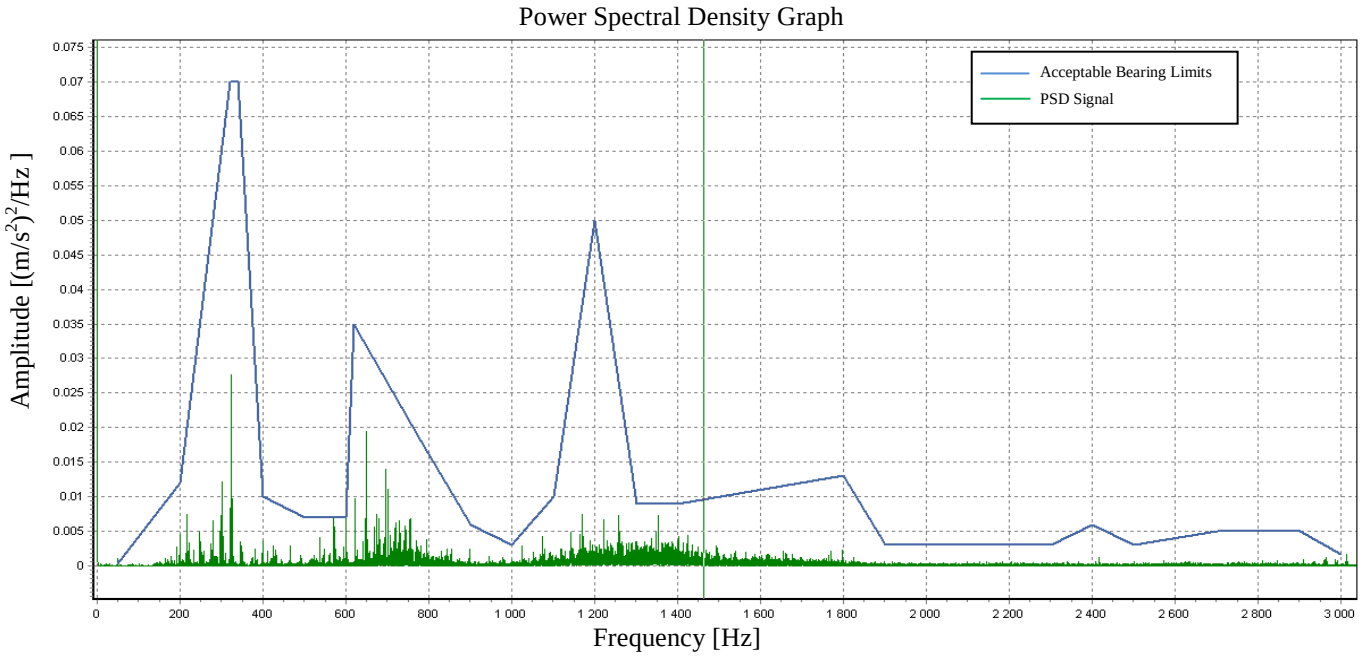

Figure F-17 – D5 non-nicked 9600Hz Butterworth 2000Hz PSD from CMS software third repeat

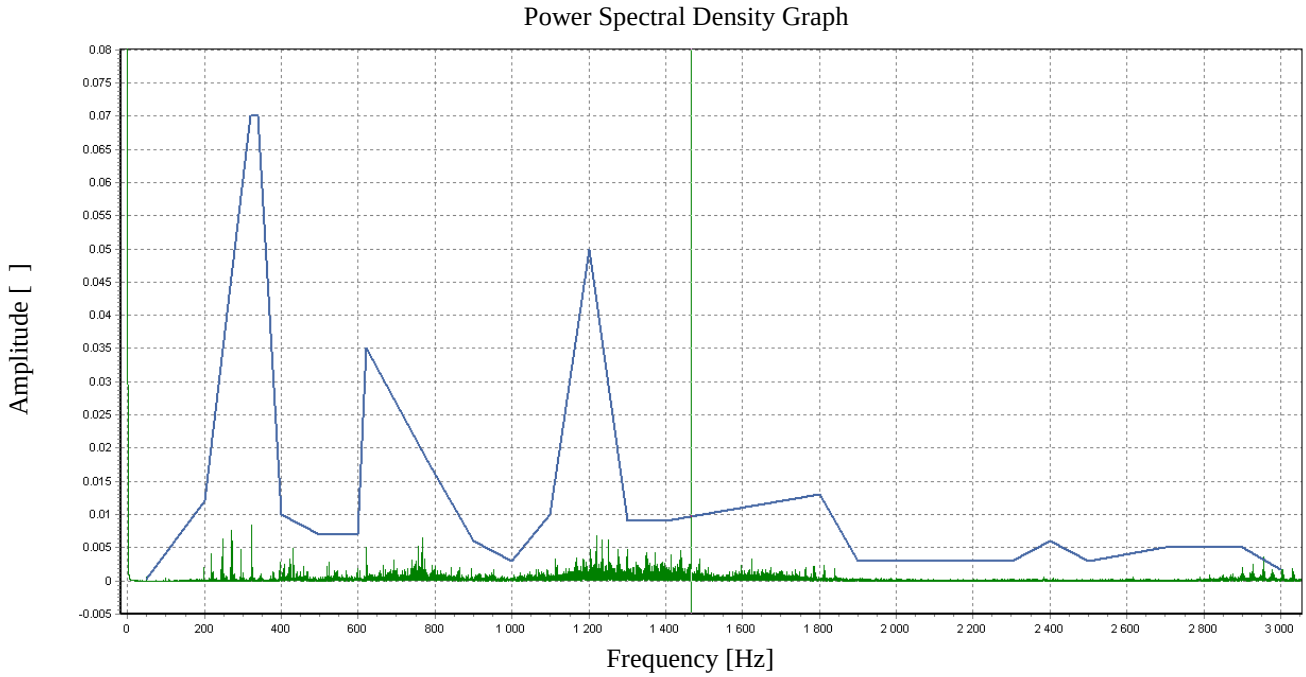

Figure F-18– Production bearing 289631 non-nicked 9600Hz Butterworth 2000Hz PSD

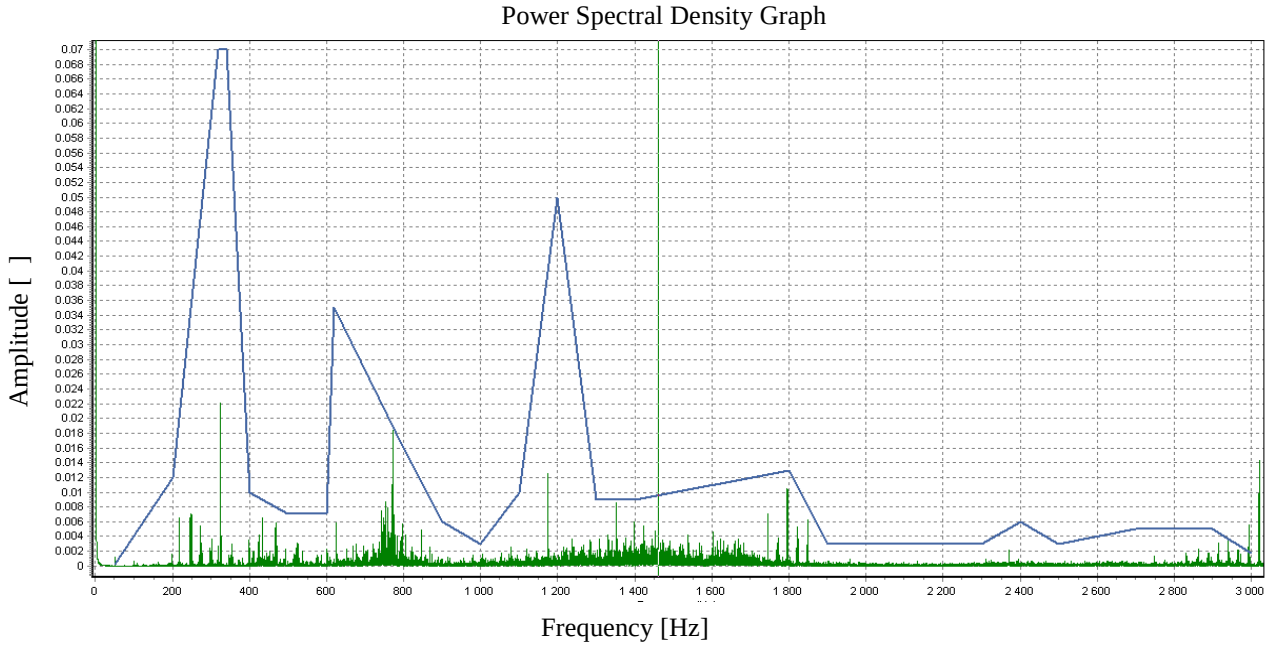

Figure F-19- Production bearing 288026 non-nicked 9600Hz Butterworth 2000Hz PSD

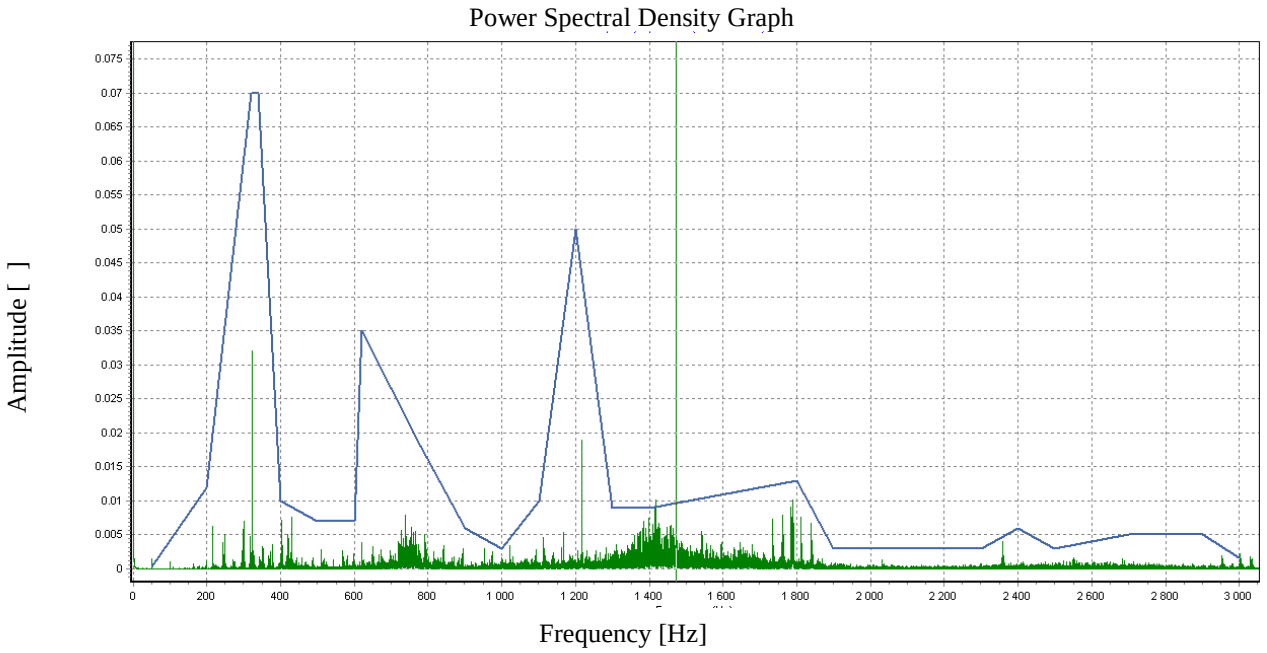

Figure F-20- Production bearing 287461 non-nicked 9600Hz Butterworth 2000Hz PSD

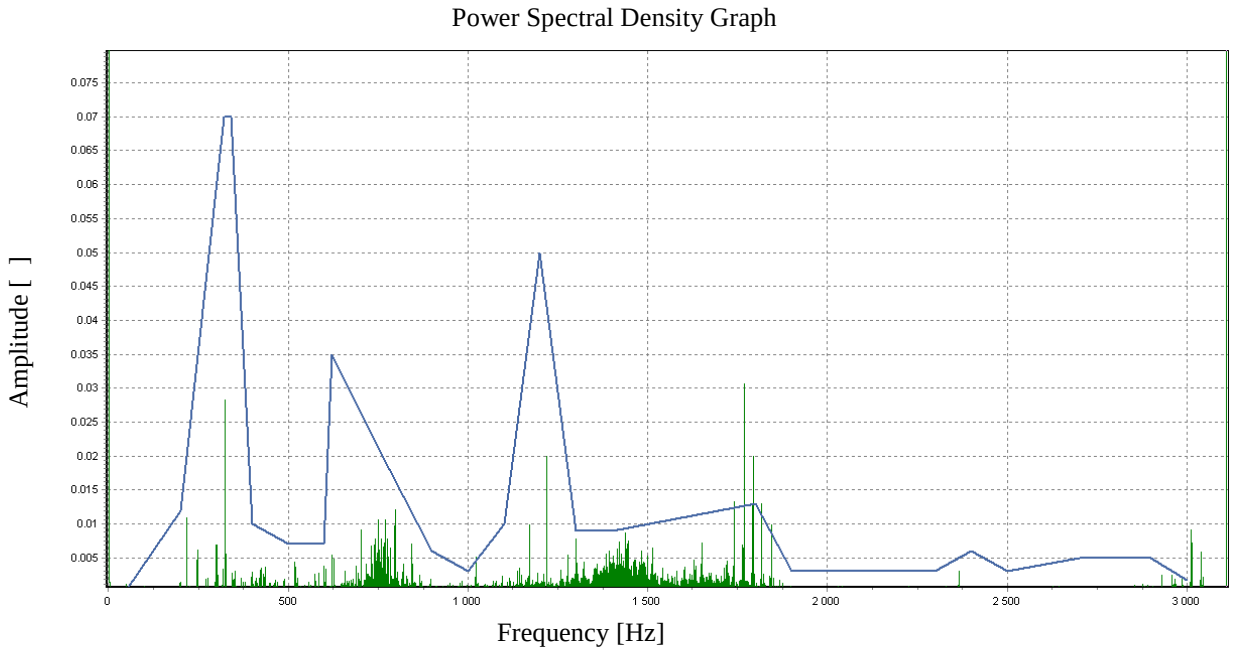

Figure F-21- Production bearing 288050 non-nicked 9600Hz Butterworth 2000Hz PSD

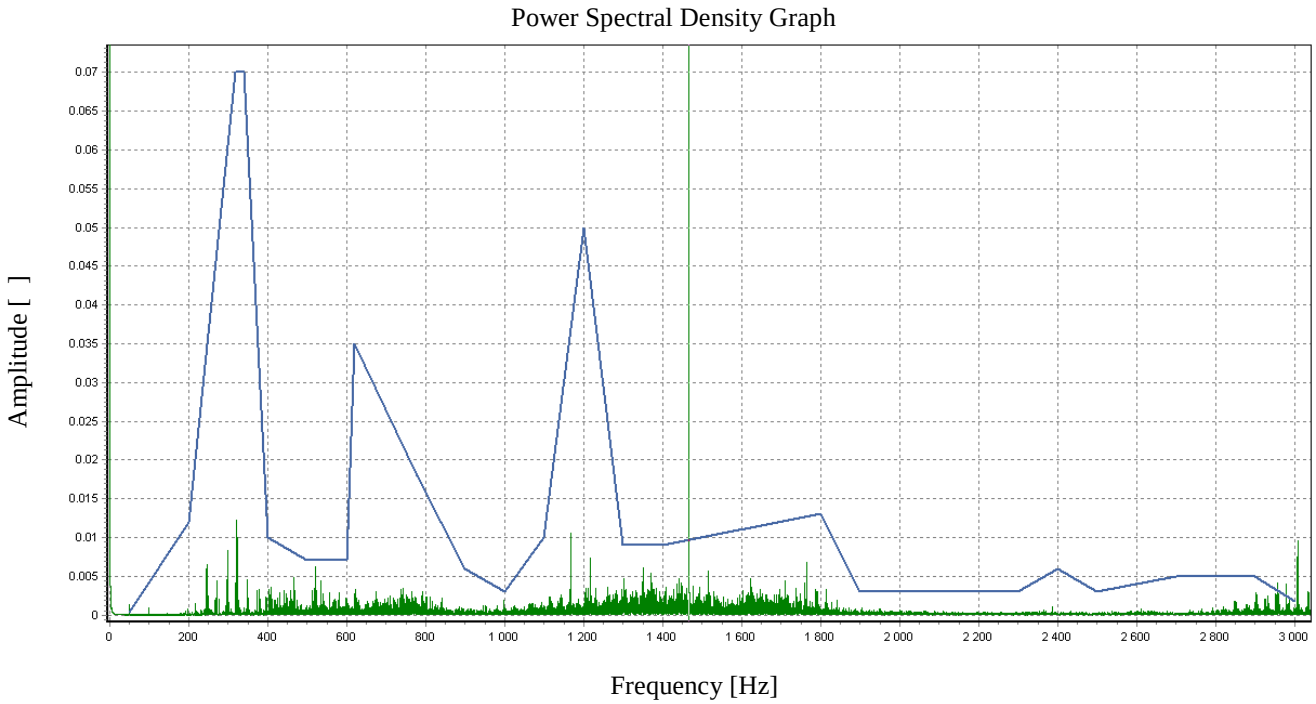

Figure F-22- Production bearing 531425 non-nicked 9600Hz Butterworth 2000Hz PSD

iv. 19.2kHz Sampling rate tests nicked and non-nicked

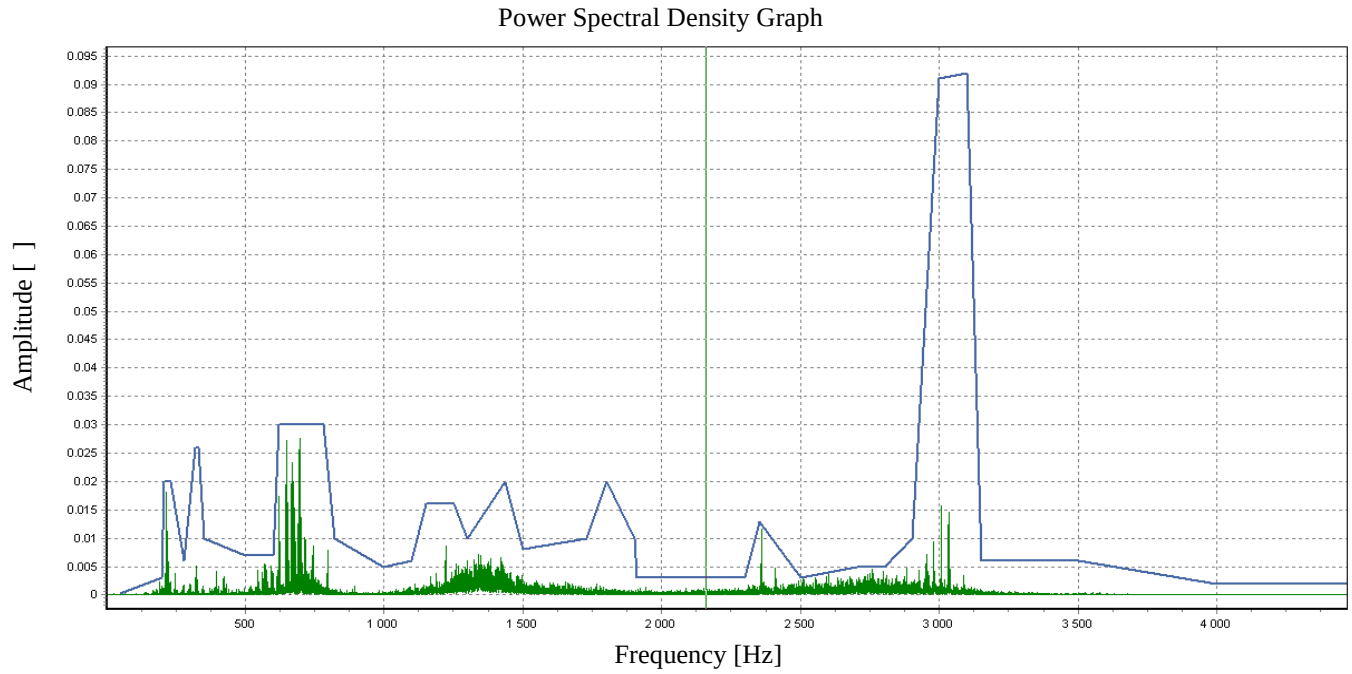

Figure F-23 – D5 non-nicked 19200Hz PSD from CMS program

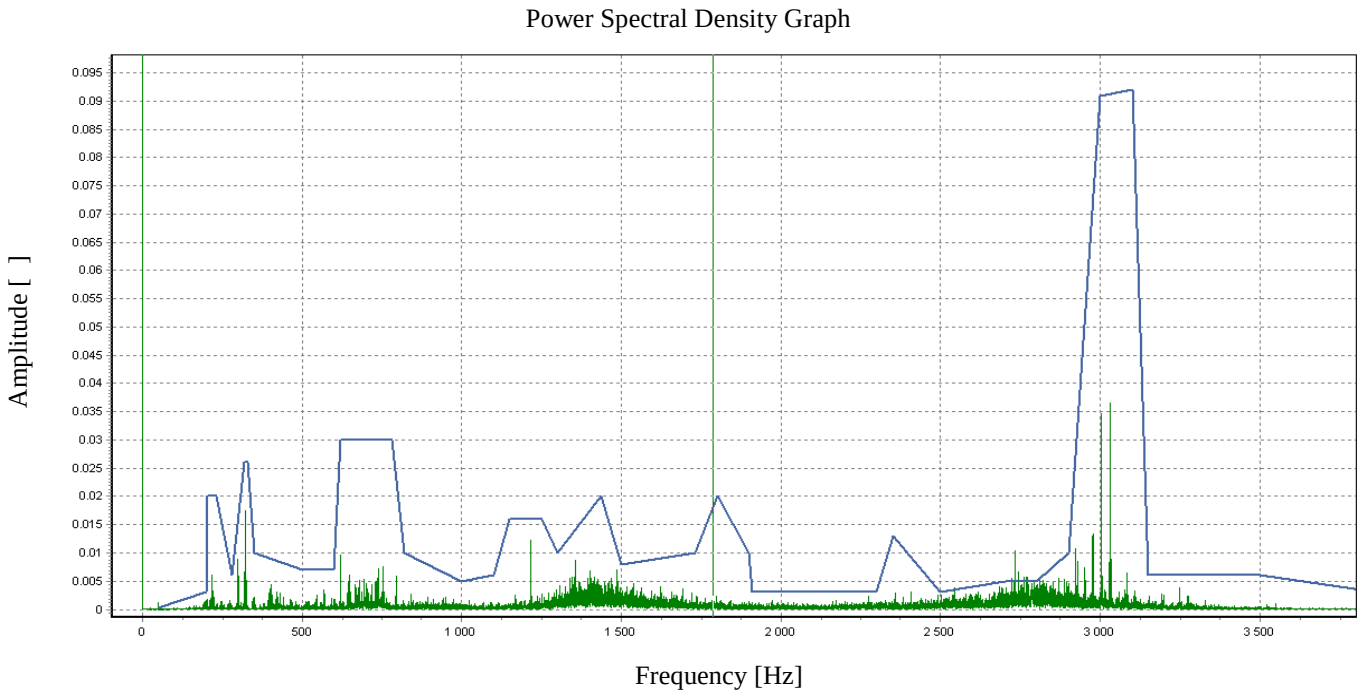

Figure F-24 – D2 nicked BEP 25.5 19200Hz PSD from CMS program

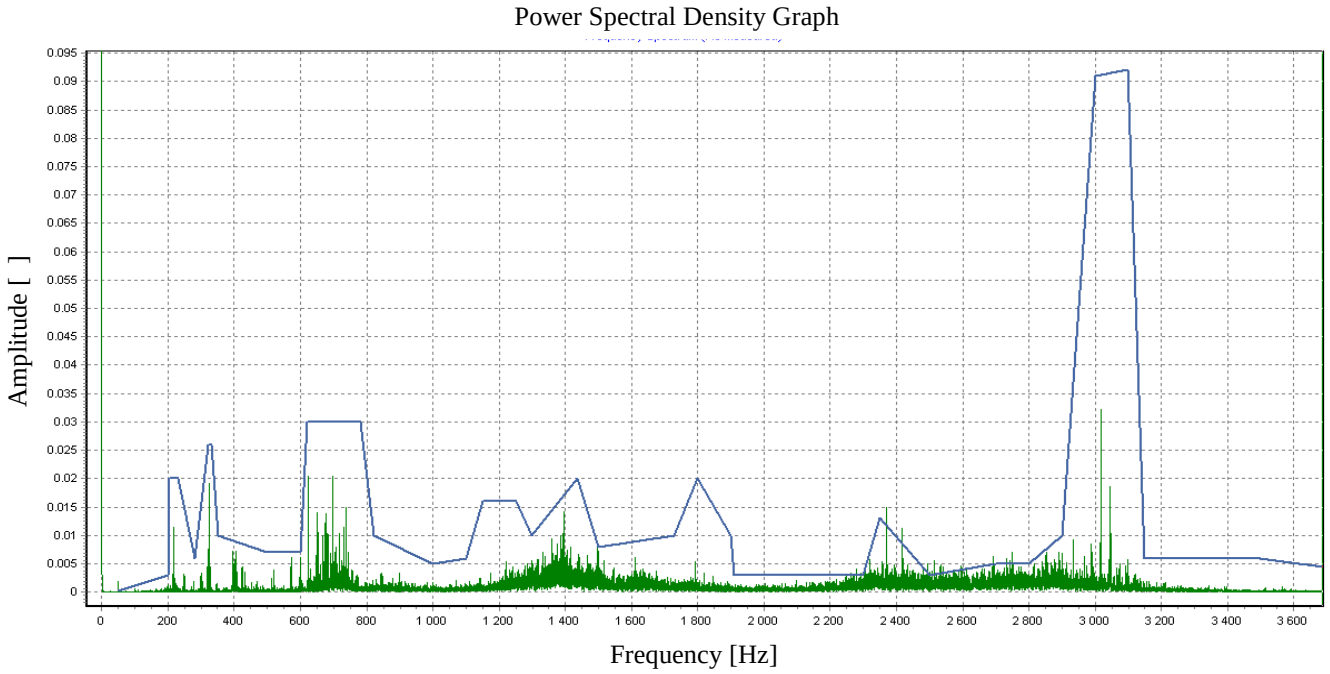

Figure F-25 – D6 nicked 19200Hz PSD from CMS program

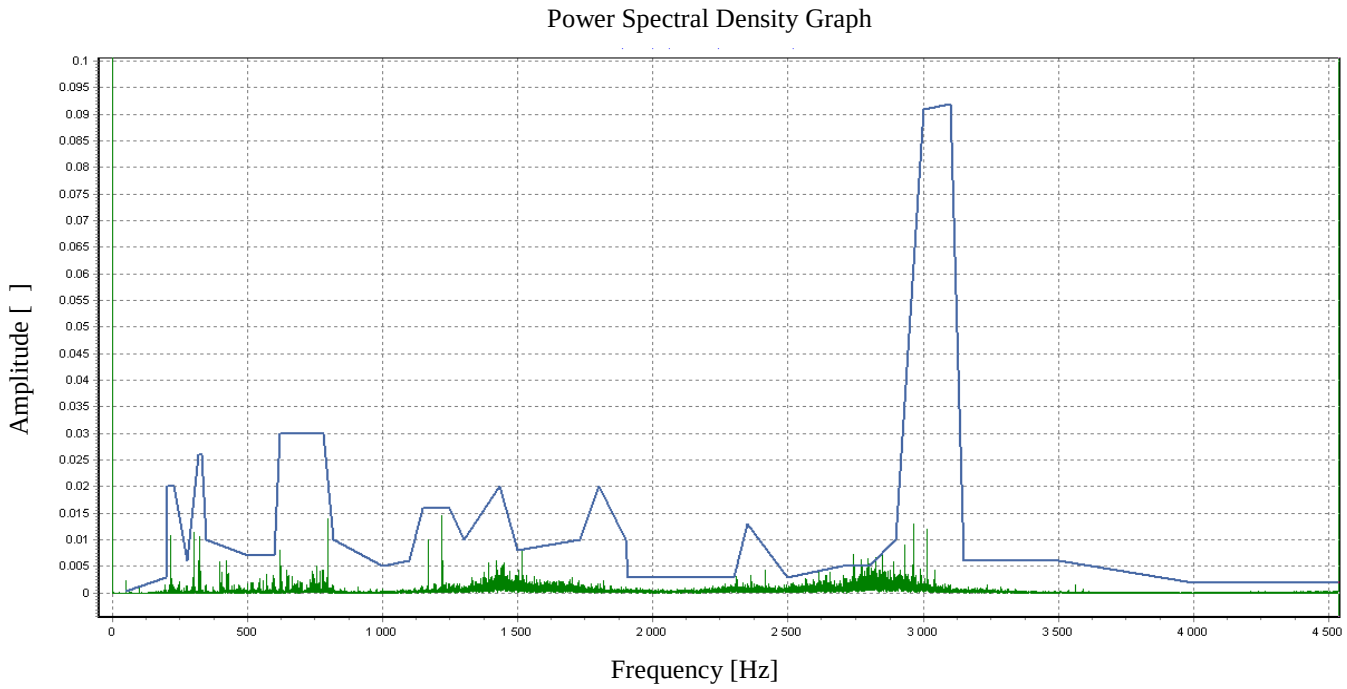

Figure F-26 – D4 nicked 19200Hz PSD from CMS program

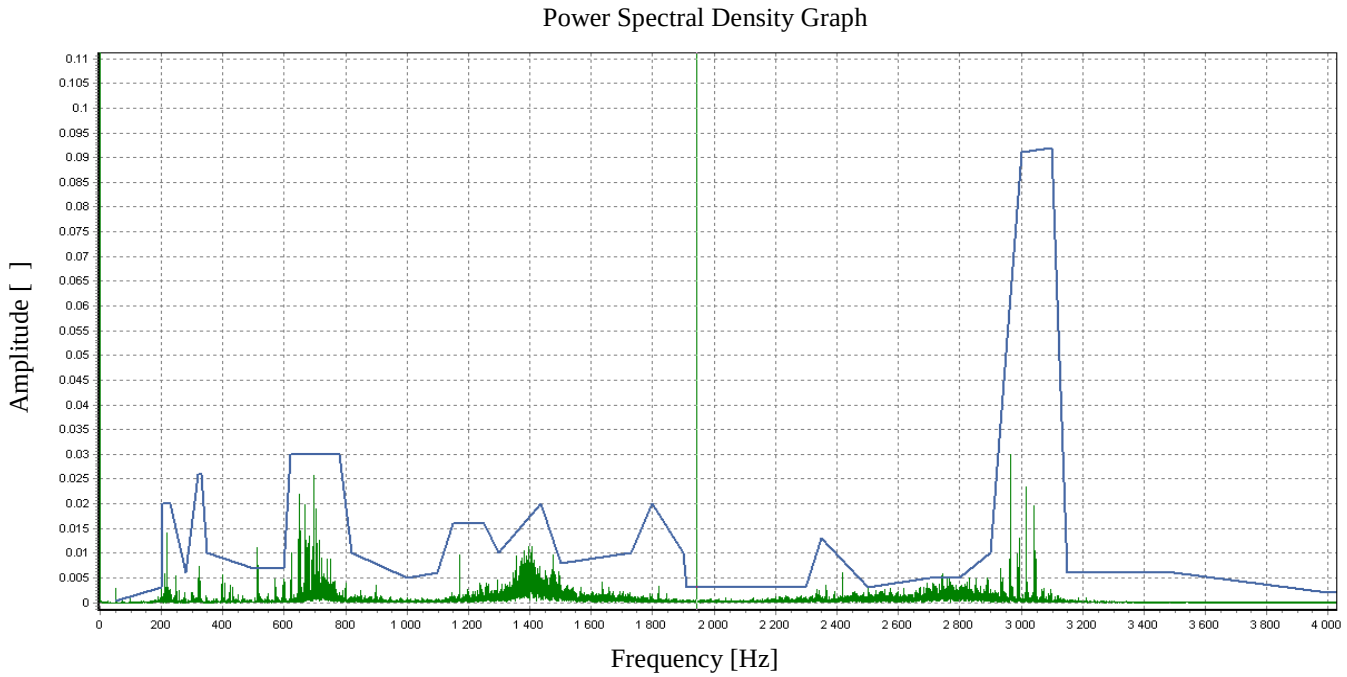

Figure F-27 – D7 nicked 19200Hz PSD from CMS program

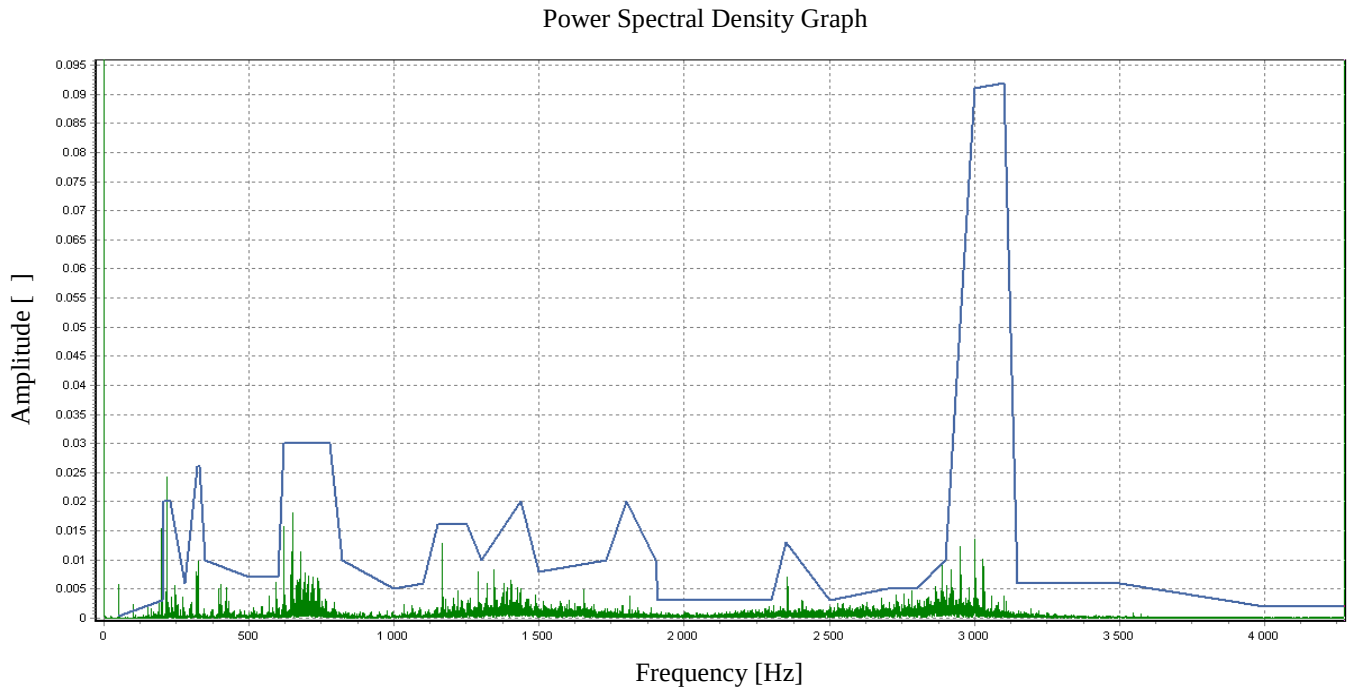

Figure F-28 – D5 cone-nicked 19200Hz PSD from CMS program